Universitat de Barcelona

From flood to drought: Transport and reactivity of dissolved organic matter along a Mediterranean river

Elisabet Ejarque Gonzalez

TESI DOCTORAL

Departament d'Ecologia
Universitat de Barcelona
Programa de Doctorat en Ecologia Fonamental i Aplicada

From flood to drought: Transport and reactivity of dissolved organic matter along a Mediterranean river

D'avingudes a sequeres: Transport i reactivitat de la matèria orgànica dissolta al llarg d'un riu mediterrani

Memòria presentada per Elisabet Ejarque Gonzalez per optar al grau de Doctora per la Universitat de Barcelona

Elisabet Ejarque Gonzalez
Barcelona, setembre de 2014

Vist-i-plau dels directors de tesi:

Dr Andrea Butturini
Director
Professor agregat, Dep. Ecologia UB

Dr Francesc Sabater Comas
Co-director
Professor titular, Dep. Ecologia UB

Als meus pares

Agraïments

Voldria començar donant les gràcies a l'Andrea per haver-me animat a emprendre aquesta aventura i per haver-me encoratjat durant els alts i baixos (que han sigut molts!). I a en Quico, per les converses de tesi sempre tant constructives. També, a tota la gent del grup, especialment a l'Eusebi per estar sempre a punt per parar l'orella i fer un cafè tant llarg com calgui; a la Marta Álvarez, per les llargues converses que hem tingut a Fuirosos; i a l'Alba, pel seu companyerisme i pragmatisme, com dic sempre: "de gran vull ser com tu!". També vull donar les gràcies a la gent del projecte Flumed: l'Anna Romaní i l'Anna Freixa, i a l'Stefano Fazi i l'Stefano Amalfitano, pel seu optimisme i alegria durant les campanyes a la Tordera. Una col·laboració mediterrània que espero que només sigui el començament. També vull donar les gràcies a aquells que han passat pel grup de manera més breu: Marta, Ana, Martí, pel suport que m'heu donat al laboratori i a les campanyes. And my special thanks to Dijana, for the great moments we shared inside and outside the lab!

També vull donar les gràcies a la Núria Catalán, en Rafa Marcé, en Marc Sala, i altres agosarats amb qui hem compartit les dificultats de la fluorescència i el PARAFAC. I a en Max, per haver-me ajudat a programar la macro per fer matrius. Això t'ho hauran d'agrair un grapat de generacions a venir!

Seguidament vull donar les gràcies a tots els companys del departament, a tots sense excepció, per crear un ambient de treball on la frontera entre feina i amistat es desdibuixa. A la Gemma, l'Octavi, l'Isa i la Laia, per acollir-me en els meus inicis al despatx de forestals. A la colla Manchester per l'amistat que hem anat construint al llarg de tots aquests anys: Mary, Júlio, Jaime, Lídia, Esther, Isis, Dani, Neus, Gonzalo, Eusebi, Alba, i les dues incorporacions recents, Astrid i Myrto, i segur que encara em deixo gent. Un grup on quasi tots us definiu com a rancis i, en realitat, reconeixeu-ho: sou la gent menys rància que he conegut mai. De converses d'ecologia n'hem tingut ben poques, però d'experiències n'hem compartit mil! tots vosaltres sou el més gran que m'ha passat aquests últims cinc anys. També vull donar les gràcies als companys de despatx, ja que conviure en un galliner no és fàcil i nosaltres ho hem aconseguit: Sílvia, Anna, Ada, Núria Catalán, Marta, Dani,

Eusebi, Tania, Elisabet, Pau Giménez, Claudia, Alba, Lluís, Sandra. I també a en Pol, en Pablo, l'Aurora, Pau Fortuño, Joan Gomà, Giorgio, Núria Sánchez, Raúl, Biel, Núria Bonada i als que ara ja esteu per paradors més llunyans: Izaskun, Carles, Iraima, Gemma, Cesc, Oriol, Said. Gràcies a tots per haver-vos creuat en el meu camí.

D'altra banda, vull donar les gràcies a en Miquel Alonso per facilitar-me un contacte que em va obrir les portes a un país únic: Mongòlia. I would like to thank Prof. Soningkhishig Nergui for giving me the opportunity to live a unique experience in Mongolia. Participating in the Orkhon project has been definately the most enriching experience during my thesis. I would also like to thank Sisira Withanachchi for his friendship, professionalism, and for sharing our daily experiences while living abroad. Also, I have special words for Azzaya Boldbaatar, who was always willing to help me with the Mongolian life. And I would like to thank all the interesting people I met within the project: the microbiologist Narantuyaa Damdinsuren, the hydrologist Tumur Sodnom, as well as all the students and professionals who participated in the field work: Ankhbold Tsogtbayar, Enkhjin, Tseegii, Deegii, Bolortsetseg Erdenee, Tsenguun Tumurkhuyag, Tamir Tamir, Odbaatar Enkhjargal, among others. And finally, I would like to thank all the people that I met besides the project which completed my Mongolian experience: Mihalis, Yannis, Thanos, Stephanie, Paula, Nara, Natsuko, Tanja, Karel, Martina, Fridi, Marcel and more, thanks!

Mil gràcies també als banyolins, per aquesta amistat que ve de lluny però que seguim compartint amb il·lusió: Irene, Alba, Elisenda, Lídia, Sergi, Riera, i en aquest cas sobretot a la Laura, perquè en la convivència del dia a dia també ha *sofert* una part d'aquesta tesi. Gràcies per escoltar-me, pels tocs a la Pedreta quan ja no podia més, pels vespres de sofà (vigila, que comença el Karakia!). A tots vosaltres, banyolins, gràcies per ser-hi!

I finalment, els agraïments més especials són per la meva família. Per en Joaquim i la Mariona, per la Núria, per l'oncle, i per l'avi i la iaia (sempre dins meu!). A tots vosaltres, gràcies per fer-me sentir estimada. I els meus agraïments més profunds, aquells que cap paraula pot descriure perquè són tot sentiment, són pels meus pares. Per demostrar-me cada dia que esteu al meu costat. Sense vosaltres aquesta tesi mai no hauria arribat a bon port.

Barcelona, 28 de setembre de 2014

Summary

Rivers play a key role in the global biogeochemical functioning, as they link the biogeochemical cycles of the terrestrial and oceanic systems. In the framework of the carbon cycle, streams and rivers receive dissolved organic matter (DOM) from a variety of sources which is subsequently transported downstream and delivered to the oceans. However, there is increasing evidence that this step involves not only a relocation of DOM from the land to the seas, but also an important in-stream processing which modifies its quality and properties and, to some extent, outgas it to the atmosphere as CO_2. However, up to now it has not been assessed how these modifications occur along a longitudinal perspective and, most importantly, the role that hydrology plays in such downstream patterns of DOM processing.

This thesis explores the transport and reactivity of DOM along a Mediterranean river (la Tordera) under a variety of hydrological conditions ranging from flash floods to summer droughts. First, the composition of DOM was determined using 3D fluorescence spectroscopy (emission-excitation matrices) and a novel chemometric approach based on a self-organising maps analysis coupled with a correlation analysis. This step allowed discerning the presence of four DOM moieties: a tyrosine-like, a tryptophan-like, and two humic-like fluorescence components.

Next, longitudinal patterns of these components are presented for a range of hydrological conditions. Along the main stem, the river exhibited three reaches with a differentiated DOM character: in the headwaters DOM had an eminent humic-like character derived from the drainage of the surrounding terrestrial catchment (high HIX); in the middle reaches (from Sant Celoni to Fogars de la Selva) there was a predominance of the protein-like component C2 reflecting the effect of direct anthropogenic water inputs (concomitant high nutrient concentrations); and the lowest part of the river was dominated by the protein-like component C1 and high FI, suggesting a predominance of microbially-derived DOM. Hydrology appeared to act as a modulator of such longitudinal patterns: during drought, the spatial heterogeneity of DOM character was maximised, whereas during flood conditions there was an homogenisation over the longitudinal dimension, consisting in a highly aromatic humic-like character.

By means of an End-Member Mixing Analysis (EMMA) approach it was observed that in-stream reactive processes were likely to be driving DOM quality, especially during non-flood conditions and at the middle and lower reaches of La Tordera. Following such evidences, the relevance of in-stream transformations over transport and physical mixing were explicitly quantified by performing a mass balance approach at thirteen consecutive downstream segments. Results of the mass balance study showed that flood events, despite their brevity in time, had the capacity to export the largest amounts of DOM, although having undergone little in-stream processing. During baseflow conditions, which have been estimated to occur annually about half of the days, there were moderate efficiencies of bulk DOM retention; however, individual fluorescence components had important in-stream generations, especially the protein-like moieties C1 and C2. In space, this processing occurred in the final segments of the river, hence exhibiting a shift from a conservative to a reactive behaviour. Finally, during drought conditions the river had the highest capacity of DOM retention and exported the least amounts of DOM. In space, retention efficiencies were homogeneous along the mainstem, except for two anthropogenically-impacted sites where the retention capacities were reduced. The mass balance study also revealed that bulk DOC processing was subject to a stoichiometric control with nitrate, even though such control was weaker during drought.

The findings of this thesis demonstrate that the riverine passage is a decisive step that defines the quantity and quality of the DOM that is finally delivered to the oceans. Moreover, the observed hydrological seasonality in La Tordera shapes a temporally-changing DOM character which may have complex repercussions for its fate once in the coastal systems.

Resum

Els rius juguen un rol essencial en el funcionament biogeoquímic global, ja que enllacen els cicles biogeoquímics terrestres amb els oceànics. En el si del cicle del carboni, els rius reben matèria orgànica dissolta (MOD) d'una gran varietat d'orígens, la qual és transportada riu avall i alliberada al mar. Hi ha evidències creixents que aquest pas, no consisteix només en un transport conservatiu, sinó que a més, té lloc un processat intern que en modifica qualitats i, fins a cert punt, l'oxida i allibera a l'atmosfera en forma de CO_2. Malgrat tot, fins ara no s'ha avaluat com ocorren aquestes modificacions des d'una perspectiva longitudinal, de capçalera a desembocadura, ni el rol que la hidrologia fluvial juga en el desenvolupament d'aquests patrons longitudinals.

Aquesta tesi explora el transport i la reactivitat de la MOD al llarg d'un riu Mediterrani (la Tordera) durant un ventall de condicions hidrològiques que comprenen des de grans avingudes fins a sequeres estivals. Primerament, es presenta un nou mètode quimiomètric per a determinar la composició de la fracció fluorescent de la MOD basat en una anàlisi neuronal amb mapes autoorganitzats de Kohonen. Aquesta anàlisi ha revelat la presència de quatre fraccions de matèria orgànica: una relacionada amb la tirosina (C1), una amb el triptòfan (C2), i dues amb substàncies húmiques (C3 i C4).

Seguidament, es presenten els patrons longitudinals d'aquestes quatre fraccions per un ventall de condicions hidrològiques contrastades. Al llarg del curs principal, el riu ha mostrat tres trams amb unes característiques de la MOD diferenciades: a la capçalera la MOD tenia un caràcter eminentment húmic i amb un HIX elevat, derivat del drenatge de la conca terrestre adjacent; en el tram mitjà (des de Sant Celoni fins a Fogars de la Selva) predominava el component proteic C2 que, coincidint amb uns elevats nivells de nutrients, reflectien l'efecte de les entrades d'aigües antropogèniques; finalment, a la part baixa del riu (des de Fogars de la Selva fins a la desembocadura) la MOD estava dominada pel component proteic C1 i un FI elevat, suggerint un predomini de substàncies derivades d'una activitat microbiana autòctona. Amb tot, la hidrologia es va mostrar com el gran modulador d'aquests patrons longitudinals: en sequera, l'heterogeneitat espacial de la MOD

era màxima, mentre que durant les crescudes s'esdevenia una homogenització al llarg de la dimensió longitudinal, que consistia en un caràcter fortament aromàtic.

Mitjançant una anàlisi de mescla d'*end-members*, es va observar que la qualitat de la MOD al llarg del curs fluvial podia estar principalment determinada per processos reactius autòctons, especialment fora de condicions de sequera, i en els trams mitjans i baixos de la Tordera. Arran d'aquestes evidències, es va quantificar i discernir la rellevància d'aquestes transformacions respecte de processos de barreja física. Això es va dur a terme mitjançant un càlcul de balanç de masses en tretze segments fluvials consecutius, localitzats entre Sant Celoni i Fogars de la Selva. Els resultats d'aquest estudi mostren que durant les crescudes, malgrat la seva brevetat en el temps, tenen una capacitat màxima d'exportar MOD; una MOD, però, que sofreix canvis composicionals mínims durant el seu transport. En condicions de cabal basal, les quals s'estima que ocorren la meitat de dies l'any, es van observar eficiències de retenció de MOD moderades, malgrat tot, individualment pels components de fluorescència hi van haver importants generacions, especialment per les fraccions proteiques C1 i C2. En l'espai, aquesta generació va tenir lloc als segments finals, mostrant així un canvi de comportament del riu des de transportador conservatiu a reactiu. Finalment, en condicions de sequera el riu va mostrar la màxima eficiència de retenció, a la vegada que exportava la mínima quantitat de MOD. En l'espai, les eficiències de retenció es mantenien homogènies al llarg del riu, excepte en dos punts subjectes a impacte antropogènic, on les eficiències de retenció es van veure reduïdes. L'estudi de balanç de masses també va revelar que el processat del carboni orgànic dissolt estava subjecte a un control estequiomètric amb el nitrat, control que en condicions de sequera es va mostrar més dèbil.

Els resultats d'aquesta tesi doctoral demostren que el pas fluvial és un pas decisiu que determina la qualitat i la quantitat de MOD que és finalment alliberada als mars. Aquesta estacionalitat temporal en la qualitat i quantitat de la MOD exportada, determinada principalment per les condicions hidrològiques, pot ser determinant pel destí que tindrà la MOD un cop al mar.

Contents

List of Figures

List of Tables

Chapter 1

General introduction

1.1 Characterisation of dissolved organic matter

1.1.1 Dissolved organic matter as a complex chemical mixture

The term dissolved organic matter (DOM) refers to the pool of organic molecules that are dissolved in water. It is ubiquitous, as it exists in all known water bodies, and it plays a key role in the global carbon cycle as it is the largest reservoir of organic carbon on Earth (Findlay and Sinsabaugh, 2003). Operationally, it is defined as the fraction of organic molecules that passes through a filter of 0.45 micrometers (McDonald et al., 2004). However, beyond this basic criterion, DOM molecules are highly heterogeneous, presenting a large range of chemical structures and properties (Filella, 2008). In biochemical terms, DOM is made up of two types of molecules: On the one hand, it contains well-known and simple biomolecular compounds, including mainly lipids, proteins and carbohydrates, and they represent about 20-40% of the total DOM. On the other hand, there is a humic fraction that includes large and complex molecules, rich in aromatic groups, whose chemical structures are very heterogeneous and not very well-known, and they represent about 50-75% of the total bulk DOM (Volk et al., 1997). These substances are the result of the long term mineralisation and decomposition of plant and animal tissue remains through a process termed humification. These humic substances have been traditionally characterised by chemical fractionation, so that we can distinguish between fulvic acids – the fraction which is insoluble at pH<2 – and humic acids – the fraction which is soluble at all pH values (Thurman, 1985). Under a physical perspective, DOM compounds span a wide range of molecular weights usually divided into low, medium and high molecular weight. As the size range is continuous, thresholds between these categories are also operational. While the low

molecular weight fraction, including the well-known biomolecules, are in the range of <1kDa, high molecular weight humic substances can be of the order of hundreds of kDa (Vázquez et al., 2007).

1.1.2 Fluorescence spectroscopy for the determination of DOM properties

Such compositional heterogeneity and complexity has therefore constituted a major challenge for the chemical characterisation of DOM. In the field of analytical chemistry, methodologies have mainly focused at elucidating the elemental and functional groups composition, with techniques like Fourier Transform Infrared Spectroscopy (FTIR), Nuclear Magnetic Ressonance Spectroscopy (NMR) and Mass Spectrometry (MS) (McDonald et al., 2004). However, these methodologies require expensive equipment, long protocols and an important manipulation of the samples, what limits the popularity and applicability of these techniques.

By contrast, fluorescence spectroscopy appeared as an analytically fast, economic and straightforward method. It is based on the fact that an important part of the molecules included in bulk DOM have the capacity to fluoresce, that is, to absorb and emit light. Whereas it is true that not all DOM molecules have this light-interacting capacity, the pool of molecules that effectively have this property include important groups of organic substances found in natural water bodies, like humic and fulvic acids, as well as some protein-like material containing tryptophan, tyrosine or phenylalanine. Each of these substances represents different roles in the environment and, hence, may provide information about a variety of ecological processes regarding DOM such as origin and transformation (Hudson et al., 2007).

The reason why the above mentioned chemical groups are optically detectable is that they contain aromatic rings in their structure. Aromatic rings have loosely held electrons that, when they are excited with incident photons, they attain a higher energy level. This is considered the absorption or excitation process. Afterwards this absorbed energy is released again in the form of light as electrons return to their original ground state, in the so-called emission process (Lakowicz, 2006). The intensity of light absorbed and emitted at a certain wavelength (λ) is dependent on the specific structure and characteristics of the aromatic groups of every molecule. Therefore the determination of the maximal wavelengths at which a substance absorbs and emits light allows the identification of that substance (Lakowicz, 2006). Highly aromatic humic substances emit light at the visible range of the light spectrum, broadly between 420 and 480 nm. At high concentrations they can be detected at naked eye by conferring a brownish or yellowish colour to the water sample. Lower aromatic humic substances appear at progressively lower emission

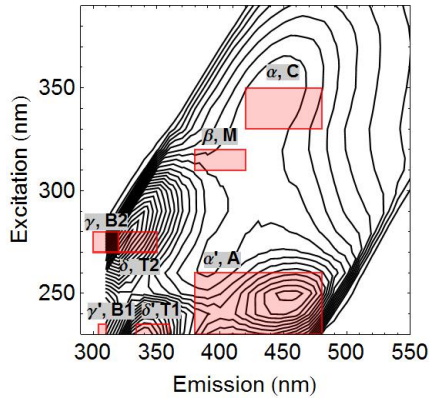

Figure 1.1 – Demonstration of an Excitation-Emission Matrix and the areas of the most commonly reported fluorophores according to Coble (1996) and Parlanti et al. (2000).

wavelengths and, aminoacids, typically appear in the ultraviolet at 300-370 nm (Fellman et al., 2010).

1.1.3 Excitation-Emission Matrices and the optical landscapes of DOM

A practical way of getting an image of the different kind of optically detectable substances that are contained in a sample is to make a full scanning over a range of emission wavelengths (λ_{em}) and excitation wavelengths (λ_{ex}). Such measurements provide an optical map in which fluorescent components appear in the form of peaks. In mathematical terms, they represent fluorescence data matrices described by two independent variables: emission and excitation. For that reason, these data sets are referred to as Excitation-Emission Matrices (EEMs) (Mopper and Schultz, 1993; Coble, 1996). In Figure 1.1 there is an example of an EEM with some typical fluorescence peaks. It should be noted here that every peak is not necessarily representing a single substance, but rather a pool of substances with close aromatic or optical properties (Stedmon and Bro, 2008). This applies especially in the present case when the analyte under consideration is DOM, containing a large diversity of organic compounds which can potentially exhibit gradients of similarities between them (Del Vecchio and Blough, 2004). Also, fluorophores can reflect internal processes such as quenching or intra molecular charge transfer (Del Vecchio and Blough, 2004; Boyle et al., 2009). For that reason, hereafter detected peaks will be referred to as fluorophores, with the aim to designate groups of compounds with similar optical properties rather than a pure chemical substance.

1.1.4 Turning spectral data into information

While the spectrofluorometric measurements in the lab are relatively fast and straightforward, the subsequent data treatment and interpretation is still a major challenge, as EEMs are the expression of a complex mixture of fluorescence signals and phenomena. Therefore it is necessary to distil the biogeochemically meaningful information out of this complex fluorescence data. Authors have used a range of approaches in order to convert EEM data sets into some simple and manageable variables or indices:

Among the earliest approaches, but still on use, is the identification of fluorophores by visual peak picking. Seminal papers on DOM EEMs relied on this approach, like in Coble (1996) and Parlanti et al. (2000), who established nomenclatures to designate fluorophores which have been used up to current dates. Such fluorphores and their locations are shown and described in Figure 1.1. Peaks A, C and M appear at the longer emissions and reflect humic-like compounds. A and C are considered to be terrestrially-derived as they have been found to be the predominant fluorescence signature in headwater streams (Hudson et al., 2007). Peak C corresponds to highly degraded humic material, whereas peak A corresponds to diagenetically younger components (Huguet et al., 2009). By contrast, peak M has been related to humic-like compounds derived from microbial activity, and have a lower aromatic character (Romera-Castillo et al., 2010). On the other hand, peaks T and B correspond to the protein-like fraction of DOM, and appear at lower emission wavelengths. Peak T reflects materials related to tryptophan, whereas peak B is related to tyrosine (Yamashita and Tanoue, 2003). Often, these peaks appear bimodal, with two excitation maxima (Henderson et al., 2009).

Further, ratios between peaks have been used to infer sistemic processes, usually by relating the intensity of any fluorophore to that of the C or α peak. The ratio T:C has been used as a tracer of anthropogenic inputs (Henderson et al., 2009) like urban and industrial sewage (Baker, 2001; Borisover et al., 2011) and farm wastes (Baker, 2002; Naden et al., 2010), based on the idea that impacted waters have a more predominant composition in tryptophan-like materials compared to humic-like ones. On the other hand, the ratio α':α has been used as an indicator of the young or mature character of the humic fraction of DOM (Coble et al., 1990; Coble, 1996; Parlanti et al., 2000). Also,γ:α gives information about the recent autochthonous character of DOM and on the productivity in the aquatic environment (Parlanti et al., 2000), as the γ fluorophore has been associated with labile compounds of protein or bacterial origin (Yamashita and Tanoue, 2003; Cammack et al., 2004).

A similar approach to the use of fluorophore ratios are fluorescence indices, in the sense that they use some specific $\{\lambda_{ex}$ - $\lambda_{em}\}$ coordinates or regions out of the whole EEM. But, instead of relying on peak maxima, they are computed over fixed

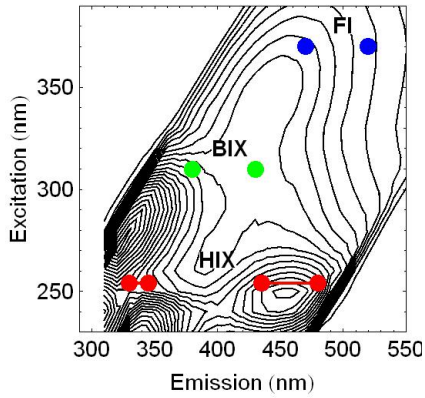

Figure 1.2 – Excitation-Emission Matrix and location of the fix wavelength coordinates used to compute the FI, BIX and HIX indices.

wavelength coordinates (Figure 1.2). The main indices used in the literature are the FI (McKnight et al., 2001), indicator of the autochthonous vs allochthonous source of DOM; the HIX (Zsolnay et al., 1999), indicating the degree of humification; and the BIX (Huguet et al., 2009), related to a predominantly autochthonous origin of DOM and to the presence of freshly released organic matter.

All the above mentioned metrics (peak intensities, ratios between peaks, fluorescence indices) have been successfully used in a wide variety of DOM studies, however, they still hold some drawbacks: (i) peak-picking-based metrics are subject to an inherent subjectivity for fluorophore identification, and (ii) all these metrics rely only on some few $\lambda_{ex} - \lambda em$ coordinates and, therefore, there is a lack of a deeper dealing with the whole complexity of the EEM signals. These drawbacks have become more important with the increasing size of EEM data sets, triggered by the recent advances in spectrofluorimetry and computer software and hardware.

1.1.5 Chemometric methods

Advances in spectrofluorimetric equipment have made it possible to automate the analysis of a large number of samples, and therefore, researchers are faced with EEM data sets of increasing sizes. Because of that, dealing with EEMs and extracting meaningful information out of them has become increasingly more challenging. The traditional approaches for identifying fluorescence components, namely visual peak picking, has become importantly limited. On the one hand, it requires a careful inspection of every single EEM of the data set, what can be very time consuming for large EEM data sets. Furthermore, visual peak detection is not always obvious: some peaks appear overlapped to wider or higher peaks, or can appear as shoulders

to other peaks. On the other hand, peak picking results among EEMs may be difficult to compare, as peaks do not consistently appear at the same coordinates, but have some variability in its location. Because of that, it is often confusing to see if an observed peak is a shifted version of an already identified peak, or whether it is a new fluorophore. Therefore, visual peak picking is not really feasible for an in-depth analysis of large EEM data sets.

Because of that, a currently active field of research is devoted to find statistical data mining tools that can objectively separate the broad signal of the EEMs into individual fluorophores, or fluorescence components, out of large EEM data sets. The most notorious advance in this sense has been the adaptation of parallel factor analysis (PARAFAC) analysis to the specific analysis of EEM data sets (Stedmon et al., 2003; Stedmon and Bro, 2008). PARAFAC is a generalisation of PCA to higher order arrays (Bro, 1997) and mathematically separates the mixture of fluorescence signals contained in the EEMs into individual constituents localised at fix $\lambda_{ex} - \lambda em$ wavelength pairs (Stedmon and Bro, 2008). It is based on the fundamental assumption that fluorophores behave independently and without interaction between them according to the Beer-Lamberts law. That is, the observed fluorescence signal results from the sum of the contribution of every fluorophore present in the sample. In practice, every component represents a group of wavelengths that vary independently to the rest of wavelengths within the data set.

PARAFAC has been successfully used in a large number of ecological studies and has enabled important advances in the scientific knowledge about the biogeochemical behaviour of DOM in marine and freshwater systems (Fellman et al., 2010). However, PARAFAC has some limitations which hinder its application to some EEM data sets. First, this model assumes that all the samples in the data set include the same number of fluorophores, but at different proportions (Stedmon and Bro, 2008), so that every component exhibits a full compositional variability within the data set. Because of that, PARAFAC is well-suited for studies characterising gradual processes of DOM modification, like samplings along gradual environmental conditions or DOM removal experiments (Stedmon and Bro, 2008). However, in the environment discontinuities and heterogeneity are usually the rule (Poole, 2002) and, therefore, this limitation is not trivial, especially for observational studies. Also, and related to that, PARAFAC is very sensitive to the presence of outliers as it relies on a least squares approach (Brereton, 2012). Because of these limitations, DOM studies have to adapt their experimental and sampling designs in order to be able to apply PARAFAC, and this means, mainly, to focus on capturing gradual changes, and avoid heterogeneity, something that cannot be foreseen beforehand in most ecological studies. Therefore, in order to further advance the understanding of DOM biogeochemistry, it is necessary to further develop statistical tools that are

less dependent on the homogeneity/heterogeneity of DOM composition, and that are less sensitive to the presence of outliers within the data set.

1.2 The biogeochemistry of DOM in fluvial systems

In ecological terms, DOM has been considered to be one of the most important variables that define the function and structure of freshwater ecosystems (Prairie, 2008). DOM is the most important active reservoir of organic carbon in aquatic environments (Findlay and Sinsabaugh, 2003), and has a fundamental ecological role, as it is implied in numerous processes which control resources availability to organisms. Namely, it mediates the transport and availability of nutrients (Taylor and Townsend, 2010) and metals (Brooks et al., 2007; Elkins and Nelson, 2002) to aquatic organisms, controls light-depth penetration and therefore light availability to autotrophs (Foden et al., 2008) because of its strong light absorbance capacity, and is a carbon and energy source for heterotrophic bacteria (Findlay, 2010).

During its transport along a riverine channel, DOM flows along changing environmental conditions and, consequently, becomes successively involved in different biogeochemical processes. Because of this interactivity, not only DOM quantity but also its quality is susceptible to change during its transport across the landscape (Jaffe et al., 2008). The quality of riverine DOM is mainly dependant on its source, and on the subsequent transformation processes it has undergone. The main DOM sources include allochthonous (terrestrially-derived), autochthonous (in-stream produced) or anthropogenic origins. Posterior transformations of DOM during its passage through the riverine system depend i) on the susceptibility of a given molecule to be transformed by a determined biogeochemical process, which can be biotic – like microbial degradation – or abiotic – like photodegradation; and ii) on the presence of the favourable environmental conditions needed for that process to take place.

1.2.1 Sources of riverine DOM

Allochthonous or terrestrially-derived DOM Typically the main source of DOM in streams and rivers originates from the drainage of the surrounding terrestrial catchment, and therefore it exhibits eminently a composition reflecting terrestrially-derived materials, that is, humic substances resulting from the humification of lignin-derived compounds in soil (McDonald et al., 2004). The prevalence of terrestrial DOM in the river depends firstly on its generation in the interstitial water in soils and, secondly, on precipitation events which flush this DOM from soils to the river. Temperature is a key factor in determining the rate of organic matter

decomposition (Christ and David, 1996) and hence, the production and availability of DOM in soil for its subsequent drainage to the stream (Freeman et al., 2001). Soil type (Clark et al., 2004) and land use (Wilson and Xenopoulos, 2009) may also generate spatial variation in the generation of DOM, for example, crops have been found to produce compounds with less structural complexity than those of forested areas (Wilson and Xenopoulos, 2009). But, ultimately, precipitation events constitute the decisive factor which controls to what extent this dissolved organic carbon (DOC) contained in soil will be effectively introduced to the river flow (Harrison et al., 2008).

Autochthonous or in-stream derived DOM In-stream biological processes constitute an authochthonous source of DOM. DOM can be released to the river water mainly by phytoplankton (Romera-Castillo et al., 2010) and macrophytes (Lapierre and Frenette, 2009), but also by microbial cell lysis, or spillage from damaged cells (Bertilsson and Jones, 2003). Even though this input pathway is often overlooked for rivers and streams, it can account for 40 to 80% of DOM sources across biomes (Webster and Meyer, 1997), especially when light availability is high and the surrounding catchment is poorly vegetated, as in arid areas. In general, autochthonously-derived DOM consists of simple and well known compounds such as lipids, polysaccharides, nucleic acids and aminoacids. Also, a release of humic substances of low molecular weight and low aromatic content has been observed (Romera-Castillo et al., 2010). At the same time, even if it can often represent a minor fraction of whole DOM in quantitative terms, it has been observed to be a highly labile fraction that support high rates of bacterial growth and therefore is rapidly utilized (Giorgio and Pace, 2008).

Anthropogenic DOM In catchments with a high human pressure, anthropogenic activities may significantly alter the quality and quantity of DOM flowing in a river. Such alteration can be caused, on the one hand, by the modification of land uses within the catchment and, on the other hand, by the direct spillage of sewage effluents to the river flow. Land use alteration creates a diffuse effect which alters the quality of the terrestrially-derived DOM which is drained from the soils during storm events. Numerous studies have recognised differentiated DOM qualities between agricultural and forested subcatchments (Wilson and Xenopoulos, 2009; Williams et al., 2010). Alternatively, direct inputs from waste water treatment plants (WWTPs), industries and urban sewage constitute point sources of anthropogenic DOM, whose composition can widely vary according to the kind of human activity that has originated it. However, some general traits have been observed that differ those of the DOM naturally flowing in the water, such as a higher con-

tribution of molecules resulting from bacterial activity and a higher proportion of protein-like material with respect to materials of humic nature.

1.2.2 Fate of riverine DOM

Once in the river water, the DOM coming from any of the above mentioned sources constitutes a complex bulk DOM mixture that is transported downstream and becomes successively involved in different biogeochemical processes – while still continuously receiving new inputs of DOM molecules. Here follow the main biogeochemical interactions in which DOM is involved.

Microbial DOM oxidation Heterotrophic bacteria essentially control DOM transformations, as they are the only biological compartment that can relevantly utilize it. This pathway represents the re-introduction of matter and energy to higher trophic levels and can be viewed as a recycling pathway of organic matter within the ecosystem (Azam et al., 1983). Bacteria can easily uptake the simple DOM compounds by transferring them directly through their membranes using permease enzymes; however more complex humic compounds have to be previously hydrolised by means of exoenzymatic enzimes (Montuelle and Volat, 1993). As a result of the bacterial degradation, DOM may be completely oxidised to CO_2, hence being completely removed from the river. For instance, in the Hudson River, bacteria have been found to be responsible for the removal of 20% of the DOC loads (Maranger et al., 2005). However, DOM can also be transformed into subproducts of lower molecular weight and higher recalcitrance (Amon and Benner, 1996). Because of that, microbes are not only controllers of DOM concentration in rivers, but also have the capacity to modify its composition and character, hence affecting the quality of the DOM that is finally delivered to oceans (Guillemette and del Giorgio, 2012). On the same time, controls on the opposite direction have been observed, so that bacterial communities may adapt their composition and function to the available DOM (Docherty et al., 2006; Judd et al., 2006). This highlights the tight coupling and complex interactivity that exists between the DOM pool and the characteristics of the bacterial communities.

Photochemical degradation During the riverine transit, the coloured fraction of DOM has been found to selectively decay (Weyhenmeyer et al., 2012). Due to its chemical ability to interact with light, the exposure of DOM to sunlight results in a decrease in the average molecular weight (Bertilsson and Tranvik, 2000) and direct mineralisation to CO_2 (Miller and Zepp, 1995). Kohler et al. (2002) reported losses of riverine DOC of 33-50%. Other fractions may not be totally mineralised but undergo profound qualitative changes (Moran et al., 2000), like a loss in the aro-

matic carbon functionality (Osburn et al., 2001) and a change in the proportion of humic substances (Kohler et al., 2002). While both the humic- and the protein-like fractions are prone to photochemical degradation, fulvic acids have been found to be more susceptible (Mostofa et al., 2007). Some authors argue that photochemical subproducts are more labile than the original DOM compounds, so that it would favour the biological uptake of DOM (Moran and Zepp, 1997). However, other studies have found a decrease in the biodegradability of DOM due to sunlight exposure, therefore the predictability of the effects of solar radiation to DOM availability is not yet well understood (Moran and Covert, 2003). However, photodegradation is well-recognised as a major pathway of DOM removal and transformation within rivers (Mostofa et al., 2007).

Other abiotic processes Microbial and photochemical degradataion and oxidation are the main pathways of DOM removal and transformation in rivers. However, DOM interacts in a variety of additional abiotic processes. For instance, DOM molecules may aggregate onto particulate organic matter (POM) particles (McKnight et al., 2002) and, furthermore, DOM molecules themselves may aggregate abiotically and form larger particles. Although it has not been tested in natural conditions, laboratory experiments indicate that it can be an important process which can consume up to 7 – 25% of DOM, at similar taxes as those observed for microbial uptake (Kerner et al., 2003). On the other hand, DOM also has the capacity to bind with free metal ions through complexation, thus decreasing the toxicity for aquatic organisms (Al-Reasi et al., 2011).

Overall, these examples highlight the wide range of interactions in which DOM is involved during the riverine transit. All of them occur at varying degrees of relevance according to changing physical and environmental conditions found downstream as DOM flows across the landscape (Jaffe et al., 2008).

1.3 Downstream transport and processing of DOM

1.3.1 Global evidences for an active transportation of DOM in rivers

Rivers play a key role in the global biogeochemical functioning, as they link the biogeochemical cycles of the terrestrial and oceanic systems. As mentioned, streams and rivers receive DOM from a variety of sources and, once in the river, these compounds are transported downstream and delivered to oceans. Traditionally, global models considered this step just as a transfer of matter from the land to the oceans. However, there are increasing evidences that important biogeochemical interactions

occur during the downstream transport, so that rivers act as filters (Bouwman et al., 2013) – as they retain DOM –, as well as bioreactors (Cole et al., 2007) – as the magnitude of DOM retention evidences that complex in-stream biogeochemical processes occur (Figure 1.3).

Recent models consistently estimate that rivers discharge between 0.8-0.9 PgC/y to the sea. However, there is an important variability in the estimations of the export of carbon from the land to the inland waters, ranging from 1.7 PgC/y (Ciais et al., 2013) to 2.7-2.9 PgC/y (Cole et al., 2007; Battin et al., 2009) and 5.7 PgC/y (Wehrli, 2013). This uncertainty is translated into variable estimates for carbon outgassing from freshwater systems as CO_2 to the atmosphere (ranging from 1 PgC/y in Ciais et al. (2013) to 4.2 PgC/y in Wehrli (2013)) and retention by burial into sediments (ranging from 0.2 PgC/y in Ciais et al. (2013) to 0.6 PgC/y in Wehrli (2013)). Despite such variability and uncertainty among models, all of them emphasize that an important proportion of the carbon is either retained or mineralised during the riverine transit. Indeed, such estimated carbon emissions to the atmosphere are similar in magnitude to global terrestrial net production and, also, burial in inland water sediments exceeds organic carbon sequestration in the ocean floor (Tranvik et al., 2009). If we consider that most of the exported C is in the form of DOM (Ludwig et al., 1996; Karlsson et al., 2005), then these figures emphasize the role that lotic systems have on the active transport of DOM. This points at rivers as interesting targets at which management strategies for climate change mitigation should be addressed (Battin et al., 2009).

1.3.2 Longitudinal patterns of river function and structure: From predictability to stochasticity

The global evidences that rivers act as sinks for DOM highlight the importance of understanding the biogeochemical behaviour of DOM during the fluvial transit, from the headwaters to the river mouth. Rivers, because of their unidirectional and longitudinal flow, are unique among freshwater ecosystems. The longitudinal dimension defined by the advective water transport constitutes the main axis along which functional and structural riverine changes occur (Wipfli et al., 2007), and therefore, it is the main dimension along which changes in DOM sources and processing occur.

In this line, the river continuum concept (RCC) (Vannote et al., 1980) already predicted fundamental changes in the carbon processing from the headwaters to the river mouth. This model of the fluvial functioning has been very influential as it provided a base for a holistic view of rivers by integrating a variety of concepts from the physical template, biological function and structure and metabolism. The RCC described rivers as predictive gradients of physical and hydrological conditions which

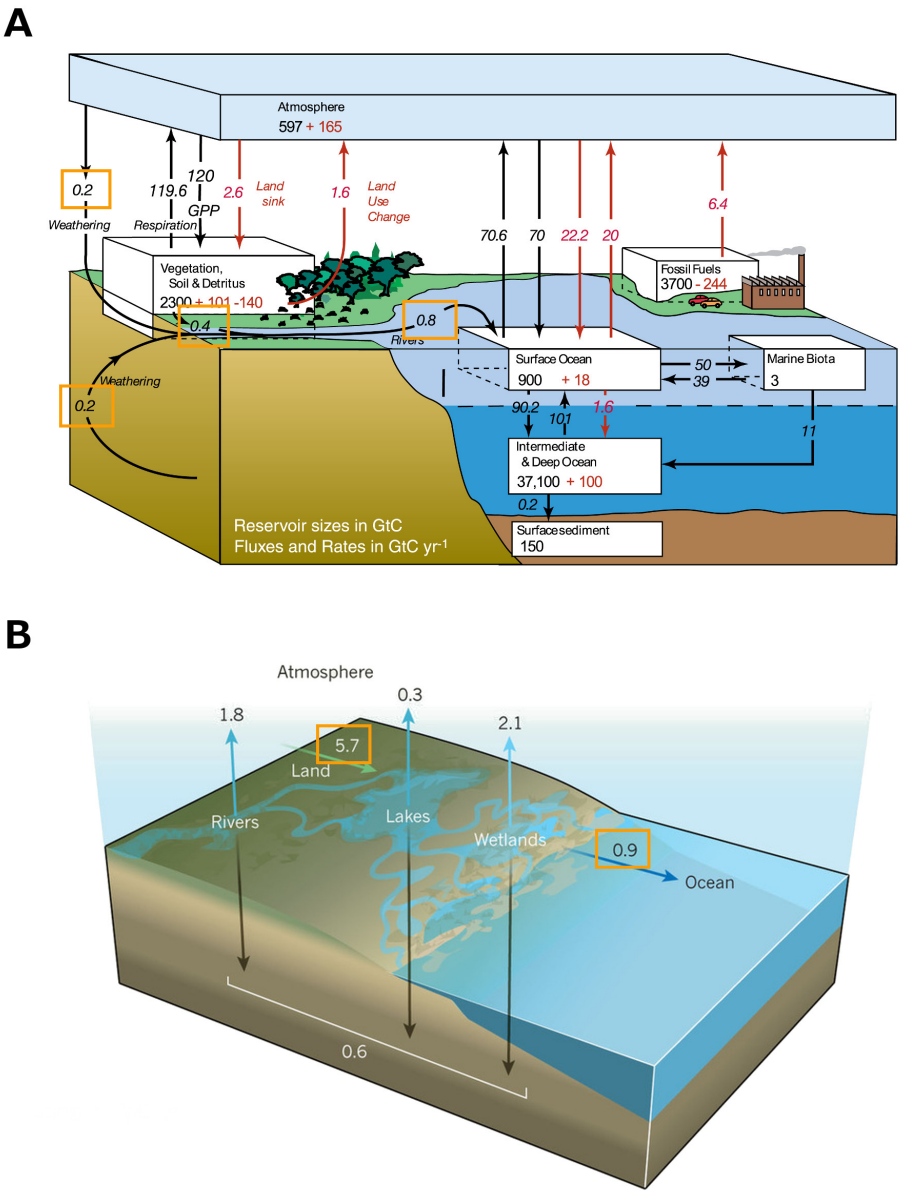

Figure 1.3 – Paradigm change in the role of rivers in the global carbon cycle. A) From Sarmiento and Gruber (2002), the amount of carbon delivered to the sea by rivers is exactly the sum of the exports from the terrestrial and atmospheric systems to the river. B) From Wehrli (2013), in-stream retention and mineralisation of carbon is taken into account.

determined a longitudinal distribution of biological communities. For carbon, it predicted a downstream decrease in the size of organic matter, as well as a decrease in the diversity of soluble organic compounds. This trend was attributed to the microbial degradation of the labile moieties, remaining a recalcitrant fraction up to the river mouth.

The RCC was soon after put into question for being over simplistic, as it ignored much of the spatial complexity that rivers actually have (Statzner and Higler, 1985; Sedell, 1989). Hence, a series of conceptual models further refined RCC by incorporating elements of stochastic spatial complexity. Namely, (Ward and Stanford, 1983) described the effects of dams and impoundments in disrupting the river continuum, and Rice et al. (2001) pointed at tributary confluences as modifiers of the river continuum. The magnitude of the disruptive effects have been associated with the relative size of the tributaries with respect to the main stem (Rice et al., 2006), and may entail consequences on the river geomorphology (Benda et al., 2004), habitat complexity and hence biodiversity (Kiffney et al., 2006), and biogeochemical rates (McClain et al., 2003; Fisher et al., 2004). Biogeochemically, tributaries may introduce water with a differentiated chemical composition with respect to the main stem. If this new water introduces complementary or missing reactants, then the convergence of both flowpaths may trigger the onset or accelerate the rate of certain biogeochemical processes (McClain et al., 2003). In this context arouse the concept of patchiness, and it was suggested that rivers, instead of continuum gradients, should be better conceptualised as a mosaic of patches (Naiman et al., 1988; Thorp et al., 2006). As the distributions of confluences are specific to every river network, these studies reflected that stochasticity plays a main role in determining longitudinal patterns of the riverine function and structure.

Despite the large number of conceptual studies that directly or indirectly predict longitudinal changes for DOM, the empirical assessment of DOM downstream transformations are seldom. Some studies found an increase in the DOC concentration downstream (Naiman et al., 1987; Massicotte and Frenette, 2011), whereas some others found a decrease (Temnerud et al., 2007) or a steady evolution (Battin, 1998). The inflow of deep groundwater was found to cause a decrease in DOC concentrations (Nakagawa et al., 2008; Brooks et al., 2007) whereas inputs from the catchment flushing (Nakagawa et al., 2008) and evaporation (Jacobson et al., 2000) caused an increase. Also, in some studies an increase in the variability of DOC concentration was observed in the final part of the river (Battin, 1998; Baker and Spencer, 2004). Despite these quantitative changes, variations in the DOM quality were also apparent. Baker and Spencer (2004) found slight decreases in the fluorescence intensity of humic-like components together with important increases in the protein-like fluorophores, which they associated with anthropogenic inputs. Overall these studies emphasize that the local characteristics and the configuration of

Author	River	Solute	Spatial domain *	Temporal domain	Retention †
Eatherall et al. (2000)	River Swale, UK	DOC	50 km	Daily scale	- 20% (3, 25 and 16%)
Duan et al. (2010)	Middle and lower Mississipi	DON	1200 km	Year scale	- 12%
Dagg et al. (2005)	Lower Mississipi	DOC	362 km	Monthly scale	- 3%
Worrall et al. (2006)	Peat catchment	DOC	11.4 km^2	Year scale	- 20-32%
Worrall et al. (2007)	Various UK river networks	DOC	87 - 9948 km^2	Year scale	- 31%
Rowson et al. (2010)	Peat catchment	DOC	7500 and 2400 m^2	Year scale	+ 29 – 85 $Mg/km^2 \cdot yr$
Moody et al. (2013)	River Tees, UK	DOC	818km^2	Year scale	- 48% - 69%

Table 1.1 – Bibliographic references reporting DOC losses or production during the riverine transit, calculated using a mass-balance approach. * km refer to reach-scale and km^2 to catchment-scale studies. † Negative values indicate losses, positive values indicate production.

the river network are important determinants of the longitudinal patterns of DOM quality and quantity. However, these studies do not elucidate to what extent the observed changes are due only to the physical mixing with inflowing waters with a different DOM composition, or whether in-stream processing is operating.

The studies that focused on verifying the occurrence of DOM reactivity during its downstream transport, have mostly eliminated the longitudinal view and applied a mass-balance approach at the catchment or reach level (Table 1.1). By comparing the DOC loads introduced by the main tributaries, with those at the outlet of the catchment, the retention of DOC can be deduced. It is common to find retentions of 20-30% with respect to the inputs, even though there is an important variability among systems (Table 1.1). These studies emphasize that the estimations at the global scale that rivers are sinks of DOC is also observable at the catchment level. However, while this mass-balance approach is very common to study the retention of inorganic nutrients (Grayson et al., 1997; Salvia et al., 1999; Bukaveckas et al., 2005; Hill et al., 2010), it has been scarcely used to evaluate DOM retentivity in catchments. Moreover, most of these few experiences addressed only quantitative terms. Qualitatively, Temnerud et al. (2009) found no relevant downstream changes in DOM optical characteristics, but (Worrall et al., 2006) found a consistent increase in the specific absorbance of DOM, although they point at an eminently conservative balanced behaviour of DOM between the sources and sinks.

Hence, in the literature there are few studies that assess the reactivity of DOM along a riverine continuum, but their results show that the net balance of DOM in individual catchments, and the relevance of the role of rivers as DOM sinks remains unclear.

1.3.3 The role of hydrology in DOM transport and reactivity

In the previous section, most of the cited works that addressed longitudinal DOM patterns and reactivity were performed during baseflow conditions, often because moderate and stable flows were considered to be the most representative (for instance, Temnerud et al. (2009)). However, most river systems are subject to seasonal changes in their discharge, due to annual patterns of rainfall, snowmelt, temperature, and other hydroclimatic variables. In some regions, like in the Mediterranean, flow variability includes extreme events of floods and droughts within every annual hydrological cycle. All the range of hydrological conditions to which a river is subject, is necessary to fully understand its functioning (Poff et al., 1997) and biogeochemistry (Fisher et al., 2004). Some theoretical studies acknowledged the importance of floods and droughts as sporadic perturbations that have a determinant repercussion on the long-term productivity and sustainability of river systems (Naiman et al., 2008) and their ecological integrity (Poff et al., 1997).

On biogeochemical terms, floods represent a rapid flush of the terrestrial catchment, exporting large amounts of DOM from the land to the river flow. Dalzell et al. (2005) reported DOC exports during flood of 90 times that of baseflow conditions. The flush response of DOM to storms is well known to produce an hysteretic relationship with discharge, so that DOM is more concentrated in the rising than in the descending limb (Butturini et al., 2006). Despite these quantitative changes, storms also cause a change to the quality of riverine DOM. Rainfall water reactivate the drainage of more superficial flowpaths thereby introducing freshly produced DOM compounds that were stored in the soils (Austnes et al., 2010) to the river flow. These diagenetically-young compounds, have been reported to have an increased availability to stream bacteria (Fellman et al., 2009a; Wilson et al., 2013). Also, floods generate lateral exchanges with the floodplains (Junk et al., 1989) and enhance the longitudinal continuum within the river system by a rapid downstream transport of water and materials.

By contrast, droughts favour the isolation of the river from the terrestrial catchment, so that in-stream processes become more relevant. The decrease in the allochthonous inputs of organic carbon and nutrients favours autotrophs, which outcompete heterotrophs (Dahm et al., 2003). Also, the longitudinal flow becomes disrupted, thus creating isolated reaches or ponds with an independent hydrochemical evolution (Vazquez et al., 2011). Lower flows and longer residence times may provide more opportunities for the biophysical retention of DOM (Battin et al., 2008) by enhancing the contact between the water column and the river sediments. Because of that, droughts represent an important perturbation that further enhance spatial patchiness (Lake, 2000; Larned et al., 2010).

Overall, the importance of the hydrological variability on the river functioning and biogeochemistry has been widely acknowledged (Lohse et al., 2009); however, to what extent they specifically effect DOM downstream transport and reactivity remains unclear due to a lack of empirical studies that have addressed this issue. Moreover, these theoretical studies concerning DOM and hydrology did not consider the longitudinal dimension. Hence, there is a lack of a concomittant perspective of the DOM riverine transport and reactivity in fluvial systems.

Chapter 2

General objectives

The aims of this doctoral thesis focus on the current challenge to better couple hydrological and biogeochemical research (Lohse et al., 2009). Specifically, this thesis aims at elucidating the influence of hydrology on the longitudinal transport and processing of dissolved organic matter (DOM).

For that, research has been conducted at three successive levels, each of which builds upon the previous ones:

Part I First of all, this thesis is devoted to develop a new methodology to discern individual fluorescence components out of large Excitation-Emission Matrix (EEM) data sets that contain an important heterogeneity of spectral shapes. Specifically, this is achieved using self-organizing map (SOM) together with a correlation analysis of the component planes. The procedure is exposed in chapter 4, entitled ***"Self-Organising Maps and correlation analysis for the analysis of large and heterogeneous EEM data sets."***, and its aims are:

- To test the suitability of Self-Organising Maps together with correlation analysis of the component planes to analyse large and heterogeneous EEM data sets, both at the object and at the variable level.
- To test the sensitivity of this method to the presence of outliers.
- To decompose the bulk fluorescence signals of our EEM data set into individual fluorescence components that can be used in the rest of the thesis to study the dynamics of DOM components.

Part II Next, the focus is moved to the biogeochemistry of DOM in a Mediterranean river – La Tordera –, by characterizing longitudinal patterns of DOM

quantity and quality under a range of hydrological conditions. This is performed in two steps, corresponding to chapters 5 and 6, and the specific objectives of each of them are:

For chapter 5, entitled ***"Preliminary assessment of longitudinal patterns in the main stem of La Tordera: Hydrochemistry and DOM quality"***:

- To provide a general biogeochemical description of the river.
- To assess longitudinal gradients of DOM quality and composition along a riverine course.
- To test how contrasting hydrological conditions alter or influence the longitudinal gradient.
- To provide a further understanding about how space and hydrology operate as inter-dependant dimensions of DOM quality.

In chapter 6, entitled ***"Multivariate exploration of DOM quality and reactivity in the main stem of La Tordera"***, more specific evidences for non-conservative transport of DOM are searched. Specifically, the aims include:

- To explore spatio-temporal variation in the DOM composition, and the relationships between the fluorescence components and other optical and chemical variables.
- To evaluate to what extent the DOM composition observed in the main stem can be explained as solely the physical mixing of input tributaries or, by contrast, whether in-stream processing may be operating.

Part III Finally, we use mass-balance calculations along the middle reaches of La Tordera (26 km long), and under a range of hydrological conditions, in order to quantify changes in DOM quantity and quality. Mass-balance calculations are used under two approaches: global, considering the whole middle part of the main stem as a single black box, and local, with the aim to recuperate the longitudinal view and characterize DOM processing along the river reach. This is developed across chapters 7, 8 and 9.

Chapter 7, entitled ***"Water balance in the middle reaches of La Tordera"*** has the aim to validate the hydrological data used to calculate the mass balances of the following chapters by specifically assessing whether

- the observed discharge in the main stem corresponds to the inputs from the upstream tributaries or if, on the contrary,

- exchanges with the alluvial aquifer are involved.

Chapter 8, entitled ***"Carbon and nitrogen mass balance: Linking DOC and nitrate"*** explores the coupling between DOM quantity (i.e. DOC and DON concentrations) and inorganic dissolved nitrogen. The specific aims are:

- To compare the reactivity of bulk DOM (DOC and DON) and dissolved inorganic nitrogen (nitrate and ammonium) along the middle reaches of La Tordera, and under a range of hydrological conditions.
- To test if the stoichiometric control between DOC and nitrate observed throughout Earth's major freshwater ecosystems (Taylor and Townsend, 2010) also applies in Mediterranean systems, including extreme hydrological events.
- To complement the evidences for any stoichiometric control between DOC and nitrate with the DOC reactivity data provided by the mass balance calculations.

Finally, chapter 9, entitled ***"Downstream processing of DOM: changes in its reactivity and composition"*** explores the transport and reactivity of individual DOM fluorescence components.

- To explore spatial patterns of the reactivity of fluorescence DOM components under contrasting hydrological conditions.
- To compare the productions/retentions observed for the individual fluorescence components with those of bulk DOC and DON reported in the previous chapter.

Chapter 3

Materials and Methods

3.1 Study site

3.1.1 The catchment of La Tordera

The catchment of La Tordera lies in the nort-eastern part of the Iberian Peninsula, in the central part of the catalan coast. It drains an area of 870 km^2 in the Prelitoral mountain range, covering the south-eastern slopes of the Montseny and Guilleries mountains, the northern slopes of the Montnegre, as well as part of the catalan Prelitoral depression. Its topography includes an important elevation gradient and aspect range. This has caused the development of a large diversity of landscapes which include the totality of the plant communities of western Europe (Bolós, 1983). In general, forest land cover dominates in the catchment (77%), especially in the upper parts. However, agriculture (16%) and urban areas and industry (7%) also have an important presence, especially in the lowland (Figure 3.1).

Because of the pluvial origin of the river, it is not possible to assign a specific source point, however the popular knowledge locates the beginning of La Tordera in the Font Bona source (broadly at 1600 m.a.s.l), in the creek of Sant Marçal, near the peaks of Les Agudes and Turó de l'Home. From its source, La Tordera flows along 60 km downstream before discharging to the Mediterranean Sea. Along its course, the river outlines sharp orographic and tectonic features, resulting in a 4-like trace characterised by two big bends. Such bends divide the river into three main reaches of similar length (approximately 20 km each), with distinct hydrogeomorphological and land cover characteristics.

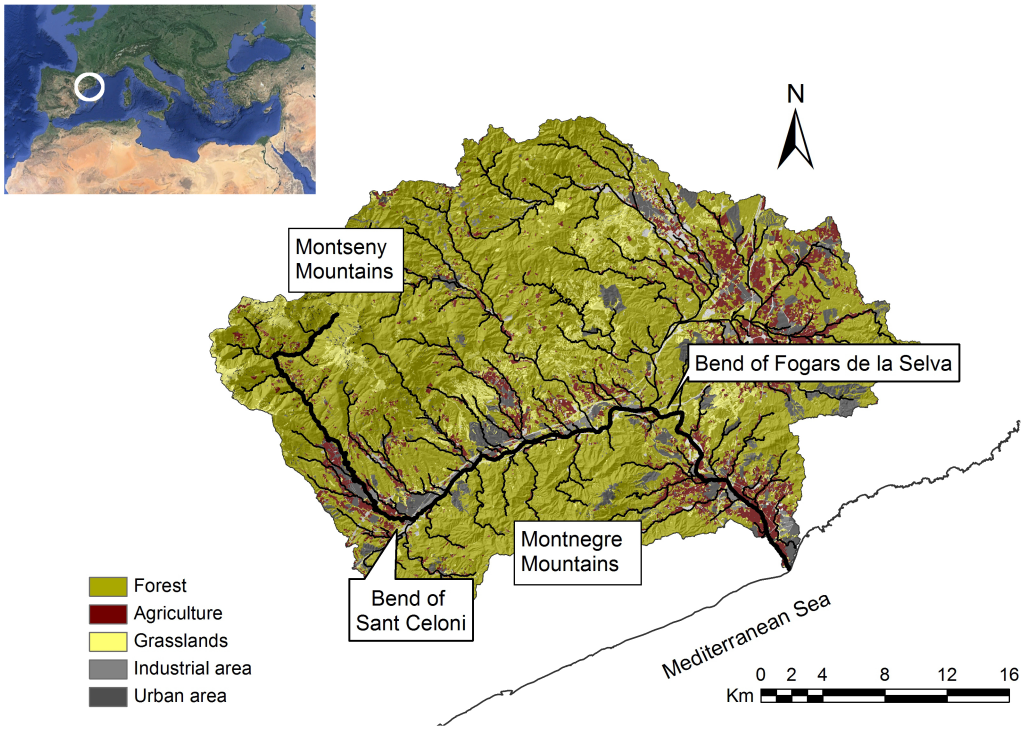

Figure 3.1 – Location of the catchment of La Tordera in the Mediterranean context, and main features of the catchment. Land covers are represented from data provided by the Center for Ecological Research and Forestry Applications (CREAF)).

The upper Tordera

In the first part, the river drains the headwaters through forested mountainsides, descending steeply from 1600 down to 150 m.a.s.l. in the town of Sant Celoni. The predominant vegetation is made up of beech forest (*Fraxinus excelsior*), while the shores of the river have a riparian area of good maturity (Boada, 2008). The geological substrate is made of igneous and metamorphic materials from the Palaeozoic, intensely modified during the hercinic orogenesis (Mayo et al., 2008).

The middle reaches

From Sant Celoni until the bend of Fogars de la Selva, the river receives the most relevant tributaries of the whole catchment in terms of drainage area and discharge contribution. From the north, it receives the waters of the streams draining the Montseny Massif. The most important ones are the creeks of Santa Coloma and

Arbúcies, followed by the creeks of Breda, Gualba and Pertegàs. Some of these tributaries bring the waters of waste water treatment plants (WWTPs) or industries received upstream. Most remarkably, the creeks of Pertegàs and Arbúcies receive a WWTP outlet just some few meters before discharging to the main stem. From the south, the river receives the streams draining the Montnegre Mountains. In this case, waters are nearly pristine, as human activities and settlements are minor in these slopes.

Contrastingly to the upper parts of the river, in the middle reaches the anthropogenic impacts are frequent and intense. This region hosts most of the economic activity of the nearby territory. Hence, here aggregate industrial zones, urban settlements and transportation routes; namely a highway, a secondary road, a railway, as well as an oil and desalination pipeline. This has resulted in a deep modification and alteration of the riparian areas. Also, the direct discharge of industrial and WWTPs effluents affects the hydrochemical characteristics of the river water (Mas-Pla and Menció, 2008).

From a hydrogeological perspective, in the transition from the upper to the middle Tordera, starts the formation of sandy deposits which appear along the main stem until its final discharge to the sea. These deposits are recent non-consolidated quaternary materials related with the sedimentary fluvial dynamics. Their depth increases gradually downstream, from 15 m in Sant Celoni, up to 30 m in Fogars de la Selva, 40 m in the city of Tordera, and finally achieving 75 m in the coastline (Mayo et al., 2008).

The high porosity and permeability of the deposits make them an important reservoir of groundwater that has a direct connection and coupled dynamics with the river course.

The lowland

Finally, the last 20 km run between the bend of Fogars de la Selva and the Mediterranean sea, where the river finally discharges. This final part is characterised by a long alluvial plain, where the river adopts a curved and meandering trace, and has a high connection between the surface and subsurface water. The contiguous plains are fertile due to the flooding dynamics of the river, and have facilitated the development of an intensive agricultural activity (Boada, 2008). In this area, where the orography is eminently plain, the river receives few tributaries. The most important one is the creek of Reixac, which receives the waters of a WWTP few meters before the confluence with La Tordera.

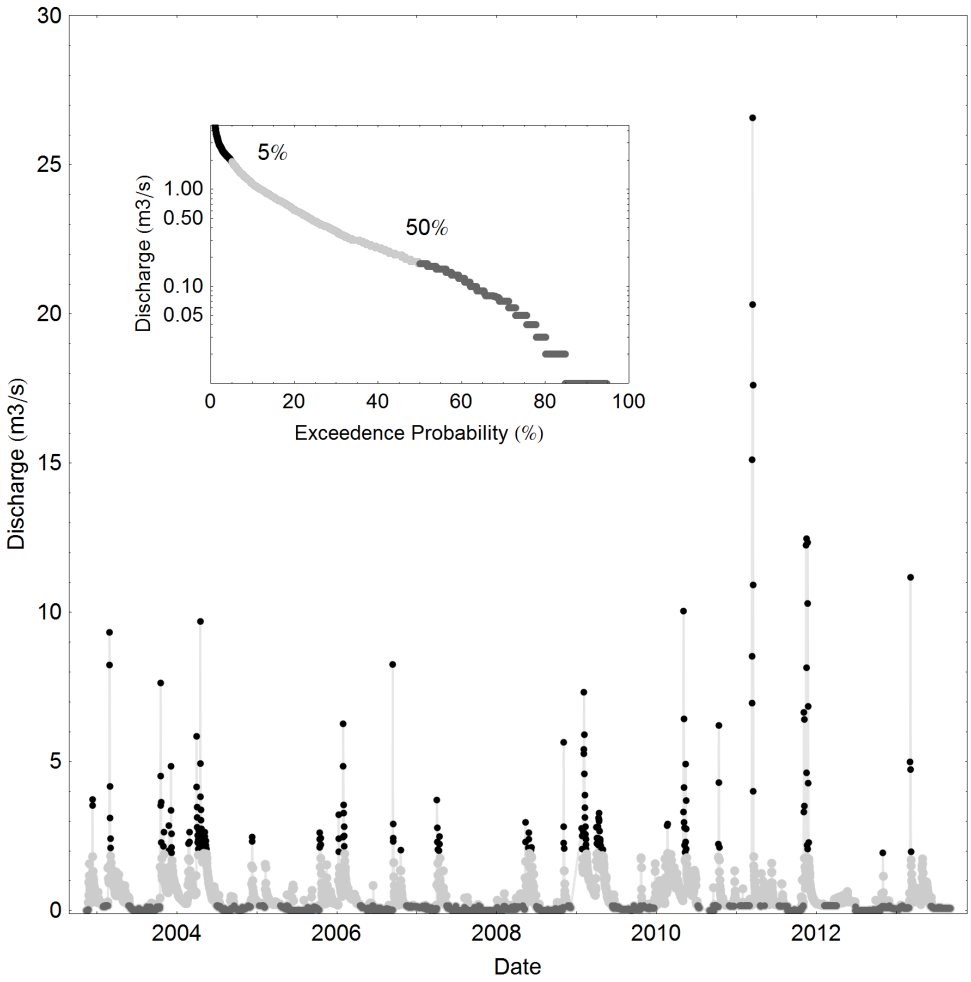

Figure 3.2 – Discharge probability distribution, based on a ten-year data series in the gauging station of Sant Celoni. Black dots indicate discharge values with and exceedence probability of 5% or less; light grey dots, between 5 and 50%; and dark grey dots, between 100 and 50%. Own elaboration from data provided by the Catalan Water Authority (Agència Catalana de l'Aigua).

3.1.2 Hydrology

Spatial variability of surface hydrology

During its course, the river of La Tordera encounters a variety of geological features. Especially, as it has been described in the previous section, from the village of Santa Maria de Palautordera until the final mouth the river flows through an

alluvial aquifer with high permeability and transmissivity which create a close relationship between the surface and the subsurface flow. Monthly water balances have revealed that the river-aquifer relationship changes over time due to changes in the precipitation regime during the year. During the first semester of the year the aquifer tends to recharge the surface flow, whereas in the second semester, the surface flow recharges the alluvial aquifer, due to low levels of water storage in the underground after the summer drought (Negre, 2004).

Moreover, at a fine spatial scale the flow is also controled by tectonic elements. Regional faults are frequent along the main stem (Insitut Cartogràfic de Catalunya, 2002), and control the drainage pattern (Mayo et al., 2008). In the middle reaches, the river flow eminently follows the trace of a major fault oriented NE-SW. Along this main fault, a series of minor faults intersect perpendicularly and may modify locally the river-aquifer flow behaviour (Mas-Pla et al., 2013).

However, the main source of spatial variability in the water flow is the successive confluence with tributaries of varying discharge contribution. Especially in the middle reaches, the river receives the waters of numerous tributaries, and the main water contributions occur after the confluences with the creeks of Arbúcies and Santa Coloma, as they are the tributaries draining the largest sub-catchments.

Temporal variability of surface hydrology

The hydrological regime of La Tordera is influenced by a Mediterranean climate, which consists in rainy and humid autumns and springs on the one hand, and dry and warm summers on the other hand. According to that, discharge exhibits extreme and contrasted events over an annual cycle, consisting on flood events in autumn and spring, and drought periods in summer.

Floods are usually short in time (in the order of hours to some few days), but intense in magnitude. In the gauging station of Sant Celoni, extreme discharge values up to 175, 203 and 267 m^3/s have been calculated to occur in return periods of 50, 100 and 267 years, respectively (Mayo et al., 2008). In a smaller time scale, including the last ten years (2003 to 2013) the hydrogram (Figure 3.2) shows the occasional occurence of stormflows peaking around 10 m^3/s, and even reaching 27 m^3/s in an event in 2011. However, such high flows are instantaneous responses to storms which are rapidly flushed out of the system, and discharges higher than 2.03 m^3/s only occurred 5% of the days during the last decade (Figure 3.2, inset).

Contrastingly, drought periods are prolonged in time. They naturally occur in summer, between the months of july and september, and their length and severity basically depend on the abundance of rains during the previous spring, as well as the temperatures during summer. However, water withdrawal from the alluvial aquifer

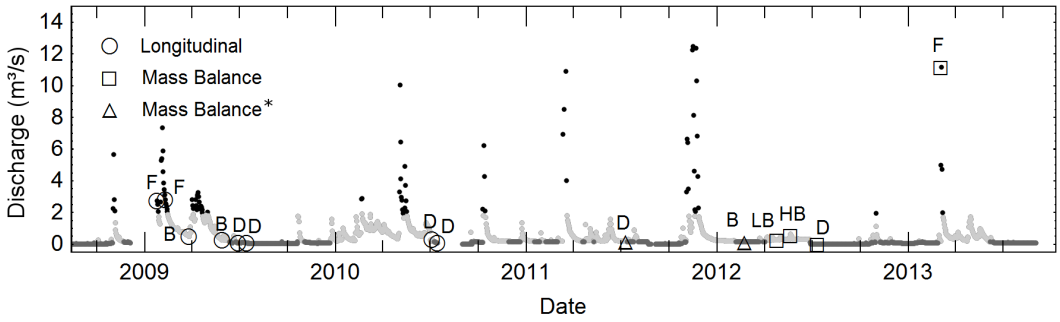

Figure 3.3 – **Hydrological contextualisation of sampling dates**, for both the longitudinal and the mass balance sampling designs. * Samplings based on the mass balance design, but where the tributaries have not been exhaustively sampled; data used to complete the data sets of chapters 4 and 6. F stands for "flood", B for "baseflow", HB for "high baseflow", LB for "low baseflow" and D for "drought". Black dots indicate discharge values with and exceedence probability of 5% or less; light grey dots, between 5 and 50%; and dark grey dots, between 100 and 50%, as shown in Figure3.2. Data provided by the Catalan Water Authority (Agència Catalana de l'Aigua).

to satisfy industrial and urban demand often accentuates the reduction of the surface flow. This was specifically observed for the years 2003-2005 (Mas-Pla and Menció, 2008), manifested by a convex shape of the recession curve of the hydrograph (Sala, 2005). In the last decade, during 50% of the the days, the gauging station of Sant Celoni registered flows of less than 0.18 m^3/s, (Figure 3.2) flows which correspond, approximately, to the minimum environmental flows threshold established by the Catalan Government (which is of 0.204 m^3/s in the summer months [1]). Moreover, these minimal flows depend, to a large extent, on the inputs from WWTPs and other anthropogenic effluents (Mas-Pla and Menció, 2008). Overall, this emphasizes the extended occurrence during the year of an hydraulic deficit in the river system.

3.2 Sampling strategy

With the aim of describing biogeochemical trends and processes during downstream riverine transport, the sampling design was focused at the main stem. Specifically, two sampling strategies were performed, hereafter referred to as *longitudinal* and *mass balance*.

[1] Pla sectorial de cabals de manteniment de les conques internes de Catalunya. Resolució MAH/2465/2006, de 13 de juliol, per la qual es fa públic l'Acord del Govern de 4 de juliol de 2006, pel qual s'aprova el Pla sectorial de cabals de manteniment de les conques internes de Catalunya. DOGC Num 4685, 27-7-2006, pàg 33808-33821.

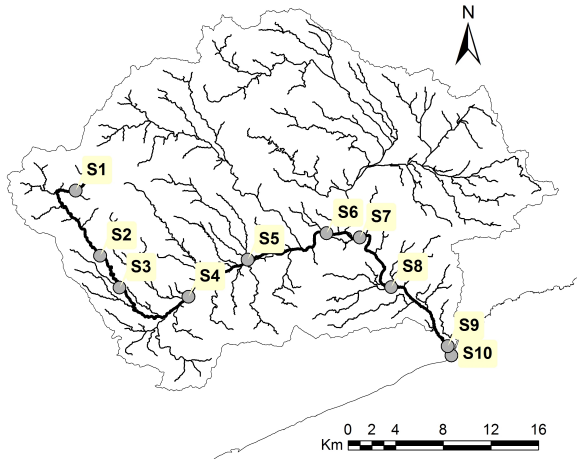

Figure 3.4 – Longitudinal sampling design. Ten sites were sampled along the main stem, from the river's source, to its mouth.

3.2.1 Longitudinal sampling

This sampling designed was aimed at providing a preliminary assessment of biogeochemical longitudinal patterns. According to that, the main stem of La Tordera was sampled in ten sites distributed from the headwaters to the river mouth (Figure 3.4), designated as sites S1 to S10. The first three sampling sites (S1-S3) were located between La Llavina and Santa Maria de Palautordera, that is, in the mountainous and forested headwaters. Next, sites S4 to S6 corresponded to the middle reaches of the river, spanning between the bends of Sant Celoni and Fogars de la Selva. Finally, sites S7 to S10 were in the lowland, were S10 corresponded to the very final river mouth.

Samplings were conducted eight times, representing three different hydrological conditions: flood, baseflow, and drought (Figure 3.3). The droughts of 2009 and 2010 differed in that the former had moderate rainfall antecedents whereas the latter had flood antecedents. Every hydrological condition was sampled twice and results were averaged. It should be noted here that site S9 was dry during drought dates. In total, 76 samples were collected, averaged to 38.

The results of these samplings constitute the base for the study presented in chapter 5. These data are also included in the data sets used in chapters 4 and 6.

3.2.2 Mass-balance sampling

This sampling design was aimed at complementing the information provided by the longitudinal sampling strategy, so that the information from the main stem could be contrasted with information about the tributaries that originate the flow of the main stem. The results from these samplings constitute the core of the mass balance study presented in chapters 7, 8 and 9.

In this sampling design, we applied a snapshot mass-balance to the middle part of the main stem, from the village of Santa Maria de Palautordera to Fogars de la Selva, comprising a total length of 26 km (Figure 3.5). This large reach was chosen because it is the part of the main stem which receives most of the tributaries of the catchment, as well as a variety of water inputs, from pristine tributaries to direct industrial effluents. In addition there is no surface water extraction in this reach and the water flow is not altered by relevant morphological barriers (i.e. dams).

The snapshot mass-balance design Grayson et al. (1997) provides an instantaneous picture of the water and mass fluxes entering and flowing out from a selected river reach or catchment area. For that, it is necessary to sample every confluence during a time period as short as possible. Hence, in this work special attention was devoted to sample all exisiting confluences along this 26-km reach as exhaustively as possible (Figure 3.5). Eight major tributaries were directly sampled. These include the creeks of Vallgorguina, Pertegàs, Gualba, Fuirosos, Breda, Arbúcies and Santa Coloma (sites A2, A3, A5, A6, A7 and A10 in Figure 3.5, their characteristics are listed in Table 3.1), as well as the main stem itself at the beginning of the reach after draining the headwaters (A0, Figure 3.5). Overall they represented a direct measure of the 85% of the catchment drainage area (Figure 3.5, dark region). The inputs from the rest of the catchment, which remained ungauged (Figure 3.5, light-coloured region), were estimated by the average specific discharge of the collindant gauged subcatchments (see Section 3.4.2 for further details). Also, 3 anthropogenic effluents discharging directly to the main stem were sampled. They corresponded to a WWTP (WWTP of Santa Maria de Palautordera, site A1, Figure 3.5) and two industries which discharged directly to the main stem (sites A4 and A9, Figure 3.5, lying in the industrial areas of Sant Celoni and Maçanet de la Selva).

As to the main stem, it was sampled before every tributary junction, as well as in some additional sites where the tributary confluences were sparser. In total, main stem sampling sites divided the whole river reach into 13 consecutive segments. The average length of each segment was 1.98 km, while the longest and the shortest were, respectively, 3.22 and 0.66 km long. The last sampling site, located in Fogars de la Selva, represented the final outlet of the mass-balance system. Besides the middle reaches, the headwaters and the lowland were also sampled, in the same sites as in

the longitudinal sampling, to provide some continuity to the data series (sites S1 to S3, and S8 to S10, Figure 3.4).

This sampling was performed on four occasions between 2011 and 2013, comprising a range of hydrological conditions: flood (156 m^3/s), baseflow (3.43 and 1.49 m^3/s) and drought (0.065 m^3/s) (discharge values corresponding to Fogars de la Selva). Overall, these samplings spanned four orders of magnitude of river flow, allowing to characterise a wide range of hydrological conditions (Hydrological characterisation in Figure 3.3).

3.3 Chemical analyses

Sample preprocessing

For the chemical and spectroscopic measurements, water was filtered with precombusted GF/F filters and next with nylon 0.22μm-pore membranes. For total organic carbon (TOC), an aliquot of 30mL was acidified 3% v/v with HCl 2M and stored refrigerated. Besides, aliquots of 10mL were kept frozen for subsequent nutrient and ion analysis. For spectroscopic measurements, 30mL aliquots were kept refrigerated in acid rinsed glass bottles and were analysed within a maximum of 5 days.

Chemical analyses

Total organic carbon (TOC) was determined by oxidative combustion and infrared analysis with a Shimadzu TOC Analyser VCSH. A coupled unit determined the total nitrogen (TN) by oxidative combustion and chemoluminescence. Ammonium concentration was measured using the salicylate method of Reardon (1969), and

Sub-catchment	Drainage area (km^2)	Average slope (degrees)	Land use (%) Forest	Agriculture	Grassland	Urban	Other
Headwaters	87.92	21.51	72.70	7.78	11.62	5.68	2.23
Vallgorguina	36.67	14.9	73.50	8.26	4.29	10.23	3.73
Pertegàs	25.35	17.96	72.21	8.87	10.07	6.06	2.79
Gualba	26.08	19.69	80.53	4.59	9.19	3.71	1.98
Breda	32.37	16.68	63.71	8.99	14.69	10.78	1.84
Arbúcies	112.07	20.52	84.46	3.78	6.21	2.95	2.59
Fuirosos	19.26	21.75	95.80	1.79	1.53	0.37	0.51
Santa Coloma	321.73	12.82	67.18	11.75	9.42	8.19	3.47

Table 3.1 – Characteristics of the tributary basins, sampled in the mass balance study.

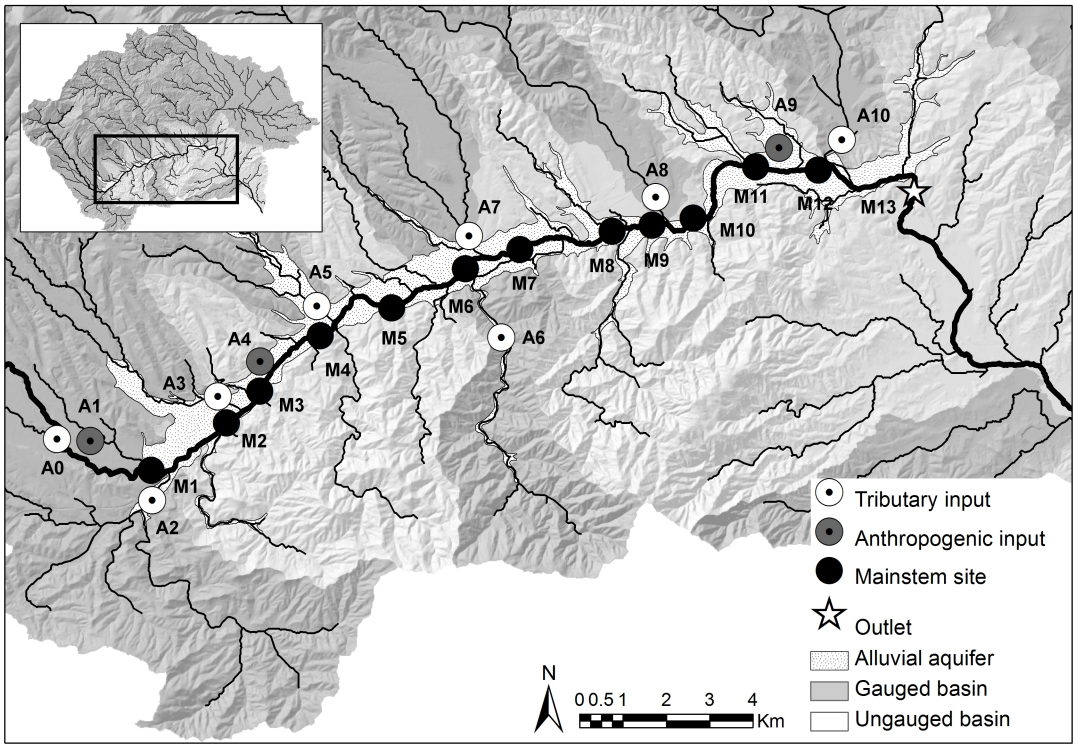

Figure 3.5 – Snapshot mass balance sampling design, performed along a 26-km river reach, spanning from Santa Maria de Palautordera to Fogars de la Selva. All relevant water inputs along were sampled before discharging to the main stem, representing 85% of the total drainage area. Also, the main stem was sampled before every confluence, as well as between confluences when tributaries were sparser.

the soluble reactive phosphor (SRF) was measured using the method of the molibdate of Murphy and Riley (1962); both methods as described in Butturini et al. (2009). Nitrates, chloride and sulphate concentrations were analysed with an ion chromatograph Metrohm 761 Compact IC with the column Metrosep A Supp5 - 150/4.0. Next, dissolved organic nitrogen (DON) was estimated by the difference between TN and the sum of nitrates and ammonia. Nitrites were not considered as they appeared under the detection limit of the ion chromatograph analyses.

Excitation-Emission Matrix analysis

Prior to analysis, samples were left in the dark to attain room temperature. Next, fluorescence analyses were performed using a Shimadzu RF-5301 PC spectrofluo-

rometer equipped with a xenon lamp and a light-source compensation system (S/R mode). For every EEM, 21 synchronous scans were collected at 1nm increments both in emission and in excitation. During each scan, excitation was measured over a wavelength range of 230 nm $< \lambda_{ex} <$ 410. Initial emission wavelengths ranged from 310 nm to 530 nm, at intervals of 10 nm. The bandwidth used for both excitation and emission was 5 nm. Spectra were acquired with a 1-cm quartz cell.

Absorption spectra used for inner filter correction purposes were measured using a UV-Visible spectrophotometer UV1700 Pharma Spec (Shimadzu). Data were collected in double beam mode with wavelength scanned from 200 to 800 nm and deionised water as the blank. The slit width was set to 1nm.

Raw EEM data were corrected and normalised to allow for inter study comparison following the steps described by Goletz et al. (2011). Spectral corrections were applied to both emission and excitation measurements to correct for wavelength-dependent inefficiencies of the detection system. An excitation correction function was determined using Rhodamine B as a quantum counter (Lakowicz, 2006), whereas for emission a correction file was obtained by comparing the reference spectra of quinine sulphate and tryptophan provided by the National Institute of Standards and Technology (NIST) according to the procedure described in Gardecki and Maroncelli (1998). Next, data were normalised by the area under the Raman peak of a deionised water sample at λ_{ex} = 350 nm and λ_{em} = 371 – 428 nm (Lawaetz and Stedmon, 2009). Inner filter effects were corrected by comparing absorbance measurements according to Lakowicz (2006), as described by Larsson et al. (2007). Finally, a blank EEM of deionised water, measured on the same day of analysis and having undergone the same correction and normalisation procedures, was subtracted from every EEM sample.

Optical indices calculation

Specific Ultra-Violet Absorbance (SUVA) was calculated according to Weishaar et al. (2003), as a measurement of bulk DOM aromaticity:

$$SUVA_{254} = \frac{Abs_{254} \times \ln(10)}{l} \times \frac{1}{[DOC]} \tag{3.1}$$

where Abs_{254} is the absorbance at 254 nm, l corresponds to the cuvette path length in m, and $[DOC]$ is the DOC concentration in $mg\ L^{-1}$.

The Humification Index (HIX) was calculated as the ratio between the area under $\{\lambda ex_{254}, \lambda em_{435-480}\}$ ("H" range) and the area under $\{\lambda ex_{254}, \lambda em_{330-345}\}$ ("L" range), as described by Zsolnay et al. (1999). The Biological Index (BIX) index was calculated by dividing the fluorescence intensity at $\{\lambda ex_{310}, \lambda em_{380}\}$ to

that at $\{\lambda ex_{310}, \lambda em_{430}\}$ (Huguet et al., 2009). Finally Fluorescence Index (FI) (McKnight et al., 2001; Cory et al., 2010) was calculated as the fluorescence intensity at $\{\lambda ex_{370}, \lambda em_{470}\}$ nm divided by that at $\{\lambda ex_{370}, \lambda em_{520}\}$ nm.

3.4 Mass-balance calculations

3.4.1 Discharge measurements

At every sampling site, discharge was determined with the velocity-area method. It consists on the summation of the product between the mean velocity ($\overline{u}_i$) and cross-sectional area (A) of a series of sub-segments along a river transect (Di Baldassarre and Montanari, 2009):

$$Q_{obs} = \sum_{i=1}^{n} \overline{u}_i \times A_i \tag{3.2}$$

The mean velocity for every subsegment was measured with a flow meter Global Water FP111, by sampling the point velocity at one half of the total depth, in the middle of the segment width.

In flooding conditions, when the river flows were too high to take in-stream measurements with the flowmeter, river discharge was estimated using the Manning's equation (Manning, 1891):

$$Q_{obs} = \left(\frac{1.49}{n}\right) \times A \times Rh^{2/3} \times S^{1/2} \tag{3.3}$$

which estimates river discharge based on the cross-sectional area (A), hydraulic radius (Rh), river bed slope (S) and the Manning's roughness coefficient (n). n was set to values between 0.05 and 0.06 following the reference tables in Chow (1959).

3.4.2 Estimation of discharge and mass fluxes from ungauged tributary basins

In order to account for those small basins which remained ungauged in our sampling design, their discharge was estimated by the Drainage-Area Ratio (Emerson et al., 2005). This method assumes that the stream flow of ungauged basins can be estimated by using the specific discharge of a nearby gauged basin as a conversion factor from basin area to discharge. Therefore, discharge in an ungauged basin (Q_{ug}) can be calculated as:

$$Q_{ug} = A_{ug} \times Q'_g = A_{ug} \times \frac{Q_g}{A_g} \tag{3.4}$$

Where A_{ug} is the drainage area of the ungauged basin and Q'_g is the specific discharge of a reference gauged basin. Q'_g is the ratio between the discharge and the drainage area and is expressed as $m^3 s^{-1} km^{-2}$. In our calculations, for every ungauged basin we used as reference the average specific discharge of the two adjoining gauged basins.

Similarly, the mass flux from ungauged basins m_{ug} was estimated as:

$$m_{ug} = A_{ug} \times m'_g = A_{ug} \times \frac{m_g}{A_g} = A_{ug} \times \frac{C_g \times Q_g}{A_g} \tag{3.5}$$

where m'_g is the specific mass flux of a reference gauged basin, that is, the ratio between the mass flux and the drainage area, expressed as $mgs^{-1}km^{-2}$. Again, in our calculations, for every ungauged basin we used as reference the average specific mass flux of the two adjoining gauged basins. For convenience, m_{ug} can also be expressed in terms of concentration as follows:

$$C_{ug} = \frac{m_{ug}}{Q_{ug}} \tag{3.6}$$

where Q_{ug} is the discharge of that given ungauged basin, as estimated in Eq. 3.4.

3.4.3 Mass balance calculations

Prior to mass-balance calculations, all the gauged and ungauged inputs joining the main stem between two given main stem sampling sites, were added. This was meant to facilitate the calculations, by considering a single tributary for every river segment i:

$$Q_{trib(i)} = Q_{g(i)} + Q_{ug(i)} \tag{3.7}$$

$$m_{trib(i)} = m_{g(i)} + m_{ug(i)} \tag{3.8}$$

Next, snapshot mass balances were calculated under two perspectives: *global* and *local*.

3.4.4 The global mass-balance

In the global mass-balance approach, the river reach was conceptualised as a big black box (Figure 3.6-A), in which all the inputs were summed together as a single overall input to the system. This input was considered both in terms of water and mass flux:

$$Q_{in} = \sum_{i=0}^{13} Q_{trib(i)} \tag{3.9}$$

$$m_{in} = \sum_{i=0}^{13} m_{trib(i)} \tag{3.10}$$

where $Q_{trib(i)}$ and $m_{trib(i)}$ correspond, respectively, to the water and mass inputs received in each of the 13 river segments (Eq. 3.7 and 3.8). Note that the summation starts at 0, as tributary 0 corresponds to the water and mass flux coming from the headwaters (F_{hw} in Figure 3.6). Overall, these total inputs correspond to the flux that we expect at the outlet of the river reach.

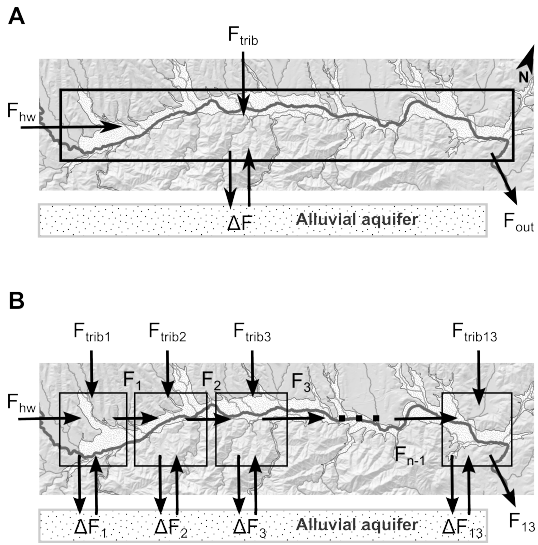

Figure 3.6 – Conceptual models of the mass balance. A) Global mass balance approach, B) Local mass balance approach. F refers to any flux, water of mass. F_{hw} corresponds to the inputs supplied by the main stem coming from the headwaters, F_{trib} are the inputs from the tributaries, and ΔF are the exchanges with the underlying alluvial aquifer, which can be an input or an output of the system, depending on the river-aquifer relationship at the specific time of sampling.

Any discrepancy between the water inputs (Q_{in}) and outputs (Q_{out}) are assumed to correspond to the amount of water that has been exchanged with the alluvial aquifer (ΔQ), that is, the amount of infiltrated or upwelled water or mass during the 26-km downstream transit:

$$\Delta Q = Q_{out} - Q_{in} \tag{3.11}$$

Positive values of ΔQ indicate an upwelling of water, whereas negative values indicate the occurrence of infiltration. The knowledge of this ΔQ is essential in order to estimate the amount of mass that we loose or gain through water exchange with the alluvial aquifer (Δm). In the absence of any in-stream reactive process, we can compute an expected mass flux at the outlet of the river reach as follows:

$$mout(exp) == m_{in} - \Delta m \tag{3.12}$$

$$\Delta m(\%) = \frac{m_{out(obs)} \times 100}{m_{out(exp)}} - 100 \tag{3.13}$$

At this point, any discrepancies between the expected and the observed mass fluxes in the outlet (Eq. 3.13) correspond to in-stream transformation processes, as all the inputs and outputs of the river reach have been taken into account. Thus, positive values of Δm indicate a net production or release along the river reach, whereas negative values indicate net retention processes. This provides information about the overall function of the river with respect to a biogeochemical componenent: whether it behaves as a source (production or generation predominates) or as a sink (loss or retention predominates).

The local mass-balance

In the local mass-balance approach, the river reach is split into 13 black boxes, each of them spanning two consecutive main stem sampling sites (Figure 3.6-B). These boxes are linked one another in series, in such a way that every main stem site represents the output of its ustream black box, as well as the input to its downstream black box. In addition, every black box receives the inputs of any tributaries that join the main stem in that specific river segment. In essence, it is the same approach of the global mass balance, but applied successively to different segments of the whole river reach. This view dissects the information provided by the global mass balances, and allows to locate on a longitudinal axis, the spatial distribution of production or retention processes.

In every river segment, inputs can be calculated as the sum of the tributaries joining that specific river segment plus the flux coming from the upstream main stem sampling site:

$$Q_{in(i)} = Q_{out(obs)(i-1)} + Q_{trib(i)} \tag{3.14}$$

$$m_{in(i)} = m_{obs(obs)(i-1)} + m_{trib(i)} \tag{3.15}$$

where $Q_{trib}(i)$ and $m_{trib}(i)$ are the water and mass flux from the catchment tributaries entering the system at the segment i, as defined in Eq. 3.7 and 3.8.

In every segment i, the difference between the inputs and the observed outputs correspond to the amount of water exchanged with the alluvial aquifer (ΔQ, calculated as in Eq. 3.11). Again, this ΔQ is essential in order to calculate the expected mass flux in the outlet of every segment i in absence of in-stream processing ($C_{out(exp)(i)}$). This $m_{out(exp)(i)}$, as well as the percentage difference between the expected and the observed mass flux at the outlet of every segment, can be calculated using the equations 3.12 to 3.13.

3.5 Statistical methods

3.5.1 EEM data mining

In order to explore patterns among EEM samples, as well as to discern and identify individual fluorescence components present throughout the data set, a new method is developed in this thesis based on a type of artifitial neural network (ANN) analysis called self-organising maps (SOMs). Therefore, all details about this statistical method are thoroughly presented in Chapter 4.

3.5.2 Multivariate analyses

In chapters 5 and 6, a non-metric multidimensional scaling (NMDS) was used in order to explore patterns among samples based on DOM fluorescence composition, as determined with SOM. An original multidimensional space, defined by the different fluorescence components, was fit to a two-dimensional space. Computations used Bray-Curtis distances and data were previously mean-centred and scaled by their standard deviation. Goodness-of-fit was assessed by two correlation-like statistics which relate ordination distances and original dissimilarities taking into account NMDS nonlinear transformations.

In order to aid the interpretation of NMDS results, hydrochemical solutes and DOM optical indices were fitted onto the NMDS analysis by means of a vector fitting analysis. Those vectors that significantly fit the ordination, a) point to the direction of maximum change and b) their length is proportional to their correlation degree within the ordination.

NMDS and vector fitting analyses were computed using R v. 2.15 (R Development Core Team, 2012) and the associated *vegan* package (Oksanen et al., 2012).

Results Part I

EEM data mining

Chapter 4

Self-Organising Maps and correlation analysis for the analysis of large and heterogeneous EEM data sets.

Elisabet Ejarque-Gonzalez and Andrea Butturini. Self-organising maps and correlation analysis as a tool to explore patterns in excitation-emission matrix data sets and to discriminate dissolved organic matter fluorescence components. *PloS one*, 9 (6), 2014. doi: 10.1371/journal.pone.0099618

4.1 Introduction

Excitation-Emission Matrices (EEMs) are three-dimensional fluorescence data that provide information about the composition of fluorescent chemical mixtures. They constitute optical landscapes that extend over the dimensions of excitation and emission wavelengths $\lambda_{ex} - \lambda_{em}$, and where fluorophores appear in the form of peaks. In the field of marine and freshwater biogeochemistry, EEMs have been used for the study of dissolved organic matter (DOM), being a comprehensive analytical technique with which to characterise a highly complex mixture of organic compounds (Hudson et al., 2007; Fellman et al., 2010; Nebbioso and Piccolo, 2013). Indeed, EEMs have served to advance scientific knowledge about the ecology and biogeochemistry of DOM in aquatic systems (Hudson et al., 2007; Fellman et al., 2010). Most importantly, they have contributed to evidence that some fractions of DOM are highly reactive organic molecules that are involved in numerous ecosystem pro-

cesses, such as bacterial uptake (Azam et al., 1983; Findlay, 2010; Cory and Kaplan, 2012), metal binding (Elkins and Nelson, 2002; Brooks et al., 2007), photoreactivity (Bertilsson and Tranvik, 2000; Mostofa et al., 2007; Osburn et al., 2009) and light attenuation (Foden et al., 2008). Overall these findings suggest the major involvement of DOM in the global carbon cycle (Cole et al., 2007; Tranvik et al., 2009).

Despite the great potential for EEMs to increase knowledge about DOM behaviour in the environment, their interpretation and statistical treatment remain a challenge (Bieroza et al., 2011). The spectral shapes of EEMs are complex mixtures of multiple and overlapping independent fluorescence phenomena, caused by the wide range of organic molecules contained in DOM. As only about 25% of these molecules have been identified (Benner, 2002), there is a lack of chemical standards to be used to separate the signal of bulk DOM into its individual components. For that reason, there is a need to develop pattern recognition methods capable of detecting and isolating the signal of different fluorescing moieties in the absence of any previous knowledge about the composition of DOM in a given sample.

A well-suited tool to satisfy these needs are self-organizing map (SOM). SOM is an artificial neural network algorithm that mirrors the biological brain function (Kohonen, 2001). Due to its unsupervised self-learning capacity, it is capable of recognizing patterns in complex data sets without following any assumptions about the data structure. Although it has been increasingly used within analytical chemistry in recent years (Brereton, 2012) it has not been until recently that SOM has been used to analyse EEM data sets (Bieroza et al., 2009, 2012), and the potential for SOM to equate or even outperform other state-of-the-art EEM data treatment methods like partial least-squares regression (PLS), principal components analysis (PCA) and parallel factor analysis (PARAFAC) has been highlighted (Bieroza et al., 2011; Brereton, 2012; Lloyd et al., 2008; Bieroza et al., 2012). The map space produced by SOM offers multiple possibilities for the graphical representation of the output, allowing to unveil patterns among samples (best matching unit and unified distance matrices), as well as to explore what variables (wavelength coordinates in the case of EEM data sets) are the most influent in creating the sample patterns (component planes) (Brereton, 2012). However, pattern recognition at the variable level has remained at a qualitative stage, and the specific need to isolate independent fluorophores has not been covered.

Furthermore, previous analyses of EEM data sets with SOM were performed on data from engineered systems, where the diversity of fluorophores was essentially homogeneous among the samples (Bieroza et al., 2009, 2012). However, EEM data sets collected in natural water systems are subject to contain a wide diversity of spectral shapes, due to the multiple environmental factors that influence DOM quality (Jaffe et al., 2008). In this case, data pattern interpretation may become

more challenging, as the presence of outliers may alter the stability of the SOM output, and hence its reliability.

In this context, this study aims at expanding the evidences that SOM is a suitable tool for the study of EEM data sets. Specifically, we focus on two aspects. On the one hand, we aim to further test the performance of SOM when a high heterogeneity of spectral shapes is contained within the data set. We address this point by assessing the stability of the quantization and the neighbourhood relations of the SOM output under a leave-one-out cross-validation approach. On the other hand, we search for independent fluorophores by extending SOM with a correlation analysis of component planes. This constitutes a novel approach to discriminate areas of the EEM (i.e. groups of wavelength coordinates) representing different fluorophores.

4.1.1 Self-Organising Maps

Self-Organising Maps (SOM) – also known as Kohonen maps – are a special type of two-layered artificial neural networks (ANNs). ANNs are mathematical models mirrored in the functioning of the biological nervous system, which have the ability to learn the patterns of input features and predict an output. They consist of an adaptive system of interconnected neurons – or processing units – that change their structure during a learning phase. In this phase, weight vectors (called prototype vectors or, in this context, prototype EEMs) that lie in the connections between neurons are adjusted to minimize the overall error of the network prediction (Kohonen, 1998).

By the end of the learning process, the EEM samples have been assigned to their best matching unit (BMU), that is, the unit that has the most similar prototype EEM. Thus, the outcome of the SOM will be a grid in which each unit will contain a prototype EEM whose spectral properties vary gradually but unevenly across the grid, according to the characteristics of the input data. By projecting the original EEMs on their BMU in the SOM grid, sample patterns can be explored.

According to Cattell (1952), this analysis can be considered as an analysis in the Q mode, as it consists of a comparison between objects (Legendre and Legendre, 1998). It can be seen as an exercise involving reduction of the dimensionality, in which samples become distributed over a two-dimensional grid, as well as a classification process, whereby samples become grouped into discrete units (Wehrens and Buydens, 2007). Moreover, in order to facilitate visual inspection of the distribution of the samples across the SOM grid, the analysis can be complemented with a clustering analysis of the neural EEM prototypes (Vesanto and Alhoniemi, 2000).

4.1.2 Correlation analysis and the determination of EEM fluorescence components

In the SOM grid, it is possible to represent the intensity of a given wavelength coordinate of the prototype EEMs throughout the different neurons using a colour scale. This kind of visualisation is called a component plane (Kohonen, 2001), and shows how the fluorescence magnitude on a given coordinate varies from neuron to neuron over the SOM grid. Two highly correlated wavelength coordinates will therefore produce two similar component planes (Barreto-Sanz and Perez-Uribe, 2007; Vesanto, 1999). When the number of variables in the data set is low, it is possible to visually compare the patterns among component planes and detect which ones are positively, negatively or not correlated (Çinar and Merdun, 2008; Mat-Desa et al., 2011). However, this becomes an unfeasible task when dealing with high-dimensional data, as is the case of EEMs (in our case, defined by 366 $\lambda_{ex} - \lambda_{em}$ coordinates). Barreto-Sanz and Perez-Uribe (2007) proposed a methodology to simplify this task by projecting the correlations between the component planes on a new SOM grid. This new projection groups highly correlated variables into the same neuron, and moderately correlated variables into nearby neurons. At this point, a hierarchical clustering analysis can be used to determine a consistent number of groups of $\lambda_{ex} - \lambda_{em}$ coordinates, each of which can be considered as a different fluorescence component. As in this case the analysis involves exploring dependences between the descriptors, it can be considered as an R-mode SOM analysis (Cattell, 1952; Legendre and Legendre, 1998).

4.2 Materials and Methods

4.2.1 Data set

Our EEM data set included 270 samples from a Mediterranean river catchment called La Tordera (865 km^2), situated to the north-west of Barcelona, Catalunya. The sampling strategy was designed in order to assess the influence of space and hydrology on the EEM spectral shapes. Accordingly, in order to characterise the longitudinal dimension, water samples were collected at 20 sites along the main stem (60 km long). The sites were operationally categorised into three main reaches, referred to as "headwaters", "middle reaches" and "lowland", divided by the bends of Sant Celoni and Fogars de la Selva (Figure 1A). Each of these three river reaches has distinctive properties. The "headwaters" section corresponds to a forested catchment area with accentuated slopes and incipient human pressure, the "middle reaches" are characterised by intensive anthropogenic activity, receiving both diffuse inputs from urban activities and point source effluents of waste water treatment plants

(WWTPs) and industries; and finally the "lowland" corresponds to a shallow and meandering geomorphology with a lower density of direct anthropogenic effluents. Eleven influent waters were also sampled upstream from the confluence with the main stem. Some of them correspond to natural tributaries with varying degrees of anthropogenic impact, whereas others correspond to WWTPs or effluents from chemical industries.

The seasonal hydrological variability was captured by sampling on 15 different dates during which a wide range of hydrological conditions was encountered: from flash floods to severe summer droughts (Figure 1B). In this case, samples were also operationally defined according to three categories: "flood" corresponds to discharges higher than 4 $m^3 s^{-1}$, "drought" to discharges lower than 1 $m^3 s^{-1}$, and "baseflow" to flows between 1 and 4 $m^3 s^{-1}$. We used discharge data from the gauging station of Fogars de la Selva, provided by the Agència Catalana de l'Aigua (Catalan Water Authority, (ACA, 2013)), as a reference.

Due to the wide variety of drained land cover, water sources and hydrological conditions included in the sampling design, the final EEM data set was expected to include a wide variety of spectral shapes.

4.2.2 Computations

SOM analysis was conducted using the Kohonen package for R (Wehrens and Buydens, 2007). The successive steps undertaken in our computations are conceptualised in the flow diagram shown in Figure 4.1. EEMs were pre-processed by normalising their fluorescence intensity by their maximum, in order remove effects of changes in concentration and focus specifically on qualitative variations (Boehme and Coble, 2000). The input matrix for the SOM analysis in the Q-mode contained 270 linearized EEMs with fluorescence data from 366 $\lambda_{ex} - \lambda_{em}$ coordinate pairs (Figure 4.1 A). The output layer was an hexagonal grid (Figure 4.1 B). Its size was chosen to be the largest size that ensured stability of the quantization error (de Bodt et al., 2002). In addition, dimensions were set to preserve the proportions of the two highest eigenvalues of the covariance matrix of the input data (Bieroza et al., 2009; Vesanto and Alhoniemi, 2000; Park et al., 2006; Céréghino and Park, 2009). During the training phase, the learning rate decreased linearly from 0.05 to 0.01. The initial neighbourhood size included two-thirds of all distances of the map units, and decreased linearly during the first third of the iterations. After that, only the winning unit was being adapted. In order to emphasise dissimilarities between the neurons of the SOM grid, a hierarchical cluster analysis with complete linkage was performed using the Lance-Williams update formula (Lance and Williams, 1967).

The influence of outliers on the performance of SOM was assessed by evaluating the quality of the SOM output in a series of leave-one-out (LOO) sample subsets.

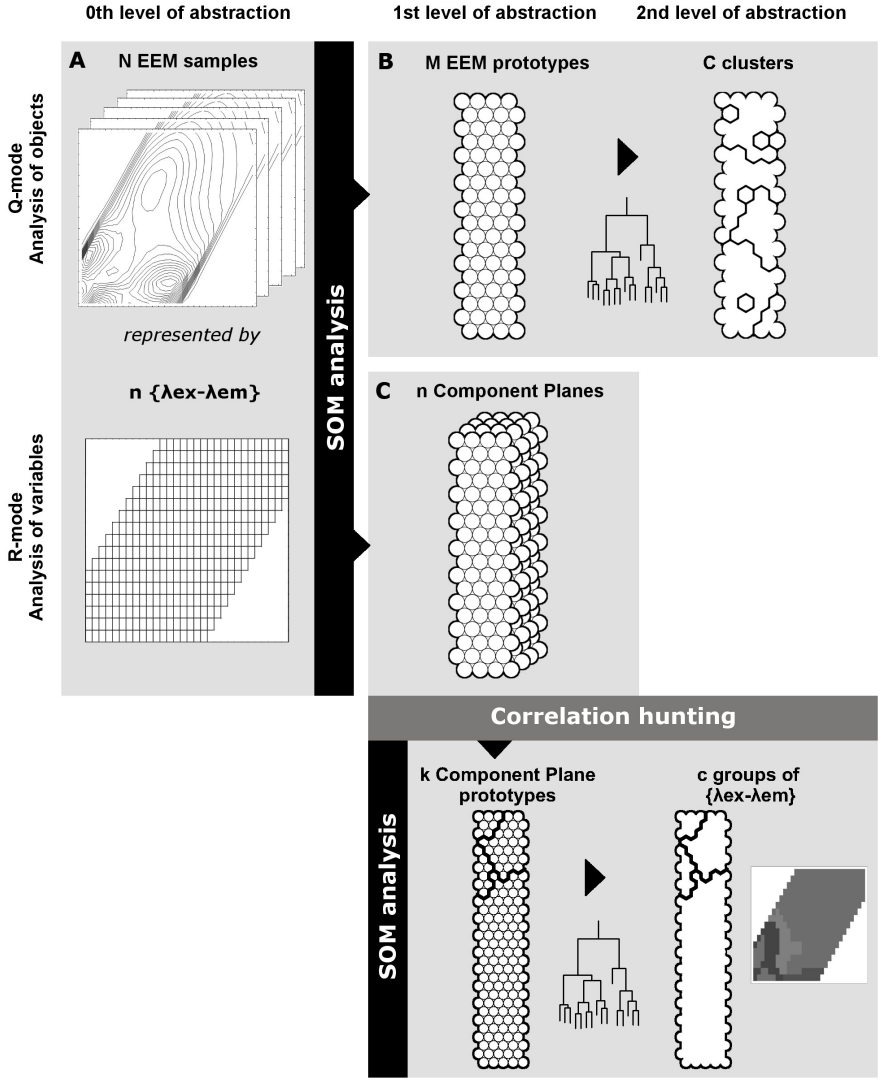

Figure 4.1 – Summary of the SOM methodology applied in this study. A) N initial samples are reduced to M prototype EEMs by SOM analysis. B) EEM prototypes are clustered to facilitate exploration of the relationships between the sample EEMs. C) SOM is performed on the correlation matrix of the component planes of the Q-mode SOM analysis. The output corresponds to an aggregation of highly correlated wavelength coordinates in a single neuron unit. D) Neuron units are clustered in order to find groups of highly correlated wavelength coordinates. E) Wavelength coordinate clusters are displayed in an EEM optical space in order to evaluate their biogeochemical meaning. Adapted and extended from Vesanto and Alhoniemi (2000).

As measures of output quality, we used the SOM reliability criteria described by de Bodt et al. (2002), which tested the stability of both the quantization and the topology of the SOM model. The stability of the quantization was assessed using the intra-class sum of squares (SSIntra) statistic, which is the sum of the squared distances between the observed data and their corresponding neural centroid. On the other hand, the stability of the neighbourhood relations was inspected by computing the histograms of all pairwise neighbourhood stabilities of a given LOO subset. SSIntra and neighbourhood stabilities were computed as described in de de Bodt et al. (2002). For every LOO subset, the statistics were averaged over 50 runs of the SOM analysis, in order to minimise the variability of the output due to random initialisation of the reference vectors (Cottrell et al., 2001).

In parallel, 366 component planes were obtained from the SOM analysis (Figure 4.1 C), one for each $\lambda_{ex} - \lambda_{em}$ coordinate that defined our original EEMs. In order to discriminate the number of fluorescence components within the samples, a correlation analysis was performed, based on the steps defined by Barreto-Sanz and Perez-Uribe (2007). These steps included:

- Transformation of the component planes into normalised vectors.
- Calculation of the Pearson's correlation between each pair of vectors, obtaining a covariance matrix of dimensions (366 x 366).
- Computation of a SOM analysis of this covariance matrix, hereafter referred to as the SOM analysis in the R-mode. In this grid, neurons grouped highly correlated $\lambda_{ex} - \lambda_{em}$ coordinates.
- Clustering of the U-matrix with a hierarchical cluster analysis with complete linkage using the Lance-Williams update formula (Lance and Williams, 1967).
- The optimal number of groups (i.e. fluorescence components) was determined by inspecting the silhouettes (Rousseeuw, 1987) of a range of partitions, from two to nine groups. The best partition had a high average $s_{(i)}$, and the fewest objects with a negative $s_{(i)}$, where $s_{(i)}$ is a measurement of how well object i matches its assigned cluster.

Eventually, the correlation analysis led to the definition of a number of EEM regions containing uncorrelated fluorescence phenomena and hence, assumed to reflect different fluorescence components. Next, the components in every sample were quantified as area-normalised fluorescence volumes, following the fluorescence regional integration (FRI) described in Chen et al. (2003).

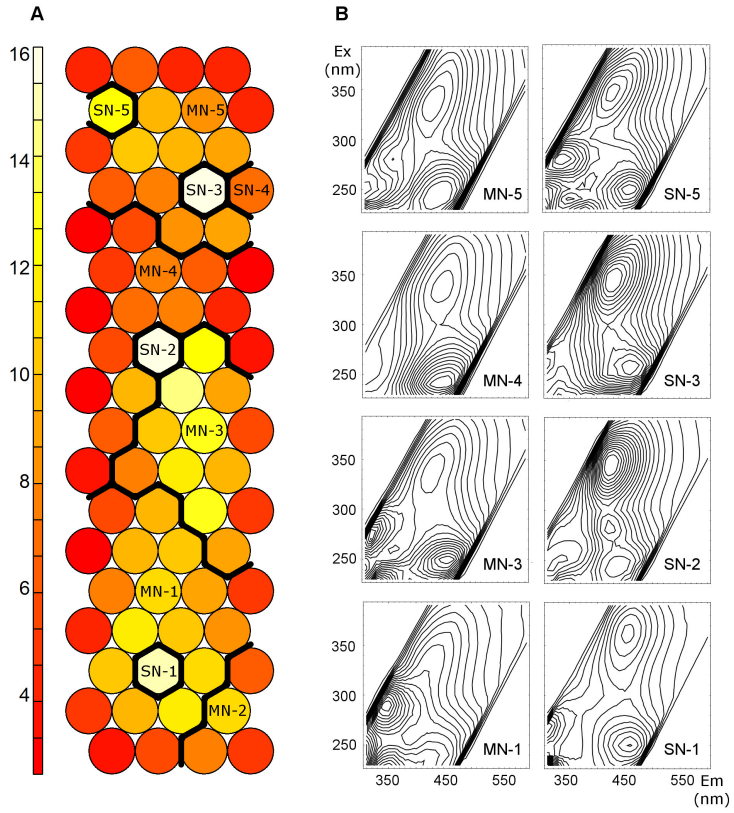

Figure 4.2 – Clustering of the U-matrix of the SOM analysis in the Q-mode. A) Ten regions were defined in the SOM grid (black solid lines), based on hierarchical clustering of the U-matrix. B) EEM prototypes representing the main SOM regions.

4.3 Results

4.3.1 SOM codebooks

The output of the SOM analysis trained on the 270-sample data set is summarised in Figure 4.2. The unified distance matrix (frequently referred to as U-matrix, Figure 4.2A) represents the distances between the EEM prototypes of neighbouring neurons using a colour scale (Ultsch and Siemon, 1990). This kind of visualisation is the most frequently used method to explore dissimilarity and clustering patterns in the SOM grid (Kohonen, 2001).

In our results, inter-neighbouring distances were clearly uneven across the SOM grid, indicating the presence of dissimilarity patterns. Low distances dominated in the upper-middle part of the U-matrix, whereas high dissimilarities were observed in the central region of the lower part of the SOM grid. In order to further emphasize and differentiate regions with higher similarities between neurons, a 10-cluster division was applied to the U-matrix (Figure 4.2A). It should be noted here that the partitioning of the U-matrix was used only for visualisation purposes. Some neurons had such a high dissimilarity to their neighbouring neurons (lowest values in the U-matrix) that they formed stand-alone clusters by themselves (hereafter referred to as SN-1 to SN-5, where SN stands for single neuron). The rest of the grid was partitioned into five multi-neuron zones (hereafter referred to as MN-1 to MN-5). The nomenclature specified in Figure 4.2 will be used hereafter to facilitate description of the distribution of samples throughout the SOM grid in order to explore relationships between samples.

4.3.2 Outlier sensitivity analysis

The outlier sensitivity test showed that the presence of a few samples with very distinctive and infrequent spectral shapes (especially those assigned to single-neuron clusters) did not affect the SOM outcome in a meaningful way. The SSIntra computed for the 270 LOO subsets followed a Gaussian distribution without any outlier values (Figure 4.3A). Moreover, the mean was almost identical to the median (92.27 and 92.17, respectively), further indicating that none of the LOO subsets exhibited a statistically relevant differentiated quantization structure.

The histograms of neighbourhood stability showed that at a radius of one and two neurons, the neighbourhood relations remained almost the same irrespective of the sample left out by the LOO subsets (Figure 4.3B). This demonstrates that the topology of the SOM output is preserved in the presence of specific outlier samples. Furthermore, all the histograms of the LOO subsets are clearly different from the theoretical histogram of a randomly organised map (Figure 4.3B). This indicates that in every SOM analysis, corresponding to different LOO subsets, the samples are meaningfully organised in the SOM grid, in a far from random distribution (de Bodt et al., 2002).

4.3.3 Samples projection

The samples in our data set were collected along a longitudinal downstream gradient, and under a variety of hydrological conditions. In order to test the influence of space and hydrology on the distributions of EEM spectral shapes, samples were projected onto the SOM grid, and coloured according to their sampling location

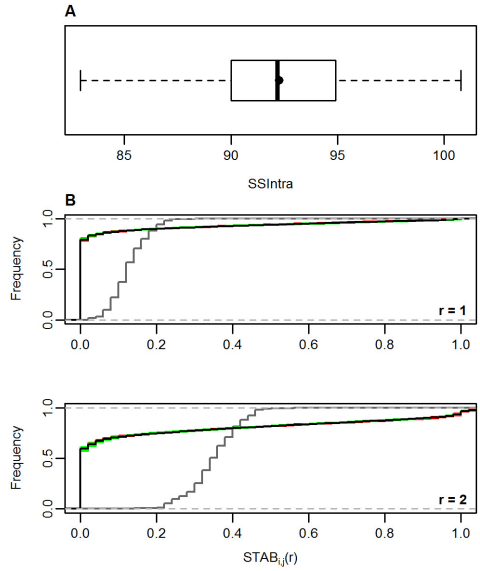

Figure 4.3 – Outlier sensitivity analysis. A) Quantization stability: variation of the average SSIntra among 270 LOO subsets. The black dot indicates the mean. The absence of outlier values of CV(SSIntra) and the similar mean and median should be noted. B) Stability of neighbourhood relations: Histograms of the stabilities over all pairs of observations. In red, histograms of the LOO subsets in which the left-out sample was assigned to a single-neuron cluster. In green, histograms of the remaining LOO subsets. In black: histogram of the whole data set. It should be noted that there is hardly any difference between them. In grey, theoretical histogram of a randomly distributed map, following a binomial distribution defined according to de Bodt et al. (2002). This demonstrates that the SOM results are organised in a far from random distribution.

("headwaters", "middle reaches" and "lowland" categories) and hydrology ("flood", "baseflow" and "drought" categories, Figure 4.4).

In terms of hydrology (Figure 4.4A), samples collected during flood conditions were grouped into three main neurons, all situated in region MN-4. However, baseflow and drought samples were distributed across the grid. In the case of space (Figure 4.4B), the three categories appeared in different parts of the SOM grid. Headwater samples appeared mainly in region MN-4, samples from the middle reaches in regions MN-3 and MN-5, and those from the lowland mainly in region MN-1. Specifically, the neurons in region MN-4, which contained samples from middle reaches or the lowland, were the very same neurons that corresponded to the flood category in the hydrological projection. This combination of a single category for hydrology (flood) and multi category for space (whole length of the river) in a single neuron suggests a homogenisation effect on the spectral shape of EEMs over the whole length of the river under flood conditions.

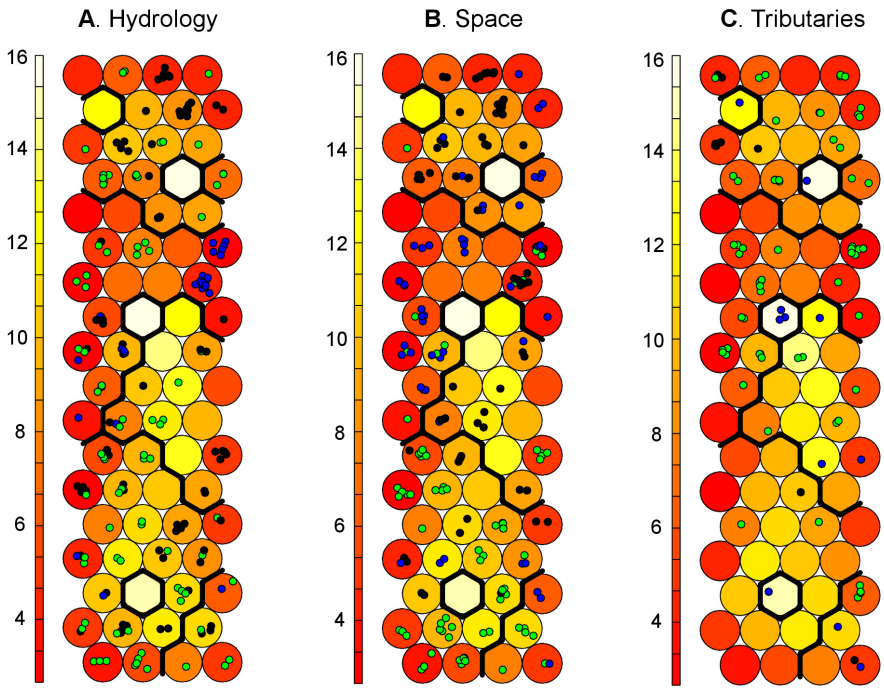

Figure 4.4 – Projection of space, discharge, and type of tributary onto the U-matrix. Neuron colour scale indicates, for every neuron, the sum of the euclidean distances to all its immediate neighbours. Samples are projected on the SOM grid and coloured according to A) hydrology: blue represents flood conditions, black represents base flow, and green drought; B) space: blue corresponds to headwater samples, black middle reaches samples, and green are the lowland samples; C) types of tributary: blue are industrial, black are WWTP, and green are natural tributaries.

Tributaries are presented separately in Figure 4.4C, coloured according to their origin: riverine, sewage-treated or industrial. It is noteworthy that single-neuron clusters contained exclusively industrial effluents, indicating that these sources produce DOM spectral shapes that are dissimilar with respect to the DOM from riverine and sewage-treated water. In contrast, WWTP samples appeared mainly in region MN-5, and natural tributaries were spread over the whole grid, but mainly in regions MN-4 and MN-5, those also associated with headwaters and middle reach sampling locations.

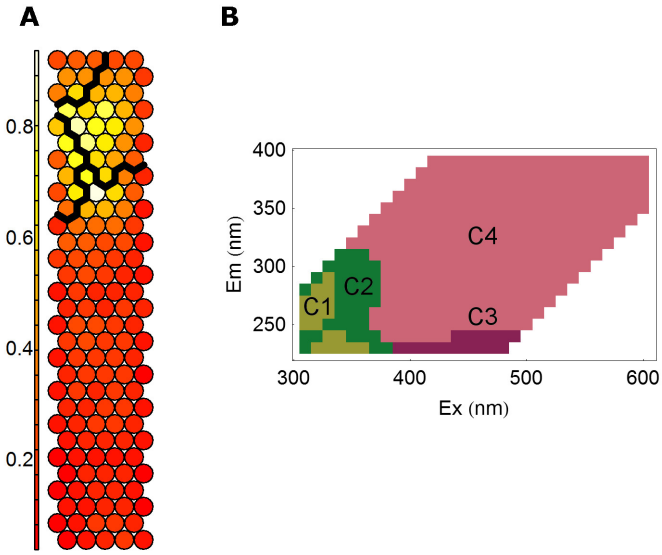

Figure 4.5 – Clustering of the U-matrix of the SOM analysis in the R-mode and fluorescence components determination. A)Every cluster groups highly correlated wavelength coordinates, representing different fluorescence components. B) Representation of the four groups on the excitation-emission space.

4.3.4 Determination of fluorescence components

The U-matrix of the SOM analysis in the R mode is shown in Figure 4.5A. It can be seen that the bottom half of the SOM grid contains highly correlated wavelength coordinates, expressed by the homogeneous dark red-coloured neurons that indicate short distances between them. In the top part, there is a central light-coloured region and darker neurons in the margins, indicating the presence of greater heterogeneity among these units. Hence, overall the SOM grid contains a high number of neurons with highly correlated wavelength coordinates, and in contrast, a small set of neurons with larger dissimilarities between them, thus containing a higher diversity of fluorescence signals.

Next, the hierarchical clustering and silhouette analysis of the SOM units showed that four clusters was the best number of fluorescence components, as it exhibited the optimal combination of the minimal number of presumably misplaced samples ($n_{(s<0)}$) and the highest average silhouette ($\bar{S}$), (Table 4.1).

The four groups of wavelength coordinates (hereafter referred to as C1 to C4) are represented on the excitation-emission space in Figure 4.5B. It can be seen that they appear spatially grouped in the optical plane and, moreover, that they over-

lap regions previously related to specific DOM fluorophores in the literature (Table 4.2). C4 corresponds to the V region of Chen et al. (2003) and broadly to peak C of Coble (1996), which were associated with humic-like substances. This component has been detected in a wide range of aquatic environments but mainly in waters draining forested catchments (Fellman et al., 2010), and hence, represents an indicator of terrestrially derived DOM (Coble, 1996). In the same emission range, but at the lowest excitation wavelengths, component C3 is apparent. Similarly to C4, it has also been associated with humic-like components of terrestrial origin but with a higher molecular weight and more freshly released character (Fellman et al., 2010; Huguet et al., 2009). In the region of the EEM with the lowest emissions are two spots centred at $\lambda_{ex}/\lambda_{em}$ = 230/330 nm and 270/310 nm (C1), similarly to the coordinates of maximal fluorescence of tyrosine (Yamashita and Tanoue, 2003). Hence, components appearing at these wavelengths have been attributed to peptide material resembling or containing tyrosine, indicating the presence of autochthonous microbially derived DOM (Cammack et al., 2004). Finally, C2 covers an area surrounding the previous protein-like spots, overlapping the region occupied by tryptophan (Yamashita and Tanoue, 2003). This component has also been reported to reflect microbial activity, and has been used as an indicator of anthropogenic DOM inputs (Baker, 2001; Henderson et al., 2009; Borisover et al., 2011).

4.4 Discussion

SOM coupled with a correlation analysis offers a flexible tool that enables, in the first stage, a similarity-based classification of EEMs and, in the second stage, a reduction of the dimensionality by grouping highly correlated $\lambda_{ex} - \lambda_{em}$ coordinates (Figure 4.1). Hence the methodology consists of two main parts: first, an analysis of the objects (i.e. sample EEMs) and second, an analysis of the variables (i.e. wavelength coordinates). In essence, the analysis of the objects is an exercise of classification of the samples, based on their spectral similarities; whereas the analysis of the variables reduces the dimensionality by grouping those coordinates that are highly correlated. This correlation analysis has meaningful biogeochemical implications, as each group of correlated wavelength pairs is assumed to be an independent fluorescent component, with consistent distributions in the $\lambda_{ex} - \lambda_{em}$ space according to the literature (Coble, 1996; Parlanti et al., 2000).

As a classification system, SOM has the advantage that it shows a low degree of dependency on the frequency at which a sample (or a spectral shape) is represented in the data set. By means of an outlier sensitivity test, the SOM quantization and topological structure was found to be robust to the presence of outlier samples. Accordingly, a single sample with unique and distinctive features can be classified on its own without affecting the classification of the other samples. In this way,

outliers are not a distorting element, but a result integrated into the whole output. In our data set, this was exemplified by the neurons SN-1, SN-3 and SN-5, each of which represented only one sample. Specifically, they represented industrial effluents, which had very different spectral shapes with respect to the river water samples. This robustness to outliers provides the advantage that a data set can be analysed irrespective of its heterogeneity. This circumvents the main limitation of other currently used and well-established methods for EEM data treatment, like PCA, PLS or PARAFAC, which are highly sensitive to the presence of outliers (Engelen and Hubert, 2011; Bro and Vidal, 2011; Stedmon and Bro, 2008) as they largely depend on least-squares solutions (Brereton, 2012). In least squares methods, the overall model is adjusted to include a better fit of an outlier, even if it results in a lower overall fit (Quinn and Keough, 2010). However, in SOM every sample only modifies its BMU and its neighbourhood, resulting in a less apparent influence of the presence of an outlier on the whole model outcome.

Furthermore, this classification stage leads not only to the grouping of samples with a high degree of similarity in terms of spectral shapes, but also to the generation of a reduced number of EEM prototypes (Figure 4.1, 0th to 1st level of abstraction). This reduced data set contains all the initial diversity of spectral shapes, but with the relative frequencies more evenly distributed. For instance, in our work, one EEM prototype could represent either a large number of samples that were very similar to one another (e.g. 13 headwater samples in a single neuron in SOM region MN-4, Figure 4.4B), or just a single sample with very unique properties (e.g. an industrial effluent in SN-1, SN-3 or SN-5, Figure 4.4C). This re-weighting effect of the representativeness within the data set allows for an analysis of correlations among variables (i.e. $\lambda_{ex} - \lambda_{em}$ coordinates) that can detect fluorophores that were initially represented at only low levels. Indeed, in our correlation analysis, we distinguished four areas in the EEM that were highly correlated (Figure 4.1, 1st to 2nd level of abstraction). Our four components had consistent properties in relation to previous descriptions in the literature (Table 4.2). Specifically, we distinguished two protein-like components, one of which appeared specifically related to anthro-

	Correspondence with		Approximate boundaries	
Component	Coble 1996	Parlanti 2000	λex (nm)	λem (nm)
C1	B	γ	250-280 and 230-240	310-330 and 320-360
C2	T	δ	240-300	340-370
C3	A	α	230-240	> 370
C4	C	α'	> 250	> 400

Table 4.1 – Wavelength coordinates boundaries of the fluorescence components. Summary of the location of the fluorescence components determined by correlation analysis and corresondence with previous components described in the literature.

#groups	S	Smin	Smax	$S_{(n<0)}$
2	0.56	-0.74	0.86	17
3	0.57	-0.50	0.8	13
4	0.54	-0.29	0.74	9
5	0.48	-0.43	0.72	13
6	0.48	-0.44	0.70	8
7	0.41	-0.23	0.70	7
8	0.42	-0.23	0.70	7
9	0.35	-0.23	0.70	16

Table 4.2 – Characteristics of the silhouettes of a range of hierarchical partitionings of the R-mode SOM grid. The silhouettes analysis (Wehrens and Buydens, 2007) corresponds to the calculation of $s_{(i)}$ for every object in the data set, where $s_{(i)}$ is a measurement of how well an object i matches its assigned cluster. $\bar{S}$ corresponds to the average $s_{(i)}$, S_{min} to the minimum $s_{(i)}$, S_{max} to the maximum $s_{(i)}$ and $S_{(n<0)}$ to the number of objects that have a negative $s_{(i)}$. Values of S near one indicate that the object is very well clustered, whereas negative S indicates that the object might be assigned to the wrong group.

pogenically derived DOM, as well as two humic-like components that coincided with the A and C areas described by Coble (1996).

This methodology for detecting fluorescence components represents a novel statistical approach. In the procedure, the partitioning of the SOM grid represents a key step where the final decision is taken about the number of fluorescence components present in the data set. This step requires particular attention. Specifically, there are several clustering techniques that could be used to classify the neurons in a SOM grid. It has been reported that SOMs create clusters similar to those created by hierarchical clustering (Vesanto and Alhoniemi, 2000; Oja et al., 2006). Indeed, we computed a hierarchical clustering with complete linkage using the Lance-Williams update formula, and our clusters were consistent with the (dis)similarity patterns of the U-matrix (Figures 3 and 6). However, in SOM grids of higher resolution (i.e., number of neurons) the U-matrix can present more complex patterns of clustering and subclustering. In this case, the results of a hierarchical clustering analysis may not follow the results of the U-matrix very closely (Vesanto and Sulkava, 2002). As a better approximation, computation of Vellido's algorithm and the use of the U-matrix neural neighbourhood distances as a cluster distance function have been proposed (Barreto-Sanz and Perez-Uribe, 2007; Vesanto and Sulkava, 2002) as, in this case, the neighbourhood conditions become explicit in the analysis and the output fits better with the results of the U-matrix. Hence, future studies should test the performance of different clustering techniques when larger data sets – and hence, larger SOM grids – are concerned.

Finally, after the regionalisation of EEMs into four fluorescence components, we quantified their contribution in every sample using the FRI technique originally described by Chen et al. (2003). This technique has been widely applied to track changes in DOM composition (Wang et al., 2009; Marhuenda-Egea et al., 2007; Shao et al., 2009). It has the advantage that it integrates the whole shape of the EEM region and accounts for the fluorescence provided by shoulders and other spectral features that would be omitted if only the maximal value of the region was taken into account. However, it has recently been pointed out that the numerical method used for integration can have important consequences for the accuracy of the results. Specifically, the Riemann summation method proposed by Chen et al. (2003) and used in this paper may result in the underestimation of the protein-like fractions, and in the overestimation of humic-like fractions (Zhou et al., 2013). In order to minimise this bias, future studies may consider the use of other methods, such as the composite trapezoidal rule or the composite Simpson's rule (Zhou et al., 2013).

In summary, our results open a new viewpoint to the statistical treatment of EEMs. Thanks to its robustness to the presence of outliers, SOM can be applied to EEM data sets including both high- and low-represented spectral shapes. This may have important practical implications especially for the study of the biogeochemical behaviour of DOM in natural systems, as sampling designs will be less restricted to the requirements of the statistical treatment, and more adaptable to research needs.

4.4.1 Next steps

In this chapter, the originally complex DOM composition of our EEM data set has been simplified into four fluorescence components which are representative of the spatio-temporal variations of DOM quality in La Tordera. These four components will be used in the following chapters of this thesis in order to investigate the transport and reactivity of DOM, not only at the bulk level but also, and most importantly, for each of these moieties.

4.5 Conclusions

In this paper, the use of SOM in combination with a correlation analysis has been presented as a powerful method to deal with large and complex EEM data sets. Specifically, our findings indicate that:

- SOM analysis coupled with a correlation analysis as described by Barreto-Sanz and Perez-Uribe (2007) allows an analysis both at the object and at the variable level. Hence, it serves not only to explore the differences in

fluorescence properties between samples, as shown by Bieroza et al. (2009, 2012), but also helps to identify particular fluorescence components, as shown herein.

- It is robust to the presence of outlier samples. That is, samples with very distinct features are discerned while having little effect on the ordination and classification of the other samples. This distinct property makes it possible to work with heterogeneous data sets.
- The correlation analysis performed on the SOM EEM prototypes has an enhanced capacity to detect fluorophores that are represented at only low levels in the original EEM data set.
- SOM analysis coupled with a correlation analysis of the component planes expands the toolbox of the fluorescence DOM researchers by enabling the analysis of complex and heterogeneous EEM data sets. This may open new possibilities for advancing our understanding of DOM character and biogeochemical behaviour.

Results Part II

Longitudinal patterns of DOM quality and reactivity

Chapter 5

Preliminary assessment of spatiotemporal patterns of DOM quality and quantity in La Tordera

5.1 Introduction

In this chapter, a first approach to the spatiotemporal patterns of dissolved organic matter (DOM) is presented. As pointed in the general introduction of this thesis (chapter 1), most conceptual models since the river continuum concept (RCC) (Vannote et al., 1980) foresee important changes in the transport and processing of organic matter along the longitude of a river (Ward and Stanford, 1983; Junk et al., 1989; Thorp and Delong, 1994); however, the empirical studies assessing such changes are seldom (Hadwen et al., 2010). Moreover, a better knowledge of the DOM interactivity during the riverine transit is of utmost importance in order to unveil the role of rivers in the carbon cycle, as there are theoretical (Cole et al., 2007; Tranvik et al., 2009) and empirical (Moody et al., 2013) evidences that rivers are major sinks of DOM. However, such evidences did not take into account how contrasting hydrological conditions can alter the capacity of a river to process DOM.

Mediterranean rivers have been little characterised in biogeochemical terms, and, however, they have a hydrological variability that makes them unique as fluvial systems. Due to the occurrence of floods in spring and autumn, and droughts during summer, Mediterranean rivers are continuously facing perturbations of alternative sign, what has shaped a characteristic seasonality and special adaptations of the bio-

logical communitites (Gasith and Resh, 1999). Also, such abrupt hydrological shifts determine specific temporal patterns in the biogeochemical functioning (Butturini et al., 2008) as they confer a spatial dynamism in terms of land-river connectivity (Vázquez et al., 2007) and longitudinal connectivity within the river corridor (Vazquez et al., 2011). Whereas the export of DOM from the land to the river has been addressed in a number of studies (Royer and David, 2005; Wiegner et al., 2009; Raymond and Saiers, 2010), especially during floods and baseflow, the successive downstream evolution of DOM has been generally overlooked. Moreover, the low flows preceding the river drying (hereafter referred to as the drought hydrological conditions) have been very scarcely characterised. Therefore, the consequences of such a variety of hydrological conditions for the transport and reactivity of DOM have not been fully assessed.

Here we present the results of a longitudinal assessment of DOM quantity and quality, performed under a range of hydrological conditions: flood (2.76 – 2.82 m^3s^{-1}), baseflow (0.57 - 0.21 m^3s^{-1}), drought (0.1 - 0.08 m^3s^{-1}) with rainy antecedents (in the previous month, the maximal discharge was 10.27 m^3s^{-1}), and drought (0.31 – 0.09 m^3s^{-1}) with non-rainy antecedents (in the previous month, the maximal discharge was 3.32 m^3s^{-1}). The main stem of La Tordera, a Mediterranean River situated in the central Catalan coast, was sampled at 10 sites distributed from the headwaters to the river mouth (see chapter 3 for full details on the sampling strategy).

Specifically, the aims of this chapter are:

- To provide a general biogeochemical description of the river. The longitudinal profiles of some physico-chemical parameters (electrical conductivity, pH, dissolved oxygen), conservative solutes (chloride, sulphides) and reactive anions (nitrate, ammonium and soluble reactive phosphor (SRP)) are presented.
- To assess the longitudinal gradients of DOM quality and composition along the riverine course: DOM is quantified as dissolved organic carbon (DOC) and dissolved organic nitrogen (DON) concentrations, and characterized using SOM fluorescence components composition as well as the optical indices of Humification Index (HIX), Fluorescence Index (FI) and Specific Ultra-Violet Absorbance (SUVA).
- To test to what extent contrasting hydrological conditions alter or influence the longitudinal biogeochemical gradients.
- To identify locations or features in space which are prone to create hydrochemical disruption.
- And finally, as a general aim, to characterise how space and hydrology operate as inter-dependant dimensions of DOM quantity and quality.

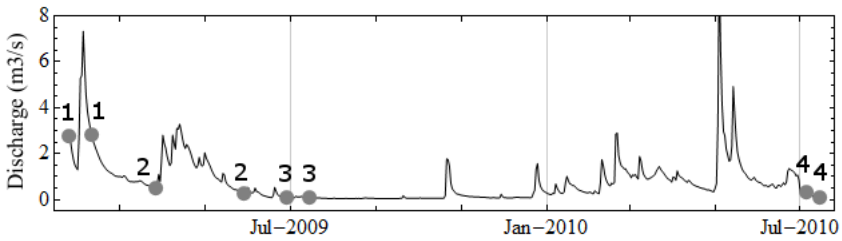

Figure 5.1 – Hydrogram of the study period, with discharge values corresponding to the gauging station of Sant Celoni. Numbers 1 to 4 indicate correspondence with the hydrological categories CH1 to CH4, in which CH1 refers to flood or stormflow conditions, CH2 baseflow conditions, CH3 drought with moderate rainfall antecedents and CH4 drought with flood antecedents. Data provided by the Catalan Water Authority (Agència Catalana de l'Aigua, ACA).

5.2 Results

5.2.1 Hydrochemical framework

In order to contextualise the hydrochemical environment, some solutes and physicochemical parameters are summarised in Table 5.1, Figure 5.2 and Figure 5.3. Conductivity (Figure 5.2a-b) showed a greater differentiation in space than over hydrological conditions. Along the river length, it was lowest in the headwaters (89.6 ± 16.6 μS/cm) [1], and maximal near the river mouth (444.9 ± 256.6 μS/cm), with an overall gradual increase disrupted by a steep rise in site S4 (located in the industrial area of Sant Celoni, at 25.5km from the river source). In relation to hydrology, despite the medians remained similar throughout the different conditions, conductivity was found to be lower during flood (369.1 ± 259.6 μS/cm) and highest during drought with moderate rainfall antecedents (461.7 ± 289.0 μS/cm). Chlorides and sulphates (Figures 5.2c-f) showed parallel patterns with conductivity (linear fits of $F_{1,34} = 205.7, P = 5.5 \times 10^{-16}, r^2 = 0.858$ and $F_{1,34} = 134.6, P = 2.3 \times 10^{-13}, r^2 = 0.798$, respectively). For the three variables, the data corresponding to the last river site, situated in the river mouth, collected during drought conditions (S10-CH3 and S10-CH4) were omitted from calculations and plottings, as due to the inland penetration of the sea-river interface they were reflecting extremely high salinity values. However, for the following solutes and physicochemical variables these data have not been omitted. It is important to keep this aspect in mind, as it indicates that site S10 during drought reflects sea water rather than the river water itself.

[1] For convention reasons, the average ± standard deviation are reported in the text, despite the described boxplots represent the medians with the four quartiles.

pH was neutral to basic (Figure 5.2g-h). The most basic conditions were found in baseflow (8.47 ± 0.38) and, in space, remained on average between 7.5 - 8 except for sites S5, S8 and S10 which reflected peaks of higher basicity (8.37 ± 0.56 to 8.91 ± 0.64). Despite a lack of data during flood, dissolved oxygen (Figure 5.2i-j) was found to be near 100% in average for the different hydrological conditions, although during drought O_2% values had a higher dispersion with extreme both high and low extreme values. In space, maximal averages were found again in S5, S8 and S10 (131.4 ± 48.4% to 166.4 ± 46.2 %), whereas it was minimal in S4 (66.6 ± 26.6%).

Nitrogen in the form of nitrate and ammonium (Figures 5.3e-h) was most concentrated in flood conditions (1.485 ± 0.656 mgN-$NO_3^- \cdot L^{-1}$, 0.200 ± 0.258 mgN-$NH_4^+ \cdot L^{-1}$); conversely, SRP (Figure 5.3i-j) was minimal under such conditions (0.057 ± 0.041 mgSRP$\cdot L^{-1}$) and maximal during drought with flood antecedents (0.351 ± 0.511 mgSRP$\cdot L^{-1}$). In space, SRP and N-NH_4^+ peak at S4 (0.633 ± 0.709 mgSRP$\cdot L^{-1}$ and 0.640 ± 0.261 mgN-$NH_4^+ \cdot L^{-1}$). Nitrate has an increasing trend over the first three headwater sites with little temporal variability. From S4 to downstream, the trend inverts and slightly decreases downstream but with an important temporal variability. Towards the river mouth, nitrate slightly increases again.

5.2.2 Variation in DOM concentration

Regarding the organic solutes, DOM was quantified both in terms of DOC and DON (Table 5.2, Figure 5.3 a-d). For the whole data set, DOC ranged between 0.598 and 7.873 mg$\cdot L^{-1}$, averaging at 2.758 ± 1.348 mg$\cdot L^{-1}$. DON ranged between non-detectable values and 4.272 mg$\cdot L^{-1}$, with an average of 0.565 ± 0.943 mg$\cdot L^{-1}$. In the headwaters were found the lowest concentrations for both DOC and DON. Then, in site S4, both solutes experience an increase. Such rise is clearer for DOC, for which the higher concentrations achieved in S4 remain constant downstream. In the case of DON, sites S4 to S10 (that is, the middle and lower reaches) have a higher variability compared to the headwaters, attaining values up to 1.5 – 2 mg$\cdot L^{-1}$. However, the medians are similarly low in the middle reaches as in the headwaters, but with a higher temporal variability. In response to hydrology, DOC median remains similar in the different conditions with higher variability during droughts. In contrast, DON differs significantly during flood ($p < 0.05$), exhibiting higher concentrations and variability with respect to baseflow and drought conditions.

5.2.3 Variation in DOM character

The indices considered in this study are the FI, HIX and SUVA, which reflect different and complementary attributes of DOM, namely the origin, humification degree and aromatic degree, respectively. The three of them exhibit clearly different patterns in space (Figure 5.4), suggesting that they respond to different ecological and biogeochemical processes. FI values ranged between 1.32 and 2.36 in the whole data set. The lowest values, which indicate a terrestrial origin of DOM, are found in the three headwater sites. Downstream, FI increases, peaking at site S7 (1.953 ± 0.270), located in the bend of Fogars de la Selva (at 45 km from source). On the other hand, HIX has a continuous decreasing trend downstream, ranging from maximal values upstream (15.085 ± 2.857) until minimal values in the river mouth (7.841 ± 3.589). Finally, SUVA has a constant average value near 5 for the whole length of the river. However, the three sites in the headwaters have a higher temporal variability compared to downstream sites.

Among the different hydrological conditions considered, different behaviours can also be observed between these indices. For SUVA, baseflow conditions largely differ from the rest for exhibiting a larger variability, although it still has a similar median. FI in flood conditions has minimal variability and low values, whereas baseflow and non-rainy antecedent drought have highest variability, indicating a more important heterogeneity of DOM sources along the river. HIX exhibits the most clear and significant differences ($p < 0.05$) in which flood conditions have highest values and minimal variability, whereas the rest of hydrological conditions have a higher variability.

5.2.4 Variation in DOM composition

The composition of DOM was assessed in terms of the fluorescence components determined by self-organizing map (SOM) analysis in chapter 4. As a reminder, these consist on four components, referred to as C1 to C4. Among them, C1 and C2 refer to protein-like material, and are similar to Coble's peaks B and T, and to Parlanti's peaks γ and δ respectively. On the other hand, C3 and C4 are related to humic-like material and can be related, respectively, to Coble's peaks A and C and to Parlanti's peaks α', β, α (Coble, 1996; Parlanti et al., 2000).

Their variation in space and over time is shown in Figure 5.5. Among the four studied hydrological conditions, all components have in common that during flood their fluorescence has little variability, indicating that they remain constant along the river length. In the case of the protein-like components, the median is maximal during baseflow, and minimal during flood (for C1) and during drought (for C2). In the case of the humic-like materials (C3 and C4), flood average is higher than

that of baseflow and similar to that of drought in the case of C4, and higher to any other hydrological condition for C3.

Regarding space, component C3 shows no clear patterns. However, the rest of components exhibit distinguishable longitudinal patterns. As for protein-like components, both C1 and C2 have the trend to successively increase downstream. However, they differ in their behaviour from site S6 (located before the confluence of the Creek of Arbúcies, at 37 km from source). In this site, there is an important decrease in the fluorescence volume. After that, component C1 recuperates the magnitude of site S5, whereas in the case of C2, the decrease effect remains and successive sampling sites remain at lower volumes, still with an increasing trend downstream. In the case of C4, there is a monotonous decreasing pattern downstream with a slight increase in the two last sampling sites, in the river mouth. This decreasing trend of the humic-like C4 component clearly opposes to the increasing one of C1 and C2.

5.2.5 Differentiation of solutes and DOM content along the longitudinal gradient

A more synthetic approach on the longitudinal variation of the water chemical composition has been addressed by computing Bray-Curtis dissimilarities of every point of the river with respect to the first sampling site, near the river source, obtaining a profile of longitudinal differentiation downstream (Figure 5.6). They indicate to what degree the water composition is different, or *dissimilar*, from site S1. Thus, a flat line would indicate a constant composition downstream, whereas higher values indicate a higher distance, and hence a higher differentiation, degree of a given site with respect to S1. These profiles have been computed for the following groups of variables: Conservative solutes (Cl^-,SO_4^{2-}, electrical conductivity), nutrients (N-NH_4^+,N-NO_3^-,SRP), DOM concentration (DOC and DON), DOM character (FI, SUVA and HIX optical indices) and DOM composition (EEM components C1 to C4). Also, dissimilarity profiles have been computed separately for every hydrological condition.

Every type of variables exhibits a different longitudinal behaviour and sensitivity to hydrology. Conservative solutes are the ones that exhibit a more consistent longitudinal pattern for the four hydrological conditions. Both during flood, baseflow and drought they gradually differentiate from the headwaters down to the river mouth, only altered by a steeper increase in the dissimilarity in site S4. Conversely, nutrients show a differentiated behaviour in the last half of the river length depending on hydrology. In the first half of the river length, nutrients composition gradually becomes dissimilar up to site S4. From there and downstream, during flood and baseflow dissimilarity becomes constant, indicating little change in the

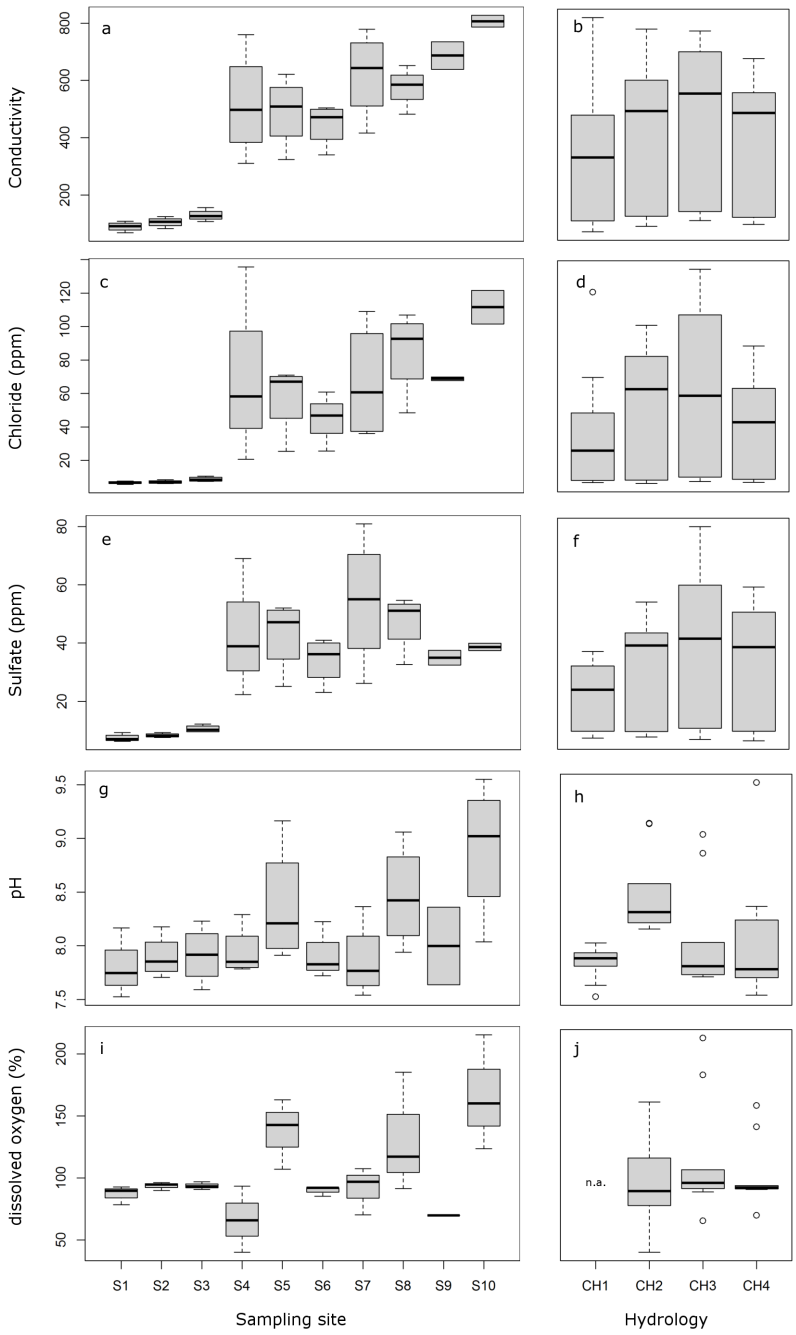

Figure 5.2 – Boxplot representation of the concentrations of conservative solutes in space and over hydrological conditions. Site S1 corresponds to the headwaters whereas site S10 corresponds to the river mouth. For the hydrological conditions, CH1 corresponds to flood, CH2 to baseflow, CH3 drought with moderate rainfall antecedents, and CH4 drought with flood antecedents. Symbol † indicates that flood concentrations are significantly different than the rest of hydrological conditions, whereas symbol ‡ indicates that flood concentrations are significantly different only with respect to baseflow, both at $p < 0.05$.

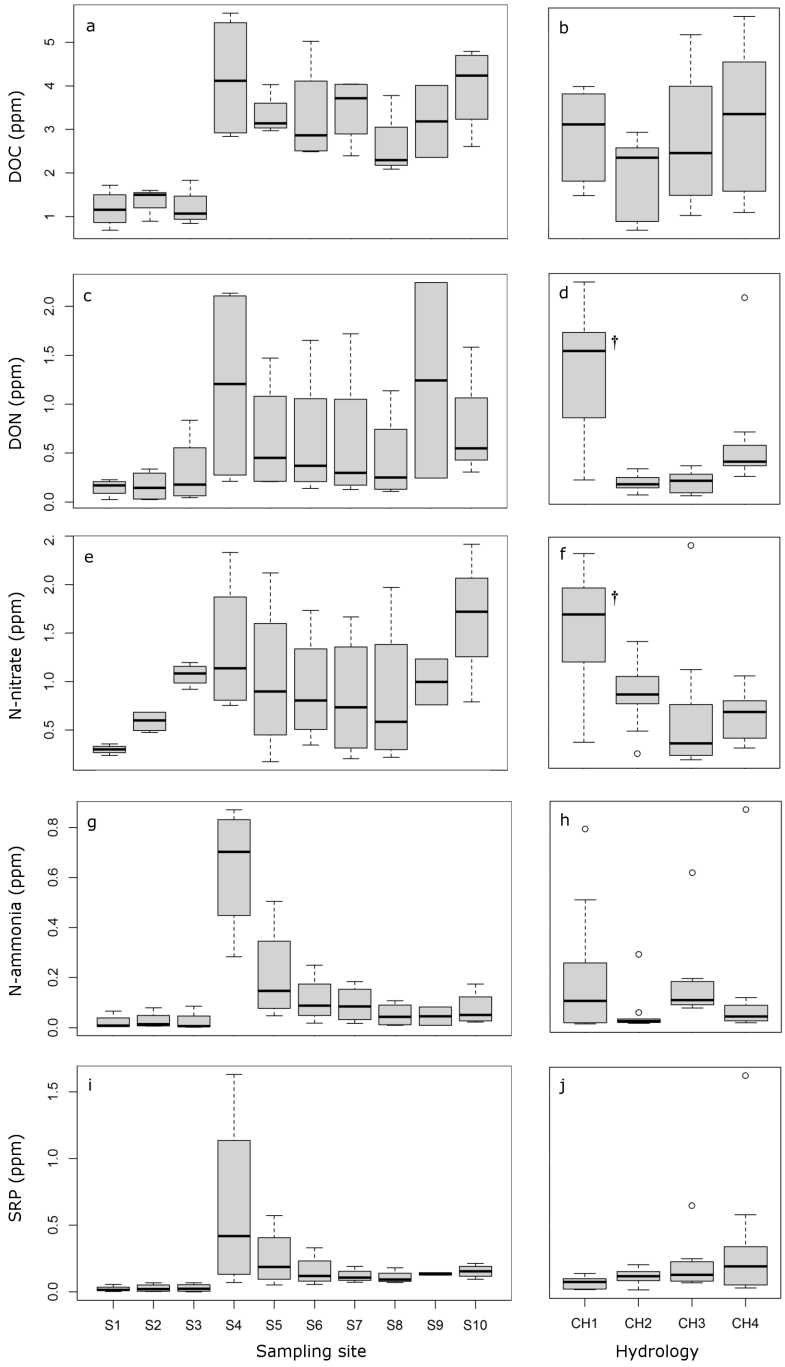

Figure 5.3 – Boxplot representation of the concentrations of non-conservative solutes in space and over hydrological conditions. Site S1 corresponds to the headwaters whereas site S10 corresponds to the river mouth. For the hydrological conditions, CH1 corresponds to flood, CH2 to baseflow, CH3 drought with moderate rainfall antecedents, and CH4 drought with flood antecedents. Symbol † indicates that flood concentrations are significantly different than the rest of hydrological conditions, whereas symbol ‡ indicates that flood concentrations are significantly different only with respect to baseflow, both at $p < 0.05$.

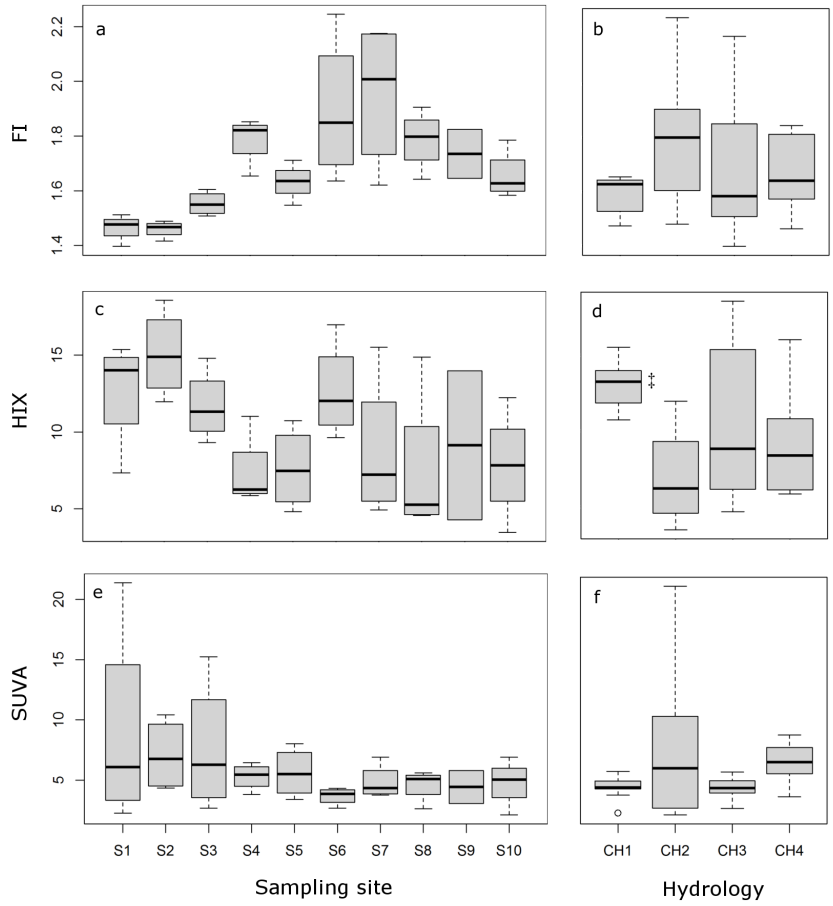

Figure 5.4 – Boxplot representation of the values of DOM optical indices in space and over hydrological conditions. Site S1 corresponds to the headwaters whereas site S10 corresponds to the river mouth. For the hydrological conditions, CH1 corresponds to flood, CH2 to baseflow, CH3 drought with moderate rainfall antecedents, and CH4 drought with flood antecedents. Symbol † indicates that flood concentrations are significantly different than the rest of hydrological conditions, whereas symbol ‡ indicates that flood concentrations are significantly different only with respect to baseflow, both at $p < 0.05$.

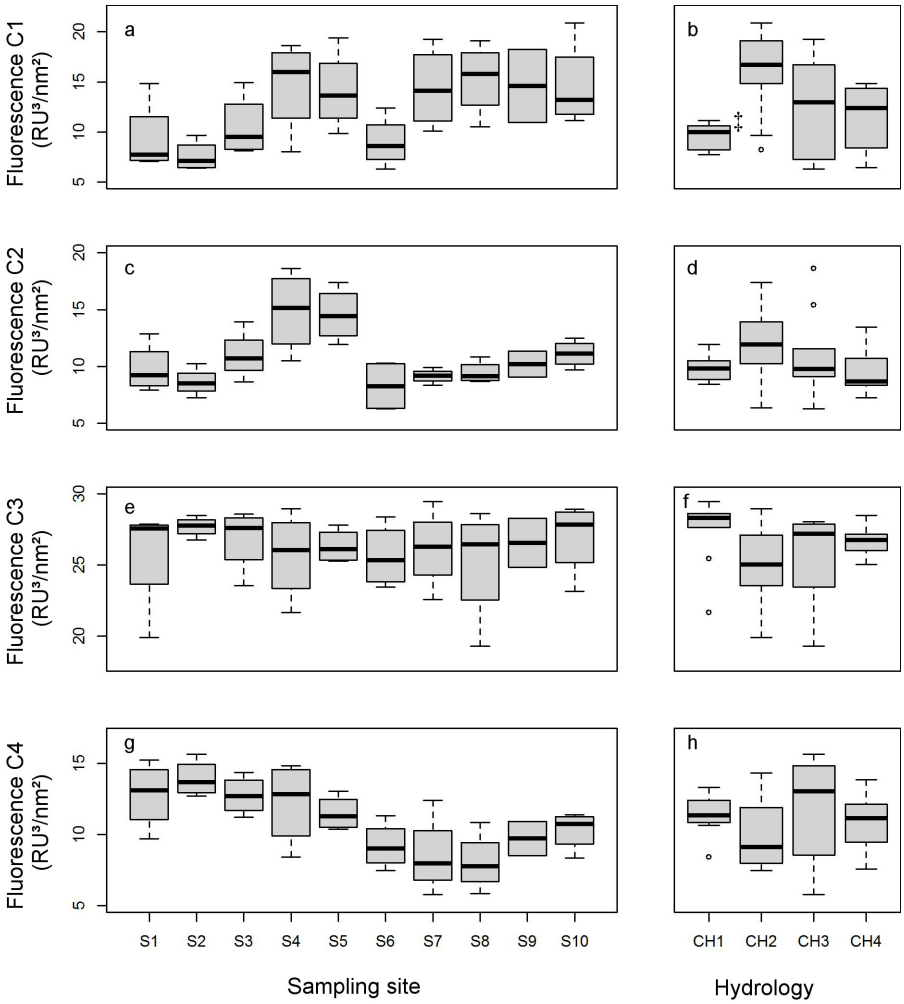

Figure 5.5 – Boxplot representation of the volumes of EEM components in space and over hydrological conditions. Site S1 corresponds to the headwaters whereas site S10 corresponds to the river mouth. For the hydrological conditions, CH1 corresponds to flood, CH2 to baseflow, CH3 drought with moderate rainfall antecedents, and CH4 drought with flood antecedents. Symbol † indicates that flood concentrations are significantly different than the rest of hydrological conditions, whereas symbol ‡ indicates that flood concentrations are significantly different only with respect to baseflow, both at $p < 0.05$.

		Spatial variability				Temporal variability									
		CH1	CH2	CH3	CH4	S1	S2	S3	S4	S5	S6	S7	S8	S9 (*)	S10 (**)
Conductivity	Mean	369.1	437.8	461.7	389.3	89.6	104.7	129.0	516.0	490.5	446.4	620.6	575.8	686.8	444.9
μS/cm	Median	331.8	495.8	557.5	488.8	91.1	106.3	126.5	497	508.8	471.0	643.5	584.8	686.8	503.5
	Std. Dev.	259.6	247.7	289.0	239.5	16.6	17.4	20.3	187.5	124.4	74.9	153.6	70.4	68.2	256.6
	n	10	10	9	9	4	4	4	4	4	4	4	4	2	2
dO_2 (***)	Mean	n.a.	8.763	9.592	8.924	8.392	8.922	9.168	5.770	11.240	7.917	7.693	10.688	6.310	12.865
(mg/L)	Median	n.a.	8.943	8.575	8.700	8.335	8.815	9.220	5.575	11.835	7.920	8.400	10.450	6.310	12.865
	Std. Dev.	n.a.	2.484	3.126	2.132	0.284	0.229	0.261	1.810	2.423	0.060	1.491	3.124	n.a.	2.675
	n	n.a.	10	10	10	4	4	4	4	4	4	4	4	1	3
dO_2 (***)	Mean	n.a.	95.5	117.4	103.5	87.0	93.7	93.7	66.6	137.6	89.9	91.7	131.4	69.9	166.4
(% sat.)	Median	n.a.	90.4	97.0	93.3	89.7	94.8	93.3	66.0	142.7	92.2	97.0	117.3	69.9	160.2
	Std. Dev.	n.a.	33.3	49.1	28.5	7.6	3.3	3.1	26.6	28.4	4.0	19.2	48.4	n.a.	46.2
	n	n.a.	10	10	10	4	4	4	4	4	4	4	4	2	4
pH	Mean	7.85	8.47	8.07	8.04	7.80	7.90	7.91	7.94	8.37	7.90	7.86	8.46	8	8.91
	Median	7.89	8.33	7.82	7.79	7.75	7.85	7.92	7.85	8.21	7.83	7.77	8.42	8	9.02
	Std. Dev.	0.16	0.38	0.52	0.63	0.27	0.20	0.27	0.24	0.56	0.22	0.36	0.48	0.51	0.64
	n	10	10	10	10	4	4	4	4	4	4	4	4	2	4
T	Mean	8.6	17.5	22.8	22.3	12.1	13.2	13.4	17.6	20.6	18.5	19.0	20.7	15.1	24.1
(^{o}C)	Median	9.0	19.7	22.8	23.0	13.1	14.5	14.8	19.4	23.5	20.9	21.2	22.4	15.1	27.2
	Std. Dev.	1.5	4.5	5.3	5.0	4.6	5.3	4.5	7.1	8.1	6.5	6.8	7.9	6.8	9.9
	n	10	10	10	10	4	4	4	4	4	4	4	4	2	4
N-NO_3^-	Mean	1.485	0.845	0.690	0.564	0.299	0.589	1.071	1.339	1.023	0.922	0.835	0.840	0.997	1.232
(mg/L)	Median	1.694	0.857	0.345	0.669	0.300	0.598	1.084	1.136	0.899	0.805	0.734	0.585	0.997	1.256
	Std. Dev.	0.656	0.325	0.721	0.320	0.049	0.109	0.117	0.722	0.821	0.593	0.660	0.793	0.335	1.057
	n	10	10	10	10	4	4	4	4	4	4	4	4	2	4
N-NH_4^+	Mean	0.200	0.042	0.166	0.132	0.022	0.028	0.025	0.640	0.212	0.111	0.092	0.051	0.046	0.075
(mg/L)	Median	0.095	0.013	0.099	0.032	0.008	0.013	0.006	0.703	0.147	0.088	0.084	0.043	0.046	0.051
	Std. Dev.	0.258	0.086	0.173	0.279	0.030	0.035	0.041	0.261	0.204	0.098	0.075	0.048	0.052	0.070
	n	10	10	10	10	4	4	4	4	4	4	4	4	2	4
SRP	Mean	0.057	0.089	0.181	0.351	0.018	0.027	0.028	0.633	0.249	0.156	0.119	0.109	0.135	0.154
(mg/L)	Median	0.062	0.102	0.116	0.180	0.009	0.020	0.023	0.417	0.187	0.119	0.107	0.093	0.135	0.154
	Std. Dev.	0.041	0.069	0.184	0.511	0.025	0.030	0.031	0.709	0.229	0.121	0.050	0.049	0.013	0.050
	n	10	10	10	10	4	4	4	4	4	4	4	4	2	4
Cl^-	Mean	36.880	55.267	61.895	40.515	6.665	7.009	8.702	68.186	57.596	45.014	66.620	85.207	68.799	55.317
(mg/L)	Median	25.538	62.808	58.849	42.847	6.684	6.744	8.430	58.219	66.981	46.772	60.762	92.727	68.799	59.025
	Std. Dev.	35.887	36.489	51.442	31.105	0.808	0.996	1.438	48.309	21.603	14.523	35.434	25.624	1.573	41.031
	n	10	10	9	9	4	4	4	4	4	4	4	4	2	2
SO_4^{2-}	Mean	22.408	33.281	39.270	33.191	7.445	8.324	10.592	42.294	42.913	34.126	54.274	47.380	34.948	35.181
(mg/L)	Median	24.133	39.540	41.938	38.906	7.053	8.191	10.263	38.923	47.208	36.230	55.020	51.108	34.948	39.130
	Std. Dev.	10.806	17.648	28.356	21.554	1.326	0.718	1.257	19.482	12.340	8.052	22.690	10.006	3.592	21.385
	n	10	10	9	9	4	4	4	4	4	4	4	4	2	2

Table 5.1 – Data of the measured physico-chemical parameters, summarised by sampling site and by hydrological conditon.

		Spatial variability				Temporal variability									
		CH1	CH2	CH3	CH4	S1	S2	S3	S4	S5	S6	S7	S8	S9 (*)	S10
DOC	Mean	3.004	2.020	2.841	3.224	1.178	1.373	1.201	4.186	3.319	3.310	3.466	2.614	3.183	3.968
(mg/L)	Median	3.150	2.376	2.486	3.394	1.152	1.500	1.065	4.119	3.139	2.865	3.715	2.293	3.183	4.235
	Std. Dev.	0.986	0.874	1.579	1.716	0.435	0.323	0.436	1.476	0.480	1.188	0.776	0.785	1.167	0.993
	n	10	10	9	9	4	4	4	4	4	4	4	4	2	4
DON	Mean	1.322	0.458	0.148	0.593	0.148	0.164	0.309	1.191	0.646	0.632	0.611	0.437	1.243	0.610
(mg/L)	Median	1.527	0.144	0.153	0.379	0.170	0.145	0.179	1.208	0.451	0.370	0.299	0.251	1.243	0.428
	Std. Dev.	0.712	0.087	0.121	0.574	0.088	0.157	0.364	1.059	0.595	0.693	0.746	0.479	1.414	0.686
	n	10	10	9	9	4	4	4	4	4	4	4	4	2	4
SUVA	Mean	4.424	7.767	4.355	6.418	0.157	7.075	7.615	5.305	5.617	3.691	4.845	4.608	4.440	4.782
	Median	4.446	6.050	4.385	6.581	0.364	6.772	6.278	5.474	5.519	3.879	4.352	5.091	4.440	5.046
	Std. Dev.	0.926	6.330	0.941	1.816	1.059	3.032	5.560	1.120	2.073	0.723	1.431	1.333	1.924	1.971
	n	10	10	9	9	4	4	4	4	4	4	4	4	2	4
FI	Mean	1.596	1.803	1.689	1.669	0.595	1.460	1.553	1.787	1.633	1.895	1.953	1.786	1.735	1.656
	Median	1.628	1.801	1.583	1.640	0.693	1.468	1.550	1.822	1.636	1.849	2.008	1.798	1.735	1.627
	Std. Dev.	0.066	0.257	0.264	0.148	0.746	0.031	0.044	0.090	0.067	0.266	0.270	0.109	0.126	0.089
	n	10	10	9	9	4	4	4	4	4	4	4	4	2	4
HIX	Mean	13.049	6.942	10.868	9.460	12.687	15.085	11.693	7.340	7.617	12.672	8.727	7.490	9.133	7.841
	Median	13.249	6.206	8.820	8.392	14.018	14.901	11.331	6.247	7.463	12.035	7.229	5.262	9.133	7.826
	Std. Dev.	1.596	2.987	5.523	3.689	4.372	2.857	2.324	2.459	2.668	3.150	4.755	4.956	6.863	3.589
	n	10	10	9	9	4	4	4	4	4	4	4	4	2	4
C1	Mean	9627	15864	12189	11429	9353	7567	10523	14655	14141	8996	14411	15309	14588	14621
	Median	9983	16693	12952	12397	7732	7109	9522	15984	13657	8621	14141	15794	14588	13227
	Std. Dev.	1271	4145	5302	3288	3700	1523	3153	4694	3963	2546	4104	3637	5144	4335
	n	10	10	9	9	4	4	4	4	4	4	4	4	2	4
C2	Mean	9807	12162	11055	9841	9802	8621	11002	14859	14541	8276	9158	9460	10211	11117
	Median	9807	11926	9766	8686	9223	8500	10730	15166	14424	8269	9196	9148	10211	11129
	Std. Dev.	1092	3356	3765	2301	2177	1228	2188	3617	2375	2259	640	991	1621	1187
	n	10	10	9	9	4	4	4	4	4	4	4	4	2	4
C3	Mean	27473	25189	25677	26662	25727	27694	26834	25669	26314	25621	26146	25199	26550	26939
	Median	28323	25041	27188	26764	27583	27758	27607	26040	26097	25334	26282	26458	26550	27840
	Std. Dev.	2312	2724	3150	996	3903	716	2269	3113	1200	2252	2819	4110	2438	2638
	n	10	10	9	9	4	4	4	4	4	4	4	4	2	4
C4	Mean	11428	10139	11501	13004	12788	13934	17250	12230	11485	9188	8521	8043	9705	10289
	Median	11350	9099	13048	13145	13117	13697	17213	12851	11262	8999	7954	7756	9705	10721
	Std. Dev.	1388	2627	3998	2407	2369	1299	1365	2973	1232	1641	2793	2088	1698	1384
	n	10	10	9	9	4	4	4	4	4	4	4	4	2	4

Table 5.2 – Data of the DOM-related variables, summarised by sampling site and by hydrological conditon.

relative composition of ammonium, nitrate and SRP, whereas during drought their composition becomes gradually more similar to the headwaters, except for the final site which might be rater reflecting the quality of sea water instead of the river water because of the inland penetration of the sea-freshwater interface. Regarding organic solutes in terms of DOC and DON, they exhibit an intermediate profile between conservative and reactive inorganic solutes. In overall, there is a gradual degree of differentiation downstream, which is greatest in site S4. But by taking a closer look, it can also be seen that flood and baseflow have a profile which is comparable to that of conservative tracers, whereas the two droughts produce a profile which is rather comparable with the non conservative nutrients because of the decreasing trend after the peak in S4.

Optical variables, both the optical indices (Figure 5.6d) and EEM components (Figure 5.6e), have distinctively different longitudinal profiles. The main difference is the lack of a consistent increase of the dissimilarity in the headwaters up to S4, observed in the three previous groups of solutes. Other than that, they reflect a strong homogenisation effect of the flooding conditions, expressed by a practically flat and horizontal profile. However, they also exhibit a certain degree of dissimilarity in the second half of the river during drought conditions. In the case of optical indices, the dissimilarity profile increases gradually downstream, being the only case in which baseflow conditions have a distinct behaviour rather than an intermediate expression between flood and drought. Despite these described features, the patterns of longitudinal differentiation for DOM quality are less clear than those of the inorganic reactive solutes.

5.2.6 Relationships between variables: a multivariate approach

The results described above provide evidence of a complex spatio-temporal relationship between types of variables. In order to further relate DOM fluorescence composition with the surrounding hydrochemical environment, we performed a multivariate statistical analysis. First, samples dissimilarities were fitted into a two-dimensional plane by computing non-metric multidimensional scaling (NMDS). The input variables were the EEM components C1 to C4, hence, the new ordination reflected sample dissimilarities in terms of DOM fluorescence composition. Next, it was tested how the rest of variables fit in this new ordination by computing a vector fit and by assessing the significance of each one.

The computed NMDS had a correlation of R^2 over 0.99 between the distances of objects in the obtained NMDS ordination and samples dissimilarities in the original 4-dimensional space. This final ordination is shown in Figures 5.7 A and 5.7 B. The scores of the four fluorescence components appear all at four different directions of the NMDS space, revealing that they are little correlated and, hence, share little

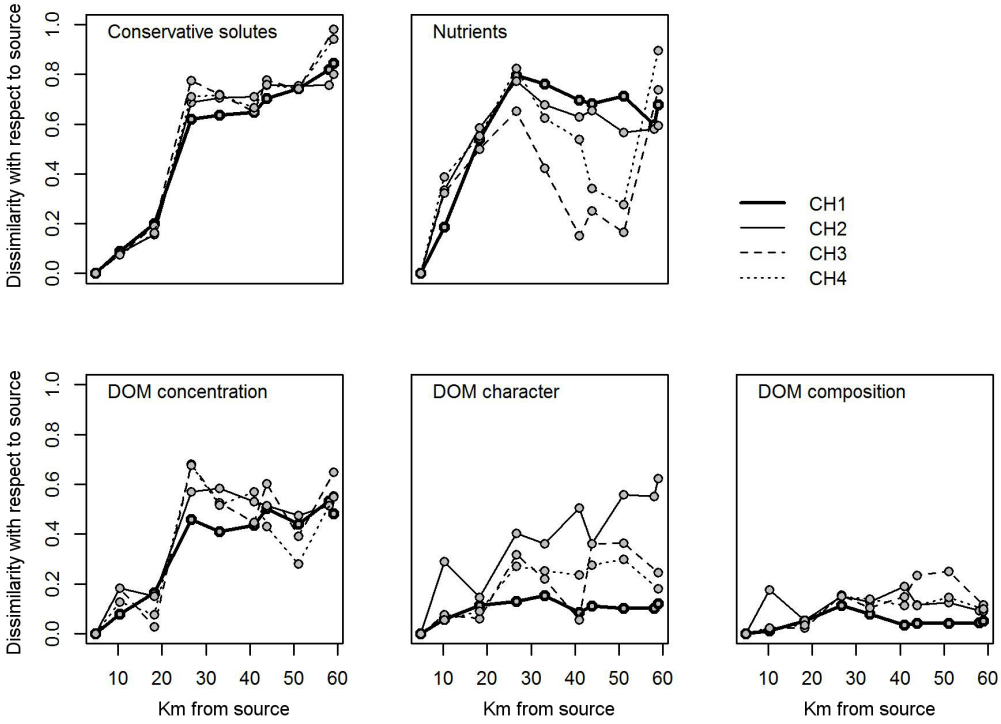

Figure 5.6 – **Biogeochemical dissimilarity profiles** of the different types of variables under study: conservative solutes (electrical conductivity, chlorides, sulfates), non-conservative solutes (nitrate, ammonia, soluble reactive phosphor), DOM concentration (DOC and DON), DOM character (HIX, FI and SUVA) and DOM composition (fluorescence components C1 to C4).

information. In overall, sample and variable scores are more widely dispersed over the first axis. In the positive side there are the two protein-like variables (C1 and C2), whereas in the negative side we find the humic-like ones (C3 and C4). Hence the first axis divides our samples according to the relevance of either protein-like of humic-like moieties. Besides, the second axis further differentiates between the two protein-like components, as C1 is oriented in the negative part, and C2 in the positive part. This suggests that the two components, despite having a similar composition, may be driven by different processes and sources.

For the sake of facilitating the interpretation of the samples distribution on the NMDS plane, samples have been grouped by sampling site Figure 5.7 A, reflecting the spatial extent; and by hydrological conditions Figure 5.7 B, reflecting the temporal extent. It should be noted there that both figures correspond to the same NMDS compoutation and only the visualisation and grouping of the samples differs. Regarding Figure 5.7 A, corresponding to the spatial extent, the location of

the centroids for the different sampling sites clearly reflects three different groups. On the negative side of the first axis appear the headwater sites S1 to S3, as well as site S6 little distance apart. They appear at the direction of the fluorescence components C3 and C4, indicating the predominance of humic-like DOM materials. On the other hand, the sites of the last part of the river (S7 to S10) appear in the positive side of the first axis, directed toward the fluorescence component C1. Finally, sites S4 and S5 appear at the positive side of the second axis, at the same direction as the fluorescence component C2. This indicates that C2 is more directly related to anthropogenic DOM sources, whereas C1 could be more directly attributed to in-stream DOM processes.

A series of hydrochemical variables have been fitted in to the NMDS ordination by means of a vector fitting analysis. Those whose fit had a significance of $p < 0.05$, have been added to the NMDS plot. Interestingly, they appear directed to the three directions described above for the sampling sites centroids. HIX appears at the direction of the headwater sites, FI together with the conservative solutes (Conductivity, chloride and sulphate) appear with the lowland river sites, and finally, DOC, ammonia and SRP appear with sites S4 and S5. Also, it is noteworthy that two variables directly related to DOM held no significance (DON and SUVA), as well as nitrate.

On the other hand, in Figure 5.7 B sample centroids reflect the hydrological extent. The confidence interval circle around the centroid indicates the dispersion degree of the samples of every hydrological condition throughout the NMDS plot. Out of that, it can be observed that during flood the samples are minimally dispersed, indicating little dissimilarities between them. During baseflow and drought, the dispersion gradually increases. Whereas the dispersion degree is similar for baseflow and drought with wet antecedents, it becomes maximal during drought with dry antecedents. Despite this difference between the two droughts in the dispersion degree, they remain similar in the position of the centroid, which indicates similar qualitative DOM trends. The centroids are located near the axes origin and the dispersion occurs throughout the whole plane. This indicates that during drought, both humic-like and protein-like DOM substances are present along the river length. However, in flood and baseflow the samples appear distributed at some specific sectors of the NMDS space. Flood is located in the negative first axis, indicating the prevalence of humic-like and humified DOM substances throughout the river. By contrast, baseflow samples are mainly located in the positive first axes, hence indicating a predominance of protein-like substances of microbial origin.

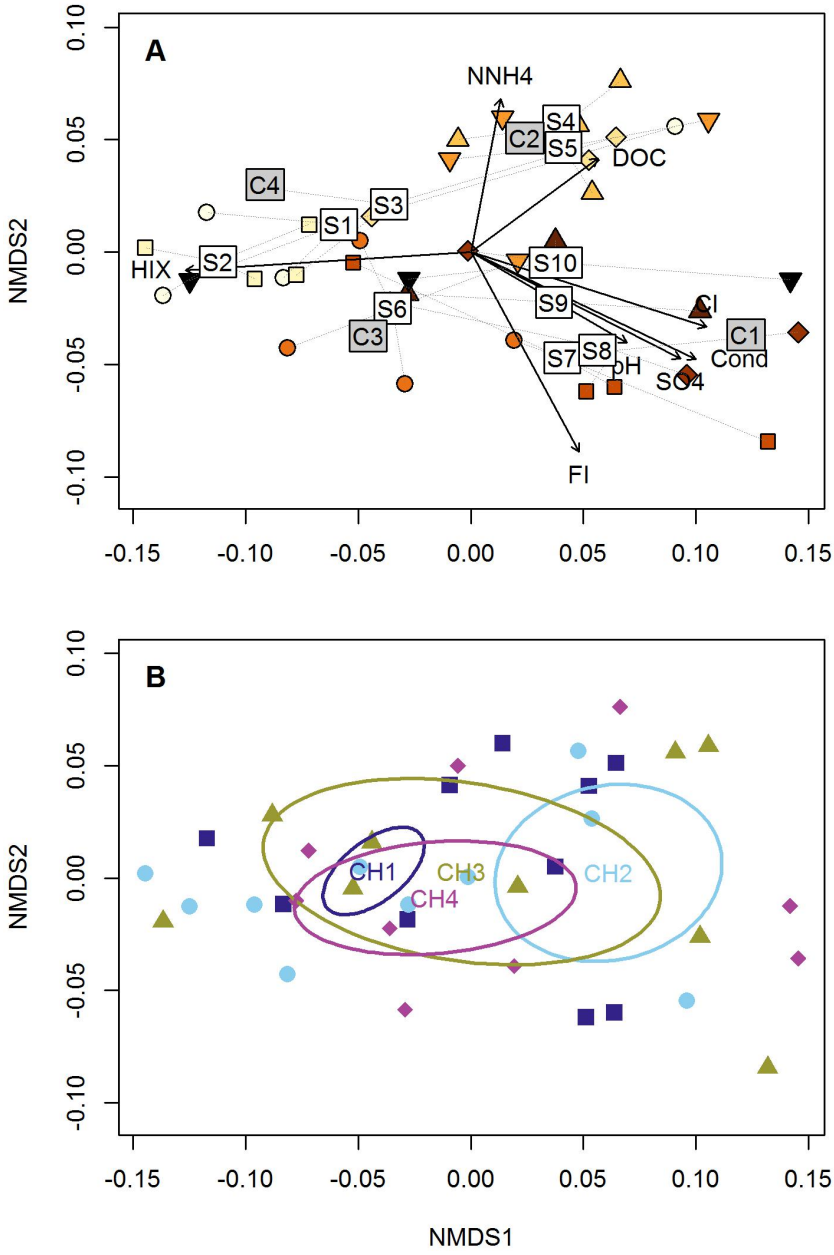

Figure 5.7 – NMDS ordination based DOM on compositional dissimilarities. Gray labels represent the fluorescence components scores, and black arrows, the chemical variables significantly fitted in the ordination ($p < 0.05$). These are only plotted in panel A, but are equivalent for panel B. A) Samples are grouped by sampling site and represented by their centroid. B) Samples are grouped by hydrological conditions. Ellipses around centroids represent confidence areas of the samples dispersion (confidence limit se = 0.95)

5.3 Discussion

5.3.1 Spatio-temporal patterns of inorganic and organic solutes

The water chemistry of La Tordera exhibits some characteristic features along the river length. One clear differentiation are the first three sampling sites, that are situated in the headwaters, from the river source until the village of Santa Maria de Palautordera (sites S1 to S3). These sites are characterised by low concentrations of all measured anions with a small seasonal variability, including both conservative and non-conservative anions. This reflects the low relevance of anthropogenic effluents, as well as a low weathering of the siliceous geological substrate in that part of the river (Mas-Pla et al., 2012).

Next to that, the river runs through the urban and industrial area of Sant Celoni. In this part of the river lies the sampling site S4, which exhibits a drastic change of the chemism. This change mainly corresponds to an increase of the concentrations of the conservative tracers of chloride, sulphate and conductivity, as well as the nutrients of N-NH_4^+, SRP and DOC, together with N-NO_3^- and DON to a certain extent. This increase remains downstream and even further augments in the case of the conservative anions. However, the rest experiment a depletion downstream, even if the influence of human activity is still present throughout sites S5 and S6. This uncoupling between the conservative and the non-conservative solutes evidences the presence of bioreactive processes that are responsible for the availability of these solutes. Some of these nutrients recuperate basal concentrations rapidly after site S4 (N-NH_4^+, SRP), while some others do it more moderately (N-NO_3^- and DON). Interestingly, DOC concentration never recuperates headwater levels, suggesting a lower bioreactive character with respect to the nitrogenated solutes. These evidences of the presence of relevant reactive processes, as well as the presence of confluences with little or non-impacted tributaries, have been previously described as attenuators of the anthropogenic pressure that operates in this central part of the river (Mas-Pla et al., 2012).

Over the different hydrological conditions assessed in this work, the longitudinal dissimilarity profiles for all the mentioned solutes provide evidence of a higher degree of biological reactivity in drought conditions with respect to flood conditions (Figure 5.6). This seasonality is clearer for inorganic than for the organic solutes (compare Figure 5.6b vs 5.6c), hence reflecting a major dependence of the bioreactive character of DOC and DON (and therefore, of DOM concentration) with the hydrological conditions.

Regarding the export capacity of the different solutes, floods are the the hydrological conditions that are more efficient especially for the nitrogenated solutes and SRP. Among them, the most accentuated difference between stormflow and the rest

of hydrological conditions occurs with DON. Pulse flood events have been found to commonly produce [DON]pulse:[DON]baseflow > 1. For Mediterranean rivers without reservoirs (Martin and Harrison, 2011) determined a [DON]pulse:[DON]baseflow ratio of 1.45 from average concentrations of 0.220 and 0.151 mgDON$\cdot L^{-1}$ during flood and baseflow conditions, respectively. In the present study, this ratio is exceeded by far (up to 10.6), and even exceeds the highest ratio reported in Martin and Harrison (2011), which is 2.22 for temperate river systems. While our averages in baseflow and drought are similar to those reported by them, our flood average is much higher (1.322 $\pm$ 0.712), which causes the ratio to increase so much. These results highlight the high potential of La Tordera to export nitrogen in dissolved organic form following flood pulses. While point sources are unlikely to be the origin of such export, because they would have become diluted by the high flows, they may be attributable to a flushing effect reflecting the characteristics of the catchment being drained, i.e. catchment land uses. Evidences in this sense can be found for instance in Lorite-Herrera et al. (2009), who reported high DON concentrations (ranging between 6.3 and 19.8 mg$\cdot L^{-1}$) and annual exports in an agricultural catchment, which were one order of magnitude higher than those from similar pristine systems. This excess was attributed to the leaching and drainage of organic nitrogen from agricultural soils.

In contrast to DON, DOC did not show any significant differences between hydrological conditions. Positive and strong correlations between DOC and discharge have been widely reported, and usually even more consistently than for DON (Clair and Ehrman, 1996). As in this study we are comparing means that include samples from the whole length of the river, spatial complexity and variability may be blurring the usually clear relationship between DOC and discharge. Indeed, statistically significant differences in space were found for DOC and not for DON.

5.3.2 Spatial trends of DOM quality

Unlike for the solutes concentrations, less clear patterns can be observed out of the boxplots in space and over hydrological conditions for the qualitative DOM variables (Figures 5.5 and 5.4). However, a multidimensional approach with an NMDS analysis was useful to elucidate associations between samples and qualitative variables and, also, to unveil interesting longitudinal patterns and hydrological influences. Indeed, the ordination of the samples in a two-dimensional space based on compositional dissimilarities showed a clear segregation of sampling sites into three main groups: one including sites from the headwaters until the middle reaches, another one representing the lowland part of the river, and finally, another one including the sites S4 and S5, situated downstream the anthropogenically impacted area of Sant Celoni. Moreover, the significant fit of optical indices provided more consistency

to this spatial differentiation based on DOM quality. Hence, it becomes clear that DOM undergoes a compositional change as it is being transported downstream.

The headwater sites S1 to S3 are related to components C3 and C4, as well as to the optical index HIX. This provides evidence that the DOM flowing in this part of the river has a predominantly humic-like nature of terrestrial origin. This is as expected, as these sites are located in a mountainous, forested area with minimal anthropogenic perturbation. In similar systems, EEMs have been reported to produce A-C shapes (equivalent to our C3 and C4 components) with high aromatic character (Hudson et al., 2007; Fellman et al., 2010).

Next, sites S4 and S5, appear differentiated in the NMDS as being related to a DOM with tryptophan-like nature (C2), as well as with the presence of nutrients (SRP, N-NH_4^+ and DOC). This differentiation in terms of DOM composition is consistent with previous findings where sewage inputs appeared to release DOM with distinguishable fluorescence signatures with respect to natural riverine DOM (Baker, 2001; Spencer et al., 2007; Henderson et al., 2009) mainly due to intense microbial transformations (Park et al., 2010). Peak T, equivalent to our C2 component, has been even used as a tracer of anthropogenic inputs (Baker, 2002).

After these two sites, the impact of the waste water treatment plant (WWTP) is no longer evident, and site S6 appears near the headwater sites. This rapid shift in the DOM composition can be due, to the one hand, to the inputs of water from non or less polluted tributaries (Fuirosos, Breda, Arbúcies) which may have diluted the upstream DOM quality. On the other hand, protein-like components are considered to be one of the most labile fractions of DOM (but see Cory and Kaplan (2012)), hence the biological uptake of these moieties may have further favoured the depletion of the C2 component. This sounds reasonable at the reaches near site S6, as the river morphology has already become more shallow with increased water residence times and open canopy which facilitate the biophysical opportunities for in-stream DOM processing (Battin et al., 2008). Also, this is in consonance with our evidences of biological retention processes in the second half of the river, described above out of the dissimilarity profiles (Figure 5.6). Another factor that may influence such minimisation of the anthropogenic inputs can be a dilution effect coming from a geological fault that creates an effluence of groundwater with little mineralisation few kilometres upstream of site S6 (named Gorg de Perxistor, described by Mas-Pla and Menció (2008)).

Finally, after the bend of Fogars de la Selva until the river mouth, the nature of DOM exhibits another shift. In this case, its composition is mainly related to C1 component, a fluorescence signal similar to that of tyrosine-like components. It represents a protein-like material, different than that observed for S4 and S5, which correlates with FI. This further suggests an in-stream origin of the DOM for the last part of the river. As in site S6, the persistence of a shallow and open canopy

characteristics, as well as because of the lack of significant tributary inputs, may explain the proliferation of an in-stream DOM production by algae and microbial activity.

5.3.3 Influence of hydrology on the determination of spatial trends

Among the different hydrological conditions sampled in this study, floods represent the conditions in which the maximal spatial homogeneity of DOM character is observed. Under these circumstances, DOM samples appear aggregated in the NMDS plane, suggesting that hardly any qualitative changes occur during the longitudinal transport. Instead, samples from low flow dates (CH3 and CH4) appear more disperse, suggesting a high heterogeneity of DOM properties.

Under flood conditions, the location of the centroid in the positive first axis of the NMDS indicates a strong predominance of humic-like substances of terrestrial origin. This allochthonous input of DOM in the river water during storms has been especially documented for forested catchments (Raymond and Saiers, 2010). During storms, hydrological flow paths shift to more superficial soil horizons richer in DOM which has been accumulated during the low flow periods (Sanderman et al., 2009). This DOM is rapidly flushed out to the riverine channel, resulting in an increase of DOM concentration (Hinton et al., 1997; Mulholland, 2003) and in a qualitative shift to vascular plant-derived humic substances (Hood et al., 2006; Fellman et al., 2009b; Nguyen et al., 2010). This flushing behaviour for DOM has already been documented for the basin of Fuirosos, one of the tributaries of the present study site (Butturini et al., 2008). Fuirosos has a completely forested land cover. In contrast, the catchment of La Tordera has a variety of land uses. Forests are distributed mainly in the upland Montseny Massif and in the Montnegre slopes whereas other land uses including agriculture and urbanisation are found in the lowland. The drainage of these areas has been found to produce a differentiated fluorescence signal in comparison to forested catchments, reflecting the inputs of labile and low humified DOM (Wilson and Xenopoulos, 2009; Williams et al., 2010). However, this signal does not appear to influence in a relevant way the samples collected during flood conditions. It has been reported that the export of DOM from crops and urban areas is primarily driven by the anthropogenic activity rather than by local rainfall events (Duan et al., 2007). Therefore, we suggest that during storms forested areas are those with the highest potential to export DOM to the river. Consequently during stormflow riverine DOM reflects mainly a terrestrial source and this character remains similar along the entire main stem, suggesting a conservative transport.

Surprisingly, this persistance of an humic-like character during flood co-occurs with a high increase of DON concentration (Figure 5.3d). This coexistence seems to discard the option that the exported DON be in the form of protein-like substances.

Rather than that, it may be part of the humic-like fraction, or just not be part of the optical fraction of DOM and hence, not reflected in the EEM components.

However, as soon as rainfall decreases in frequency and in intensity, the dominance of the DOM terrestrial character observed during flood gives way to a longitudinal differentiation of DOM fluorescence properties. During the drying process, not only does discharge decrease, but also change the flowpaths which feed the river (Hinton et al., 1998) and the connection between the river and the terrestrial catchment becomes weaker. The drainage of DOM-rich subsurface soil horizons gradually ceases and the river surface water is mainly sustained by deep groundwater which is poor in DOM. Therefore, drought minimizes the terrestrial sources of riverine DOM, which only remain in the headwater sites (S1-S3). Downstream, samples appear associated to the presence of protein-like substances, either resulting from anthropogenic or in-stream sources.

During low flows the river loses dilution capacity and, therefore, any inputs such as natural tributaries or WWTP effluents have a major impact on the properties of the bulk DOM of the main stem. On the other hand, as flows decrease the connectivity between river reaches diminishes and appear retention areas where water residence times are high. These areas constitute sections of the river channel which increase the microbial opportunities for DOM in-stream processing (Battin et al., 2008), as well as for autotrophic DOM production (Peduzzi et al., 2008). Thus in overall, drought maximises the variety of processes that can potentially modify the bulk DOM pool, and these processes vary along the main stem due to the variety of land uses, anthropogenic influence, and geomorphologic features in the catchment (Jaffe et al., 2008). Therefore during dry conditions the local characteristics and environmental conditions of each riverine reach become the primary drivers of bulk DOM properties, and this results in a spatial mosaic of varied DOM fluorescent signatures. Also, our results suggest that the hydrological antecedents regulate the magnitude of such spatial differences, where longer previous dry periods contribute to amplify the longitudinal heterogeneity of DOM character.

5.3.4 Next steps: Transport vs Reaction, integrating information from the tributaries

Between the contrasted hydrological conditions of flood and drought, baseflow shows an intermediate degree of dispersion in the NMDS plot, and appears clearly differentiated from flood by being centred at the negative first axis, near to the direction of the C1 component and FI. This sharp segregation between the samples of flood and baseflow conditions shows a clear differentiation of DOM quality as soon as the stormflow ceases. This shift from humic-like to protein-like substances, as well as to the shift from terrestrial to in-stream DOM sources suggests that as soon as storm-

flows cease, in-stream processes start to operate and to structure a longitudinal pattern of DOM quality.

Hence, this chapter suggests that lower flows increase the chances for DOM in-stream processing and favour a higher spatial variability of DOM quality and quantity. However, with the sampling design used in this study the relevance of in-stream reactivity over downstream transport cannot be demonstrated. Along the main stem, and especially along the middle reaches, La Tordera receives the waters of numerous tributaries draining a variety of land uses, as well as a number of anthropogenic point sources whose dynamics respond more to socio-economic aspects rather than hydro-climatic. Therefore, the higher spatial variability observed during low flows could be due to the fact that the river has a lower dilution capacity of these inputs and tributaries that join the main stem successively downstream.

Because of that, in order to take a step further and assess the relevance of in-stream processing in shaping the longitudinal patterns of DOM quality and quantity, the longitudinal sampling design used in this study should be complemented with comprehensive information about the waters that the main stem receives along its length.

5.4 Conclusions

The results of this study highlight the importance of hydrology and space in the determination of DOM quantity and quality:

- Along the main stem, the river exhibits three reaches with a consistent differentiated DOM character: the headwaters, the region near the town of Sant Celoni, and the low part of the river flowing between the bend of Fogars de la Selva and the river mouth.
- In the headwaters, DOM has an eminent humic-like character coming from the drainage of the surrounding terrestrial catchment. During flood conditions, this character remains downstream.
- Near Sant Celoni, there is a shift in the DOM quality, expressed as a predominance in the protein-like component C2. A concomitant increase in the chlorides and nutrients content of the water suggests that this shift in the DOM quality is caused by the direct outlets of a WWTP and possibly other industries in the beginning of the river reach.
- In the lower part of the river, high water residence times and light availability favour the conditions for in-stream DOM production and transformation,

which results in an increased FI and predominance of the protein-like EEM component C1.

- Whereas flood conditions induce an homogenisation of the DOM character over the longitudinal dimension, baseflow and drought favour spatial differentiation resulting from the influence of the local characteristics of the river at every reach.

- The hydrological antecedents of a drought period determine the magnitude of the spatial differentiation of DOM character. A longer previous dry period contributed to an amplification of the longitudinal differentiation.

- This suggests a seasonal role of the river with respect to DOM, shifting between transporter and transformer. Such alternation in the transport and processing of DOM can have further implications for the understanding of the carbon cycling at higher scales, and may contribute to the ongoing debate on the role of inland waters on the global carbon cycle.

Chapter 6

Multivariate exploration of DOM quality and reactivity in the main stem of La Tordera

6.1 Introduction

In the previous chapter, a longitudinal assessment of dissolved organic matter (DOM) quality revealed that, at low discharge conditions, there was an emergence of spatial heterogeneity in DOM quantity, fluorescence composition and character. The Fluorescence Index (FI) suggested that in-stream processes could be favouring such spatial heterogeneity, especially in the lower reaches of the river. However, the sampling design did not take into account the quality of the tributaries joining the main stem. Hence, it could not be concluded whether such longitudinal changes were effectively the result of in-stream processes, or on the contrary, the result of the physical mixing with the waters of the tributaries, inputting a diversity of DOM compositions and character.

In order to provide more evidences about the relevance of DOM in-stream processing over transport, in this chapter we use coupled data from the main stem, as well as from the tributaries that originate the water and solutes flow of the main stem. With the use of an end-member mixing analysis (EMMA) approach, we explore to what extent the DOM composition observed in the main stem can be attributed to the physical mixing of the tributaries or, by contrast, whether it responds to biogeochemical interactions during its downstream transport.

Multivariate ordinations have been widely used to study water mixing processes in catchments since the seminal papers of Hooper et al. (1990) and Christophersen

and Hooper (1992). Its most common use has been to identify the water sources in catchments (Hooper, 2001) or groundwater systems (Long and Valder, 2011), hence the ordination is based on conservative tracers (Christophersen and Hooper, 1992), and their main challenge is to identify the adequate number of end-members that can effectively explain the water sources within the system. That is, conservative transport is assumed, and the unknown are the water sources (Barthold et al., 2011; Valder et al., 2012). Here, we use an alternative approach in which the reasoning is the opposite: the sources are well-known (i.e. the tributaries) and the conservative versus non-conservative transport is tested.

For this assessment, six additional surveys were performed in which the tributaries and anthropogenic outlets discharging at the main stem were comprehensively sampled. These water inputs effectively represented the solutes and water flux along the main stem, as it is later shown in Chapter 7. Also, the sampling effort in the main stem was intensified especially in the middle reaches, where the confluences are most frequent. These six additional surveys were conducted between July 2011 and March 2013, and were sought to span a range of hydrological conditions. In this case, we captured an extreme flood event of 156 m^3/s, which was four orders of magnitude higher than the lowest flows conditions, of 0.065 m^3/s. Between these two hydrological extremes, we sampled baseflow (3.10, 1.90 and 1.532 m^3/s) and drought (0.47 m^3/s) conditions (see section 3.2.2 for further details on the sampling strategy). These surveys, added to the longitudinal ones, created altogether a data set of 270 samples, including a longitudinal gradient, a variety of tributaries and anthropogenic outlets, as well as a range of hydrological conditions. This large data set provided the opportunity to better explore spatio-temporal patterns of DOM quality in La Tordera, as well as relationships between chemical and optical parameters.

According to that, the main objectives of this chapter were two-fold:

1. To explore spatio-temporal variation in the DOM composition, and the relationships between the fluorescence components and other optical and chemical variables.

2. To evaluate to what extent the DOM composition observed in the main stem can be explained as solely the physical mixing of input tributaries or, by contrast, whether in-stream processing may be operating.

To address these aims, we performed a fluorescence composition-based non-metric multidimensional scaling (NMDS) analysis with the whole 270-samples data set. This analysis a) was complemented with a vector fit analysis to attain objective 1, and b) was used to create mixing diagrams to address objective 2, as in Christophersen and Hooper (1992): Based on the EMMA approach, we follow the rationale

that if the water composition in the main stem is only the physical mixing of the tributaries, then the main stem samples will lie within the polygon formed by the tributaries in the NMDS ordination.

6.2 Results

6.2.1 Characteristics of the tributaries

The most concentrated inputs of DOM to the main stem of La Tordera corresponded to two industrial effluents (Industry 1 corresponding to site A4 and Industry 2 corresponding to site A8 as shown in Figure 3.5) and the creek of Reixac. The industries represent direct inputs of anthropogenic waters, whereas the creek of Reixac represents a semi-direct input, as it receives the effluents from a waste water treatment plant (WWTP) just some few meters before the confluence with the main stem. The effluent of Industry 1, situated in the industrial area of Sant Celoni, had the highest average dissolved organic carbon (DOC) concentration, consisting of 43.13 $\pm$ 14.19 mg L^{-1}, ranging between 29.86 and 67.6 mg L^{-1}. The effluent of Industry 2, situated in the industrial area of Hostalric, introduced DOC at an average concentration of 18.94 $\pm$ 19.39, ranging between 1.89 and 46.64 mg L^{-1}. The creek of Reixac, situated in the lower part of the river (at 53 km from the river source, and at 8 km to the river mouth) had an average DOC concentration of 13.14 $\pm$ 9.55 mg L^{-1}, ranging between 3.46 and 24.11 mg L^{-1}. All these three inputs had a median DOC concentration (38.72, 13.61 and 12.49, respectively) over the general one (4.46 mg L^{-1}). Regarding dissolved organic nitrogen (DON) concentrations, the same trend could be observed, so that Industry1, Industry2 and the creek of Reixac had a higher median DON concentration than the general one. Again, the most notable DON input was found for Industry 1, which had an average DON concentration of 4.40 $\pm$ 4.80, ranging between 0 and 10.94 mg L^{-1}. Industry 2 and the creek of Reixac had lower average DON concentrations (0.91 $\pm$ 0.82, ranging between 0 and 1.75 mg L^{-1}; and 1.62 $\pm$ 1.92 mg L^{-1}, ranging between 1.92 and 4.49, respectively), although their median (0.95 and 0.80 mg L^{-1}, respectively) was still higher than the overall one (0.221 mg L^{-1}).

For the fluorescence components, it could also be observed that anthropogenic waters had higher intensities than the natural tributaries with little impact, although the differences were not as pronounced as for the quantitative parameters of DOC and DON. For the protein-like fluorescence represented by component C2, the inputs which had a higher median than the overall one (11522 r.u.^{3} nm^{-2}) were the WWTP of Santa Maria de Palautordera, the creek of Pertegàs, Industry1 and the creek of Reixac (whose means were, respectively, 26884, 21258, 31737 and 31477 r.u.^{3} nm^{-2}). The WWTP of Santa Maria de Palautordera are direct inputs

of anthropogenic waters, whereas the creeks of Pertegàs and Reixac are semi-direct inputs, as they receive the waters of a WWTP just some few meters before their confluence with the main stem of La Tordera. The same effluents also had a higher median humic-like fluorescence compared to the overall one, which was of 14390 r.u.^{3} nm^{-2}. The medians of the WWTP of Santa Maria de Palautordera, the creek of Pertegàs, Industry1 and the creek of Reixac were, respectively, of 26884, 21258, 31737 and 31477 r.u.^{3} nm^{-2}, respectively.

6.2.2 Fluorescence composition-based NMDS ordination

Characteristics of the ordination: Variable loadings and vector fitting analysis

The NMDS analysis fitted the original four-dimensional space (defined by the four fluorescence components) into two dimensions with a high goodness of fit (non-metric fit R^2=0.997; linear fit R^2=0.988). As it can be seen in Figures 6.3 and 6.4 the first axis separates the humic-like components C3 and C4 (negative side) from the protein-like components C1 and C2 (positive side).

The results of the vector fitting analysis are overlaid as white labels. Humification Index (HIX) is oriented to the negative side of the first axis, whereas FI and Biological Index (BIX) appear towards the positive direction of the first axis, all with a high level of significance ($p < 0.001$, except Specific Ultra-Violet Absorbance (SUVA) for which $p < 0.05$). This reinforces the interpretation of the components, so that C1 and C2 are related to autochthonously derived components, whereas C3 and C4 are related to terrestrially-derived components.

The secondary axis separates C1 and C3 from C2 and C4, suggesting further differentiation within the protein- and the humic-like groups of components. SUVA appears directed towards the negative secondary axis and C3 ($p < 0.05$). It is noteworthy, though, that SUVA and HIX appear perpendicular, showing independence from one another. A series of chemical solutes, such as DOC, total nitrogen (TN), ammonium and soluble reactive phosphor (SRP) were significantly ($p < 0.01$) oriented to the positive side of the second axis, near C2. This indicates that samples appearing at that direction may be related to nutrient-enriched sites. On the other hand, the chemical solutes with the most conservative behaviour (nitrate, chloride, sulfate and electrical conductivity), did not fit significantly ($p > 0.05$) to the fluorescence DOM-based NMDS ordination.

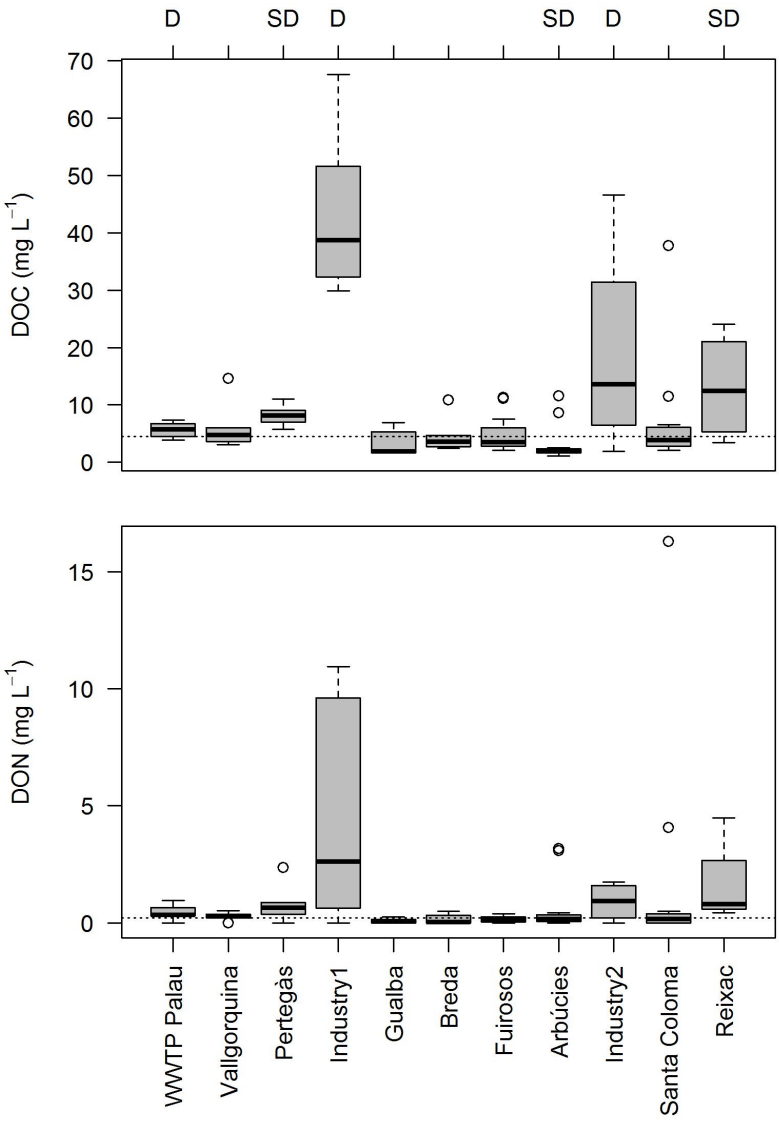

Figure 6.1 – DOC and DON inputs from the tributaries. The top axis indicates whether the inputs refer to D=direct or SD=semi-direct inputs of anthropogenic effluents. The horizontal line corresponds to the overall mean.

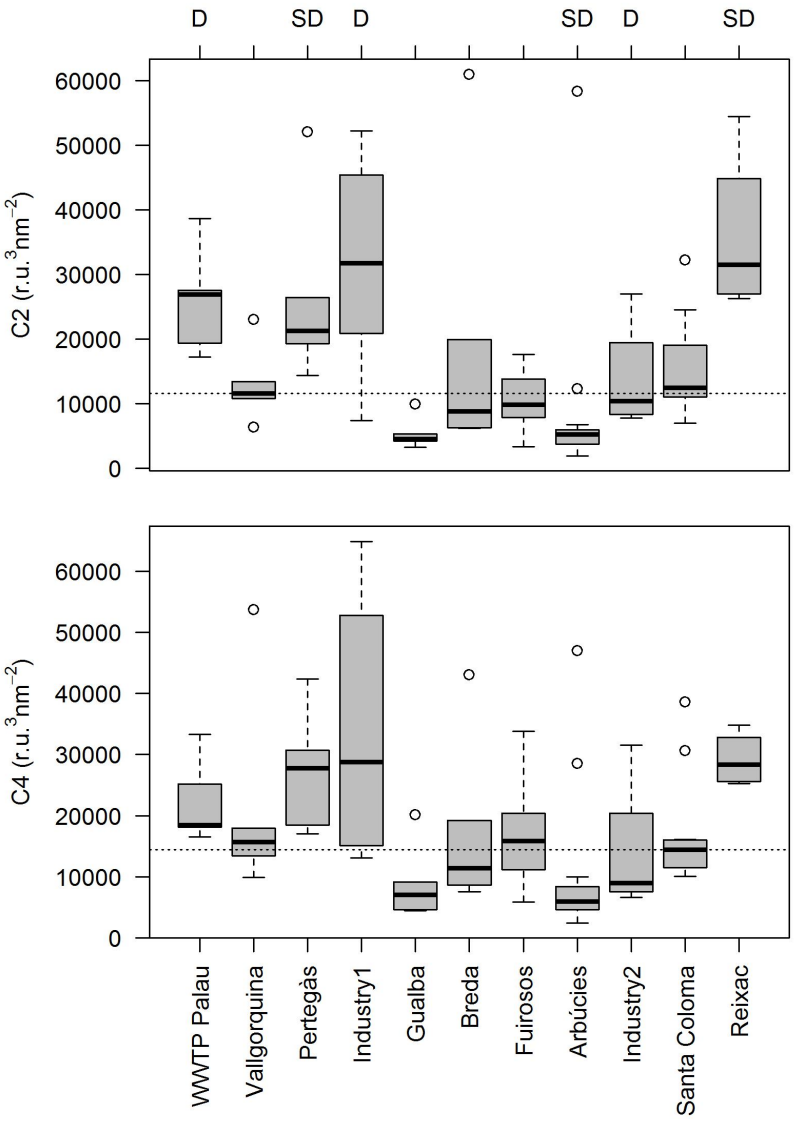

Figure 6.2 – Humic-like and protein-like inputs from the tributaries. The top axis indicates whether the inputs refer to D=direct or SD=semi-direct inputs of anthropogenic effluents. The horizontal line corresponds to the overall mean.

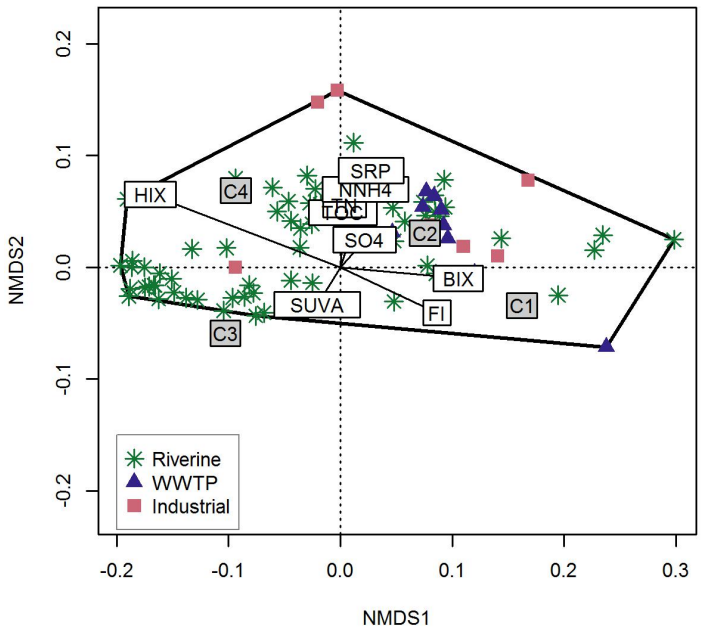

Figure 6.3 – NMDS showing the ordination of the end-members. NMDS analysis, in which only the tributaries and anthropogenic outlets have been plotted. Sites have been coloured to distinguish between natural tribuaties, WWTPs and industries. The polygon outlines the mixing domain defined by all the tributaries (i.e. end-members).

Tributaries as end-members of DOM composition in the main stem

Figure 6.3 shows the tributary sites, which comprise a mixture of natural and anthropogenic water types. The samples corresponding to natural tributaries with minimal anthropogenic impact (riverine category) appear spread over the whole NMDS plane, occupying the space of both sides of the primary and secondary axes. However, industrial effluents appear only in the positive side of the secondary axis. As for WWTP effluents, they show a very clear relationship with the fluorescence compnent C2, suggesting a relationship between C2 and sewage-derived DOM.

Altogether, they delineate a polygon region hereafter referred to as *endmember polygon*. This polygon disginguishes between two regions: the inner region contains samples which can be potentially due to the physical mixing of the waters from the tributaries; and the outer regions, where the composition of the samples cannot be explained solely by the tributaries and, hence, is indicative of the presence of in-stream processing deriving such compositional changes.

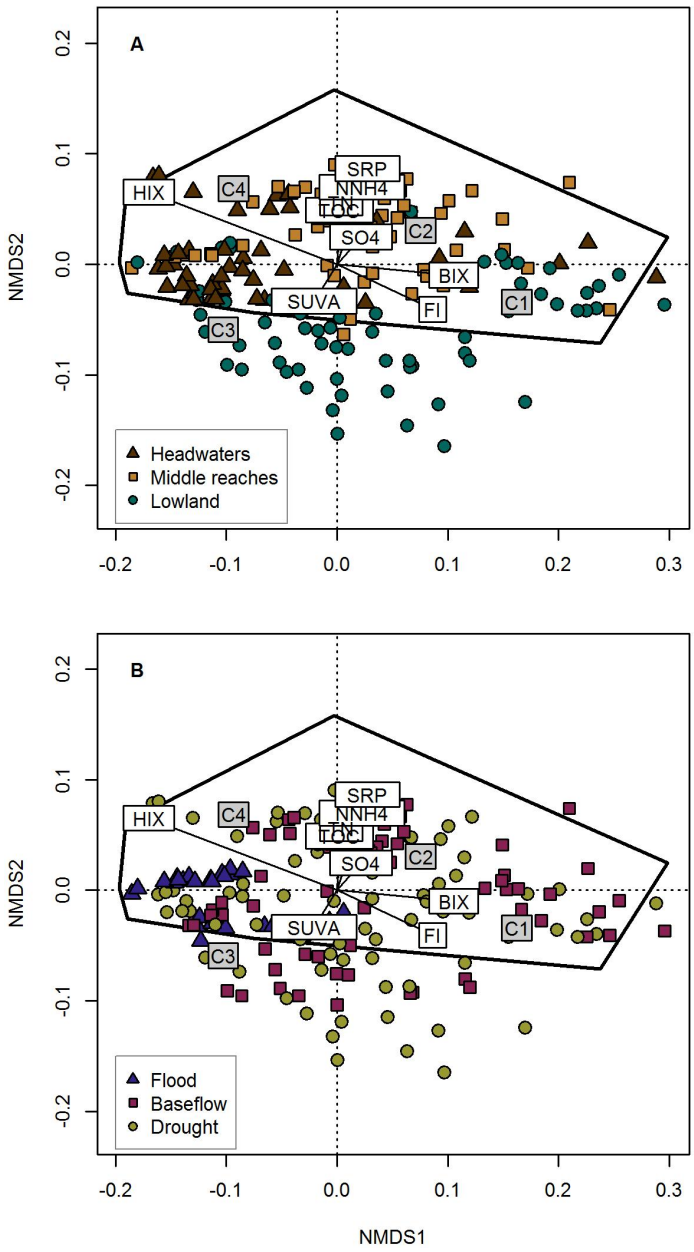

Figure 6.4 – NMDS showing the ordination of the main stem sites. NMDS plot in which only the main stem sites have been plotted and coloured according to their river reach (A), and the hydrological conditions under which they were sampled (B). In panel A, space categories correspond to Headwaters (0 to 20 km from source), middle reaches (20 to 40 km) and lowland (40 to 60 km, i.e. river mouth). In panel B, hydrology categories correspond to flood ($> 4m^3/s$), baseflow (4 to 1 m^3/s) and drought ($< 1m^3/s$) – Discharge measured in Fogars de la Selva.

Ordination patterns due to hydrology and space

In order to explore spatio-temporal patterns of DOM composition in the main stem, Figure 6.4 shows only the main stem sites, as well as the endmember polygon derived in the previous section.

In space (panel A), the most important segregation occurs on the second axis. The sites from the lowland appear on the negative side, whereas those from the headwaters and the middle reaches are found on the positive side. Furthermore, headwater samples appear slightly more concentrated in the region between C3 and C4, similarly to the situation for flood samples in panel B. In relation to the vector fitting analysis, the headwater samples are mainly related to HIX, the sites from the middle reaches to the chemical nutrients and Spectral Ratio (SR), and the lowland sites with the indices BIX and FI, as well as with SUVA and Spectral slope (S). It is noteworthy that all the samples that appear outside of the polygon formed by the tributaries correspond to sites of the lowland.

In panel B, objects are coloured according to the discharge category under which they were sampled. The samples collected during flood conditions appear clearly aligned between the region of C3 and C4. Samples from baseflow and drought conditions appear more broadly distributed throughout the whole NMDS plane. Drought samples seem to be more dispersed and, together with some baseflow samples, occupy the negative secondary axis outside the polygon formed by the tributaries.

6.2.3 Mixing diagrams at a range of hydrological conditions

In order to explore the relevance of in-stream processing over transport, mixing diagrams have been build for those surveys with data about the tributary inputs (Figure 6.5). From the whole NMDS analysis, only the samples from every specific survey have been plotted in each panel, with their corresponding endmember polygon.

During the flood survey, all the main stem samples appear aggregated inside the endmember polygon, at the negative side of the primary axis. This suggests that the DOM composition in the main stem is the result of the physical mixing of some few tributaries, and that those located at the positive side of the primary axis do not have much impact on the final composition in the main stem.

However, in the rest of hydrological conditions, an important number of samples lie in the outer region of the endmember polygon. Lowland sites appear practically always outside the polygon, however, samples from the middle reaches and even from the headwaters can also be found in this outer region, i.e. panels C, D and F.

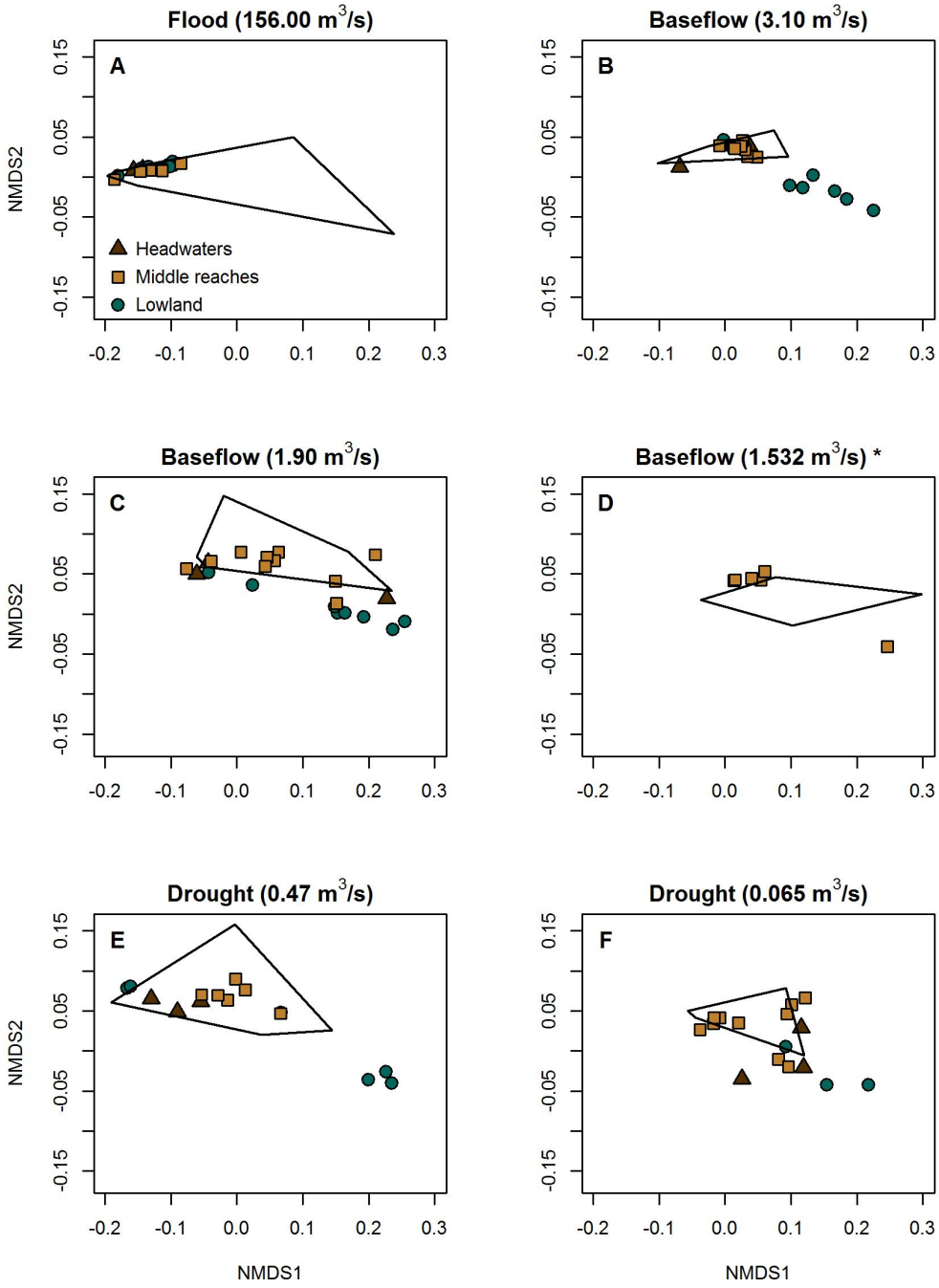

Figure 6.5 – Mixing diagrams at a range of hydrological conditions, derived from the NMDS ordination. The discharge stated in the plot labels was recorded in Fogars de la Selva. (*) In the survey of 1.53 m^3/s only the middle reaches were sampled.

6.3 Discussion

The characteristics of the NMDS ordination perfomed on the complete data set yielded very similar results as the NMDS analysis performed only on the longitudinal samplings (previous chapter). However, here we improved the spatio-temporal resolution, hence obtaining more robust results; and most importantly, we gained the information provided by the tributaries, which revealed the presence of some samples whose composition could not be the result of the physical mixing of the tributaries but, on the contrary, had to be the result of in-stream processing.

6.3.1 Spatio-temporal patterns of DOM composition in the main stem

The NMDS analysis performed in this chapter reinforced the evidences that flood conditions homogenise DOM composition along the whole river length. During such extreme high flows, DOM composition consisted of a high prevalence of humic-like substances, defined by components C3 and C4, and its bulk properties were characterised by a high humification degree. This demonstrates a strong connection of the riverine DOM with the terrestrial catchment, typical of stormflow events in forested catchments (Vidon et al., 2008; Nguyen et al., 2010). However, out of flood conditions, there was a clear segregation of samples according to their longitudinal distribution along the main stem (Figure 6.4).

Headwater sites appeared clustered with the samples collected during flood, suggesting that during such high flows, DOM composition of headwater sites remained constant along the whole length of the river. The middle reaches appeared mainly accumulated in the positive secondary axis, spanning the space between C4 and C2 loadings, and towards the direction of the nutrients from the vector fitting analysis. If we consider the finding that C2 is directly related to WWTP outlets (Figure 6.3), then it follows that the middle reach sites exhibit a gradual shift in its composition from a predominance of C4 – characteristic of the headwaters –, to a predominance of C2 – indicator of sewage water. The relationship with nutrients provided by the vector fitting analysis reflects the fact that the main tributaries discharge to the main stem in these middle reaches. Most of these tributaries flow along important towns and receive the waters of a number of industries and WWTPs. For instance, the creek of Arbúcies receives the waters of the WWTP of Arbúcies in the headwaters, and those of the WWTP of Hostalric in its lower part, right before discharging to La Tordera. Similarly, the creek of Breda receives first the outlet of the WWTP of Breda and then that of the WWTP of Riells i Viabrea. The creek of Gualba receives the waters of the WWTP of Gualba in its middle reaches, and the creek of Pertegàs receives the waters from the WWTP of Sant Celoni a few meters before

its confluence with La Tordera. Finally, Vallgorguina receives the outlets of the WWTPs of the towns of Vallgorguina and Vilalba Sasserra. Therefore when they reach the main stem they are nutrient enriched (Mas-Pla and Menció, 2008).

Finally, the lowland sites appear separated on their own, but dispersedly distributed at the same time, in the area of the negative secondary axis. There, samples appear between the loadings of C3 and C1, hence also exhibiting a range between humic-like and protein-like components, but different from those in the middle reaches. Here, C1 appears to be closely related with high values of BIX and FI, therefore indicating that C1 is the result of in-stream biological activity (McKnight et al., 2001; Huguet et al., 2009). The distance between C1 and the DON endmembers would suggest that, whereas C2 may reflect protein-like components of anthropogenic origin, C1 may be indicator of protein-like components generated in-stream. This would be in line with evidences of non-conservative DOM transport along these lowland sites.

BIX, FI and HIX exhibited a consistent behaviour according to the predominant interpretation of these indices in the literature (Fellman et al., 2010). BIX and FI, as indicators of an in-stream origin of DOM, were related to the protein-like component C1 as well as to lowland sites were non-conservative transport has been found to be predominant. On the other hand, HIX is inversely related to BIX and FI, as it indicates the presence of highly humified humic substances, here related with headwater sites and flood periods when the water DOM reflects the terrestrial drainage of the catchment.

But, more surprisingly, HIX and SUVA vectors appeared at perpendicular directions, showing little relationship between DOM humification degree and aromaticity. Both aspects (humification and aromaticity) have been found to be linked in a number of organic materials (Fuentes et al., 2006); therefore, HIX and SUVA would be expected to covary. However, both indices have been found to provide uncoupled results when compared one another (Singh et al., 2014). Such inconsistencies may arise from the fact that as both indices are obtained with different methods (fluorescence and absorbance) they may be affected by different types of interferences. While SUVA has been found to be very specifically linked to the percent aromatic content (Weishaar et al., 2003), HIX may reflect more complex properties, as it is derived from the shape of a whole emission spectrum. The presence of protein-like fluorescence can interfere with the HIX value because they create a peak in the L spectral region used to calculate HIX (see section 3.3 of the Materials and Methods). In this sense, previous studies found a consistent trend of HIX with the proportion of protein- to humic-like fluorescence ratio (Kowalczuk et al., 2013), together with a strong correlation between HIX and humic-like components (Hunt and Ohno, 2007; Kowalczuk et al., 2013). Overall these inconsistencies reflect that there is not still a good understanding of the chemical properties underlying HIX

and SUVA indices, and therefore, the interpretations of the results may be difficult to generalise beyond the framework of a specific study. Also, this underlines the difficulties of using optical proxies and the cautiousness that should be taken in its systematic application.

6.3.2 The relevance of in-stream processing

The distribution of the tributaries over the NMDS plane delimited the mixing domain of the tributaries for the whole data set (Figure 6.3). Figure 6.4 showed that a series of lowland sites, both collected under baseflow and under drought conditions, appear consistently outside this endmember polygon. This refutes the possibility that these samples result from the physical mixing of the tributaries and, therefore, suggest that DOM composition is driven by in-stream processes. This is not an especially surprising result, if we consider the fact that in this part, the river practically does not receive any relevant tributary; on the contrary the river flows along a shallow floodplain, at conditions that maximize the possibilities for DOM processing: low flow velocities would favour microbial degradation (Battin et al., 2008), and shallow geomorphologies together with an open canopy would favour DOM photochemical oxidation by direct solar radiation (Mostofa et al., 2007). Therefore it seems reasonable to find that along this final river reach, the DOM composition becomes gradually modified from its upstream composition.

On the other hand, the middle reaches are the part of the river that directly receives the inputs of the most important tributaries of the catchment in terms of drainage area and discharge. Although in this part there are also conditions that could favour DOM processing such as direct solar radiation and shallow morphology, the prevalence of in-stream processing over transport may not be so apparent at first, as the water flows faster and confluences occur frequently, at relatively short distances (average distance between confluences of 2 km). Indeed, in the overall view of the NMDS analysis, the middle reaches sites appear inside the endmember polygon. However, when considering every survey separately (Figure 6.5), the mixing diagrams show that in-stream processing may also be operating in the middle reaches, even if at a lower intensity than in the lowland sites.

Furthermore, the mixing diagrams performed for a range of flows (Figure 6.5) revealed that flood conditions were the only ones in which the DOM composition of the whole main stem could be attributed solely to the inputs of the tributaries, and emphasise the evidences for a conservative transport of DOM during flood.

Next steps

Given the evidences of the presence of physical mixing and in-stream processes driving DOM changes along the middle reaches of La Tordera, the following chapters will be devoted to quantify such DOM downstream changes by means of an hydrological (chapter 7) and biogeochemical (chapters 8 and 9) mass balance approach. This will allow to further understand the fate of DOM along a large river reach subject to an important anthropogenic pressure and high variability in the local riverine characteristics; as well as to discern the relevance of in-stream processes as a biogeochemical source or sink of DOM under variable hydrological conditions.

6.4 Conclusions

The NMDS performed on a data set with a higher spatio-temporal resolution, reinforced most of the conclusions drawn in the previous chapter. Moreover, the addition of information from the tributaries which feed the main stem of La Tordera, provided strong evidences of a non-conservative transport of DOM.

- The homogenisation of DOM properties observed along the river length during flood conditions has been effectively found to be due to a conservative transport.
- The longitudinal patchiness in DOM properties that appears at lower flows do not only reflect the successive mixing with tributaries providing DOM with varying properties, but are also due to the occurrence of in-stream processing.
- The lowland sites, located between Fogars de la Selva and the river mouth, exhibited a downstream DOM gradient mainly driven by in-stream processing.
- The headwater sites exhibited consistently a humified humic-like character irrespective of the hydrological conditions, with conservative transport being the main driver of DOM downstream evolution.
- The sites from the middle reaches were found to respond to a more intricate relationship between physical mixing and processing, due to the high frequency of tributary inputs providing a variety of water types, from low to highly polluted.

Results Part III

Mass balance

Chapter 7

Water balance in the middle reaches of La Tordera

7.1 Introduction

The Mediterranean climate is characterised by an annual precipitation accumulated in autumn and spring, while severe droughts typically occur in summer. For this reason, rivers of pluvial origin present an hydrology with an extreme annual seasonality: in winter and autumn rapid flash floods are frequent, whereas in summer, the reduction of the discharge can result in a fragmentation of the longitudinal flow, creating disconnected ponds and even drying out completely.

This variability and seasonality of extreme hydrological events shapes the structure and processes of rivers (Naiman et al., 2008; Poff et al., 1997). In particular, hydrological conditions determine the biogeochemical functioning of the river, as they modify the origin of the solutes and materials that arrive to the river water, modulate the degree of connectivity between the surrounding terrestrial catchment and the river itself, and also determine the opportunities of transformation during the riverine transit (Fisher et al., 2004).

Hence, in order to understand the biogeochemical functioning of La Tordera, first the hydrology needs to be assessed in detail. This chapter is devoted to characterise the longitudinal variation of water flows along a 25-km reach situated in the middle part of La Tordera, between the bends of Sant Celoni and Fogars de la Selva (Figure 3.1 in section 3.1). This is performed by means of a water balance approach. This methodology takes into account all the tributaries that join all along the river reach, as water inputs to the system, and are compared to the flow in the final sampling site, as the outputs of the system. In this study, a mass balance approach is used to

determine whether a) the discharge in the main stem is solely the result of the sum of the upstream receiving tributaries, or b) interactions with the alluvial aquifer are also involved.

Two modelling approaches to predict water discharge along the river length are discussed. Accurate and reliable predictions will be essential in order to perform, in the next chapters, a mass balance study for biogeochemical and microbiological components.

7.2 Results and discussion

7.2.1 The water inputs to the main stem

In our conceptualisation of the water balance system, the inputs correspond either to natural tributaries draining the terrestrial catchment, or to anthropogenic effluents derived from waste water treatment plants (WWTPs) and industries. The main tributaries, draining 85% of the catchment area, were directly measured in-situ. These included the creeks of Vallgorguina, Pertegàs, Breda, Arbúcies, Santa Coloma and Fuirosos. The discharge resulting from the drainage of the remaining 15% of the catchment area was estimated by the Drainage-Area Ratio (see section 3.4.3, Eq. 3.4). During drought, though, these ungauged catchments were so small that they were considered to be dry and not to contribute to the main stem discharge.

During the wetter periods —flood, high and low baseflow —most of the water inputs to the main stem came from natural tributaries (Table 7.1). Especially, the creeks of Arbúcies and Santa Coloma contributed nearly to the half of the total inputs in all three sampling dates. The slopes of the Montseny mountains contributed proportionately with their drainage area in the three sampling dates. However, the slopes of the Montnegre mountains showed a more variable character: during baseflow their contribution was minimal (2.2 and 2.9%), whereas during flood it was especially relevant (15.2%). The headwaters also showed a variable contribution, which was found to be maximal during high baseflow (21.7%).

In the case of drought, though, the inputs of natural origin were minimal, and most of them came from WWTPs and industries (73.3 %). The creeks of Arbúcies and Santa Coloma, who were the main discharge contributors during the wetter dates, had conversely negligible input percentages in summer. This may be due to the fact that, as being the most important tributaries in the catchment, they have a well-developed alluvial formation in their final part before discharging to the main stem. In these reaches they may have lost an important part of their discharge through infiltration, before reaching the main stem. In the case of Santa Coloma, infiltration is so important that the tributary became completely dry by

	Area (km^2)	Discharge (%) Flood	High bf	Low bf	Drought
Natural Measured					
Headwaters	11.2	2.9	21.7	9.5	0.9
Vallgorguina	4.7	4.2	1.9	2.5	7.9
Pertegàs	3.2	6.6	3.9	3.7	3.3
Gualba	3.3	6.6	5.5	5.7	14.7
Breda	4.1	8.6	4.2	5.0	0.0
Arbúcies	14.3	22.3	20.9	25.1	0.0
Sta.Coloma	41.1	17.9	23.0	22.8	0.0
Fuirosos	2.5	4.8	0.3	0.4	0.0
Natural Estimated					
Montnegre	7.3	15.2	2.2	2.9	0.0
Montseny	8.3	8.2	6.4	7.2	0.0
Anthropogenic$^{(*)}$					
WWTPs and Ind.	n.a.	2.9	10.0	15.3	73.3

Table 7.1 – Water inputs to the main stem for every sampling date. * Anthropogenic inputs include industrial and WWTP effluents that are discharged to the main stem both directly, or through some of the natural tributaries (i.e. Vallgorguina, Pertegàs, Gualba, Breda and Arbúcies.)

the confluence. Hence, it did not contribute to the main stem discharge through surface runoff, but, due to the continuity of the alluvial formation in the main stem, it is possible that it did contribute through the groundwater, and probably, that water may have later raised to the surface, as will be discussed in the next sections. In the case of Arbúcies, as well as Breda, the flow was not completely depleted, but still 0.008 and 0.004 $m^3 s^{-1}$, respectively, arrived to the main stem. Our sampling design does not allow to infer what proportion of that final discharge was due to the tributary itself or to the anthropogenic inputs. However, anthropogenic inputs were likely to represent an important part - if not all - of the discharge, as the upstream inputs from the WWTPs were one order of magnitude higher (0.028 and 0.023 $m^3 s^{-1}$, respectively).

In overall, it can be seen that the inputs from anthropogenic sources gradually became more relevant as the river flows decreased (Table 7.1). Thus, during flood they were practically negligible (2.9 %), whereas during drought they represented about two thirds of the total water inputs. This reflects the diminishing dilution capacity of the river as its natural flows decreased.

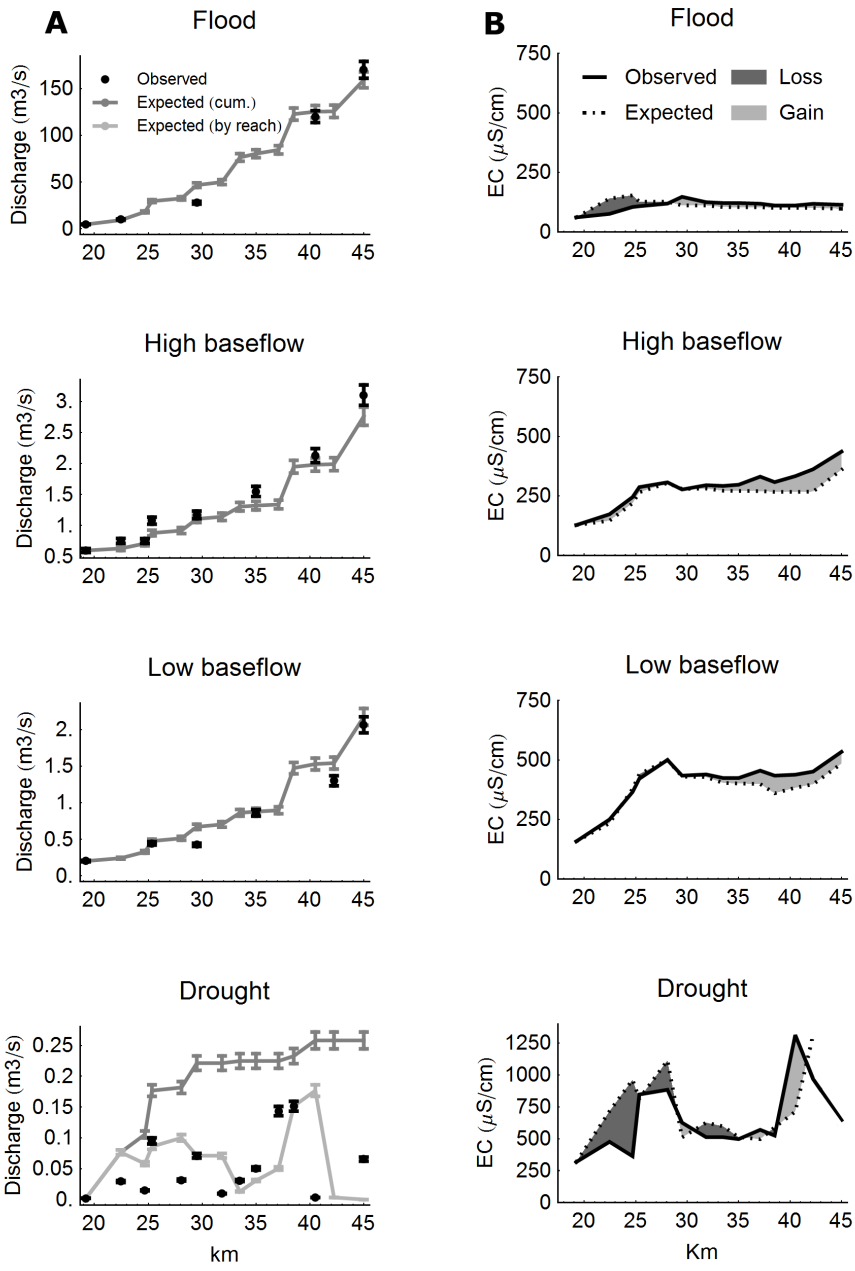

Figure 7.1 – Longitudinal profiles of the river flow and electrical conductivity. A) Longitudinal profiles of the observed and expected river flows. B) Longitudinal profiles of the observed and expected electrical conductivity. Note the change in the y-axis scale for drought, when the conductivities were much higher than in the other dates.

7.2.2 Prediction of the longitudinal discharge by water balance

In order to predict how the flows evolve along the main stem, two mass balance approaches have been used: a *cumulative* one, and a *reach-by-reach* one.

The *cumulative model* calculates the discharge at a given sampling site, assuming that the water flow corresponds to the sum of all the tributaries that joined the main stem upstream (see further details and the specific equations used in section 3.4.3).

According to this model, during flood, high and low baseflow, there was a high correspondence between the observed and the predicted water flows (Figure 7.1 A). This correspondence with empirical data suggests that, under these hydrological conditions, the surface water flow is eminently conservative; that is, there is little interaction between the river and the underlying alluvial aquifer, and all the water flow is the result of the previous tributary inputs.

However, a very different behaviour was observed during drought. In that date, the observed discharge was lower, by far, than the expected one according to the cumulative model. Moreover, the observed discharge along the river did not monotonically increase as it occurred in the wetter periods. Instead, it presented oscillating values between 0 and 0.15 $m^3 s^{-1}$. This important discrepancy suggests that during summer drought there were important water exchanges with the alluvial aquifer which should be taken into account, in order to better predict the longitudinal water flow.

For that purpose, the reach-by-reach model was computed for that sampling date. This model predicts discharge at a given sampling site as the sum of the discharge at the previous sampling site of the main stem, plus the inputs from any tributaries which may have joined in between (see further details and the specific equations used in section 3.4.3). In this way, the difference between every pair of observed-expected discharge values indicates the amount of sourced or infiltrated water in that specific river segment.

By observing the differences between the observed and the expected discharge values at every sampling site (Fig 7.2) it can be seen that there was a longitudinal alternation of a gaining and loosing character along the river. In overall, infiltration exceeded effluence, as it would be naturally expected during that season, characterised by a lack of rainfall and high evapotranspiration rates. Moreover, groundwater withdrawals might have been over-inducing this loss of surface water flow (Sala, 2005).

However, in some specific spots an effluence of groundwater was observed (Figure 7.2). It occurred most importantly in two reaches: one which spanned from 34 to 37 km from source, in an area called Perxistor; and another one which lied in the final part of the studied river length, corresponding to Fogars de la Selva. Both

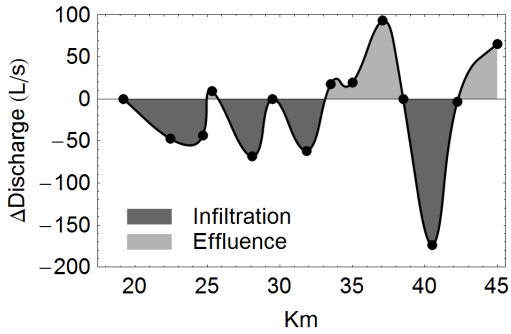

Figure 7.2 – Longitudinal profile of infiltration during the summer drought date. ΔDischarge refers to the difference between the observed water flow, and that predicted by the reach-by-reach model. In overall, as infiltration (0.398 m^3 s^{-1}) exceeded effluence (0.205 m^3 s^{-1}), there was a net loss of water (0.193 m^3 s^{-1}).

in Perxistor and in Fogars de la Selva, this effluent character was already inferred by comparison with the water table in nearby wells, and by the observation of a dilution of the river chemistry (Mas-Pla and Menció, 2008). Besides, in the sampling site located at 25 km from source, after the Pertegàs creek, a very modest water effluence was also detected. Even if the amount of gained water was so low that it could be neglected, it showed indeed a very differentiated character with respect to its neighbouring sampling sites, which were clearly influent. This effluent trend in this specific spot has been previously reported (Mas-Pla et al., 2013) and attributed to an upflow of deep groundwater through regional fault lines. This reasoning may also apply to our site located at 30 km from the river source, where a local modest behaviour is also detected, as it also lies on a regional fault.

7.2.3 Suitability of the models

In light of the results described in the previous section, the cumulative model was found to be suitable to predict the discharge along the main stem during the hydrological conditions of flood, high and low baseflow. This approach has the advantage that only data from the joining tributaries are necessary. This represents a methodological advantage, especially in those wetter periods in which the high flows in the main stem make it difficult to measure discharge by the usual methods (flow-meter or slug addition).

However, during drought the reach-by-reach model was found to be more suitable, in order to take into account the local gains and losses of water. This approach requires an additional sampling effort, as it is necessary to measure discharge at every site in the main stem where we want to calculate a theoretical value. However,

such additional effort during drought is feasible, as the low discharges flowing in the main stem make the task easier.

7.2.4 Verification by the mass balance of a conservative solute

In order to assess the suitability of the cumulative and reach-by-reach approaches for the successive calculation of biogeochemical mass balances, both models have been used to predict electrical conductivity (EC) along the river length under study (Figure 7.1 B). EC is a suitable parameter to test the method as, due to its conservative nature, its changes in concentration downstream should be uniquely a consequence of dilution or concentration processes resulting from the physical mixing with tributaries or inputs of different concentrations. Therefore, if changes in discharge are adequately modelled, the expected EC should ideally be equal to the observed one.

Such correspondence between the observed and the expected EC effectively occurred during flood, high and low baseflow (Figure 7.1 B). There was just a slight discrepancy in the final part of the river reach, in which the observed EC was slightly more concentrated than expected. As it corresponds to an industrial area, this minimal discrepancy can be due to some waste water effluents of little discharge but rich in dissolved salts that have not been taken into account in our sampling design.

However, during drought, the differences between the observed and the expected EC were comparatively more important. Most likely, this may reflect that 14 sampling sites do not have enough resolution to capture the longitudinal variability of the hydrological behaviour of the river. That is, even if between two successive sampling sites we detected a net amount of water infiltration or effluence, it is possible that it resulted from the balance of a complex combination of water loosing and gaining, making it difficult to predict changes in the mass fluxes with exactitude. However, despite these difficulties to empirically characterise such spatially heterogeneous hydrological behaviour, it is noteworthy that both profiles - expected and observed - clearly follow the same trend, especially in the central part (30 to 40 km from the river source). The most important discrepancies are in the second and third sampling sites, indicating that infiltration or withdrawal processes are being underestimated. Also, in the last site there is a notable difference. This is due to the fact that, as in the previous main stem and joining tributary sites the river was completely dry, any observed flow or concentration resulted from an effluent process. This is in line to what was observed in Figure 7.2, where a gaining character of the river was observed in this very final part of the river reach.

7.2.5 Next steps

The verification of the water balance performed in this chapter provided evidence that the cumulative and the reach-by-reach approaches are useful to describe the water balance in La Tordera. These hydrological data will provide the necessary framework to perform, in chapters 8 and 9, a mass balance study for bulk dissolved organic matter (DOM) and its individual fluorescence components, as well as for inorganic nitrogen solutes.

7.3 Conclusions

The results of this chapter mainly highlight that the hydrological behaviour of the water flow along the middle part of the main stem of La Tordera is different during drought or non-drought conditions.

During flood, high and low baseflow:

- most of the water inputs to the main stem of La Tordera come from the natural drainage of the terrestrial catchment, mainly through the creeks of Arbúcies and Santa Coloma.
- The main stem discharge is the result of the sum of the previous water inputs received upstream. This indicates a minor interaction between the river and the underlying alluvial and groundwater aquifers.
- Under these circumstances, the cumulative approach is useful to predict longitudinal changes in water and conservative solutes along the main stem.

Conversely, during summer drought:

- most of the water inputs to the main stem come from anthropogenic sources (either WWTPs or industries). The contribution of these inputs may be essential to maintain the flows in certain sections of the river.
- The river exhibits important interactions with the underlying aquifers, linked to the geo-tectonic structure of the physical environment. Because of that, there is an important spatial heterogeneity of the hydrological behaviour of the river, alternating between a gaining and a loosing character.
- Despite the occurrence of a net infiltration of water over the whole length of the river reach, there are some specific spots that have an effluent character, located consistently with previous findings in the literature.

- Under these circumstances, a reach-by-reach approach has been found to be necessary to predict longitudinal changes in water and conservative solutes along the main stem, in order to take into account local water gains and losses.

Chapter 8

Carbon and nitrogen mass balance: Linking DOC and nitrate

8.1 Introduction

One of the main problems derived from global change is the transformation of the nitrogen cycle. Due to agriculture intensification and the use of synthetic fertilizers, as well as to the increase in fossil fuel combustion, the amount of reactive nitrogen in the environment has increased by an order of magnitude since the industrial revolution (Galloway et al., 2008). This has resulted in a significant nutrient enrichment of rivers, which poses a series of threats like eutrophication, acidification, generation of nitrogen oxides emissions and alteration of the function and structure of the ecosystem (Vitousek et al., 1997) . Because of that, a better understanding of the sources and sinks of nitrogen in rivers is currently of utmost importance, as it may allow improving the capacity to predict nitrogen fate in the ecosystem, hence improving management strategies.

Kinetic studies have improved our understanding of dissolved inorganic nitrogen (DIN) dynamics in rivers (Thouin et al., 2009). However, as these methods are based solely on ambient molecular concentrations (Mulholland et al., 2002; Payn et al., 2005), they overlook the fact that nitrogen transformations are highly dependent on other biogeochemical elements, mainly carbon (Lutz et al., 2011; Johnson et al., 2012). Nitrogen and carbon are concomitantly required by organisms at predictable ratios to satisfy their energetic and nutritional needs (Sterner and Elser, 2002). Therefore, studies with an approach concerning both nitrogen and carbon

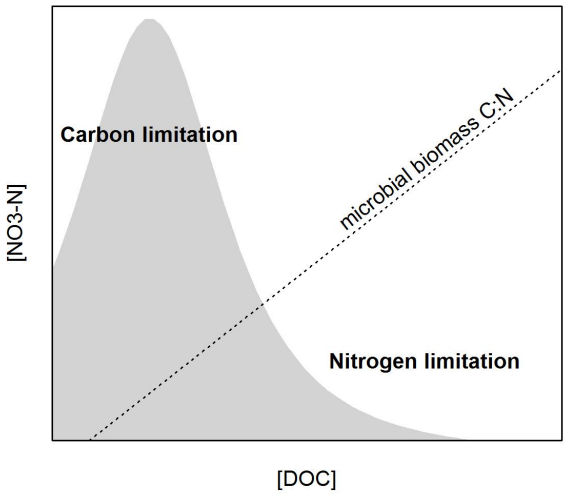

Figure 8.1 – Theoretical framework of the stoichiometric relationship between DOC and nitrate in aquatic ecosystems. Nitrate will accumulate or be depleted from streamwater in relation to its stoichiometric relationship with DOC. The breakpoint between carbon and nitrogen limitation is determined by the C:N ratio of microbial biomass. Modified from Taylor and Townsend (2010)

may provide more accurate insights about the role and fate of DIN in the river system and, moreover, may emphasize the importance of dissolved organic matter (DOM) in regulating the nitrogen cycle. The work of Taylor and Townsend (2010) highlights this link by evidencing a stoichiometric control of nitrate and organic carbon concentrations throughout a wide range of aquatic systems. According to their model, a shift between nitrogen to carbon limitation for microbial heterotrophs is a key determinant of nitrate accrual or depletion in the environment (Figure 8.1). Organic carbon:nitrate ratios lower than the minimum carbon:nitrogen ratio of microbial biomass (which range widely between 3 and 20, (Taylor and Townsend, 2010)) lead to carbon limitation and, therefore, to an accumulation of nitrate in the water; whereas under higher organic carbon:nitrate ratios, nitrogen limitation enhances nitrate depletion and an accumulation of organic carbon. Their findings are consistent with previous observations of negative and nonlinear relationships between dissolved organic carbon (DOC) and nitrate concentrations (Goodale et al., 2005; Evans et al., 2006), and highlight the potential importance of DOM to regulate DIN dynamics in rivers.

Despite the robust trend observed in Taylor and Townsend (2010) – as they included samples from the major Earth ecosystems – their model did not take into account environmental factors. Most notably, hydrology has been identified as a key factor controlling in-stream biogeochemical transformations (Gao et al., 2014), as they modify the periodicity and spatial distribution of areobic – anaerobic conditions (Pinay et al., 2002) and modify the opportunities of interaction between the solutes and the benthic and hyporrheic microbial communities (Battin et al., 2008). Because of that, changing hydrological conditions could alter or modify the strength of the relationship between DOM and DIN.

In this study, we explore the potential role of DOM to control DIN in streamwater by i) complementing the stoichiometric view with a mass-balance approach, and ii) by taking into account contrasting hydrological conditions, including flood, high baseflow, low baseflow and drought. Specifically, we approach and develop this topic in two steps. First, we present the results of the mass balance study performed in the middle reaches of the Tordera (for more details, see chapter 3.1) in order to explore sinks and sources for nitrogen and carbon solutes, independently (including nitrate, ammonium, dissolved organic nitrogen (DON) and DOC). We present the results of the mass balances performed at two scales: a) at the global scale (or reach scale, i.e. the whole river reach is considered as a single big black box) and b) at the local scale (or segment scale, i.e. the whole reach is divided into 13 successive downstream segments, for each of which mass balance was performed). Both views complement each other, as the global mass balance reveals the net function of the river, whereas the local mass balance provides insight about the processing that takes place during the riverine transit. Specifically, our aims are:

- To identify spatio-temporal patterns of nitrogen and carbon processing. That is to say, to explore the longitudinal evolution of nitrogen and carbon processing, and to what extent these spatial patterns vary according to the hydrological conditions.
- To compare the information provided by the global and local mass balances. We explore to what extent the net processing observed at the whole-reach scale is representative of what happens at the segment scale or, conversely, to assess the importance of local characteristics to create a spatial variability of the river biogeochemical function.

Next, we explore to what extent any coupling between carbon and nitrogen processing exists in our study site, for a range of hydrological conditions. The main contribution of this study is that we assess carbon-nitrogen coupling not only in terms of concentrations (as in previous studies, i.e. Goodale et al. (2005); Evans et al. (2006)), but also and most importantly, in terms of mass flux and processing.

For this part, we specifically focus on DOC and nitrate, as they are the most abundant carbon and nitrogen solutes, respectively. In order to explore any potential relationship between DOC and nitrate:

- We further evaluate the role of DOM to control dissolved nitrogen behaviour by comparing our data with the framework described in Taylor and Townsend (2010). With that we aim to contextualize our data, including extreme hydrological events of a Mediterranean system, to the trends observed for a wide range of environments throughout Earth's major freshwater ecosystems.
- We examine correlations between DOC:nitrate stoichiometric ratios and nitrate processing. With that, we aim to complement the stoichiometric approach with the information provided by the mass balance.

According to what was described in (Taylor and Townsend, 2010), we expect that at low DOC:nitrate stoichiometric ratios, nitrate will be either neutrally transported or generated, whereas under high DOC:nitrate ratios, nitrate will be eminently retained.

8.2 Results

8.2.1 Dissolved nitrogen concentrations

In terms of concentrations, nitrate was the most abundant solute in all hydrological conditions (Figure 8.2, first row). During the flood event, the average concentration (2.326 ± 1.099 mg L^{-1}) was slightly higher than that during high and low baseflow (1.157 ± 0.185 and 1.430 ± 0.470 mg L^{-1}, respectively). During baseflow the longitudinal profile of nitrate concentration was eminently steady, however, during flood and drought it exhibited an important spatial variation. During flood there was a prominent peak of nitrate concentration at 25.5 km, after the discharging point of the waste water treatment plant (WWTP) of Sant Celoni. This peak, which exhibited a maximal value of 5.848 mg L^{-1} rapidly returned to basal concentrations in the next few kilometres. On the other hand, in drought nitrate had the largest longitudinal variability (1.107 ± 2.253 mg L^{-1}). It exhibited one main peak in the upstream-most site (8.7 mg L^{-1}) which was rapidly depleted to concentrations lower than 0.5 m L^{-1}, and it was not until km 37-40 that some minor peaks occurred.

Besides nitrate, ammonium and DON had comparatively low concentrations. Ammounium was higher and longitudinally more variable during drought (0.371 ± 1.001 mg L^{-1}) than during flood, high and low baseflow (0.060 ± 0.020, 0.196 ± 0.412 and 0.084 ± 0.102 mg L^{-1}, respectively). For DON, concentrations were

slightly lower during flood (0.116 ± 0.129 mg L^{-1}) than during drought, when concentrations were maximal (0.259 ± 0.327 mg L^{-1}). Baseflow conditions exhibited intermediate DON concentrations. During drought, DON and especially ammonium had a peak in their concentrations after the confluence with the WWTP of Sant Celoni. In the next 5 km, the basal concentrations of both ammonium and DON were recuperated.

8.2.2 Dissolved organic carbon concentrations

During flood conditions, DOC remained steady in space (9.293 ± 1.412 mg L^{-1}) with a slight increasing trend downstream (Figure 8.3, first row). Contrastingly to what was observed for nitrate, DOC did not exhibit any peak after the confluence with the outlet of the WWTP of Sant Celoni. During both high- and low-baseflow, longitudinal profiles of DOC similarly exhibited minimal variability. For each survey, respectively, DOC concentration averaged 2.203 ± 0.405 and 2.360 ± 0.816 mg L^{-1}. In this case, though, the WWTP of Sant Celoni did have some effect, causing a moderate increase in DOC concentrations at 25.5 km.

On the other hand, during drought there was a maximal downstream variability of DOC concentration. Basal values (oscillating near 2 mg L^{-1}) were interrupted by two main peaks: one at 25.5km, after the junction with the WWTP of Sant Celoni (6.972 mg L^{-1}); and another one at 41 km, after the junction with the WWTP of Hostalric (5.670 mg L^{-1}). In both cases, peak concentrations returned to basal values in the following 5-7 kilometers.

8.2.3 Global mass balance: net function of the river

When comparing the sum of the mass that enters the river through the tributaries, with the mass which is flowing out through the downstream-most site, it can be seen that retention predominates both for the dissolved nitrogen solutes and DOC but in different intensities throughout the four hydrological conditions. During flood the retention efficiencies (i.e. retained mass with respect to the inputs) are low and gradually increase through high and low baseflow, until drought when they are maximal (Table 8.1).

During flood nitrate and ammonium have retention efficiencies near 15%, and DOC a production of 5.1%. These low efficiencies indicate a rather conservative behaviour of these solutes during their downstream passage. However, due to the high flows discharging on that date, these low percentages represent the largest amount of retained nitrogen, especially in the form of nitrate, which was the most abundant nitrogen solute (67.58 g NO_3^--N). Also, this was the most conservative survey for DOC, despite the fact that its 5.1% of generation represented a considerable source

Solute	Flood	High baseflow	Low baseflow	Drought
	Δm in gN/s or gC/s (Δm in %)			
N-NO3	-67.58 (-14.7%)	+0.28 (9.3%)	-0.20 (-7.0%)	-0.15 (-81.5%)
N-NH4	-1.48 (-15.2%)	-0.23 (-54.3%)	-1.01 (-90.5)	-0.61 (-92.3%)
DON	-19.85 (-100.0%)	-0.78 (-71.4%)	-0.22 (-40.5%)	-0.10 (-100.0%)
DOC	+80.99 (+5.1%)	-0.69 (-9.8%)	-1.25 (-21.2%)	-1.52 (-73.7%)

Table 8.1 – Global mass balance for the nitrogen and carbon solutes, considering the whole river reach as a single black box. Δm values indicate the difference between the inputs (sum of the tributaries) and the outputs, in absolute (gN or gC) or relative terms (%). Positive values indicate released or produced mass, whereas negative values indicate retained or uptaken mass.

of carbon mass (81.00g/s of DOC). Overall, these results emphasize that small efficiencies during flood represented the most important amounts of mass release or retention in absolute terms.

At lower flows retention efficiencies increased, especially in the case of ammonium. In high baseflow, the retention of ammonium was already important (54.3%), and was followed by a retention of 90% during low baseflow and drought. Nitrate and DOC, though, remained at low efficiencies during baseflow, and it was only during drought when they had importantly high retentions (81.47% and 73.7%, respectively). Despite these high efficiencies during drought, in absolute terms this represented the lowest amounts of retained mass among the four surveys.

DON, in its turn, was an exception to this overall trend, and exhibited high retention rates higher than 70% during drought, high baseflow and flood conditions. In absolute terms, due to the low concentrations of DON in streamwater, these high retention efficiencies represented similar mass amounts as the nitrogen retained as ammonium or nitrate.

8.2.4 Local mass balances: Processing heterogeneity along the main stem

The results of the local mass-balances, performed at successive river segments throughout the whole river reach under study, further refines the black box view described in the previous section. Figure 8.2 and Figure 8.3 (second and third rows) show the longitudinal distribution of mass generation and retention for the dissolved nitrogen and carbon solutes, calculated for the four different surveys.

All surveys exhibit a clear predominance of mass retention in most river segments. For nitrogen, the results in terms of absolute mass flux (Figure 8.2, second row) show an increasing trend downstream of the retained mass which is consistent

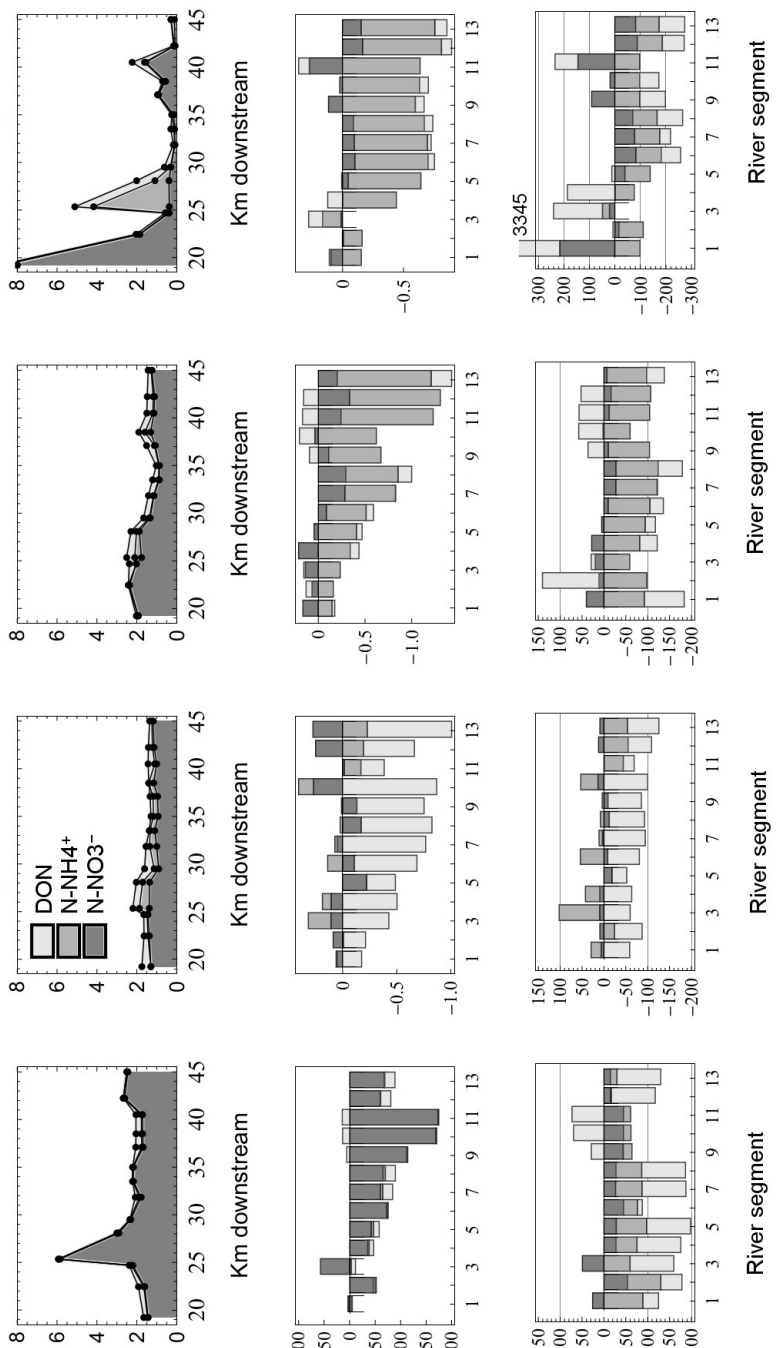

Figure 8.2 – Concentrations and mass fluxes for nitrogen compounds along the main stem of the Tordera. First row corresponds to observed concentrations. The other rows correspond to the differences between the inputs and the outputs in every river segment, expressed in absolute terms (second row, the different scale of the y-axis for the flood survey should be noted) and as percentage (third row, the different scale of the y-axis for the drought survey should be noted). Positive mass fluxes indicate release or generation, whereas negative mass fluxes refer to retention or assimilation processes. In all plots, the different categories (i.e. solutes) are stacked.

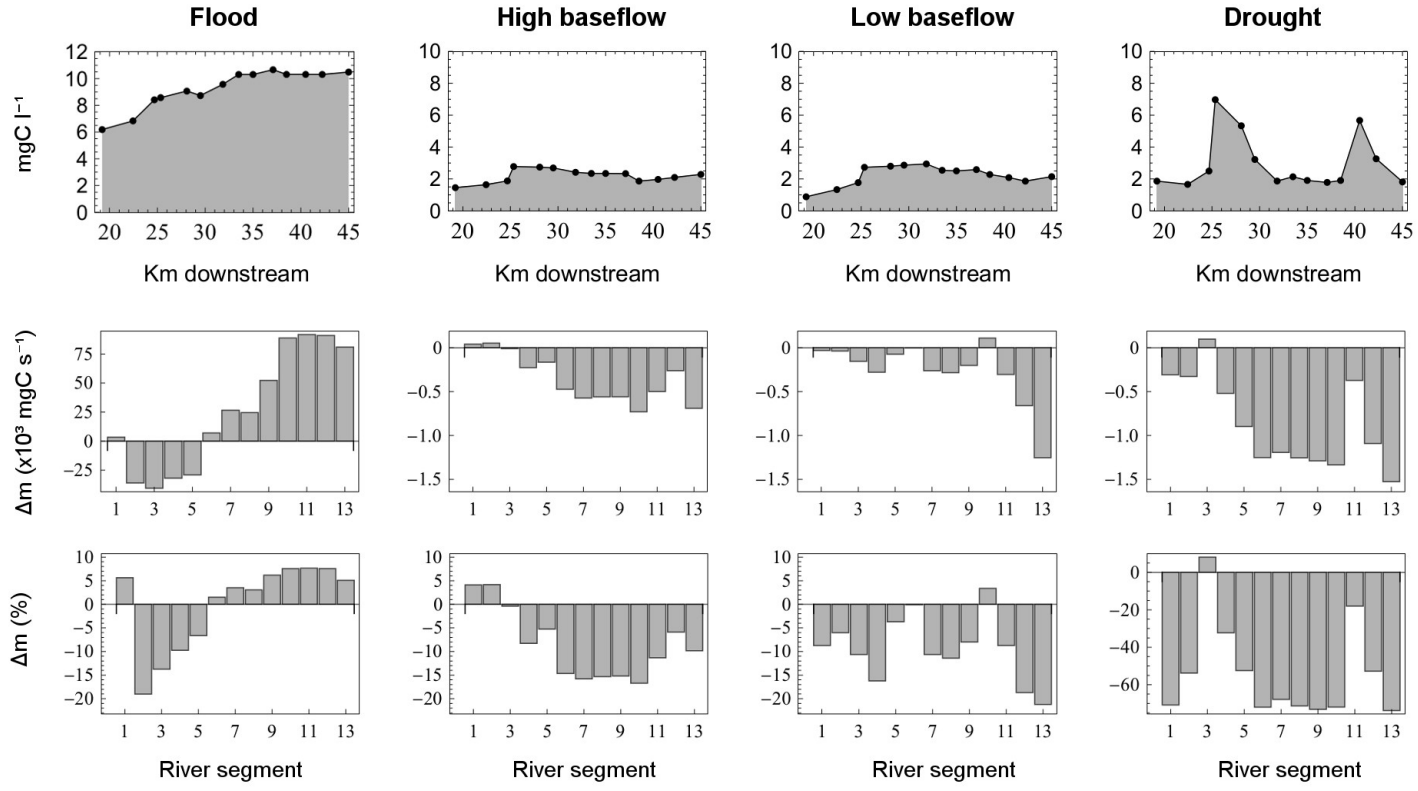

Figure 8.3 – Concentrations and mass fluxes for DOC along the main stem of the Tordera. First row corresponds to observed concentrations. The other rows correspond to the differences between the inputs and the outputs in every river segment, expressed in absolute terms (second row, the different scale of the y-axis for the flood survey should be noted) and as percentage (third row, the different scale of the y-axis for the drought survey should be noted). Positive mass fluxes indicate release or generation, whereas negative mass fluxes refer to retention or assimilation processes. In all plots, the different categories (i.e. solutes) are stacked.

throughout all four hydrological conditions. However, the main form of assimilated nitrogen differed in every survey. While in high-baseflow most of the retained nitrogen mass was in the form of DON, in low-baseflow and drought assimilation occurred mainly in the form of ammonium. Finally during flood most nitrogen mass retention was in the form of nitrate.

In the case of DOC, from high baseflow to drought there was also a predominance of retention, especially in the downstream-most sites (Figure 8.3, second row). During drought, though, segments 3rd and 10th – coinciding with the outlets of the WWTPs of Sant Celoni and Hostalric – had comparatively reduced retentions. In both cases, the retention capacity was rapidly recuperated in the following two segments. During flood, a different pattern was observed, and it was characterised by a gradual shift from mass retention in the first half of the main stem, to mass generation in the second half.

During high and low baseflow, the mass balance results in absolute terms (i.e. absolute processed mass) are consistent with what was observed in relative terms (i.e. mass processing efficiency). That is, the solute that had the largest amounts of mass retentions, also exhibited the largest retention efficiencies. Specifically, during high baseflow DON was both the most efficiently retained solute, as well as the main form of nitrogen mass retention; whereas during low baseflow, the same occurs with ammonium. However, during flood and drought, retention preferences are not so consistent between the two viewpoints. During flood, in most segments DON is the most efficiently retained nitrogen solute, despite that most of the retained mass is in the form of nitrate. In drought all three nitrogen solutes exhibit similarly high retention efficiencies. The exceptions are the 1st, 3rd, 4th and 11th segments, in which generation efficiencies are higher than retentions.

The longitudinal variability in the generation or retention efficiencies for every solute at the different hydrological surveys is shown in Figure 8.4. In there, it becomes apparent that every solute had a different behaviour. DOC and nitrate, especially from flood to low baseflow, exhibit little spatial variability and an eminently conservative character. However, DON and ammonium, as well as nitrate during drougth, have an important spatial variability and exhibit a wide range of processing efficiencies, from complete depletions to mass generations which can even triplicate the inputs (DON during drought). This alternation between retention and generation within the river length suggests that net retentions observed in the global mass balances may be underestimating both the total processed mass, as well as the overall processing efficiency. This is because the global mass balance approach only considers the inputs that join the river through the tributaries, but do not take into account further solute generation or retention that takes place in-stream.

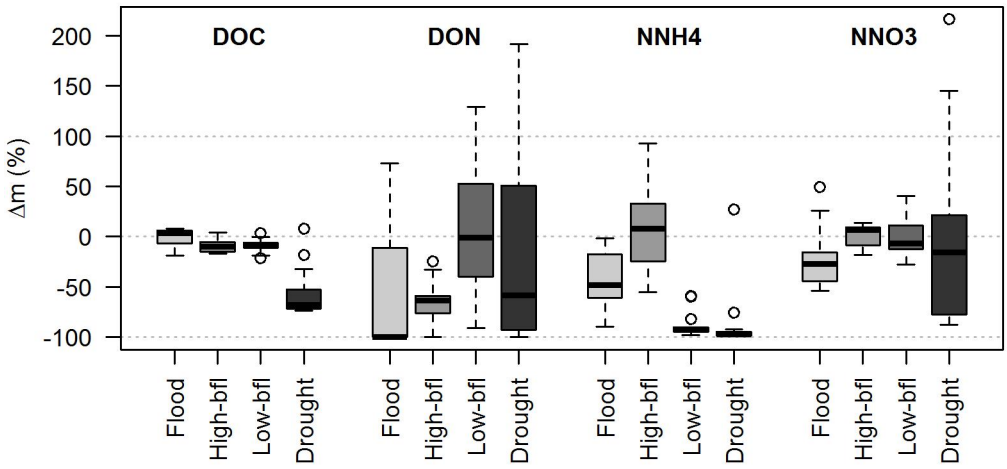

Figure 8.4 – Average retention efficiencies of dissolved nitrogen and carbon solutes, for each of the four hydrological surveys. Every box represents de distribution of the efficiencies among the 13 river segments were local mass balances were performed. *bfl* stands for *baseflow*.

8.2.5 Coupling between DOC and nitrate

With the aim to explore potential couplings between carbon and nitrogen, we examined the relationship between DOC and nitrate concentrations, as they represented the major forms of dissolved carbon and nitrogen, respectively (Figure 8.2 and 8.3, first rows). In order to better reconstruct the trends between those solutes in our study site, we added the data from all the surveys conducted in this thesis, which span a range of hydrological conditions from flood to drought (see section 3.2).

Similarly to what was ascertained in (Taylor and Townsend, 2010) we broadly observed a negative nonlinear relationship between DOC and nitrate, with a breakpoint which separated a region of nitrate accumulation at low DOC concentrations, and a region of nitrate depletion at high DOC concentrations. An accumulation of nitrate occurred at low DOC concentrations around 200 μmol/L, occupying the region between the stoichiometrical DOC:nitrate ratios of 1 and 3-6. Most samples in this area corresponded to the samples collected during baseflow. At higher DOC concentrations, together with higher DOC:nitrate ratios, nitrate concentrations became minimal and there was rather an accumulation of DOC. In this area, most samples corresponded to the drought survey. At DOC:nitrate ratios lower than 1

there was only one sample with important nitrate concentration. It corresponded to a sample collected during drought, located at the upstream-most main stem site (especifically, site A0, see map in Figure 3.5, chapter 3.1).

However, the main difference between our samples and the results presented in Taylor and Townsend (2010) is found for the samples collected during flood. These samples do not fit into the general nonlinear negative relationship between DOC and nitrate, but rather exhibit a positive linear trend between both solutes. It should be noted that their linear trend overlaps the stoichiometric region between DOC:nitrate = 3 and 6, which corresponds to the breakpoint between carbon and nitrogen limitation. The other grey points that appear in the breakpoint region also correspond to samples collected during the flood episode, but are not marked as such because these samples were not included in the mass-balance study (they belong to sites located further upstream or downstream from the river reach used for mass-balance).

Next, in order to test to what extent these results relate to the findings based on the mass balance approach, we examined the relationship between DOC:nitrate and the retention efficiency of nitrate. Figure 8.6 shows the reference DOC:nitrate ratios identified in Figure 8.5, at which a change in the behaviour of the retention efficiency should be observed. Results show a gradual change from nitrate generation to nitrate retention as the ratio DOC:nitrate increased, following a logarithmic decay (Δm N-NO_3^-(%)=13.9-22.2log(x), $R^2 = 0.416$, $p < 0.001$, fig. 8.6). The shift between generation and retention occurs at a DOC:nitrate ratio $\simeq 3$, which corresponds to the lower limit of the breakpoint where the shift from carbon to nitrogen limitation is attributed. Even though all samples followed the general negative relationship, some of them appeared sparser and did not fit the logarithmic model. These samples corresponded mainly to the summer drought, and specifically to segments 1 (initial site), 3 and 4 (which are after the outlet of the WWTP of Sant Celoni) and 9 and 11 (located after the outlet of the WWTP of Hostalric). During flood, there were also two outlier samples that were excluded from the mode. These were segments 1 and 3; again, the upstream-most site and the segment after the WWTP of Sant Celoni.

This logarithmic behaviour is most clearly observed for the samples collected during flood, high and low baseflow. Contrastingly, those samples corresponding to the summer drought, even though they also exhibit a general linear negative relationship, the trend is less clear as they appear sparser in the plot.

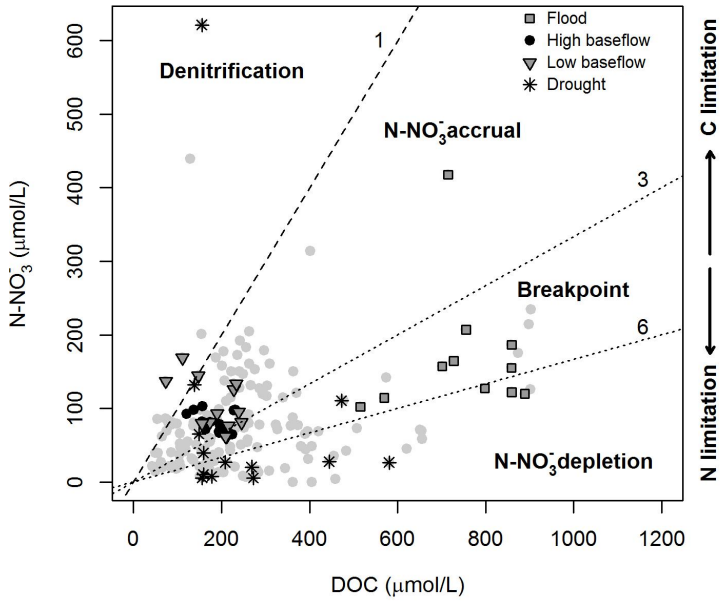

Figure 8.5 – Correlation between nitrate and DOC concentrations. Solid gray dots correspond to samples from the main stem of the Tordera, collected either in sites or on sampling dates not included in the mass balance study, which have been added to the plot for completion purposes. Diagonal lines represent reference DOC:nitrate stoichiometric ratios which divide, from left to right, the areas of denitrification, nitrate accumulation due to carbon limitation, breakpoint between carbon and nitrogen limitation, and nitrate depletion due to nitrogen limitation.

8.3 Discussion

Rivers are conduits that transfer nutrients from the land to the coast, hence linking the terrestrial and the marine systems. However, rivers also have an important in-stream processing capacity (Alexander et al., 2000; Cole et al., 2007), which has been found to be responsible for the retention or removal of substantial amounts of nitrogen (Peterson et al., 2001), and DOC (Moody et al., 2013). In line with these general findings, our results showed that the middle reaches of the Tordera are eminently a sink for both dissolved nitrogen and carbon. However, hydrology was found to be a great modulator of the magnitude of the sink, both in absolute (total mass retained) and relative terms (retention efficiency).

8.3.1 The net function of the river

Despite that in all surveys a predominance of retention was observed, the river as a whole was more efficiently retaining nitrogen and carbon at successively lower flows, achieving its maximal sink character during drought. Under such extremely low flows, retention efficiencies ranged between 73.3 and 100%. Similarly, several studies have found that uptake efficiency increases with declining discharge (Alexander et al., 2000; Peterson et al., 2001; Grimm et al., 2005). This is attributed to the fact that the low flows minimize the proportion between water volume and river bed surface, thereby enhancing the contact between the water column and the sediments where most biogeochemical transformations occur (Trimmer2012). Also, slow water velocities favour the diffusion of the solutes from the water column to the sediments, and lengthen the duration of the time contact between the water and the sediments (Pinay et al., 2002) thereby maximizing the processing rates of nitrogen and carbon.

By contrast, during flood the river had the lowest retention efficiencies. However, these low percentages represented, in absolute terms, the largest amounts of retained nitrogen (88.92 gN including nitrate, ammonium and DON nitrogen). This underlines the importance of flash floods in the nitrogen cycle. Despite they usually last for some hours to days, the large amounts of exported materials may make it possible that small retention efficiencies represent important amounts of cycled nitrogen in absolute mass. Indeed, in one second during flood it was processed the same amount of nitrate mass that was processed in 7.5 min during drought.

Despite this general trend of higher retention efficiencies with decreasing river flows, DON appears as an exception, as it exhibits important retention rates irrespective of the hydrological conditions. DON retention efficiencies only became moderate during low baseflow. Hence in the global scale, DON appears to be the nitrogen fraction which is most efficiently removed from the system irrespective of the hydrological conditions.

DOC, with respect to nitrogen, was found to have a more conservative character, and only during drought had an important net retention efficiency. During flood to baseflow, the processed mass percentage was rather low (+5.1% to -21.2%) compared to the -73.7% of retention in summer drought. Interestingly, the flood survey was the only one in which the river was a net source of DOC, even if at a moderate efficiency (+5.1%).

8.3.2 Inside the black box

Most studies calculate mass balance fluxes only at the outlet of a catchment. This approach ignores in-stream processes that may have occurred during the riverine transport prior to that point (Moody et al., 2013). This may result in an over- or

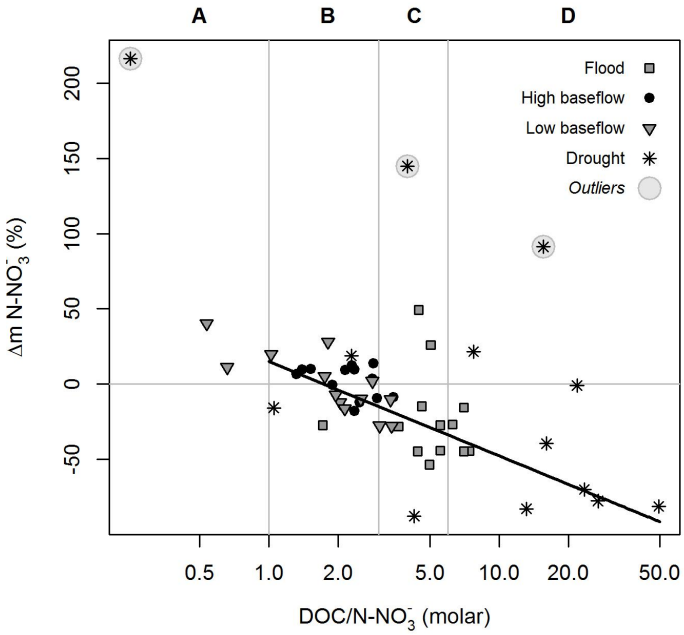

Figure 8.6 – Retention efficiency of nitrate as a function of the DOC:nitrate ratio. The log scale of the x axis should be noted. Vertical lines represent reference stoichiometric ratios which divided the areas of A) denitrification, B) carbon limitation, C) breakpoint and D) nitrogen limitation in Figure 8.5. A logarithmic model was significantly fitted to the data (see text for further details). Outlier samples were not included.

underestimation of the processing capacity of a river. In this study, this discrepancy has become apparent through the complementary approaches of the global and the local mass blances.

Even though most solutes have an overall net retention, when considering the mass fluxes in the 13 consecutive river segments it becomes evident that some solutes experience an alternation of generation and retention along the river (Figure 8.4). This is especially the case for DON. For instance, during flood and drought it had a net balance of 100% retention of the inputs. However, the local mass balances revealed that along the river reach, DON processing had an important variability, so that some river segments exhibited more moderate retentions, and even some DON generation took place in some specific segments. Such spatial heterogeneity is also importantly observed for nitrate during drought, and ammonium during high baseflow.

Overall these results underline that in the occurrence of local heterogeneity, the global and the local scales may not be extrapolable between them. Similarly, in sediment transport studies local variation was identified to produce large errors to whole reach mass balance calculations (Grams et al., 2013). Also, Moody et al. (2013) found evidences that catchments may be smaller DOC sinks than what is suggested by whole-catchment mass balances if the DOC losses within the catchment streams are taken into account. This evidences the key importance of spatial variability in choosing the right scale for determining the boundaries in mass-balance studies in order to make accurate determinations of the biogeochemical role of a river reach or chatchment.

Finally, we also found that hydrology intervenes, for every solute, in the extent of the spatial variability.

8.3.3 DOC mass balance

The importance of elucidating DOC mass balances in streams and rivers is widely recognised in the literature, but it is rarely empirically quantified (Moody et al., 2013). Among the few previous studies, DOC budgets are usually presented as annual budgets and have been performed using a whole catchment as a single black box. Thus annual DOC losses have been quantified from 12-18% in a 2-km river reach (Dawson et al., 2001) to 40% in a peat catchment (Worrall et al., 2006) and 31% accross the whole UK river network (Worrall et al., 2007). These figures are useful to understand the carbon cycle at the big picture level, however, they lack resolution of spatiotemporal patterns in DOC processing. Eatherall et al. (2000) calculated net DOC in-stream losses during baseflow and flood conditions, and their results revealed a shift from a conservative (3% removal) to a sink behaviour (25% DOC removal). Their results emphasize the importance of the hydrological conditions in the net effect of the river passage on the DOC processing, even though they find an opposite pattern compared to our results, that is, they find that high flows enhance the retention efficiency. However, they discuss the limitations of their sampling strategy to capture all inputs of DOC along the catchment and highlight the importance of detailed mass balance samplings in order to better determine the net DOC processing.

On the other hand, to our knowledge our study is the first one to provide a longitudinal characterisation of DOC mass balance, under a range of hydrological conditions. We indeed found an important longitudinal variability in the biogeochemical processing of DOC in the river. Interestingly, all previous studies always report net losses for DOC, however in our study we detect net sources in the second half of the river during flood conditions. The relevance of in-stream DOC sources is well documented in the literature (Bertilsson and Jones, 2003), as the periphy-

ton can be a relevant source of DOC. However it is surprising we detect DOC net sources during such high flow conditions, as it has been argued that in-stream processes would have their chance to occur relevantly at lower flows, when the residence times of DOC are higher and there are more opportunities for it to interact with the environment (Battin et al., 2008).

Also, during the flood survey it is interesting to observe such gradual longitudinal variation of the DOC processing efficiency, which shifts from retention in the upstream segments to release or generation in the downstream segments. This gradual downstream evolution suggests that changes in DOC processing during flood are not controlled by local drivers but rather by the different biogeochmical compartments flowing together downstream, i.e. they would be more related to planktonic-driven changes rather than benthonic-driven transformations. One reason supporting this idea may be that during such high flows, the river bed sediments were importantly resuspended and flowing downstream together with the water discharge and the solutes within. However, it should be noted that efficiencies were low throughout the river reach (between -20% and 10%).

Contrastingly, during drought retention efficiencies were high in most river segments, near 80% (Figure 8.3). Such high retention efficiencies, though, were reduced after the outlets of the WWTPs of Sant Celoni and Hostalric. This effect has been reported for inorganic solutes (Marti et al., 2004; Merseburger et al., 2011), however up to now it has not been explicitly evaluated for DOC. Even though sewage-treated DOM has been described to be a labile (Fellman et al., 2009a, 2010) and photoreactive fraction (Meng et al., 2013), such reduction in the removal efficiency may be due to the high loads, which may saturate the in-stream capacity to process the DOC inputs, similarly as for inorganic nutrients. The important lability may be later reflected in the rapid recuperation of basal DOC removal in the next few kilometers downstream.

8.3.4 Dissolved nitrogen mass balance

In contrast with DOC, DIN has received wider attention in river mass balance studies. In Mediterranean rivers, the retention capacity of nitrate has been found to be higher (23% and 52%, Aguilera et al. (2012) and Caille et al. (2012), respectively) than that found in other European watersheds, which have been estimated to be around 10-20% (Grizzetti et al., 2005). Aguilera et al. (2012) argue that increased retention efficiencies in Mediterranean watersheds may be due to the relatively lower flows with respect to the main European rivers. This agrees with the variable retention efficiency that we observed among hydrological conditions, especially for ammonium which gradually varied from 15.2% retention during flood to 92.3%

during drought. Nitrate remained relatively better conserved within the system, as found in House and Warwick (1998).

In the spatial dimension, the effect of the WWTPs was less clear than was observed for DOC. In this case, an increase in the nitrogen concentration was translated not only into a decrease in the retention efficiency, but even into a net release of nitrogen in that river segment. This occurs in the first, third and eleventh segments. As mentioned, the third and the eleventh segments correspond with the inputs of the WWTPs of Sant Celoni and Hostalric, respectively. The first segment, even though does not have any WWTP or industry, might have received some point source anthropogenic input by the time the sampling was performed. Reduced retention efficiencies downstream of anthropogenic nitrogen inputs are in line with previous findings that nitrogen loading saturates the capacity of the biological and physical uptake mechanisms (Martin et al., 2011; Marti et al., 2004; Merseburger et al., 2011).

8.3.5 Seasonal shift in the type of nitrogen retention

In all surveys nitrate was the most concentrated form of dissolved nitrogen. However, the longitudinal profiles of nitrogen retentions revealed that it was usually the least efficiently retained. Despite that, in absolute terms, during flood nitrate was, by far, the main form of retained nitrogen. In terms of retention efficiency, the main form of nitrogen uptake changed from high (flood and high baseflow) to low flows (low baseflow and drought) along the 13 river segments. Specifically, there was a shift from DON to ammonium preferential uptake (Figure 8.2, third row).

During flood and high baseflow, DON was the most efficiently removed form of nitrogen. Enhanced assimilatory DON uptake by heterotrophic bacteria, instead of inorganic nitrogen, has been associated with either a limitation of carbon, which can inhibit denitrification (Johnson et al., 2012), or colimitation of carbon and inorganic nitrogen, which may favour assimilatory DON uptake (Lutz et al., 2011; Brookshire et al., 2005). Surprisingly, our results do not show any contrasting values of ambient nitrate and DOC concentrations between the high and low baseflow surveys. Carbon limitation could occur not only by changes in DOC concentration, but also by changes in its quality and lability. However our results do not show either any changes in DOM lability specifically from high to low baseflow (Figure 8.7) which could support such change in the preferred form of retained nitrogen. Otherwise, a simpler explanation would be that a change in the DON lability itself occurred. In this case, a qualitative change was most likely to be blind to spectrophotometric methods. It has been reported that the main labile fraction of DON are proteinaceous fractions contained in combined form (Maie et al., 2006; Yu et al., 2002) which may not be reflected in Excitation-Emission Matrices (EEMs)

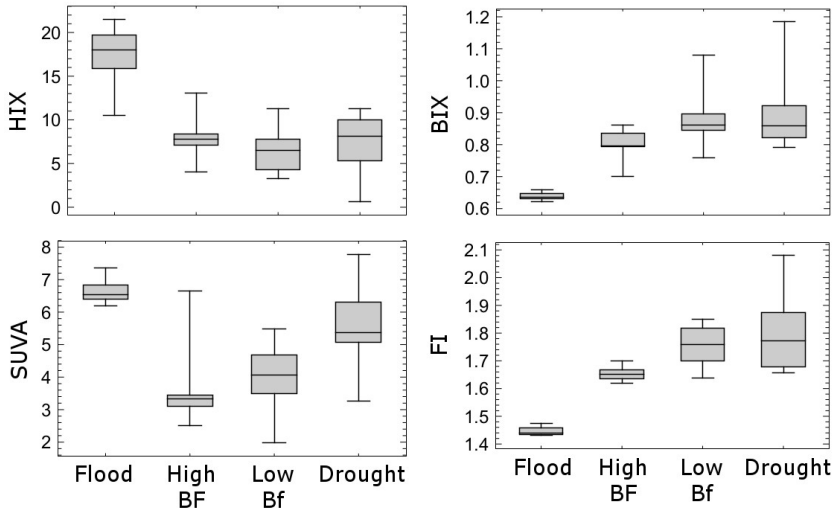

Figure 8.7 – Average DOM quality of main stem sites in the mass balance surveys. High BF and Low BF refer to high baseflow and low baseflow, respectively

and therefore, in optical indices. Similarly, Inamdar et al. (2012) did not find any association between DON and any EEM-derived metric.

On the other hand, in lower flows (low-baseflow and drought surveys), the highest retention efficiencies were attributed to ammonium. This shift in the main assimilated N form may be due to a series of modifications of the biophysical environment following the flows decrease that favour ammonium retention. Namely, lower flowing velocities, shallow geomorphologies and high light availability favour the proliferation of filamentous algae. The consequent high autotrophic activity may modify the redox conditions in the sediments surface to more oxidising conditions, inhibiting denitrification (Arnon et al., 2013). Also, ammonium may be directly assimilated by the algae, as most aquatic plant species prefer ammonia as nitrogen nutrient (Kadlec and Knight, 1996). Finally, laminar flows may also maximize the abiotic retention of ammonium especially in adsorption to sediments due to its high adsorption capacity (Vogeler et al., 2011).

8.3.6 (Un)coupling between DOC and nitrate

General trends among major Earth ecosystems suggest that DOC can play a key role in regulating the accumulation of nitrate (e.g. DIN) in stream water (Taylor and Townsend, 2010; Goodale et al., 2005; Evans et al., 2006). It was consistently found that nitrate accumulates at low DOC concentrations, whereas it is depleted at high DOC concentrations. A suite of microbial processes were identified as the

underlying regulators of such stoichiometrically coupled behaviour between DOC and nitrate concentrations. However, these studies explicitly only used baseflow samples in their models, and the role of hydrology was not specifically addressed. In this study, we contribute to fill this gap by comparing the behaviour between DOC and nitrate in different hydrological conditions, including extreme events like flood and drought.

Our results show that DOC and nitrate concentrations from a Mediterranean river broadly have a similar behaviour as those from tropical, temperate, boreal and arctic regions (Taylor and Townsend, 2010). Visually, we identified a shift between nitrate accumulation and depletion between the DOC:nitrate ratios 3 and 6, which are in the lower limit of those identified across a range of aquatic biomes (Taylor and Townsend, 2010), which also correspond to the lowest C:N ratios observed in microbial tissues (Cleveland and Liptzin, 2007).

Within this general framework, in our system every specific hydrological survey had a different DOC:nitrate stoichiometric relationship. During baseflow, there was mostly an accumulation of nitrate. Samples exhibited concomitantly low DOC concentrations (around 200 μmol/L), and DOC:nitrate ratios between 1 and 3-6. Between these ratios, carbon is considered to be the limitant for the microbial assimilatory activity (Taylor and Townsend, 2010). On the other hand, at DOC:nitrate ratios higher than 6 – and therefore, in the area of nitrogen limitation – samples corresponded exclusively to the drought survey. However, not all drought samples had such high ratios, but instead, appeared in all ranges of ratios: both in the region of preferential denitrification (DOC:nitrate < 1), as well as in that of carbon limitation (DOC:nitrate between 1 and 3-6) hence making it apparent that during drought there was a wide diversity of stoichiometric conditions.

At DOC:nitrate ratios lower than 1, it is considered that there are the optimal stoichiometric conditions for denitrification, and therefore nitrate should be minimal. In our data set, most of the data are close or below the 1:1 line (Figure fig:DOCNNO3-retNNO3). Only two clear exceptions were observed, which may consist on sites that that received nitrate inputs recently upstream and therefore, stoichiometric ratios could still not adapt to general DOC:nitrate dynamics.

However, during flood samples did not fit the general framework of Taylor and Townsend (2010). In that survey, samples did not exhibit a negative nonlinear relationship but, on the contrary, a positive linear trend was observed. One hypothesis would be that, under such extreme flash flood conditions, both nitrate and DOC would result from the rapid flushing of the terrestrial catchment, therefore exhibiting such positive relationship (William and Grant, 1979; Martin and Harrison, 2011; Hood et al., 2006). However, our results from the mass balance suggest that, despite the rapid downstream water and solute transport, in-stream processing of carbon and nitrogen took place to an important extent. Therefore, our results

rather suggest a differentiated processing which modifies the relative carbon and nitrogen cycling, thereby altering the relationship between nitrate and DOC.

When relating the DOC:nitrate molar ratio with the nitrate mass flux, we observed a general negative linear trend and a continuum between the samples from the different surveys and, in this case, flood appeared integrated within the general trend. The general trend was consistent with our hypothesis and hence, with the framework of Taylor and Townsend (2010). That is, under a carbon stoichiometrical limitation, nitrate had a tendency to be neutrally transported or to have slight in-stream releases, whereas at higher DOC:nitrate ratios, nitrate had higher retention efficiencies. Therefore, our mass-balance results support the hypothesis of a stoichiometrical coupling between DOC and nitrate. In our river, the breakpoint was found to be at a DOC:nitrate ratio of 3, which corresponds to the lowest range of reported C:N ratios of microbial biomass (Cleveland and Liptzin, 2007). However, drought did not follow the same trend as the flood and baseflow samples, as they presented an important dispersion. Therefore, in that hydrological condition the relationship between the nitrate processing and the streamwater DOC:nitrate ratio was not clear. It would be necessary to have more data on nitrate retention efficiencies in order to draw conclusions with the same confidence as in the DOC vs nitrate concentrations relationship.

8.4 Conclusions

In this study, we described the longitudinal patterns of DOC and dissolved nitrogen concentrations and mass balance along a 26 km river reach in a Mediterranean catchment under a range of contrasting hydrological conditions. Our main findings have been:

- Retention predominated for the dissolved nitrogen and organic carbon solutes. However, the efficiencies of the net retentions in the river were different according to the hydrological conditions: it was maximal during drought and minimal during flood.
- During flood, even though the processing efficiencies were the lowest among hydrological conditions, in absolute terms it was the date in which the largest amount of nitrogen and DOC mass was retained and released, respectively. This emphasizes the importance of such extreme events, even if they last just for some few hours or days.
- DON had a distinct behaviour with respect to DIN and DOC, as it exhibited high net retentions in all hydrological conditions, as well as an important spatial variability in its processing.

- In space, the retained mass consistently increased downstream in all hydrological conditions. However, the main nitrogen solute removed in every survey differed. From flood to drought, they corresponded to nitrate, DON and ammonium.
- In terms of removal efficiencies, spatial patterns were not clear and had an important longitudinal variability.
- In space, after the confluences with the WWTP inputs, there was a reduced retention efficiency both for DOC and dissolved nitrogen.

Regarding the coupling between DOC and nitrate:

- Our results showed that in the studied Mediterranean river, the stoichiometrical relationship between DOC and nitrate streamwater concentrations was consistent with that observed in the major Earth systems, especially during baseflow conditions.
- During flood, the general nonlinear negative trend was shifted to a linear positive relationship.
- Results of the mass balance were consistent with the stoichiometric findings, and showed that nitrate processing changed into higher retention efficiencies at higher DOC:nitrate ratios. In this case, the drought period did not follow the general trend and showed a weak relationship between nitrate processing and DOC:nitrate stoichiometry.
- Finally, we emphasize the determinant role that hydrology plays in the definition of longitudinal patterns of carbon and nitrogen biogeochemical processing, as well as in the definition of its coupling.

Chapter 9

Downstream processing of DOM: changes in its reactivity and composition

9.1 Introduction

Understanding the fate of dissolved organic matter (DOM) in the environment is currently a major challenge, difficult to unveil due to the complex simultaneity of different biogeochemical processes in which it is involved, and to the uneven effects that they have on individual fractions of DOM. Often, DOM retention in space has been modelled as a first-order decay function where it is assumed that the amount of retained DOM is a function of its own initial concentration (Raymond and Bauer, 2000; Weyhenmeyer et al., 2012; Baldwin et al., 2014). However, DOM transformations may follow more intricate longitudinal patterns due to the complexity of DOM environmental interactivity. The main processes responsible for the degradation of DOM are the UV radiation and microbial activity, both of which have the capacity to completely oxidise DOM to CO_2, as well as to alter its composition, as it has been detectable in its fluorescence composition (Lee and Hur, 2014; Gao and Zepp, 1998; Cory and Kaplan, 2012).

Bacteria have been widely recognised to be important DOM consumers, responsible for the re-introduction of organic carbon to the food webs (Azam et al., 1983), as well as to the outgassing of CO_2 to the atmosphere (Battin et al., 2008; Tranvik et al., 2009). Also, they can degrade and modify the quality of bulk DOM, and convert it into more labile (Cammack et al., 2004; Guillemette and del Giorgio, 2011) or recalcitrant (Ogawa et al., 2001) fractions. This traditional view of bacte-

Traditional view	Recent evidences
Bacteria as consumers of DOM	Dual role of bacteria as consumers and producers of DOM (Guillemette and del Giorgio, 2012)
Protein-like components as very labile fraction	Protein-like components can range from labile to recalcitrant. (Maie et al., 2007)
Humic-like fraction as a recalcitrant fraction	Humic-like fraction can be utilised and directly outgassed as CO2 (Fasching et al., 2014)
Microbially-derived components always labile	Bacteria can produce recalcitrant humic-like components. (Jiao et al., 2010; Guillemette and del Giorgio, 2012; Fasching et al., 2014; Asmala et al., 2014)

Table 9.1 – Commonly accepted views regarding DOM sources and lability being challenged in recent studies.

ria eminently as consumers, though, is currently being revised due to the increasing evidences that bacteria have a dual role as consumers and as producers (Guillemette and del Giorgio, 2012). On the one hand, they can produce protein-like compounds which have been traditionally considered to be highly labile and rapidly uptaken from the water (Rosenstock and Simon, 2001; Fellman et al., 2009b), even though it has also been found that a fraction of the protein-like components can include humic molecules of low-molecular weight with a recalcitrant character (Maie et al., 2007; Cory and Kaplan, 2012). On the other hand, bacteria have also been found to produce highly aromatic humic-like substances, which have been commonly attributed to be originated exclusively in terrestrial systems (Ogawa et al., 2001; Jiao et al., 2010; Asmala et al., 2014) and to exhibit a recalcitrant character (Cory and Kaplan, 2012). But recently, there are evidences that such humic-like substances, derived either from bacterial activity or the terrestrial drainage, can be utilised by bacteria under certain conditions and represent a potentially important pathway of carbon loss through outgassing as CO_2 (Guillemette et al., 2013; Fasching et al., 2014). Overall these findings emphasize the difficulty to predict the fate of DOM in freshwater ecosystems (Table 9.1), as its lability is a highly relative concept which depends also on the structure and function of the microbial communities and their capacity to degrade specific DOM compositions (Judd et al., 2006).

UV radiation has also been found to be an important process directly converting DOM into CO_2 (Miller and Zepp, 1995), or modifying its composition (Mostofa et al., 2007). Studies have demonstrated that sunlight breaks DOM molecules into blue-shifted compounds (Lee and Hur, 2014) of lower-molecular weight (Osburn et al., 2001). The lability of DOM photoproducts have been found to range from labile (Moran and Zepp, 1997) to recalcitrant (Tranvik and Kokalj, 1998). Again, there is such an important specificity between the molecule being photodegraded, the nature of the photoproducts, and the microbial community present to utilise

that material, that it is especially complex to predict what will be the fate of DOM in a natural system, subject to both photo- and bio-degradation.

Moreover, all the cited works assessing the relationship between DOM and bacteria have tested their hypothesis using laboratory incubations thereby controlling the environmental conditions. Such experiences are important because they elucidate the potential interactivity between bacteria and DOM, however, it is difficult to translate such potential observations to what effectively occurs in natural systems.

In this chapter we contribute to expand the understanding of DOM fate during downstream riverine transport by providing direct field evidence on the generation or retention of specific DOM fractions. For that, we use the mass balance approach of the previous chapters to evaluate the downstream reactivity of individual fluorescence components (as determined in chapter 4), and further, we test the role of hydrological conditions in determining longitudinal reactivity patterns. The performance and suitability of SOM-derived fluorescence components has been previously assessed as shown in the Annex of this thesis.

Our aims are addressed according to the following specific objectives:

- To quantify the extent of in-stream processing of the DOM fluorescence components on the whole-reach scale: we first show the global effect of the passage of DOM along the whole river reach on each of the fluorescence components, considering it as a single black box. Next, we present the longitudinal patterns of generation/retention processes along the river reach, corresponding to the mass balances performed at each of the thirteen successive downstream segments.

- To assess the effect of hydrological conditions at shaping DOM processing both at the reach (global) and at the segment (local) scale.

- To test the coupling between quantitative and qualitative DOM changes, both i) in terms of concentrations (for dissolved organic carbon (DOC) and dissolved organic nitrogen (DON)) and fluorescence intensities (fluorescence components), and ii) in terms of generation or retention efficiencies.

- To assess to what extent the DOM processing in each river segment can be predicted from its own initial characteristics in the beginning of each river segment, in terms of i) initial concentrations and ii) initial character, as described by the optical indices Fluorescence Index (FI), Humification Index (HIX), Biological Index (BIX) and Specific Ultra-Violet Absorbance (SUVA).

9.2 Results

9.2.1 Fluorescence intensities of DOM components

The longitudinal profiles of the intensities of DOM components (Figure 9.1, first row) show that the four components followed similar trends downstream, but their relative intensities differed among surveys. During flood, the highest intensities were found for component C3 (56.051 $r.u.^3nm^{-2}$), followed by C4 (32 839.8 $r.u.^3nm^{-2}$), that is, the humic-like fraction. Conversely, during high-, low-baseflow and drought, there was a predominance of the protein like fraction. C1 was the most intense component (17 735.6, 12079.0 and 29660.2) followed by C2 (8220.2 , 10657.6 and 18497.4 for high-, low-baseflow and drought, respectively).

The longitudinal profiles of the fluorescence intensities exhibited gradual downstream evolutions during flood and the two baseflow surveys, with a slight increasing trend. During baseflow, intensities (represented mainly by component C1) became higher in the last kilometres of the river reach (6.5 km in high baseflow and 11.5 km in low baseflow). The effect of the waste water treatment plant (WWTP) of Sant Celoni (at 25 km from source) could be noted as a small peak, although very modestly. During flood, such differentiation of the last km was not observed, but there was rather a steady oscillation along the whole river length, with minimal values in the upstream-most sites.

During drought, such gradual downstream patterns were replaced by an important variability in the fluorescence intensities, consisting in two main peaks. The first one, at 25 km from the river source, was located after the inputs from the WWTP of Sant Celoni, whereas the second one, at 40 km, appeared after the inputs from the industrial area of Hostalric. In both cases, though, concentrations recuperated basal intensities in the following two sampling sites (within a 5 km downstream distance). The peak at 25 km was represented by all for components at similar proportions; however at 40 km the peak was mainly due to the increase in the fluorescence intensity of C1 and, to a lesser extent, of C2.

9.2.2 Global mass balance

If we consider the whole 26-km river reach as a big black box, we can compare the total sum of the inputs (sum of the flow-weighted fluorescence intensities of the tributaries) with the outputs (flow-weighted fluorescence intensity flowing at the final main stem site, in Fogars de la Selva). The differences between the inputs and the outputs for every fluorescence component and for every survey are presented both in absolute terms and as percentages with respect to the inputs, also hereafter referred to as processing efficiencies (Table 9.2).

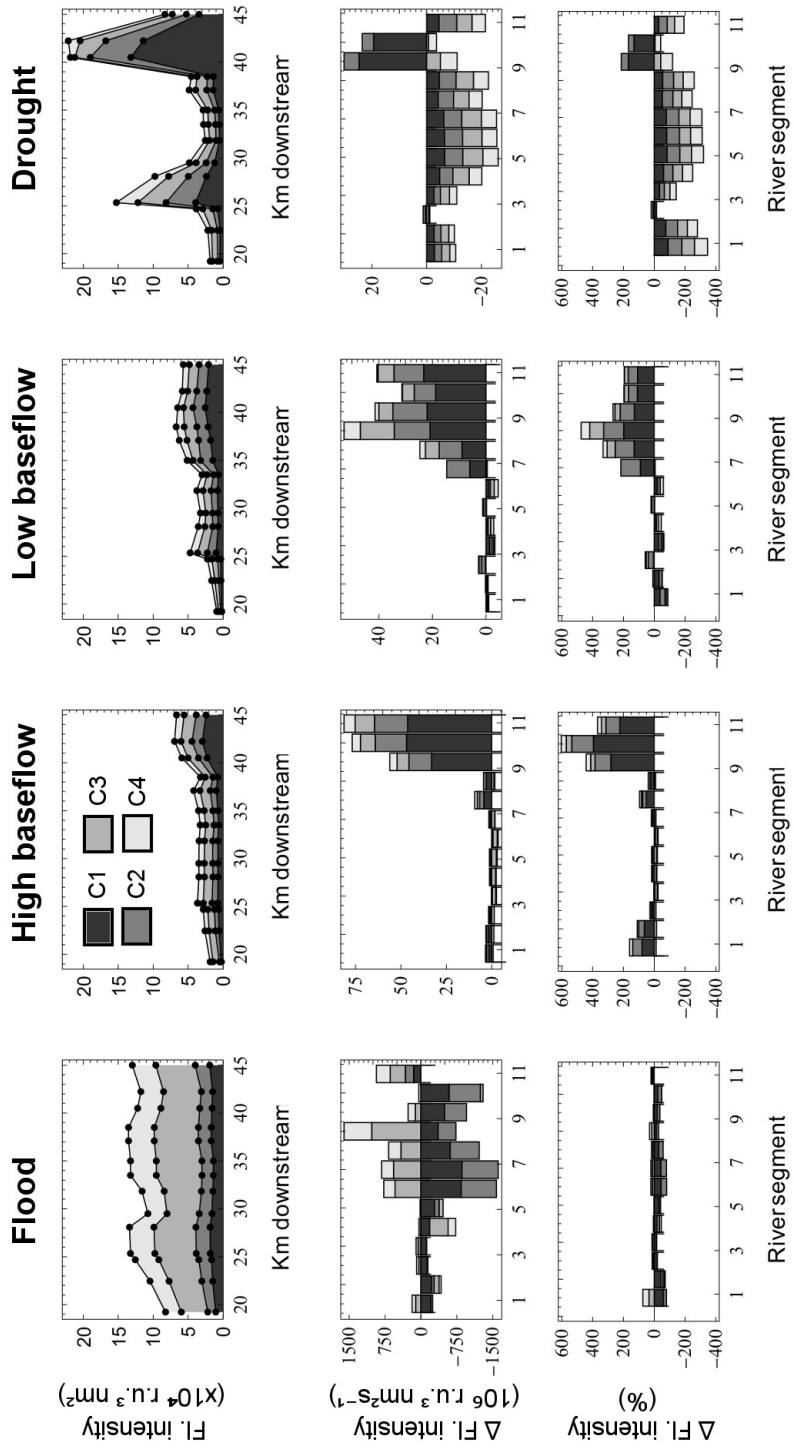

Figure 9.1 – Fluorescence intensity and mass fluxes for DOM fluorescence components along the main stem of the Tordera. First row corresponds to the observed fluorescence intensities; second and third rows correspond to the difference between the inputs and the outputs at every river segment expressed in absolute terms and as percentage, respectively. Positive values indicate release or generation, whereas negative values refer to retention or assimilation of the components. In all plots, the different categories (i.e. fluorescence components) are stacked.

Solute	Flood	High baseflow	Low baseflow	Drought
		$r.u.^3nm^{-2}$ ($\times 10^6$)		
C1	152.9 (5.4%)	46.2 (223%)	23.2 (107.8%)	-4.4 (-37.3%)
C2	172.2 (5.5%)	18.3 (90%)	11.1 (60.4%)	-6.5 (-58.7%)
C3	316.9 (3.7%)	10.6 (28.7%)	5.9 (24.5%)	-5.6 (-50.8%)
C4	289.7 (5.7%)	6.1 (25.5%)	0.4 (2.3%)	-4.8 (-62.5%)

Table 9.2 – Global mass balance for the DOM fluorescence components. Values refer to the differences between the inputs and the outputs in the whole river reach, between brackets these differences are expressed as percentages with respect to the inputs. Positive values indicate produced fluorescence intensity, whereas negative values indicate depleted fluorescence intensity during the riverine passage.

During flood, the amount of processed fluorescence intensity in absolute terms represented the largest amounts of generated fluorescence intensity throughout this study (in the order of 10^8r.u., Table 9.2). However, these generations, when compared to the inputs, correspond to very low generation efficiencies (3.7 to 5.7%) what suggests that in essence there is a conservative passage of the fluorescence components through the riverine transit.

Under lower flows, processing efficiencies became prominent. During high- and low-baseflow, the river represented a source of fluorescence intensity, especially for the protein-like fractions: component C1 was tripled (+223.0 %) and duplicated (+107.8%) under high- and low-baseflow, respectively; and component C2 was practically duplicated in both hydrological conditions (+90.0 % and +60.4%, respectively). Increases in the humic-like fraction were more moderate, exhibiting productions between 20%-30%, with the exception of C4 during low-baseflow which appeared conservative (2.3%).

During drought, the opposite trend occurred: All four components experienced retentions during the riverine passage. The highest retention efficiency was observed for the humic-like component C4 (-62.5 %), followed by the protein-like component C2 (-58.7%). The component that underwent the least net retention rate was C1 (-37.3%).

9.2.3 Longitudinal profiles of retention and release

The mass balances performed at 13 successive river segments refine the findings of the global mass balances (Figure 9.1, second and third rows) on the longitudinal perspective.

During flood conditions, processing efficiencies for all four fluorescence components ranged between -60% to 39%, averaging -7.5% (Figure 9.2). These efficiencies were much lower than those observed in the other surveys with lower flows. In absolute terms (Figure 9.1, second row) it can be seen that, despite the first half of the river reach exhibiting little fluorescence processing, the final half concentrates the processing of large amounts of fluorecence intensity. Due to the low percentages that they represent with respect to the inputs (i.e. low processing efficiencies), it cannot be assured with enough confidence whether such differences in the intensities are due to ecological processes or analytical errors. However, in this second half of the river, it is consistently observed that depletions occur for the protein-like fractions C1 and C2, whereas the humic-like components C4 and C5 undergo notable productions especially between the 7th and 10th segments (located at 31 to 38.5 km from source). These results suggest that, despite an eminently conservative transport, a weak DOM processing occurs in the middle sections of the river that operate differentially for the humic-like versus the protein-like components.

During baseflow, the river reach appeared clearly divided into two parts, both in absolute and relative terms: a first part with little or nil processing, and a second part undergoing important fluorescence intensity generations. During high-baseflow conditions, this final reactive part of the river reach spanned 3 segments (6.5 km long), whereas during low-baseflow it spanned a longer distance, including 6 segments (11.5 km long). The main DOM fraction experiencing net generations in these final river segments was the fluorescence component C1, followed by C2. By contrast, components C3 and C4 showed more moderate generation efficiencies.

Finally, during drought there were net depletions of all four fluorescence components in all segments (averaging -26.2 $\pm$ 82.8 % for C1, -46.7 $\pm$ 47.2 % for C2, -53.2 $\pm$ 24.2 % for C3 and -61.4 $\pm$ 21.7 % for C4, Figure 9.2). In some segments, this pattern was reduced (segment 3) or even inverted (segments 11 and 12) for components C1 and C2 (Figure 9.1). In segment 3, located at the outlet of the WWTP of Sant Celoni, processing efficiencies of all four components were reduced to very low values, between -9.3% (C3) and 11.9% (C2), indicating a conservative transport of fluorescent DOM in these site. By contrast, in segments 11-12 (which follow the confluence with the Creek of Arbúcies, including the outlet of the WWTP of Hostalric), retentions of protein-like fractions were inverted to generations of 167% (C1) and 45% (C2). Such important generations of protein-like intensity in these segments may balance the retentions experienced in the rest of segments, and may explain the fact that the net retentions in the whole river reach are lower for the protein-like than the humic-like fraction. Indeed, if we compute the average retention among segments, excluding segments 3, 11 and 13, we obtain very similar retention efficiencies (-64.7 $\pm$ 21.0 % for C1, -69.9 $\pm$ 17.4 % for C2, -63.4 $\pm$ 13.7 % for C3 and -68.0 $\pm$ 12.0 % for C4). This emphasizes that, in the absence of direct

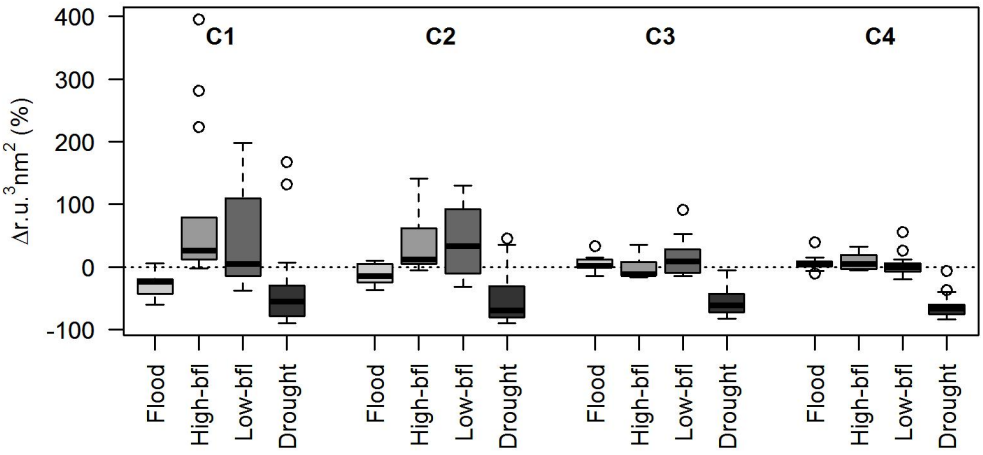

Figure 9.2 – Average retention efficiencies of the fluorescence components, for each of the four hydrological surveys. Every box represents de distribution of the efficiencies among the 13 river segments were local mass balances were performed. *bfl* stands for *baseflow*.

WWTP inputs, the four fluorescence components are indistinctly removed from the river water.

9.2.4 Quantitative and qualitative coupling of DOM processing

Coupling between DOM concentrations and fluorescence components intensities

Linear models were computed between DOM concentration (as DOC and as DON) and the intensities of the fluorescence components along the middle reaches, in order to explore the relationships between quantitative and compositional aspects of DOM. That is, linear correlations were computed between DOC or DON concentration, and the intensities of the fluorescence components.

When all the surveys were considered together, DOC concentrations had a strong positive linear relationship with the fluorescence intensities of components C3 (R^2 = 0.942, p <0.001, df=51) and C4 (R^2 =0.936, p <0.001, df=51; Figure 9.3A). Samples sites exhibited a clear linear continuity where the samples from higher flows appear at higher DOC concentrations and higher fluorescence intensities. However, this linear relationship was not observed for the protein-like components C1 and C2 (Figure 9.3B). For these components, the sites collected during drought, low-

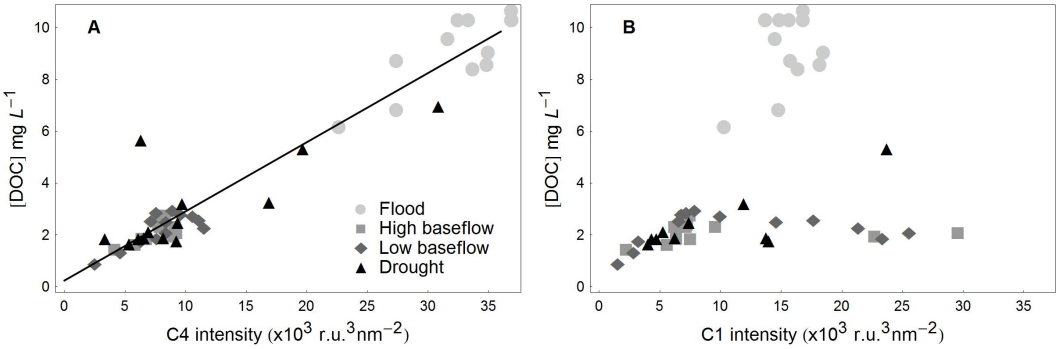

Figure 9.3 – Relationship between DOC concentration and the fluorescence intensity of C4 (A) and C1 (B). The solid line in panel A describes the significant relationship between DOC concentration and the fluorescence intensity of C4. See text for further details.

and high-baseflow exhibited a saturation curve, in which for fluorescence intensities between 0 and 10^4 $r.u.^3nm^{-2}$ DOC exhibited a coupled linear increase, whereas at fluorescence intensities higher than 10^4 $r.u.^3nm^{-2}$ DOC remained at concentrations near 2 mg L^{-1}. On the other hand, the samples collected under flood did not appear in this saturation curve, but as a cluster situated at higher DOC concentrations ($9.29 \pm 1.4 mgL^{-1}$) and intermediate fluorescence intensities ($15.6 \times 10^3 \pm 2.2 \times 10^3$ $r.u.^3nm^{-2}$). This indicates that, out of flood conditions, samples remained at low DOC concentrations but variable degrees of protein-like fluorescence compounds, whereas during flood, there was an increase in DOC concentration which was not directly reflected as an increase in the protein-like fluorescence signal. Overall, there was an uncoupling between DOC concentration and the protein-like fluorescence intensity, which was especially disrupted during flood conditions.

Contrastingly, when the qualitative-quantitative coupling was assessed with DON, no relationship was observed. The linear correlations between DON and the fluorescence components always had R^2 less than 0.132 and p higher than 0.07. The lack of any statistically significant correlation between DON concentration and the fluorescence intensity of any of the fluorescence components highlighted the uncoupling between the fluorescence composition and the DON content in the samples.

Coupling between the processing of DOM and that of the fluorescence components

Next the coupling between bulk DOM and the individual fluorescence components was assessed in terms of biogeochemical processing. This was addressed by computing linear models between the mass retentions/generations of DOC and DON,

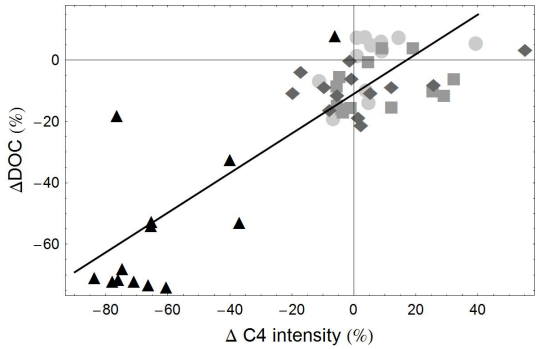

Figure 9.4 – Relationship between the processing efficiency of DOC and C4. The solid line represents the significant linear correlation between both variables, see text for further details. Every symbol represents a different hydrological condition, as defined in Figure 9.3.

versus the fluorescence intensity retentions/generations efficiencies of the fluorescence components.

Similarly to what was observed in the previous section, the best correlations were found between DOC and the humic-like components, although in this case with a lower statistical strength. The processing of bulk DOC explained more than 50% of the processing of the components C3 and C4 (for C3, $R^2 = 0.571$, $p = 9.6 \times 10^{-11}$, df=51; for C4, $R^2 = 0.740$, $p = 2.9 \times 10^{-16}$, df=51; Figure 9.4). Conversely, no significant – or very weak statistical correlations were found for the protein-like components (for C1, $R^2 = 0.089$, $p = 0.03$, df=51; for C2, $R^2 = 0.277$, $p = 6.1 \times 10^{-5}$, df=51).

The graphical representation of the relationship between the processing of DOC and fluorescence components (Figure 9.4) reveals that the survey that mainly contributed to the linear relationship between both parameters is that of drought conditions. While the samples corresponding to the surveys of flood, high- and low-baseflow appear forming a cloud around the axis origin, those from drought appear linearly distributed at the negative axis of both DOC and fluorescence components processing efficiencies, so that higher retentions of DOC implicated higher retentions of the fluorescence components. This relationship could be perceived for all fluorescence components, but as mentioned it was maximised and statistically relevant for C3 and C4.

The retained or produced mass of DON did not significantly correlate with the fluorescence intensity retention or release of any of the four components (R^2 always less than 0.084, and p always higher than 0.053).

9.2.5 Can the input characteristics of DOM determine its downstream biogeochemical processing?

Relationship between the initial intensities of DOM fluorescence components and their processing

Next it was assessed to what extent the degree of biogeochemical processing of DOM was dependent on the initial concentrations at the beginning of every river segment. Very similar patterns were found for DON, C3 and C4. In the case of C4 (Figure 9.5) baseflow and flood samples did not show a clear trend but rather a cluster-like distribution centered near 0% of processing efficiency (5.76 $\pm$ 16.95 %). However, they presented different fluorescence intensities at the beginning of the river segments: baseflow samples (both high- and low-baseflow) were centered at 7801 $\pm$ 2038 $r.u.^3nm^{-2}$, whereas flood samples were centered at 32776 $\pm$ 4472 $r.u.^3nm^{-2}$. However, during drought samples had some linear behaviour, so that higher retention efficiencies were obtained for lower fluorescence intensities. There were some sites, though, that appeared as outliers to this linear trend. In the case of the fluorescence components C3 and C4, the outliers corresponded to the segment 1 sampled during flood, and to the segments 3 and 11 sampled during drought. In the case of DOC, the outliers corresponded to the segments 3 and 12. Segment 1 is located after the WWTP of Santa Maria de Palautordera, segment 3 after the WWTP of Sant Celoni, and segments 11 and 12 are located after the WWTP of Hostalric. These outlier sites appeared together with the samples collected during high- and low- baseflow. Under such conditions, samples appeared clustered at low intensities and low production/retention efficiencies.

Contrastingly, DON and components C1 and C2, did not show any relationship between their processing percentage and their initial concentrations, at any of the sampled hydrological conditions.

Relationship between the optical indices and the processing of the fluorescence components

In order to answer this question, the correlations between the optical indices at the beginning of every segment and the production/retention of fluorescence intensity for the different fluorescence components were computed (Figure 9.6).

The most clear statistical relationship was found for the FI during drought (Figure 9.6A), which could significantly explain the retentions of the four fluorescence components. The strongest correlations were found for components C2 ($R^2 = 0.746$, $p = 6 \times 10^{-4}$, df=10) and C3 ($R^2 = 0.731$, $p = 4 \times 10^{-4}$, df=11). In the case of C2, segments 3 and 11 were excluded as outliers, whereas for C3, segment 3 was ex-

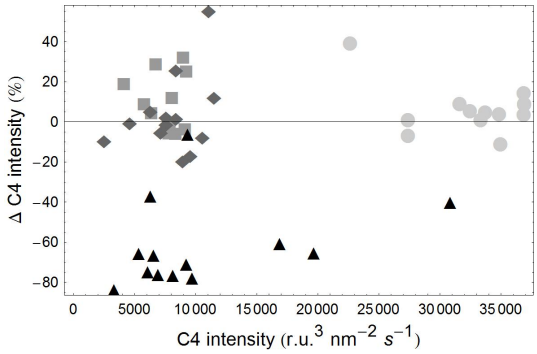

Figure 9.5 – Relationship between the processing of C4 and its initial concentrations. Every symbol represents a different hydrological condition, as defined in Figure 9.3.

cluded. For components C1 and C4, FI explained less than 70% of its variance (for C1, $R^2 = 0.673$, $p = 2 \times 10^{-3}$, df=10; for C5, $R^2 = 0.532$, $p = 7 \times 10^{-3}$, df=11). In the rest of surveys (that is, from low baseflow to flood), no statistical relationships were found, as the variability in the FI values were too small compared with the variation in the retention/release of fluorescence intensity.

In the case of HIX, there was no significant statistical relationship with the biogeochemical processing of any of the components. However, it could be observed that at higher values of HIX, the dispersion in the biogeochemical percentages gradually decreased, and became centered to zero, indicating a gradually lower biogeochemical processing of the fluorescence components towards higher HIX values, represented by the flood samples (Figure 9.6B). This pattern could be observed for all the four components.

Finally, SUVA and BIX did not have any statistically relevant ability to predict the biogeochemical processing of fluorescence components.

9.3 Discussion

The main conclusion that can be drawn from the results of this chapter is that hydrology plays a key role in determining both the global reactivity of the river reach, as well as the longitudinal distribution of such reactivity. This is especially important for systems like the Mediterranean ones, which are subject to high intra-annual hydrological variability; and provides further evidence that the biogeochemical functioning of these systems is tightly linked to hydrology.

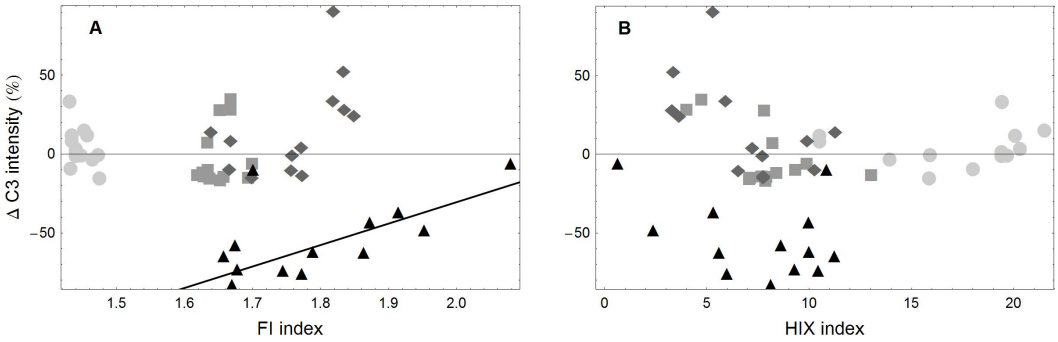

Figure 9.6 – Relationship between the processing of fluorescence component C3 and the values of FI (A) and HIX (B) optical indices at the beginning of the river segments. In A, the solid line describes the relationship between both variables during drought conditions (see text for further details). Every symbol represents a different hydrological condition, as defined in Figure 9.3.

9.3.1 Hydrology and the biogeochemical processing of DOM fluorescence components

Baseflow

During baseflow conditions the river reach as a whole was found to be a net source of fluorescence components, especially of the protein-like component C1, followed by C2, but also of the humic-like components C3 and C4. This was an interesting result given that for bulk DOM (that is, DOC and DON), the whole river reach was not found to be a net source in any of the hydrological conditions. This suggests that there are processes that operate modifying the composition of DOM without altering its overall quantity. Therefore, this points to an uncoupling between the quantitative and the qualitative dynamics of DOM. The production of fluorescence intensity of specific components parallel to bulk DOC decreases has already been observed (Asmala et al., 2014; Guillemette and del Giorgio, 2012) and has been pointed to the capacity of microorganisms to convert uncoloured DOM forms into coloured ones (Guillemette and del Giorgio, 2012). In the case of this study, most of the produced intensity corresponded to protein-like components, what is in line with common knowledge that protein-like substances are usually derived from autochthonous microbial activity (Henderson et al., 2009). However, to a lesser extent but still remarkably, humic-like components were also generated. These findings add evidence to the recent revision of the traditional conception that humic-like substances are solely of terrestrial origin and that, on the contrary, microbial activity can be an important source of humic-like material (Ogawa et al., 2001; Jiao et al., 2010).

The longitudinal profiles for the baseflow conditions showed that most of this DOM production observed during high- and low-baseflow occurred in the final segments of the river reach, which spanned the last 6.5 km during high baseflow, and 11.5 km during low baseflow. That is, with lower flows the length of the final reactive part of the river became longer. This could be related to increased residence times in lower segments where the river morphology becomes shallower downstream, as it has been described that low residence times may favour the opportunities for DOM processing (Battin et al., 2008; Weyhenmeyer et al., 2012). Also, with the lengthening of the reactive part it could be observed that the generation percentage increased gradually downstream, what suggested that downstream changes were not directly related to local features but rather to global environmental factors.

The fact that such generations were translated into higher fluorescence intensities in stream water which remained downstream suggest that, at least to a certain extent, these in-stream generated components are persistent and therefore, recalcitrant to biological or photochemical degradation. This is in line with observations that microbially-produced protein-like or humic-like components can be persistent in the environment (Jiao et al., 2010; Maie et al., 2007).

The hydrological extremes: drought and flood

The opposite biogeochemical functioning was found during drought, when the river reach as a whole behaved as a sink for the fluorescence components; in this case, consistently with what was found in quantitative terms for DOC and DON. However, retention efficiencies for the fluorescence components (ranging between 37.3% and 62.5%) were much moderate than those observed for DOC and DON (which were of 73.3% and 100%, respectively). This could be explained by two hypothesis: on the one hand, this could reflect that the fluorescence fraction of DOM is more refractory than the non-fluorescence compounds. This would be in accordance with the general conception in the scientific literature that well-known biochemical compounds, most of which are not aromatic and hence, do not have fluorescence properties, are the most labile and rapidly utilised fractions of DOM (Montuelle and Volat, 1993). On the other hand, another explanation would be that such reduced retention efficiencies of the fluorescence components with respect to bulk DOC might be due to parallel generations of fluorescence DOM which would counter-balance the net retentions. This second hypothesis would be sustained by our finding that, during drought, higher FI values are related to lower retention efficiencies (Figure 9.6), as such relationship would indicate that lower net retentions are related to a higher prevalence of in-stream produced fluorescence DOM.

Along the longitudinal axis it was found that, similarly to what was observed for DOC, after the confluences with the WWTP there was a decrease in the re-

tention efficiency of the fluorescence components (segment 3, Sant Celoni), or even an inversion into generation (segments 11-12, Hostalric). This further suggests a saturation in the system that surpasses the natural capacity of the river to uptake fluorescent DOM, as it has been similarly observed for inorganic nutrients (Marti et al., 2004; Martin and Harrison, 2011; Merseburger et al., 2011). In Sant Celoni the inputs from the WWTP were translated into an increase in the retention efficiencies of all four fluorescence components at similar proportions which, together with a paractically null processing efficiency, suggests that in that site there was only a physical mixing of the inputs which caused the observed increase in the fluorescence intensities. By contrast, in Hostalric there was mainly an increase in the fluorescence intensity of the protein-like components (mainly C1 but also C2), which in this case were the result of in-stream generations, which could be triggered by the inputs from the WWTP, which could have introduced either missing reactants or a different microbial community capable of undergoing such important generations of protein-like components (McClain et al., 2003). In both cases, though, such increases in the intensities of fluorescence components were rapidly depleted in the following downstream river segments, as evidenced by the net retentions and rapid recuperations of basal fluorescence intensities in the following segments. Overall these results evidence a high lability of both the allochthonous/anthropogenic DOM inputs, and the in-stream generated fluorescence components.

Under flood conditions, the river reach as a whole behaved mainly as a pipe, as the differences between the inputs from the tributaries, and the outputs at Fogars de la Selva were practically identical (differences between 3.7% for C3 to 5.7% for C4, Table 9.2). In absolute terms, the river transported large amounts of fluorescent DOM downstream. To make these magnitudes more apparent, if we consider that during flood the river generated 289.7 r.u./s of C4, and that in drought the river retained 4.8 $r.u.^3 nm^{-2} s^{-1}$, (Table 9.2) then it follows that in flood conditions the river exported in 1s the same amount that it would be capable of retaining in 1 minute during drought.

In the longitudinal perspective, it could be observed (similarly to what was found for baseflow conditions) a shift from a first part in which the river segments were very conservative, and a second part where the segments were more reactive. Fluorescence generations were observed for the protein-like components, although their magnitudes represented little percentages with respect to the inputs and, therefore, such non-conservative transport could not be confidentially assumed. However, some retention was indeed likely to occur in the final reaches (7,8,9 and 12), for the humic-like components C3 and C4.

9.3.2 Relevance of different hydrological conditions in the framework of the Mediterranean seasonality

Overall these results highlight the key role that the hydrological conditions play in determining the biogeochemical processing of DOM. On the one hand, it determines the role of the whole river reach, as it shifts from behaving as a conservative pipe during flood, to a source during baseflow, and to a sink during drought. On the other hand, it also determines how DOM processing is distributed in space.

Baseflow conditions are those that are most common throughout the year. In the last 10 years, La Tordera had water flows between those sampled during high- and low-baseflow surveys during 17.34 % of the days, although according to the operational hydrological categories defined in the Materials and Methods (Chapter 3, Figure 3.3) and used in chapters 5 and 6, baseflow conditions may represent the flows that occurred 45% of the days of the last 10 years. Under these circumstances, if we assume that the final quilometers of the river which were not included in the mass balance behave like the second reactive part, then the river may mainly deliver freshly produced protein-like components to the coast.

By contrast, floods are very short in time. The flows sampled in the flood survey have only been exceeded 0.18 % of the days during the last 10 years, and could represent the flows of 5% of the days according to the categories defined in Figure 3.3. However such flash-flood episodes are very intense, and they can represent an important flux of DOM export in quantitative terms as it has been widely acknowledged in the literature (Dalzell et al., 2005; Wiegner et al., 2009; Wilson et al., 2013). However, in qualitative terms, it has been widely accepted that the rapid flash-floods transport DOM without much opportunities for its in-stream processing. Whereas here we did not obtain enough confidence to conclude the opposite, we did find trends that in the lower part of the river reach some processing of the fluorescence components took place. Future studies would be necessary to better assess to what extent any preprocessing of the DOM occurs prior to be discharged to the coast under flash-flood circumstances.

Finally, drought conditions may span a variable length of time every year, typically lasting up to 2 or 3 of months. The specific flows sampled in the drought survey were equal or lower in 15.23 % of the days of the last 10 years, and could represent up to 50% of the days (according to the categories defined in Figure 3.3). During drought, DOM deliveries to the coast are minimal, as the river flow is rapidly reduced and completely depleted at the river mouth and an inland intrusion of the river/sea water interface occurs (as was evidenced in chapter 5 with the high salinities at the last sampling sites during the drier periods). Therefore, under such circumstances the export of DOM from the land to the sea would be minimal,

and, if still any flux of DOM would occur, it would deliver highly processed DOM material.

Hence, these results highlight that hydrology determines a seasonality of the quantitative and qualitative delivery of DOM to the coastal system which may determine its temporal functioning.

9.3.3 Biogeochemical reactivity of DOM fluorescence components

Some of our findings support recent revisions of traditional conceptions about the sources and lability of fluorescence DOM components (Table 9.1). Specifically, we found evidences for an important in-stream generation of fluorescence DOM which could be due to the recently described dual role of bacteria as consumers and as producers (Guillemette and del Giorgio, 2012). The generation role of fluorescent DOM was especially apparent during baseflow conditions, when the fluorescence components altogether increased by 75% (high baseflow) and 50% (low baseflow). Linked to that, we found evidences that the bacterially-derived components, be either humic-like or protein-like, were likely to be recalcitrant, as net generations remained at successive segments downstream. By contrast during drought the generation of DOM could not be proved, as net depletions were observed. However, generations may be likely to occur, as their counter-balancing effect may explain the relatively low retention efficiencies observed during drought.

On the other hand, we found a lack of relationship between the reactivity of bulk DOC and DOM concentrations and their initial intensity at the beginning of every river segment. That is, the reactivity of bulk DOC and that of fluorescence components could not be predicted from their initial characteristics. Such relationship would be expectable in case that their retention in space followed a first-order decay function (Raymond and Bauer, 2000; Weyhenmeyer et al., 2012; Baldwin et al., 2014). The lack of such relationship in this study can be explained by two assumptions: on the one hand, we found evidences of in-stream generations of fluorescence DOM that would occur in parallel with DOM uptake, so that such generations would blur the final net retentions detected. On the other hand, in every segment there is a different time residence and, because of that, every pair of retention efficiency and initial concentration may not be comparable.

Also, with the exception of FI during drought, optical indices did not explain either the efficiencies of DOM processing. This emphasizes the decoupling between DOM composition and its lability in the environment, and further emphasizes the complexity and relativity of the lability concept.

9.4 Conclusions

The main conclusions that arouse in this chapter are the following:

- Hydrology is a key environmental factor that determines the transport and reactivity of DOM in the Mediterranean river under study.
- Whereas in terms of DOC and DON the river was found to behave as a pipe during flood and high baseflow, and as a sink during drought, in terms of fluorescence composition the river behaved as a pipe during flood, as a source during baseflow, and as a sink during drought.
- Even though a reactive transport of fluorescence DOM during flood could not be assessed with enough confidence, there were evidences of some protein-like depletions and humic-like generations during the riverine passage.
- During baseflow conditions there were important generations of protein-like components which triplicated (high-baseflow) and doubled (low-baseflow) the inputs. Humic-like components were also generated, although at lower efficiencies.
- In drought conditions, all four fluorescence components exhibited retentions along the river length, with the only exceptions of segments under the influence of anthropogenic inputs, in which retentions were reduced or even inverted to generations.
- In space, during flood and baseflow DOM processing occurred in the final segments of the river reach. Contrastingly, during drought DOM reactivity took place homogeneously along the river reach, except in the anthropogenically-influenced segments.
- In our field observations, the degree of DOM processing could not be predicted from its initial characteristics (i.e. initial intensities and character in terms of optical indices).
- Some of our findings support recent revisions of traditional views, providing observations which are in line with studies reporting a dual role of bacteria as both consumers and producers of fluorescence DOM and a recalcitrant character of in-stream produced components.

Chapter 10

General discussion

Dealing with dissolved organic matter (DOM) implies dealing with complex organic molecules. This arises from the fact that DOM is composed of an amalgam of organic molecules spanning a range of chemical structures – most of them unknown and highly humified (McDonald et al., 2004) – and also spanning a range of interactivity with the environment – as different groups of molecules will present a varying degree of susceptibility to be involved in different biogeochemical processes, whether microbial or photochemical degradation, sediment sorption or flocculation (Jaffe et al., 2008).

The main aim of this thesis was to better understand transport and reactivity of DOM during its downstream riverine passage, and to elucidate to what extent and in what manner hydrological conditions influence such downstream transport of DOM. Assessing the in-stream reactivity of DOM requires previous knowledge about its composition, as it is not enough to calculate the differences in overall DOM quantity (e.g. dissolved organic carbon (DOC)). Such difference would explain the net amount of DOM which has been added or removed from the system. However, it would not explain underlying DOM transformations (Fisher et al., 2004). Microbial and photochemical degradation processes very often do not complete mineralise DOM to CO_2, but either break it into new compounds of lower molecular weight, or even aggregate and transform different molecules into larger and more complex compounds (Bertilsson and Tranvik, 2000). These new molecules present a different ecological and biogeochemical role with respect to the original ones, as they will subsequently have a different lability degree. Therefore, understanding DOM reactivity requires not only understanding quantitative changes, but also variations in its composition.

10.1 Unveiling DOM composition: Self-Organising Maps and correlation analysis

In order to study DOM, it is necessary to systematise and simplify the originally complex DOM composition into some few representative constituents which can then be used as independent data variables. Such simplification is a key step, as it will determine our perception of DOM and, therefore, the knowledge that we build about it. The challenge is to find a statistical methodology that performs that simplification process in an objective way and that finds a number of DOM components which are as representative as possible of the diversity of spectral shapes of a given data set.

Up to now, the main methodologies used for that purpose have been peak-picking and parallel factor analysis (PARAFAC). Peak picking (Coble, 1996; Parlanti et al., 2000) reduces large Excitation-Emission Matrices (EEMs) into some few coordinates corresponding to peak maxima. Data reduction is important, but still the definition of a finite number of fluorescence components remains ambiguous and at the subjectivity of the researcher. PARAFAC (Andersen and Bro, 2003; Stedmon and Bro, 2008) overcomes this limitation and resolves the overall signal of EEMs into a number of fluorescence components that appear at fix coordinates among the samples of an EEM data set. However, as this method is based on least squares solutions, it is highly sensitive to the presence of outliers (Brereton, 2012). This is an important limitation, as it requires that experimental and sampling designs are planned in order to suit PARAFAC requirements, namely, to span a gradual range of compositional changes (Stedmon and Bro, 2008). In this sense, we aimed at finding a tool which would give DOM researchers more freedom in their experimental designs, and therefore, which would expand the number of research questions that can be addressed about DOM.

In chapter 4 we presented the use of self-organising maps (SOMs) (Kohonen, 1998) to explore patterns in EEM data sets, as well as to resolve the composition of DOM into some finite fluorescence components. SOM is an unsupervised self-learning algorithm that makes no preassumptions about the data structure, and has a high flexibility to interpret and manage the results: it performs on the same time, a reduction of the dimensionality (distribution onto a two-dimensional grid) and a clustering (distribution among discrete units) of the original data, and offer many graphical possibilities to explore and analyse results (Vesanto, 1999). It has already been used successfully in chemometrics (Brereton, 2012) for one (Mat-Desa et al., 2011) and two (Rhee et al., 2005; Bieroza et al., 2009) dimensional spectral data in order to find patterns among samples. Here, the novelty of our approach was to couple SOM with a correlation analysis of its component planes (Barreto-Sanz and Perez-Uribe, 2007), so that a finite number of fluorescence components could

also be determined. According to our results, SOM had i) little outlier sensitivity and ii) enhanced resolution of component separation. The latter was possible due to the re-weighting of the representativeness of different spectral shapes within the data set, as the correlation analysis is performed on the codebooks of the SOM analysis, and not on the original samples. Even though in this thesis we did not present a systematic comparison between SOM and PARAFAC capabilities, we previously performed peak picking and PARAFAC analysis which produced weaker results: with peak picking, there was a high dispersion in the peaks location that created a lot of ambiguity to define different fluorescence components, whereas with PARAFAC, only two fluorescence components could be validated (Figure 10.1). Moreover, the two-component PARAFAC model produced systematic patterns in the residuals matrices, indicating a weak fitting of the model (Stedmon and Bro, 2008).

The SOM analysis presented in chapter 4 revealed the presence of four fluorescence components: two humic-like and two protein-like moieties, similar to the previously identified B, T, A and C components (here referred to as C1, C2, C3 and C4, respectively). These components were used thereafter in the rest of the thesis in order to unveil their biogeochemical behaviour during their downstream transport in La Tordera, under three contrasting hydrological conditions: flood, baseflow and drought.

10.2 Flood: Inert conduit of DOM from the land to the sea

In the mass balance study we had the opportunity to sample a very extreme flood event. In Fogars de la Selva, the outlet of our mass balance design, there was a discharge of 156 m^3s^{-1}, a water flux that in the last 10 years has only been equalled or exceeded on three rainfall events (according the discharge data of the last 10 years provided by Agència Catalana de l'Aigua). However, this event may also be representative of stormflows of $> 4m^3s^{-1}$, as characterised in chapters 5 and 6. Such flows occurred 5% of the days in the last 10 years, and represented the export of 40% of the total water, highlighting the relevance of the export capacity of stormflows, even though they are short in time. In such high flows, we observed an homogeneous DOM composition throughout the river length with a predominance of the humic-like components C3 and C4, together with a highly humified character as expressed by high Humification Index (HIX) values (chapters 5 and 6). Such homogeneity suggested little processing during the DOM downstream transport under such high flows, assumption that was later demonstrated in the mass balance study.

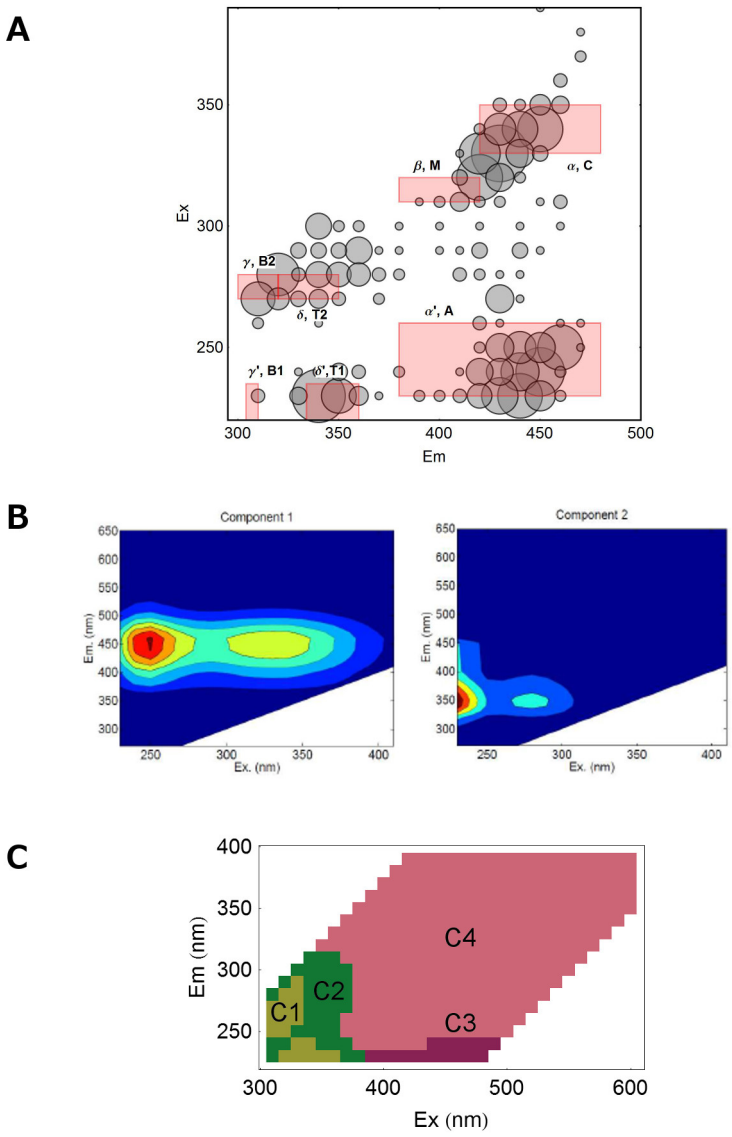

Figure 10.1 – Different data mining methods applied to our EEM data set: peak picking analysis (A), PARAFAC (B) and SOM (C).

In chapters 8 and 9 we observed that the amount of DOM exported in Fogars de la Selva was practically the same than the DOM that entered the river through the tributaries, both in terms of bulk DOM – for which the differences between the inputs and the outputs were -5.1 for DOC –, and of fluorescence components – for which the differences were -5.4 ± 0.3 % for C1, -5.5 ± 0.3 % for C2, -3.7 ± 0.2 % for C3 and -5.7 ± 0.3 % for C4. Such low percentages could still represent higher amounts of DOM retention than those reported in periods of lower flows, however the uncertainties associated to those percentages do not allow to confidentially assess the extent of such retention. The only exception to that eminent retentive character was dissolved organic nitrogen (DON), which exhibited a global depletion of 100%.

These results demonstrated that during flood, the river behaved eminently as a pipe, inertly transporting DOM downstream. That is, during this flood event, every second the river was delivering at least 81 mg of highly humified, terrestrially-derived DOC. If we assume that this behaviour can be made extensive for the stormflows of $> 4m^3s^{-1}$ (as suggested in chapter 5), then the amount of exported DOM may represent up to the 47% of the DOC export (computed over the last 10 years). The lowland sites of the river were not included in the mass balance study, however if we consider that the DOM composition remained homogeneous also in this final part of the river, we can assume that DOM was effectively discharged to the sea having undergone hardly any processing.

10.3 Baseflow: Spatial variability of DOM transport and reactivity, and dual biogeochemical role of the river

In chapter 5, the direct observation of the intensities of fluorescence DOM components revealed an important variability along the main stem, so that the river had three parts with clearly different DOM compositions. The headwaters had a predominance of humic-like materials, which reflected the drainage of the forested land covers of the upper parts of the catchment. In Sant Celoni (the beginning of the middle part of the river) there was a change in the water chemistry, consisting in an increase in component C2, together with conservative anions (chlorides, sulphates and electrical conductivity) as well as nutrients (nitrate, ammonium, soluble reactive phosphor (SRP)). These increases indicated the predominance of inputs of anthropogenic origin. Finally, in the lower part of the river, there was a predominance of component C1 and increasing values of the Fluorescence Index (FI).

In fact, this approach provided evidence of the changing predominant sources of DOM along the river: from terrestrial in the headwaters, to anthropogenic in the middle reaches, and autochthonously-derived in the lower part of the river. This

emphasized that the variability of the concentrations and relative proportions of fluorescence DOM components along the river were mainly driven by the predominant sources. However, beyond a downstream switch in the main DOM sources, the direct observation of the intensities of fluorescence components was not sufficient to demonstrate the extent at which DOM processing was taking place, and to what extent any downstream compositional changes could be due simply to the physical mixing of input waters providing a different water composition.

Some intuition in this sense was achieved by means of an end-member mixing analysis (EMMA) approach. It was evidenced that the composition of some sites could not be explained solely as the result of the mixing of upstream water inputs, as they appeared outside of the endmember (i.e. tributaries) mixing domain. Therefore, the intensities of the fluroescence components had the be the result of in-stream processing at least to some extent. This was most evident for the lowland sites, and also expectable, as during the last 20 km the river flows along a mild terrain that hardly receives any tributaries. Hence, any observed increases in FI and C1 intensities should be due to in-stream processes. However, in the middle reaches the degree of reactivity was less clear. Even though sites appeared mainly within the end-member mixing domain, on some dates during base flow and drought they appeared highly disperse and outside it, suggesting that in-stream transformations could be operating and shaping the main stem fluorescence intensities. Also, due to the frequent confluences within the middle reaches, and to the different nature of their compositions, the relationship between transport and reactivity in this part of the river seemed less obvious.

The mass balance study (chapters 8 and 9) provided direct insight in this sense, and evidenced that an important in-stream processing of DOM took place. Most remarkably, it was found that there was an uncoupling between the processing of bulk DOM and that of the individual fluorescence components. Bulk DOM experienced moderate net retentions (differences of -9.8 during high baseflow and -21.2% during low baseflow for DOC between the total inputs and the outputs in Fogars de la Selva). Contrastingly, fluorescence components experienced higher reactivity efficiencies, consisting on net generations. This was especially found for the protein-like components which were tripled (C1) and doubled (C2) during their riverine transport. Therefore, while the river was behaving as a moderate sink for bulk DOC, there were high generations of fluorescence components. This evidenced the importance and relevance of intermediate transformations of DOM, rather than its complete oxidation to CO_2. Even though our sampling design does not allow to infer what specific of biogeochemical processes were operating, our findings may add evidence to recent findings that bacteria can be important producers of fluorescence DOM (Guillemette and del Giorgio, 2012).

In baseflow conditions, the global mass balances were representative of what could be observed locally, at the segment level. That is, locally we also observed generations of fluorescence DOM, mainly consisting on components C1 and to a lesser extent, C2. However, such reactive processes only occurred in the final part of the middle reaches, which spanned 11.5 km during high baseflow (3.43 m^3s^{-1}) and 6.5 km during low baseflow (1.49 m^3s^{-1}), while in the previous segments there was an eminent conservative transport of fluorescent DOM. If we assume that the reactivity that we observed in the final segments remains similar in the lower part of the river, then the DOM delivered to the coast will be rich in fresh and in-stream produced protein-like components.

The two baseflow surveys performed during baseflow captured the discharges of 1.49 and 3.43 m^3s^{-1}, therefore, the findings corresponding to these dates represent the state and functioning of the river at least 17.34 % of the days (according the discharge data of the last 10 years provided by Agència Catalana de l'Aigua). However these findings may be extensive to the flows between 1 and 4 m^3s^{-1}, characterised as baseflows in chapters 5 and 6. These conditions are mainly relevant due to their duration over time and moderate flows, as they occurred 45% of the days during the last 10 years, and exported 53% of the water, which in DOC terms, represents an export capacity of up to one half of the total annual exported DOC (as computed over the last 10 years).

10.4 Drought: The river as a filter

During summer low flows, the spatial variability of DOM composition was similar to that observed during baseflow conditions. That is, a humic-like character in the headwaters turned into a C2-dominated composition in the middle reaches and, finally, into a C1-dominated and high FI predomination in the lowland. However, such spatial differentiation and heterogeneity of DOM composition and character was maximised during drought, as shown in chapters 5 and 6.

Contrastingly with these heterogeneity in terms of DOM composition, in the mass balance study it was found that in terms of biogeochemical functioning, there was an eminent spatial homogeneity throughout the middle reaches. Globally, this part of the river retained -73.7% of DOC, a similar percentage of the retention that the fluorescence components experienced, on average, in the different segments along the middle reaches. Such longitudinal homogeneity was only disrupted at the outlets of anthropogenic inputs. In Sant Celoni, the discharge of sewage water from the waste water treatment plant (WWTP) caused an interruption of the retentions and, locally, DOC was conservatively transported. This was despite the fact that in this site, important increases in DOM concentration and fluorescence intensities

were detected. The lack of retentions could be due to a decreased capacity of the river to uptake DOM, similarly to what has been observed for inorganic nitrogen (Martin et al., 2011; Marti et al., 2004; Merseburger et al., 2011). By contrast, in Hostalric, there was not just a depletion of the retention capacity but, conversely, there was a generation of fluorescence components and DOC. This suggests that there was not just a depletion of the retention capacity of the system, but rather, the anthropogenic inputs of DOM locally caused a differentiated biogeochemical processing of DOM which resulted in a generation of protein-like moieties. This could be due to some complementary effect between the DOM and/or bacterial inputs and those found in the river water which may have triggered the onset of such protein-like DOM generation, as suggested in (McClain et al., 2003); even though it had little repercussion on the overall balance of DOM, as retention still predominated in the system as whole.

The behaviour of the river observed during drought conditions may be representative of up to 50% of the days of the last 10 years, although due to the extreme low flows these periods only account for 7% of the total exported water. Hence, during such periods of minimal flows, the inputs of DOM to the coast are minimal, as they contribute to approximately the 4% of the total DOC export (computed over the last 10 years) and may deliver highly degraded organic materials.

10.5 The role of DOM in the regulation of inorganic nitrogen

Even though the main focus of this thesis is on DOM, its relationship with inorganic nitrogen has also been assessed, due to the coupled biogeochemical behaviour observed between both kinds of substances (Lutz et al., 2011; Johnson et al., 2012). Globally it has been observed that nitrate accumulation in water bodies is regulated by its stoichiometric relationship with DOM, as it regulates a suite of microbial processes that couple both substances (Taylor and Townsend, 2010). This results in an inverse and nonlinear relationship between nitrate and DOC concentrations (Goodale et al., 2005). However, such relationships have been assessed with baseflow conditions. In chapter 8 we assessed to what extent different and contrasting hydrological conditions fit into this stoichiometric framework, and to what extent changes in the nitrogen mass fluxes could be related to changes in its stoichiometric relationship with DOC.

Our results showed that despite most samples followed the nonlinear negative relationship between the concentrations of DOC and nitrate previously described in the literature (Goodale et al., 2005; Taylor and Townsend, 2010), flood conditions were an exception, and exhibited a positive linear relationship. We argued

that, most likely, the reason for this behaviour would be that the rapid downstream transport during such high flows do not allow for any biogeochemical coupling between DOC and nitrate, and this may be supported by the low processing efficiencies found for both in the global mass balances in flood conditions (-14.7% for nitrate and 5.1% for DOC).

On the other hand, the results of the mass balance study were consistent with the stoichiometric findings, so that higher retention efficiencies of nitrate were found at higher DOC:nitrate ratios. The samples from all the hydrological conditions contributed to this relationship, even though during drought samples were more dispersed. However, overall these results highlight the role of DOM in coupling the cycles of carbon and nitrogen.

10.6 Implications and future research

Mediterranean rivers are highly dynamic systems over time due to the large intraanual variability of their flows regime, which have shaped its ecological structure and function (Gasith and Resh, 1999). In this thesis it has been evidenced that such hydrological variability, unique of Mediterranean systems, has also a determinant role in the biogeochemical functioning of rivers with respect to DOM. Whereas during extreme high flows downstream transport controls DOM export, during lower flows in-stream processes dominate over transport and shape the quantity and composition of the DOM that is finally exported from the river. Hence, the seasonal variability of the Mediterranean river flows were found to have a determinant role in shaping the quantity and quality of DOM which is finally exported to the sea: From large amounts of highly humified and little processed DOM during short and intensive storm events, to moderate amounts of protein-like and freshly produced DOM during baseflow, and small amounts of highly processed DOM during extreme low flows, that may extend up to half of the days of the year.

As rivers link the carbon cycle of the terrestrial and marine systems, it is of utmost importance to better understand the consequences that such qualitatative changes of DOM, derived from the riverine passage, have on the subsequent lability of DOM in the sea. While there are evidences that marine bacterioplankton can readily degrade riverine DOM (Bonilla-Findji et al., 2009) even at higher rates than riverine bacteria (Stepanauskas et al., 1999), the quality of exported DOM may regulate the relative relevance of bacterial production and CO_2 outgassing (Xu et al., 2014). Therefore, the observed seasonality in La Tordera of the quantity and quality of exported DOM to the coast may have complex repercussions on the capacity of bacterial communities to degrade such temporally-changing DOM and, therefore, to further funnel DOM through the carbon cycle.

Unveiling the fate of riverine DOM in the sea involves facing a current challenge of DOM research, which is to better understand the coupling between DOM composition and the structure and function of bacterial communities. DOM and bacteria have a close relationship as substrate - consumer, however such relationship, far from being straightforward, is intricate and recursive (Judd et al., 2006; Docherty et al., 2006) due to the plasticity of bacterial communities in their carbon metabolism, allowing them to use DOM pools of different compositions (Rochelle-Newall et al., 2004). A better understanding on the adaptability of bacterial communities to changing characteristics of DOM may provide a better understanding on the lability of DOM, a concept that still remains relative to the specific bacterial communities and DOM pools sampled in every study.

Also, a better understanding of the coupling between DOM and bacteria may provide a further understanding of the underlying processes controlling the biogeochemical processing observed in this thesis. In this sense, this thesis contributed to expand the current knowledge about DOM transport and reactivity in lotic systems by providing direct evidence of in-situ generation/retention of DOM fractions along a Mediterranean river. However, our field-based approach did not allow to discern the specific biogeochemical processes (namely bacterial and photochemical degradation) that are directly controlling the observed retentions/productions, nor the relative importance of each of them. Therefore, the findings of this work could be expanded by better understanding the controls that the bacterial communities exert on DOM composition and concentration.

Chapter 11

General conclusions

PART I

Chapter 4: Self-Organising Maps and correlation analysis for the analysis of large and heterogeneous EEM data sets.

1. Self-organizing map (SOM) analysis coupled with a correlation analysis allows an analysis both at the object and at the variable level. Hence, it serves not only to explore the differences in fluorescence properties between samples, but also helps to identify particular fluorescence components.

2. SOM analysis is robust to the presence of outliers. That is, samples with very distinct features are discerned while having little effect on the ordination and classification of the other samples. This distinct property makes it possible to work with heterogeneous data sets.

3. The correlation analysis performed on the SOM Excitation-Emission Matrix (EEM) prototypes has an enhanced capacity to detect fluorophores that are represented at only low levels in the original EEM data set.

4. SOM analysis coupled with a correlation analysis of the component planes expands the toolbox of the fluorescence dissolved organic matter (DOM) researchers by enabling the analysis of complex and heterogeneous EEM data sets. This may open new possibilities for advancing our understanding of DOM character and biogeochemical behaviour.

PART II

Chapter 5: Preliminary assessment of spatiotemporal patterns of DOM quality and quantity in La Tordera

5. Along the main stem, the river exhibited three reaches with a consistent differentiated DOM character: the headwaters, the region near the town of Sant Celoni, and the low part of the river flowing between the bend of Fogars de la Selva and the river mouth.

6. In the headwaters, DOM has an eminent humic-like character coming from the drainage of the surrounding terrestrial catchment. During flood conditions, this character is transferred downstream.

7. Near Sant Celoni, there is a shift in the DOM quality, expressed as a predominance in the protein-like component C2. A concomitant increase in the chlorides and nutrients content of the water suggests that this shift in the DOM quality is caused by the direct outlets of a waste water treatment plant (WWTP) and possibly other industries in the beginning of the river reach.

8. In the lower part of the river, high water residence times and light availability favour the conditions for in-stream DOM production and transformation, which results in an increased Fluorescence Index (FI) and predominance of the protein-like EEM component C1.

9. Whereas flood conditions induce an homogenisation of the DOM character over the longitudinal dimension, baseflow and drought favour spatial differentiation resulting from the influence of the local characteristics of the river at every reach.

10. The hydrological antecedents of a drought period determine the magnitude of the spatial differentiation of DOM character. A longer previous dry period contributed to an amplification of the longitudinal differentiation.

11. This suggests a seasonal role of the river with respect to DOM, shifting between transporter and transformer. Such alternation in the transport and processing of DOM can have further implications for the understanding of the carbon cycling at higher scales, and may contribute to the ongoing debate on the role of inland waters on the global carbon cycle.

Chapter 6: Multivariate exploration of DOM quality and reactivity in the main stem of La Tordera

12. The homogenisation of DOM properties observed along the river length during flood conditions has been effectively found to be due to a conservative transport.

13. The longitudinal patchiness in DOM properties that appears at lower flows do not only reflect the successive mixing with tributaries providing DOM with varying properties, but are also due to the occurrence of in-stream processing.

14. The lowland sites, located between Fogars de la Selva and the river mouth, exhibited a downstream DOM gradient mainly driven by in-stream processing.

15. The headwater sites exhibited consistently a humified humic-like character irrespective of the hydrological conditions, with conservative transport being the main driver of DOM downstream evolution.

16. The sites from the middle reaches were found to respond to a more intricate relationship between physical mixing and processing, due to the high frequency of tributary inputs providing a variety of water types, from low to highly polluted.

PART III

Chapter 7:Water balance in the middle reaches of La Tordera

During flood, high and low baseflow:

17. Most of the water inputs to the main stem of La Tordera come from the natural drainage of the terrestrial catchment, mainly through the creeks of Arbúcies and Santa Coloma.

18. The main stem discharge is the result of the sum of the previous water inputs received upstream. This indicates a minor interaction between the river and the underlying alluvial and groundwater aquifers.

19. Under these circumstances, the cumulative approach is useful to predict longitudinal changes in water and conservative solutes along the main stem.

Conversely, during summer drought:

20. Most of the water inputs to the main stem come from anthropogenic sources (either WWTPs or industries). The contribution of these inputs may be essential to maintain the flows in certain sections of the river.

21. The river exhibits important interactions with the underlying aquifers, linked to the geo-tectonic structure of the physical environment. Because of that, there is an important spatial heterogeneity of the hydrological behaviour of the river, alternating between a gaining and a loosing character.

22. Despite the occurrence of a net infiltration of water over the whole length of the river reach, there are some specific spots that have an effluent character, located consistently with previous findings in the literature.

23. Under these circumstances, a reach-by-reach approach has been found to be necessary to predict longitudinal changes in water and conservative solutes along the main stem, in order to take into account local water gains and losses.

Chapter 8: Carbon and nitrogen mass balance: Linking DOC and nitrate

24. Retention predominated for the dissolved nitrogen and organic carbon solutes. However, the efficiencies of the net retentions in the river were different according to the hydrological conditions: it was maximal during drought and minimal during flood.

25. During flood, even though the processing efficiencies were the lowest among hydrological conditions, in absolute terms it was the date in which the largest amount of nitrogen and dissolved organic carbon (DOC) mass was retained and released, respectively. This emphasizes the importance of such extreme events, even if they last just for some few hours or days (as floods).

26. dissolved organic nitrogen (DON) had a distinct behaviour with respect to dissolved inorganic nitrogen (DIN) and DOC, as it exhibited high net retentions in all hydrological conditions, as well as an important spatial variability in its processing.

27. In space, the retained mass consistently increased downstream in all hydrological conditions. However, the main nitrogen solute removed in every survey differed. From flood to drought, they corresponded to nitrate, DON and ammonium.

28. In terms of removal efficiencies, spatial patterns were not clear and had an important longitudinal variability.

29. In space, after the confluences with the WWTP inputs, there was a reduced retention efficiency both for DOC and dissolved nitrogen.

Regarding the coupling between DOC and nitrate:

30. In La Tordera, the stoichiometrical relationship between DOC and nitrate streamwater concentrations was consistent with that observed in the major Earth aquatic systems, especially during baseflow conditions.

31. During flood, the general nonlinear negative trend was shifted to a linear positive relationship.

32. Results of the mass balance were consistent with the stoichiometric findings, and showed that nitrate processing changed into higher retention efficiencies at higher DOC:nitrate ratios. In this case, the drought period did not follow the general trend and showed a weak relationship between nitrate processing and DOC:nitrate stoichiometry.

33. Results emphasize the determinant role that hydrology plays in the definition of longitudinal patterns of carbon and nitrogen biogeochemical processing, as well as in the definition of its coupling.

Chapter 9: Downstream processing of DOM: changes in its reactivity and composition

34. Hydrology is a key environmental factor that determines the transport and reactivity of DOM in the studied Mediterranean river.

35. Whereas in terms of DOC and DON the river was found to behave as a pipe during flood and high baseflow, and as a sink during drought, in terms of fluorescence composition the river behaved as a pipe during flood, as a source during baseflow, and as a sink during drought.

36. Even though a reactive transport of fluorescence DOM during flood could not be assessed with enough confidence, there were evidences of some protein-like depletions and humic-like generations during the riverine passage.

37. During baseflow conditions there were important generations of protein-like components which triplicated (high-baseflow) and doubled (low-baseflow) the inputs. Humic-like components were also generated, although at lower efficiencies.

38. In drought conditions, all four fluorescence components exhibited retentions along the river length, with the only exceptions of segments under the influence of anthropogenic inputs, in which retentions were reduced or even inverted to generations.

39. In space, during flood and baseflow DOM processing occurred in the final segments of the river reach. Contrastingly, during drought DOM reactivity took place homogeneously along the river reach, except in the anthropogenically-influenced segments.

40. In our field observations, the degree of DOM processing could not be predicted from its initial characteristics (i.e. initial intensities and character in terms of optical indices).

41. Some of our findings support recent revisions of traditional views, providing observations which are in line with studies reporting a dual role of bacteria as both consumers and producers of fluorescence DOM and a recalcitrant character of in-stream produced components.

Appendix

Evaluation of the capacity of DOM optical variables to quantify mixing processes

Introduction

One of the main challenges for unveiling the role of dissolved organic matter (DOM) in rivers, is to understand its sources and fate. In this context, spectroscopic DOM measurements have found their success, because of their ability to detect DOM moieties from different sources in a DOM mixture, and to track them after mixing. This *fingerprinting* capacity has been used and addressed in a number of studies, aiming at tracking downstream the impact of sewage (Baker, 2001; Borisover et al., 2011; Carstea et al., 2009), farm wastes (Bilal et al., 2010; Ruggiero et al., 2006; Naden et al., 2010), the contribution of different flowpaths to the river discharge during stormflow events (Fellman et al., 2009b; Hood et al., 2006; Nguyen et al., 2010) or to discern an authochthonous versus allochthonous production of DOM (Battin, 1998; McKnight et al., 2001). For that, a large variety of discrimination indices have been used, like the Fluorescence Index (FI) (McKnight et al., 2001; Carstea et al., 2009), the Humification Index (HIX) (Nguyen et al., 2010), the Specific Ultra-Violet Absorbance (SUVA) (Hood et al., 2006) and the intensity or ratio between parallel factor analysis (PARAFAC) components (Fellman et al., 2009b; Borisover et al., 2011), as well as between fluorescence components determined by fluorescence regional integration (FRI) (Bilal et al., 2010).

Despite the numerous evidences that fluorescence measurements can serve as a good tool to track DOM from different sources, most studies have remained at a qualitatiave stage. Only few examples can be cited that tested the capabilities of fluorescence metrics to quantify mixing processes at subtle levels, and, most of them highlighted that their use should be critically examined (Yang and Hur, 2014). In order for a variable to have good discrimination capabilities, it should follow a

property balance principle; that is, it should exhibit a linear response at intermediate mixtures of two or more DOM sources. Some studies, like in Hur et al. (2006), Korak et al. (2014) and Yang and Hur (2014) tested the discrimination capacity of a several optical metrics using an end member validation approach was used. That is, well-defined end-member samples were used to create intermediate artificial mixtures at known proportions in order to check the capacity of different indices to predict their values for intermediate mixtures. Hur et al. (2006) evaluated a total of 18 metrics corresponding to HPLC-SEC chromatograms, fluorescence and absorbance spectra. Yang and Hur (2014) tested the property balance of PARAFAC components, absorption coefficients, spectral slopes, peak ratios, HIX and FI, and Korak et al. (2014) tested the performance of fluorescence components determined by visual peak-picking, as well as the FI index. Their work shows that not all the variables are equally valid for predicting mixtures by mass-balance. Property balance was found to be well preserved for fluorescence components, either determined by PARAFAC (Yang and Hur, 2014) or visual peak picking (Korak et al., 2014). However, the discrimination capacity of indices based on spectral ratios showed a variety of behaviours. Hur et al. (2006) observed a good property balance for SUVA and a fulvic- to protein-like ratio, whereas FI and HIX have not been found to exhibit a linear behaviour with respect to end-member mixing ratios (Hur et al., 2006; Yang and Hur, 2014).

As self-organizing map (SOM) analysis is a novel approach to determine Excitation-Emission Matrix (EEM) components, we consider it necessary to evaluate the behaviour of such components in mixing processes. Also, given that there are few previous studies testing the discrimination capacity of optical indices, and that there are some disparities in their results, we also test the performance of SUVA, FI and HIX. For the SOM components, we used two methods to quantify them: maximal fluorescence intensity, and regional integration. The former method simply takes the maximal fluorescence intensity of every component region, and follows the traditional peak-picking approach; while the latter integrates the area under the surface of every component region using a Riemann summation as described in Chen et al. (2003). This will allow to compare the performance of the two quantification methods in mass-balance calculations.

Objectives

The specific objectives of this appendix are:

- To test the source discrimination capacity of the fluorescence components determined using Self-Organising Maps and correlation analysis (chapter 4).

- To test the best quantification of SOM components in order to optimise their discrimination capactiy: maximal intensity of regional integration.
- To test the property balance performance of other optical variables, namely SUVA, FI HIX and Biological Index (BIX), in order to provide more experiences to the scientific literature.

The results of this analysis will provide the basis to decide which variables are suitable to be used in the DOM mass-balance study, chapters 9.

Procedures

In order to verify the linear relationship of an optical variable during DOM mixing from different sources, we performed two artificial mixture banks. The first one used as end-members a sample from the effluent of the waste water treatment plant (WWTP) of Sant Celoni, and a pristine river water, corresponding to the creek of Fuirosos. The second mixture bank used as end-members the same WWTP effluent, with a slightly impacted river water, corresponding the creek of Pertegàs. The WWTP of Sant Celoni and the creek of Pertegàs are located upstream of site A3 (Figure 3.5), the creek of Fuirosos corresponds to site A6 (Figure 3.5).

End-member samples were collected in the field as described in section 3.3. Every pair of end-members were mixed at proportions of 100:0, 99:1, 90:10, 70:30, 50:50, 30:70, 10:90, 1:99, 0:100; and after that, all mixtures were analysed for EEM fluorescence, absorbance spectra and dissolved organic carbon (DOC) concentration as described in section 3.3. Next, expected values at intermediate mixtures were calculated according to standard mass-balance calculations:

$$C_{predicted} = \frac{C_1 \times V_1 + C_2 \times V_2}{V_1 + V_2} \tag{11.1}$$

where C corresponds to a spectral variable or index, C_1 and C_2 the values of the spectral variable of each end-member and V_1 and V_2 the proportional volumes of each end-member in the mixture. Finally, the expected values were compared with the measured ones by linear regression.

Results and discussion

EEM components

The EEMs of the end-members and some of the intermediate mixtures are shown in Table 11.1. The EEM of Fuirosos exhibited two peaks centered at $\lambda_{ex} = 240$ and 350 nm for λ_{em}=450. These correspond to peaks A and C (Coble, 1996), largely reported for streams draining forested catchments (Hudson et al., 2007; Vazquez et al., 2011). On the other hand, the end-member from Pertegàs had an additional peak at $\lambda_{ex}, \lambda_{em} = 290, 420$, closer to the coordinates previously identified as peak M (Coble, 1996). This third peak lied near peak C with slightly higher intensity, therefore confering a shoulder-like shape to peak C. Finally, the end-member from the WWTP had a clearly distinct EEM shape. It showed 5 peaks, 3 of them centered at $\lambda_{em} = 425$ nm and exciting at $\lambda_{ex} = 320$, 270 and 240; whereas the other two were centered at $\lambda_{em} = 350$ nm, exciting at $\lambda_{ex} = 285$ and 240 nm. The first three appeared at the lower emission range for humic-like substances, whereas the latter two appeared to the coordinates attributed to tryptophan-like material. The humic-like and the protein-like moieties appeared with similar intensity, what has been identified as a typical feature of sewage DOM (Baker, 2001; Henderson et al., 2009). Throughout the intermediate mixtures between the WWTP and Fuirosos or Pertegàs, it can be seen that the characteristic shape of the WWTP was already apparent at low proportions of this end-member.

In Table 11.2 there is a summary of the linear regression models between the measured and the predicted values of the EEM components. In the first two groups of rows appear the results for the EEM components determined by SOM. It is noticeable that both types of quantification (i.e. maximal intensity or regional integration) have very high goodness-of-fit values ($r^2 > 0.9900$) and mean % differences lower than 10%. This indicates the good ability for both quantifications to predict the composition of end-member EEM mixtures. Moreover, the slope remains near 1, indicating that there is no consistent pattern toward over- or underestimating the predicted values with respect to the actual ones.

Despite the high performance of the SOM components under both types of quantification, a closer look to the mean % differences between the predicted and observed values, indicates that in the quantification using maximal intensity values, the mean % differences are slightly higher than in the quantification using regional integration. Such trend is statistically significant for the Pertegàs - WWTP mixtures (t-test, $p < 0.05$). Therefore, regional integration would be preferable to picking the maximal intensity of a SOM region, as it seems to be able to provide more accurate predictions.

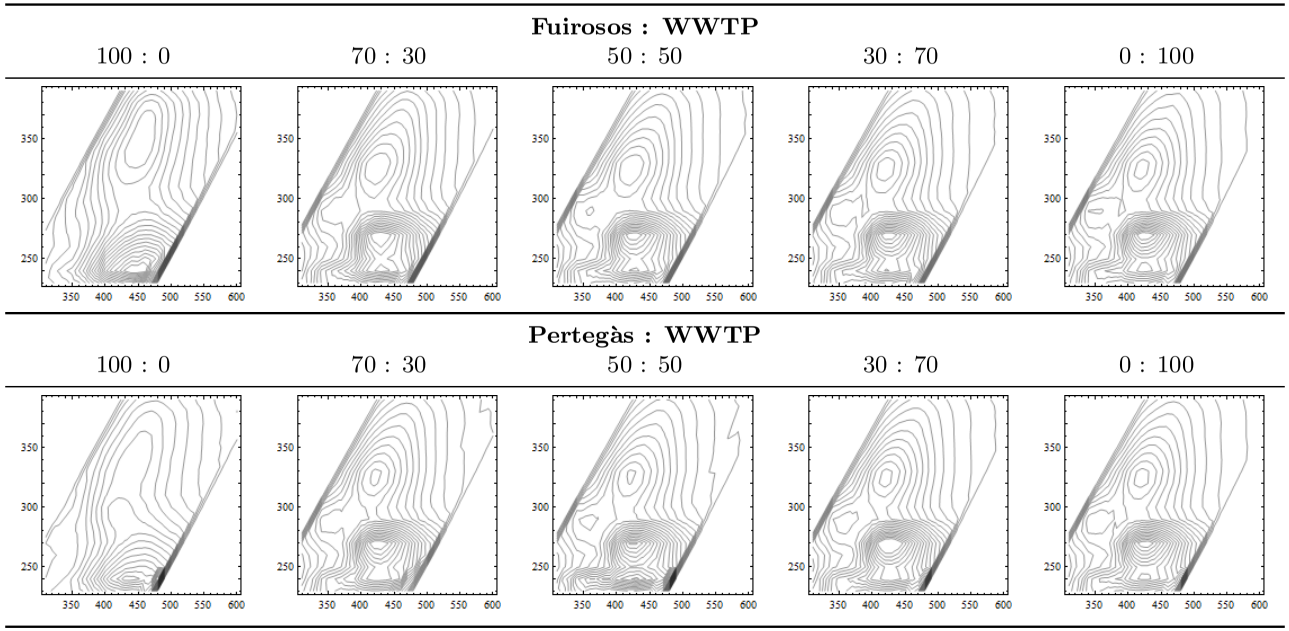

Table 11.1 – EEMs of the end-members and some of the intermediate mixtures.

variable	Fuirosos - WWTP r^2	slope	mean % difference*	Pertegàs - WWTP r^2	slope	mean % difference*
C1.vol	0.9970	0.974	7.80	0.9983	1.009	5.98
C2.vol	0.9966	0.963	7.97	0.9981	1.01	6.63
C3.vol	0.9986	0.985	2.36	0.9966	1.025	5.49
C4.vol	0.9987	0.998	1.9	0.9974	1.009	4.13
C1.int	0.9945	0.961	9.36	0.9973	0.999	5.92
C2.int	0.9965	0.959	6.83	0.9945	1.002	6.46
C3.int	0.9980	1.004	2.31	0.9699	1.044	9.9
C4.int	0.9943	1.016	5.83	0.9976	1.017	7.58
FI	0.9745	1.000	1.29	0.8236	0.921	3.89
HIX	0.4848	0.533	40.99	0.4891	0.561	46.54
BIX	0.5161	0.532	6.48	0.5592	0.637	7.98
SUVA	0.0355	1.066	6.09	0.1855	0.663	2.90

Table 11.2 – Summary of the linear model parameters for the different variables evaluated. * Percentage differences between the predicted and the measured values.

Among fluorescence components, the mean % difference between actual and predicted values remains similar for the four components in the intermediate mixtures of Pertegàs : WWTP. However, in the intermediate mixtures of Fuirosos : WWTP, the protein-like components (C1.vol and C2.vol, C1.int and C2.int) have a higher % difference than their corresponding humic-like components. This is evident in the two types of EEM components determination (maximal intensities and regional integration), but slightly more accentuated with the components determined by maximal intensity. This indicates that while the humic-like fraction behaves consistently in a linearly additive way, the protein-like substances are more prone to non-linearity additions in mixtures. In order to better understand this phenomena, it is worth doing an attentive inspection of the expected versus the actual values of the intermediate mixtures (Tables 11.3, 11.4 and 11.5). In there it can be seen that those mixtures containing the highest proportions of river water with respect to WWTP water (99:1 to 70:30), also have the highest mean % differences between the actual and the predicted vaues. This is especially notorious for protein-like components, which can have mean % differences up to 20 - 50 %. In contrast, dilutions from 50:50 to 1:99 (predominance of WWTP water) have very low mean % differences ($< 5\%$) indicating very accurate predictions in this range.

This asymetry over the range of mixing proportions could be attributable to the large differences between the end-members. However, this asymetric response was also evident in many of the variables evaluated by Hur et al. (2006), even though they were working with two end-members of more similar nature (humic acids and

fulvic acids, standards from the International Humic Substances Society (IHSS) and Sigma-Aldrich respectively). According to that, this asymetry is more likely to be independent of the original composition of the end-members, and more subject to the behaviour of fluorescence to mixing processes.

Differentiated prediction capacity among SOM components

The high overall capacity of fluorescence components to predict the composition of intermediate mixtures, implies the assumption that the EEM shape results from the linear sum of independently fluorescing components. This is indeed one of the main premises assumed in current DOM research methods, like PARAFAC, peak picking and the fingerprinting approaches mentioned in the introduction.

However, in this study a further in-depth analysis of the mixing process showed that the prediction accuracy was unequal at varying proportions of the end-members. These observations, consistent with findings in Hur et al. (2006), may unveil the occurrence of intramolecular electronic interactions, which may ultimately affect the fluorescence of the bulk DOM mixture (Del Vecchio and Blough, 2004; Boyle et al., 2009).

Whether the fluorescence of bulk DOM results from an non-interactive or interactive sum of individual components is currently a matter of debate (Murphy et al., 2014). The role of electronic interactions such as intramolecular energy transfer, spectral shifting and charge transfer have been evidenced in laboratory analyses performed at very controlled chemical conditions (Del Vecchio and Blough, 2004; Boyle et al., 2009; Ma et al., 2010). On the other hand, the non-interacting additive approach has predominated in field-based research and has triggered substantial advances over the last decade (Fellman et al., 2010). In our results, the non-interactive addition approach appears to have the main role, as it explains more than the 99% of the data variability, Table. 11.2). However, the influence of non-interactive phenomena may explain the subtle poorer predictions observed in certain end-member proportions.

Spectral indices

In contrast with EEM components, the spectral indices exhibited a poor capacity to predict the quality of DOM in intermediate mixtures. Out of the four studied indicies, FI is the one which has the best linear adjust, with a high r^2, a slope of 1 and a very low mean mean % difference (1.29, Table 11.2). The r^2, though, is slightly lower than those observed for EEM components (0.9745). This indicates that, even though it shows a good linear additive behaviour, its behaviour in mass balances should be interpreted in terms of trends, rather than for fine quantification

purposes. The authors of the FI index themselves (McKnight et al., 2001) discourage the use of this index to quantify the relative proportions of precursor end-members of a given sample. They state that the quantitative use of FI is influenced by the DOC concentration and the variation in fluorescence intensity per mg C of the different fulvic acids. Korak et al. (2014) has found that FI behaves non-linearly with end-member mixing ratios, and they attribute that to the fact that both the emission at with peak C has its maximal intensity, as well as its curvature, vary simultaneously. Because of that, the fluorescence intensities at the coordinates of the numerator and the denominator used to calculate the FI change at different rates and this causes the non-linearity behaviour along a mixing gradient. Because of this reason, Yang and Hur (2014) found that all the metrics based on a spectral ratio had a poor balance property, and this may also explain what we observe for the rest of optical indices.

SUVA, like FI exhibited good prediction capability, observed from the low mean % difference (6.09). However, the very low r^2 reveals a lack of linear additivity over the end-member mixtures. Interestingly, this contradicts the findings of Hur et al. (2006), who found SUVA to be the best parameters performing linear additions. In view of the above-mentioned reasoning, this disparity could be due to the fact that in the set of mixtures used in Hur et al. (2006) the rate of change of DOC concentration and the absorbance coefficent at 254 nm may be more moderate than in our case.

HIX has no linear behaviour (r^2 =0.4848 and 0.4891) and has extremely low prediction capacity (mean % difference of 40.99 - 46.54). Therefore, in our study this variable should be discarded to be used in mass-balance calculations. Similarly, BIX also showed a poor linear additive character, with an r^2 of 0.5161 and 0.5592 and slopes near to 1, although the average percentage differences between the expected and the observed values where not as high as for HIX. This poor source discriminant behaviour is in line with the findings of Yang and Hur (2014) and may also be explained by the fact that they are calculated as a ratio between two spectral regions of different rates of change.

Conclusions

The specific findings of this annex include:

- EEM components were found to have a more robust linear additive behaviour irrespective of their method of determination (maximal intensity or regional integration). By contrast, the spectral indices, showed a weak (FI) or no ability (HIX and SUVA) to predict values in mixtures.

- Among spectral indices, FI was the only one that exhibited linear behaviour. However, its weak linear fit discourages its use in mass-balance calculations.
- The SOM components determined by regional integration obtained the highest accuracies in the linear models ($r^2 > 0.99$, mean % difference $< 5\%$). This further underlines the potential of the use of the SOM analysis resolve EEMs into meaningful components.
- By comparing between the four components, the protein-like fraction was found to be more prone to non-linear additivity, despite a good overall linear fit.

		Fuirosos : WWTP			Pertegàs : WWTP		
		Measured	Predicted	Diff.(%)	Measured	Predicted	Diff.(%)
C1.vol	100 : 0	2667	2667	n.a.(*)	2100	2100	n.a.
	99 : 1	4709	3137	33.3	3171	2557	19.3
	90 : 10	8250	7372	10.6	5747	6667	16
	70 : 30	14529	16782	15.5	17760	15800	11
	50 : 50	24997	26193	4.7	25668	24933	2.8
	30 : 70	34964	35603	1.8	34206	34066	0.4
	10 : 90	44216	45013	1.8	44277	43198	2.4
	1 : 99	48025	49248	2.5	48242	47308	1.9
	0 : 100	49718	49718	n.a.	47765	47765	n.a.
C2.vol	100 : 0	3496	3496	n.a.	2270	2270	n.a.
	99 : 1	6100	3973	34.8	3703	2738	26
	90 : 10	9512	8267	13	6228	6953	11.6
	70 : 30	15720	17808	13.2	18524	16319	11.9
	50 : 50	26440	27350	3.4	26667	25686	3.6
	30 : 70	36107	36892	2.1	35503	35052	1.2
	10 : 90	45132	46434	2.8	45865	44418	3.1
	1 : 99	49494	50728	2.4	49824	48633	2.3
	0 : 100	51205	51205	n.a.	49102	49102	n.a.
C3.vol	100 : 0	12534	12534	n.a.	9408	9408	n.a.
	99 : 1	13561	13077	3.5	8851	9999	12.9
	90 : 10	18765	17966	4.2	12547	15322	22.1
	70 : 30	26958	28829	6.9	25562	27150	6.2
	50 : 50	38396	39693	3.3	41984	38979	7.1
	30 : 70	50416	50556	0.2	50820	50807	0
	10 : 90	60658	61420	1.2	63079	62635	0.7
	1 : 99	65057	66309	1.9	67679	67958	0.4
	0 : 100	66852	66852	n.a.	68550	68550	n.a.
C4.vol	100 : 0	7425	7425	n.a.	4474	4474	n.a.
	99 : 1	7951	7766	2.3	4633	4843	4.5
	90 : 10	10998	10833	1.5	6714	8160	21.5
	70 : 30	16344	17649	7.9	17251	15532	9.9
	50 : 50	23529	24466	3.9	22833	22904	0.3
	30 : 70	31007	31282	0.8	30202	30277	0.2
	10 : 90	37937	38098	0.4	37974	37649	0.8
	1 : 99	41027	41166	0.3	40960	40966	0
	0 : 100	41506	41506	n.a.	41335	41335	n.a.

Table 11.3 – Measured and predicted values calculated using mass balance (Eq. 11.1), for the SOM components determined by regional integration. (*) n.a. stands for not applicable.

		Fuirosos : WWTP			Pertegàs : WWTP		
		Measured	Predicted	Diff.(%)	Measured	Predicted	Diff.(%)
C1.int	100 : 0	0.127	0.127	n.a.(*)	0.104	0.104	n.a.
	99 : 1	0.292	0.147	49.7	0.152	0.123	19.3
	90 : 10	0.370	0.322	12.8	0.264	0.295	11.7
	70 : 30	0.634	0.713	12.4	0.763	0.677	11.2
	50 : 50	1.050	1.103	5	1.154	1.059	8.2
	30 : 70	1.469	1.493	1.6	1.458	1.441	1.1
	10 : 90	1.868	1.883	0.8	1.850	1.823	1.4
	1 : 99	2.019	2.059	1.9	2.003	1.995	0.4
	0 : 100	2.078	2.078	n.a.	2.014	2.014	n.a.
C2.int	100 : 0	0.222	0.222	n.a.	0.150	0.150	n.a.
	99 : 1	0.309	0.244	21.1	0.224	0.171	23.6
	90 : 10	0.485	0.437	9.9	0.335	0.358	6.9
	70 : 30	0.770	0.866	12.4	0.859	0.775	9.7
	50 : 50	1.223	1.295	5.8	1.380	1.192	13.5
	30 : 70	1.644	1.724	4.8	1.601	1.609	0.4
	10 : 90	2.077	2.153	3.6	2.073	2.026	2.2
	1 : 99	2.257	2.346	3.9	2.256	2.213	1.8
	0 : 100	2.367	2.367	n.a.	2.234	2.234	n.a.
C3.int	100 : 0	0.584	0.584	n.a.	0.505	0.505	n.a.
	99 : 1	0.590	0.607	2.8	0.385	0.529	37.4
	90 : 10	0.809	0.811	0.2	0.595	0.741	24.6
	70 : 30	1.151	1.263	9.7	1.189	1.213	2
	50 : 50	1.642	1.716	4.5	2.169	1.685	22.3
	30 : 70	2.099	2.169	3.3	2.191	2.157	1.5
	10 : 90	2.617	2.622	0.1	2.651	2.629	0.8
	1 : 99	2.818	2.825	0.2	2.827	2.841	0.5
	0 : 100	2.848	2.848	n.a.	2.865	2.865	n.a.
C4.int	100 : 0	0.553	0.553	n.a.	0.367	0.367	n.a.
	99 : 1	0.580	0.587	1.3	0.351	0.403	15
	90 : 10	0.800	0.899	12.3	0.508	0.729	43.4
	70 : 30	1.276	1.590	24.6	1.512	1.454	3.8
	50 : 50	2.059	2.282	10.8	2.089	2.178	4.2
	30 : 70	2.888	2.973	2.9	2.859	2.902	1.5
	10 : 90	3.642	3.665	0.6	3.625	3.627	0
	1 : 99	3.973	3.976	0	3.937	3.952	0.3
	0 : 100	4.010	4.010	n.a.	3.989	3.989	n.a.

Table 11.4 – Measured and predicted values calculated using mass balance (Eq. 11.1), for the maximal intensity of the SOM components (*) n.a. stands for not applicable.

		Fuirosos : WWTP			Pertegàs : WWTP		
		Measured	Predicted	Diff.(%)	Measured	Predicted	Diff.(%)
FI	100 : 0	1.56	1.56	n.a.*	1.48	1.48	n.a.
	99 : 1	1.55	1.57	0.9	1.49	1.49	0.2
	90 : 10	1.63	1.6	1.6	1.64	1.53	6.6
	70 : 30	1.72	1.68	2.4	1.83	1.62	11.6
	50 : 50	1.82	1.76	3.1	1.88	1.71	8.9
	30 : 70	1.89	1.84	2.6	1.91	1.8	5.6
	10 : 90	1.94	1.92	0.7	1.92	1.89	1.8
	1 : 99	1.95	1.96	0.3	1.93	1.93	0.3
	0 : 100	1.96	1.96	n.a.	1.93	1.93	n.a.
HIX	100 : 0	17.64	17.64	n.a.	18.19	18.19	n.a.
	99 : 1	8.7	17.53	101.4	10.57	18.08	71
	90 : 10	9.67	16.52	70.8	8.79	17.05	93.9
	70 : 30	8.66	14.28	64.7	7.7	14.77	91.6
	50 : 50	6.95	12.03	73	6.91	12.49	80.7
	30 : 70	6.72	9.79	45.7	6.69	10.21	52.7
	10 : 90	6.66	7.55	13.2	6.43	7.93	23.2
	1 : 99	6.55	6.54	0.1	6.53	6.91	5.8
	0 : 100	6.42	6.42	n.a.	6.79	6.79	n.a.
SUVA	100 : 0	3.84	3.84	n.a.	3.74	3.74	n.a.
	99 : 1	4.09	3.84	6	3.83	3.74	2.4
	90 : 10	3.9	3.83	1.9	4.08	3.76	7.8
	70 : 30	4.34	3.81	12.2	3.8	3.81	0.3
	50 : 50	4.48	3.79	15.3	4.11	3.86	5.9
	30 : 70	4.2	3.77	10.2	4.22	3.91	7.3
	10 : 90	3.95	3.75	5.1	4.01	3.96	1.2
	1 : 99	3.9	3.74	4.1	3.93	3.98	1.2
	0 : 100	3.73	3.73	n.a.	3.98	3.98	n.a.
BIX	100 to 0	0.65	0.65	n.a.	0.64	0.64	n.a.
	99 to 1	0.80	0.66	17.8	0.75	0.64	14.6
	90 to 10	0.80	0.67	15.2	0.79	0.66	16.7
	70 to 30	0.79	0.71	9.6	0.82	0.70	15.2
	50 to 50	0.84	0.75	10.2	0.83	0.73	11.2
	30 to 70	0.83	0.79	4.4	0.84	0.77	7.8
	10 to 90	0.84	0.83	0.5	0.86	0.81	5
	1 to 99	0.85	0.85	0.6	0.84	0.83	1.3
	0 to 100	0.85	0.85	n.a.	0.83	0.83	n.a.

Table 11.5 – Measured and predicted values calculated using mass balance (Eq. 11.1), for spectral indices. * n.a. stands for not applicable.

Bibliography

Bibliography

ACA. Consulta de dades - Xarxes de control, 2013. URL aca-web.gencat.cat/aca/.

Rosana Aguilera, Rafael Marce, and Sergi Sabater. Linking in-stream nutrient flux to land use and inter-annual hydrological variability at the watershed scale. *The Science of the total environment*, 440:72–81, 2012. ISSN 1879-1026. doi: 10.1016/j.scitotenv.2012.08.030.

Hassan a Al-Reasi, Chris M Wood, and D Scott Smith. Physicochemical and spectroscopic properties of natural organic matter (NOM) from various sources and implications for ameliorative effects on metal toxicity to aquatic biota. *Aquatic toxicology (Amsterdam, Netherlands)*, 103(3-4):179–90, June 2011. ISSN 1879-1514. doi: 10.1016/j.aquatox.2011.02.015. URL http://www.ncbi.nlm.nih.gov/pubmed/21470554.

RB Alexander, RA Smith, and GE Schwarz. Effect of stream channel size on the delivery of nitrogen to the Gulf of Mexico. *Nature*, 403(February):758–761, 2000. URL http://www.nature.com/nature/journal/v403/n6771/abs/403758a0.html.

Rainer MW Amon and Ronald Benner. Bacterial utilization of different size classes of dissolved organic matter. *Limnology and ...*, 41(1):41–51, 1996. URL http://www.riversystems.washington.edu/lc/RIVERS/77_amon_rmw_41-41-51.pdf.

C M Andersen and R Bro. Practical aspects of PARAFAC modeling of fluorescence excitation-emission data. *Journal of Chemometrics*, 17(4):200–215, 2003. ISSN 0886-9383. doi: 10.1002/cem.790.

Shai Arnon, Keren Yanuka, and Ali Nejidat. Impact of overlying water velocity on ammonium uptake by benthic biofilms. *Hydrological Processes*, 27(4):570–578, February 2013. ISSN 08856087. doi: 10.1002/hyp.9239. URL http://doi.wiley.com/10.1002/hyp.9239.

E. Asmala, R. Autio, H. Kaartokallio, C. a. Stedmon, and D. N. Thomas. Processing of humic-rich riverine dissolved organic matter by estuarine bacteria: effects of predegradation and inorganic nutrients. *Aquatic Sciences*, 76(3):451–463, February 2014. ISSN 1015-1621. doi: 10.1007/s00027-014-0346-7. URL http://link.springer.com/10.1007/s00027-014-0346-7.

Kari Austnes, Christopher D Evans, Caroline Eliot-Laize, Pamela S Naden, and Gareth H Old. Effects of storm events on mobilisation and in-stream processing of dissolved organic matter (DOM) in a Welsh peatland catchment. *Biogeochemistry*, 99(1-3):157–173, 2010. ISSN 0168-2563. doi: 10.1007/s10533-009-9399-4.

F Azam, T Fenchel, J G Field, J S Gray, L A Meyerreil, and F Thingstad. The Ecological Role of Water-Column Microbes in the Sea. *Marine Ecology-Progress Series*, 10(3):257–263, 1983. ISSN 0171-8630. doi: 10.3354/meps010257.

A Baker. Fluorescence excitation-emission matrix characterization of some sewage-impacted rivers. *Environmental science & technology*, 35(5):948–953, 2001. ISSN 0013-936X. doi: 10.1021/es000177t.

A Baker. Fluorescence properties of some farm wastes: implications for water quality monitoring. *Water research*, 36(1):189–195, January 2002. ISSN 0043-1354. doi: 10.1016/S0043-1354(01)00210-X.

A Baker and R G M Spencer. Characterization of dissolved organic matter from source to sea using fluorescence and absorbance spectroscopy. *Science of the Total Environment*, 333(1-3):217–232, October 2004. ISSN 0048-9697. doi: 10.1016/j.scitotenv.2004.04.013.

Darren S. Baldwin, Kerry L. Whitworth, and Claire L. Hockley. Uptake of dissolved organic carbon by biofilms provides insights into the potential impact of loss of large woody debris on the functioning of lowland rivers. *Freshwater Biology*, 59 (4):692–702, April 2014. ISSN 00465070. doi: 10.1111/fwb.12296. URL `http://doi.wiley.com/10.1111/fwb.12296`.

Miguel A Barreto-Sanz and Andres Perez-Uribe. Improving the correlation hunting in a large quantity of SOM - Component planes classification of agro-ecological variables related with productivity in the sugar cane culture. *LECTURE NOTES IN COMPUTER SCIENCE*, 4669:379–388, 2007. ISSN 0302-9743; 978-3-540-74693-5.

Frauke K Barthold, Christoph Tyralla, Katrin Schneider, Kellie B Vache, Hans-Georg Frede, and Lutz Breuer. How many tracers do we need for end member mixing analysis (EMMA)? A sensitivity analysis. *Water Resources Research*, 47: W08519–W08519, August 2011. ISSN 0043-1397. doi: 10.1029/2011WR010604.

T J Battin. Dissolved organic matter and its optical properties in a blackwater tributary of the upper Orinoco river, Venezuela. *Organic Geochemistry*, 28(9-10): 561–569, 1998. ISSN 0146-6380. doi: 10.1016/S0146-6380(98)00028-X.

Tom J Battin, Louis A Kaplan, Stuart Findlay, Charles S Hopkinson, Eugenia Marti, Aaron I Packman, J Denis Newbold, and Francesc Sabater. Biophysical controls on organic carbon fluxes in fluvial networks. *Nature Geoscience*, 1(2): 95–100, 2008. ISSN 1752-0894. doi: 10.1038/ngeo101.

Tom J Battin, Sebastiaan Luyssaert, Louis A Kaplan, Anthony K Aufdenkampe, Andreas Richter, and Lars J Tranvik. The boundless carbon cycle. *Nature Geoscience*, 2(9):598–600, 2009. ISSN 1752-0894. doi: 10.1038/ngeo618.

L Benda, K Andras, D Miller, and P Bigelow. Confluence effects in rivers: Interactions of basin scale, network geometry, and disturbance regimes. *Water Resources Research*, 40(5):W05402–W05402, May 2004. ISSN 0043-1397. doi: 10.1029/2003WR002583.

R Benner. Chemical composition and reactivity. In DA Hansell and CA Carlson, editors, *Biogeochemistry of Marine Dissolved Organic Matter*, chapter 3, pages 59–90. Academic Press, Elsevier Science, New York, 2002. ISBN 978-0-12-323841-2.

S Bertilsson and L J Tranvik. Photochemical transformation of dissolved organic matter in lakes. *Limnology and Oceanography*, 45(4):753–762, 2000. ISSN 0024-3590.

Stefan Bertilsson and Jeremy B. Jones. Supply of Dissolved Organic Matter to Aquatic Ecosystems: Autochthonous Sources. In Stuart Findlay and Robert L Sinsabaugh, editors, *Aquatic Ecosystems: Interactivity of Dissolved Organic Matter*. Elsevier, 2003.

M Bieroza, A Baker, and J Bridgeman. New data mining and calibration approaches to the assessment of water treatment efficiency. *Advances in Engineering Software*, 44(1):126–135, February 2012. ISSN 0965-9978. doi: 10.1016/j.advengsoft.2011.05.031.

Magdalena Bieroza, Andy Baker, and John Bridgeman. Exploratory analysis of excitation-emission matrix fluorescence spectra with self-organizing maps as a basis for determination of organic matter removal efficiency at water treatment works. *Journal of Geophysical Research-Biogeosciences*, 114:G00F07–G00F07, December 2009. ISSN 0148-0227. doi: 10.1029/2009JG000940.

Magdalena Bieroza, Andy Baker, and John Bridgeman. Classification and calibration of organic matter fluorescence data with multiway analysis methods and artificial neural networks: an operational tool for improved drinking water treatment. *Environmetrics*, 22(3):256–270, May 2011. ISSN 1180-4009. doi: 10.1002/env.1045.

Muhammad Bilal, Anne Jaffrezic, Yves Dudal, Cedric Le Guillou, Safya Menasseri, and Christian Walter. Discrimination of Farm Waste Contamination by Fluorescence Spectroscopy Coupled with Multivariate Analysis during a Biodegradation Study. *Journal of Agricultural and Food Chemistry*, 58(5):3093–3100, March 2010. ISSN 0021-8561. doi: 10.1021/jf903872r.

Martí Boada. Unitats de paisatge diferenciades: els cursos de la Tordera. In Martí Boada, Sílvia Mayo, and Roser Maneja, editors, *Els sistemes socioecològics de la*

conca de la Tordera, page 541. Institució Catalana d'Història Natural, Barcelona, first edit edition, 2008. ISBN 978-84-7283-983-0.

J R Boehme and P G Coble. Characterization of colored dissolved organic matter using high-energy laser fragmentation. *Environmental science & technology*, 34 (15):3283–3290, August 2000. ISSN 0013-936X. doi: 10.1021/es9911263.

Oriol Bolós. *La vegetació del Montseny*. Servei de Parcs Naturals. Diputació de Barcelona., Barcelona, 1983.

O Bonilla-Findji, E Rochelle-Newall, Mg Weinbauer, Md Pizay, Me Kerros, and Jp Gattuso. Effect of seawater–freshwater cross-transplantations on viral dynamics and bacterial diversity and production. *Aquatic Microbial Ecology*, 54 (January):1–11, January 2009. ISSN 0948-3055. doi: 10.3354/ame01256. URL `http://www.int-res.com/abstracts/ame/v54/n1/p1-11/`.

Mikhail Borisover, Yael Laor, Ibrahim Saadi, Marcos Lado, and Nadezhda Bukhanovsky. Tracing Organic Footprints from Industrial Effluent Discharge in Recalcitrant Riverine Chromophoric Dissolved Organic Matter. *Water Air and Soil Pollution*, 222(1-4):255–269, November 2011. ISSN 0049-6979. doi: 10.1007/s11270-011-0821-x.

a. F. Bouwman, M. F. P. Bierkens, J. Griffioen, M. M. Hefting, J. J. Middelburg, H. Middelkoop, and C. P. Slomp. Nutrient dynamics, transfer and retention along the aquatic continuum from land to ocean: towards integration of ecological and biogeochemical models. *Biogeosciences*, 10(1):1–22, January 2013. ISSN 1726-4189. doi: 10.5194/bg-10-1-2013. URL `http://www.biogeosciences.net/10/1/2013/`.

Erin S Boyle, Nicolas Guerriero, Anthony Thiallet, Rossana Del Vecchio, and Neil V Blough. Optical Properties of Humic Substances and CDOM: Relation to Structure. *Environmental science & technology*, 43(7):2262–2268, April 2009. ISSN 0013-936X. doi: 10.1021/es803264g.

Richard G Brereton. Self organising maps for visualising and modelling. *Chemistry Central journal*, 6 Suppl 2(Suppl 2):S1, January 2012. ISSN 1752-153X. doi: 10.1186/1752-153X-6-S2-S1. URL `http://www.pubmedcentral.nih.gov/articlerender.fcgi?artid=3395104\&tool=pmcentrez\&rendertype=abstract`.

Rasmus Bro. PARAFAC. Tutorial and applications. *Chemometrics and Intelligent Laboratory Systems*, 38(2):149–171, 1997. URL `http://www.sciencedirect.com/science/article/pii/S0169743997000324`.

Rasmus Bro and Maider Vidal. EEMizer: Automated modeling of fluorescence EEM data. *Chemometrics and Intelligent Laboratory Systems*, 106(1):86–92,

March 2011. ISSN 01697439. doi: 10.1016/j.chemolab.2010.06.005. URL http://linkinghub.elsevier.com/retrieve/pii/S0169743910001152.

Marjorie L Brooks, Diane M McKnight, and William H Clements. Photochemical control of copper complexation by dissolved organic matter in Rocky Mountain streams, Colorado. *Limnology and Oceanography*, 52(2):766–779, 2007. ISSN 0024-3590.

E N J Brookshire, H M Valett, S A Thomas, and J R Webster. Coupled cycling of dissolved organic nitrogen and carbon in a forest stream. *Ecology*, 86(9):2487–2496, 2005. ISSN 0012-9658. doi: 10.1890/04-1184.

P. a. Bukaveckas, D. L. Guelda, J. Jack, R. Koch, T. Sellers, and J. Shostell. Effects of Point Source Loadings, Sub-basin Inputs and Longitudinal Variation in Material Retention on C, N and P Delivery from the Ohio River Basin. *Ecosystems*, 8(7):825–840, October 2005. ISSN 1432-9840. doi: 10.1007/s10021-005-0044-3. URL http://link.springer.com/10.1007/s10021-005-0044-3.

Andrea Butturini, Francesc Gallart, Jérôme Latron, Eusebi Vazquez, and Francesc Sabater. Cross-site Comparison of Variability of DOC and Nitrate c–q Hysteresis during the Autumn–winter Period in Three Mediterranean Headwater Streams: A Synthetic Approach. *Biogeochemistry*, 77(3):327–349, February 2006. ISSN 0168-2563. doi: 10.1007/s10533-005-0711-7. URL http://link.springer.com/10.1007/s10533-005-0711-7.

Andrea Butturini, Marta Alvarez, Susana Bernal, Eusebi Vazquez, and Francesc Sabater. Diversity and temporal sequences of forms of DOC and NO3-discharge responses in an intermittent stream: Predictable or random succession? *Journal of Geophysical Research-Biogeosciences*, 113(G3):G03016–G03016, 2008. ISSN 0148-0227. doi: 10.1029/2008JG000721.

Andrea Butturini, Sergi Sabater, and Anna M. Romaní. La química de las aguas. los nutrientes. In Arturo Elosegui and Sergi Sabater, editors, *Conceptos y técnicas en ecología fluvial.* Fundación BBVA, 1st edition, 2009. ISBN 978-84-96515-87-1.

F Caille, J L Riera, and A Rosell-Mele. Modelling nitrogen and phosphorus loads in a Mediterranean river catchment (La Tordera, NE Spain). *Hydrology and Earth System Sciences*, 16(8):2417–2435, 2012. ISSN 1027-5606. doi: 10.5194/hess-16-2417-2012.

W K L Cammack, J Kalff, Y T Prairie, and E M Smith. Fluorescent dissolved organic matter in lakes: Relationships with heterotrophic metabolism. *Limnology and Oceanography*, 49(6):2034–2045, 2004. ISSN 0024-3590.

Elfrida M Carstea, Luminita Ghervase, Gabriela Pavelescu, and Dan Savastru. Assessment of the Anthropogenic Impact on Water Systems by Fluorescence Spectroscopy. *Environmental Engineering and Management Journal*, 8(6):1321–1326, 2009. ISSN 1582-9596.

R B Cattell. *Factor Analysis: An Introduction and Manual for the Psychologist and Social Scientist*. Harper, New York, USA, 1952. ISBN 9780837166155.

Özer Çinar and Hasan Merdun. Application of an unsupervised artificial neural network technique to multivariant surface water quality data. *Ecological Research*, 24(1):163–173, April 2008. ISSN 0912-3814. doi: 10.1007/s11284-008-0495-z. URL `http://link.springer.com/10.1007/s11284-008-0495-z`.

R. Céréghino and Y.-S. Park. Review of the Self-Organizing Map (SOM) approach in water resources: Commentary. *Environmental Modelling & Software*, 24(8): 945–947, August 2009. ISSN 13648152. doi: 10.1016/j.envsoft.2009.01.008. URL `http://linkinghub.elsevier.com/retrieve/pii/S1364815209000188`.

W Chen, P Westerhoff, J A Leenheer, and K Booksh. Fluorescence excitation - Emission matrix regional integration to quantify spectra for dissolved organic matter. *Environmental science & technology*, 37(24):5701–5710, December 2003. ISSN 0013-936X. doi: 10.1021/es034354c.

Ven Te Chow. *Open-channel hydraulics*. McGraw-Hill, New York, USA, 1959.

Martin J. Christ and Mark B. David. Temperature and moisture effects on the production of dissolved organic carbon in a Spodosol. *Soil Biology and Biochemistry*, 28(9):1191–1199, September 1996. ISSN 00380717. doi: 10.1016/0038-0717(96)00120-4. URL `http://linkinghub.elsevier.com/retrieve/pii/0038071796001204`.

N Christophersen and R P Hooper. Multivariate-Analysis of Stream Water Chemical-Data - the use of Principal Components-Analysis for the End-Member Mixing Problem. *Water Resources Research*, 28(1):99–107, January 1992. ISSN 0043-1397. doi: 10.1029/91WR02518.

Philippe Ciais, Christopher Sabine, Govindasamy Bala, Laurent Bopp, Victor Brovkin, Josep Canadell, Abha Chhabra, Ruth DeFries, James Galloway, Martin Heimann, Christopher Jones, Corinne Le Quéré, Ranga B Myneny, Shilong Piao, and Peter Thornton. Carbon and Other Biogeochemical Cycles. In TF Stocker, D Qin, G K Plattner, M Tignor, S K Allen, J Boschung, A Nauels, Y Xia, V Bex, and P M Midgley, editors, *Climate Change 2013: The Physical Science Basis. Contribution of Working Group I to the Fifth Assessment Report of the Intergovernmental Panel on Climate Change*, chapter 6, pages 465–570. Cambridge University Press, Cambridge, United Kingdom and New York, NY, USA., 2013.

T A Clair and J M Ehrman. Variations in discharge and dissolved organic carbon and nitrogen export from terrestrial basins with changes in climate: A neural network approach. *Limnology and Oceanography*, 41(5):921–927, July 1996. ISSN 0024-3590.

M.J. Clark, M.S. Cresser, R. Smart, P.J. Chapman, and a.C. Edwards. The influence of catchment characteristics on the seasonality of carbon and nitrogen species concentrations in upland rivers of Northern Scotland. *Biogeochemistry*, 68(1): 1–19, March 2004. ISSN 0168-2563. doi: 10.1023/B:BIOG.0000025733.07568.11. URL `http://link.springer.com/10.1023/B:BIOG.0000025733.07568.11`.

Cory C. Cleveland and Daniel Liptzin. C:N:P stoichiometry in soil: is there a "Redfield ratio" for the microbial biomass? *Biogeochemistry*, 85(3):235–252, July 2007. ISSN 0168-2563. doi: 10.1007/s10533-007-9132-0. URL `http://link.springer.com/10.1007/s10533-007-9132-0`.

P G Coble. Characterization of marine and terrestrial DOM in seawater using excitation emission matrix spectroscopy. *Marine Chemistry*, 51(4):325–346, 1996. ISSN 0304-4203. doi: 10.1016/0304-4203(95)00062-3.

P G Coble, S A Green, N V Blough, and R B Gagosian. Characterization of Dissolved Organic-Matter in the Black-Sea by Fluorescence Spectroscopy Rid B-7727-2009. *Nature*, 348(6300):432–435, November 1990. ISSN 0028-0836. doi: 10.1038/348432a0.

J J Cole, Y T Prairie, N F Caraco, W H McDowell, L J Tranvik, R G Striegl, C M Duarte, P Kortelainen, J A Downing, J J Middelburg, and J Melack. Plumbing the global carbon cycle: Integrating inland waters into the terrestrial carbon budget RID B-9108-2008 RID E-9767-2010 RID B-4951-2011. *Ecosystems*, 10(1): 171–184, February 2007. ISSN 1432-9840. doi: 10.1007/s10021-006-9013-8.

Rose M Cory and Louis A Kaplan. Biological lability of streamwater fluorescent dissolved organic matter. *Limnology and Oceanography*, 57(5):1347–1360, September 2012. ISSN 0024-3590. doi: 10.4319/lo.2012.57.5.1347.

Rose M Cory, Matthew P Miller, Diane M McKnight, Jennifer J Guerard, and Penney L Miller. Effect of instrument-specific response on the analysis of fulvic acid fluorescence spectra. *Limnology and Oceanography-Methods*, 8:67–78, 2010. ISSN 1541-5856.

M Cottrell, E De Bodt, and M Verleysen. A Statistical Tool to Assess the Reliability of Self- Organizing Maps. In *Advances in Self-Organising Maps*, number June, pages 7–14, Lincoln (United Kingdom), 2001. Springer Verlag. ISBN 1852335114.

M J Dagg, T S Bianchi, G A Breed, W J Cai, S Duan, H Liu, B A McKee, R T Powell, and C M Stewart. Biogeochemical characteristics of the lower Mississippi River, USA, during June 2003. *Estuaries*, 28(5):664–674, 2005. ISSN 0160-8347. doi: 10.1007/BF02732905.

Clifford N. Dahm, Michelle a. Baker, Douglas I. Moore, and James R. Thibault. Coupled biogeochemical and hydrological responses of streams and rivers to drought. *Freshwater Biology*, 48(7):1219–1231, July 2003. ISSN 0046-5070. doi: 10.1046/j.1365-2427.2003.01082.x. URL `http://doi.wiley.com/10.1046/j.1365-2427.2003.01082.x`.

Brent J Dalzell, Timothy R Filley, and Jon M Harbor. Flood pulse influences on terrestrial organic matter export from an agricultural watershed. *Journal of Geophysical Research-Biogeosciences*, 110(G2):G02011–G02011, November 2005. ISSN 0148-0227. doi: 10.1029/2005JG000043.

JJC Dawson, MF Billett, and D Hope. Diurnal variations in the carbon chemistry of two acidic peatland streams in north-east Scotland. *Freshwater Biology*, 46: 1309–1322, 2001. URL `http://onlinelibrary.wiley.com/doi/10.1046/j.1365-2427.2001.00751.x/full`.

Eric de Bodt, Marie Cottrell, and Michel Verleysen. Statistical tools to assess the reliability of self-organizing maps. *Neural networks : the official journal of the International Neural Network Society*, 15(8-9):967–78, 2002. ISSN 0893-6080. URL `http://www.ncbi.nlm.nih.gov/pubmed/12416687`.

R Del Vecchio and N V Blough. On the origin of the optical properties of humic substances. *Environmental science & technology*, 38(14):3885–3891, July 2004. ISSN 0013-936X. doi: 10.1021/es049912h.

G Di Baldassarre and A Montanari. Uncertainty in river discharge observations: a quantitative analysis. *Hydrology and Earth System Sciences*, 13(6):913–921, 2009. ISSN 1027-5606.

Kathryn M Docherty, Katherine C Young, Patricia a Maurice, and Scott D Bridgham. Dissolved organic matter concentration and quality influences upon structure and function of freshwater microbial communities. *Microbial ecology*, 52(3):378–88, October 2006. ISSN 0095-3628. doi: 10.1007/s00248-006-9089-x. URL `http://www.ncbi.nlm.nih.gov/pubmed/16767520`.

Shuiwang Duan, Thomas S Bianchi, and Troy P Sampere. Temporal variability in the composition and abundance of terrestrially-derived dissolved organic matter in the lower Mississippi and Pearl Rivers. *Marine Chemistry*, 103(1-2):172–184, January 2007. ISSN 0304-4203. doi: 10.1016/j.marchem.2006.07.003.

Shuiwang Duan, Thomas S Bianchi, Peter H Santschi, and Rainer M W Amon. Effects of tributary inputs on nutrient export from the Mississippi and Atchafalaya Rivers to the Gulf of Mexico. *Marine and Freshwater Research*, 61(9):1029–1038, 2010. ISSN 1323-1650. doi: 10.1071/MF09235.

A Eatherall, M S Warwick, and S Tolchard. Identifying sources of dissolved organic carbon on the River Swale, Yorkshire. *Science of the Total Environment*, 251: 173–190, May 2000. ISSN 0048-9697. doi: 10.1016/S0048-9697(00)00381-8.

Elisabet Ejarque-Gonzalez and Andrea Butturini. Self-organising maps and correlation analysis as a tool to explore patterns in excitation-emission matrix data sets and to discriminate dissolved organic matter fluorescence components. *PloS one*, 9(6), 2014. doi: 10.1371/journal.pone.0099618.

K M Elkins and D J Nelson. Spectroscopic approaches to the study of the interaction of aluminum with humic substances. *Coordination Chemistry Reviews*, 228(2): 205–225, 2002. ISSN 0010-8545. doi: 10.1016/S0010-8545(02)00040-1.

Douglas G. Emerson, Aldo V. Vecchia, and Ann L. Dahl. Evaluation of Drainage-Area Ratio Method Used to Estimate Streamflow for the Red River of the North Basin , North Dakota and Minnesota Scientific Investigations Report 2005 – 5017 Evaluation of Drainage-Area Ratio Method Used to Estimate Streamflow for th. Technical report, U.S. Department of the Interior and U.S. Geological Survey, 2005.

Sanne Engelen and Mia Hubert. Detecting outlying samples in a parallel factor analysis model. *Analytica chimica acta*, 705(1-2):155–65, October 2011. ISSN 1873-4324. doi: 10.1016/j.aca.2011.04.043. URL `http://www.ncbi.nlm.nih.gov/pubmed/21962358`.

Christopher D. Evans, Brian Reynolds, Alan Jenkins, Rachel C. Helliwell, Christopher J. Curtis, Christine L. Goodale, Robert C. Ferrier, Bridget a. Emmett, Michael G. Pilkington, Simon J. M. Caporn, Jacky a. Carroll, David Norris, Jennifer Davies, and Malcolm C. Coull. Evidence that Soil Carbon Pool Determines Susceptibility of Semi-Natural Ecosystems to Elevated Nitrogen Leaching. *Ecosystems*, 9(3):453–462, April 2006. ISSN 1432-9840. doi: 10.1007/s10021-006-0051-z. URL `http://link.springer.com/10.1007/s10021-006-0051-z`.

Christina Fasching, Barbara Behounek, Gabriel a Singer, and Tom J Battin. Microbial degradation of terrigenous dissolved organic matter and potential consequences for carbon cycling in brown-water streams. *Scientific reports*, 4:4981, January 2014. ISSN 2045-2322. doi: 10.1038/srep04981. URL `http://www.pubmedcentral.nih.gov/articlerender.fcgi?artid=4021337\&tool=pmcentrez\&rendertype=abstract`.

Jason B Fellman, Eran Hood, David V D'Amore, Richard T Edwards, and Dan White. Seasonal changes in the chemical quality and biodegradability of dissolved organic matter exported from soils to streams in coastal temperate rainforest watersheds. *Biogeochemistry*, 95(2-3):277–293, 2009a. ISSN 0168-2563. doi: 10.1007/s10533-009-9336-6.

Jason B Fellman, Eran Hood, Richard T Edwards, and David V D'Amore. Changes in the concentration, biodegradability, and fluorescent properties of dissolved organic matter during stormflows in coastal temperate watersheds. *Journal of Geophysical Research-Biogeosciences*, 114:G01021–G01021, 2009b. ISSN 0148-0227. doi: 10.1029/2008JG000790.

Jason B Fellman, Eran Hood, and Robert G M Spencer. Fluorescence spectroscopy opens new windows into dissolved organic matter dynamics in freshwater ecosystems: A review. *Limnology and Oceanography*, 55(6):2452–2462, 2010. ISSN 0024-3590. doi: 10.4319/lo.2010.55.6.2452.

Montserrat Filella. Freshwaters: which NOM matters? *Environmental Chemistry Letters*, 7(1):21–35, May 2008. ISSN 1610-3653. doi: 10.1007/s10311-008-0158-x. URL `http://link.springer.com/10.1007/s10311-008-0158-x`.

S Findlay and RL Sinsabaugh. *Aquatic Ecosystems: Interactivity of Dissolved Organic Matter*. Academic Press, Elsevier Science, 2003.

Stuart Findlay. Stream microbial ecology. *Journal of the North American Benthological Society*, 29(1):170–181, 2010. ISSN 0887-3593. doi: 10.1899/09-023.1.

Stuart G. Fisher, Ryan A. Sponseller, and James B. Heffernan. HORIZONS IN STREAM BIOGEOCHEMISTRY : FLOWPATHS TO PROGRESS. *Ecology*, 85 (9):2369–2379, 2004.

J Foden, D B Sivyer, D K Mills, and M J Devlin. Spatial and temporal distribution of chromophoric dissolved organic matter (CDOM) fluorescence and its contribution to light attenuation in UK waterbodies. *Estuarine Coastal and Shelf Science*, 79(4):707–717, 2008. ISSN 0272-7714. doi: 10.1016/j.ecss.2008.06.015.

C Freeman, C D Evans, D T Monteith, B Reynolds, and N Fenner. Export of organic carbon from peat soils. *Nature*, 412(6849):785, 2001. ISSN 0028-0836. doi: 10.1038/35090628.

Marta Fuentes, Gustavo González-Gaitano, and José Ma García-Mina. The usefulness of UV–visible and fluorescence spectroscopies to study the chemical nature of humic substances from soils and composts. *Organic Geochemistry*, 37(12):1949–1959, December 2006. ISSN 01466380. doi: 10.1016/j.orggeochem.2006.07.024. URL `http://linkinghub.elsevier.com/retrieve/pii/S0146638006001896`.

James N Galloway, Alan R Townsend, Jan Willem Erisman, Mateete Bekunda, Zucong Cai, John R Freney, Luiz A Martinelli, Sybil P Seitzinger, and Mark A Sutton. Transformation of the Nitrogen Cycle :. *Science*, 320(May):889–892, 2008.

H Z Gao and R G Zepp. Factors influencing photoreactions of dissolved organic matter in a coastal river of the southeastern United States. *Environmental science & technology*, 32(19):2940–2946, 1998. ISSN 0013-936X. doi: 10.1021/es9803660.

Yang Gao, Bo Zhu, Guirui Yu, Weiliang Chen, Nianpeng He, Tao Wang, and Chiyuan Miao. Coupled effects of biogeochemical and hydrological processes on C, N, and P export during extreme rainfall events in a purple soil watershed in southwestern China. *Journal of Hydrology*, 511:692–702, April 2014. ISSN 00221694. doi: 10.1016/j.jhydrol.2014.02.005. URL `http://linkinghub.elsevier.com/retrieve/pii/S0022169414001024`.

J A Gardecki and M Maroncelli. Set of secondary emission standards for calibration of the spectral responsivity in emission spectroscopy. *Applied Spectroscopy*, 52(9): 1179–1189, September 1998. ISSN 0003-7028. doi: 10.1366/0003702981945192.

A Gasith and VH Resh. Streams in Mediterranean climate regions: abiotic influences and biotic responses to predictable seasonal events. *Annual review of ecology and systematics*, 30(1999):51–81, 1999. URL `http://www.jstor.org/stable/221679`.

Paul Del Giorgio and ML Pace. Relative independence of dissolved organic carbon transport and processing in a large temperate river: the Hudson River as both pipe and reactor. *Limnol Oceanogr*, 53(1):185–197, 2008. URL `http://www.avto.aslo.info/lo/toc/vol\_53/issue\_1/0185.pdf`.

Charlotte Goletz, Martin Wagner, Anika Gruebel, Wido Schmidt, Nathalie Korf, and Peter Werner. Standardization of fluorescence excitation-emission-matrices in aquatic milieu. *Talanta*, 85(1):650–656, July 2011. ISSN 0039-9140. doi: 10.1016/j.talanta.2011.04.045.

Christine L. Goodale, John D. Aber, Peter M. Vitousek, and William H. McDowell. Long-term Decreases in Stream Nitrate: Successional Causes Unlikely; Possible Links to DOC? *Ecosystems*, 8(3):334–337, May 2005. ISSN 1432-9840. doi: 10.1007/s10021-003-0162-8. URL `http://link.springer.com/10.1007/s10021-003-0162-8`.

Paul E. Grams, David J. Topping, John C. Schmidt, Joseph E. Hazel, and Matt Kaplinski. Linking morphodynamic response with sediment mass balance on the Colorado River in Marble Canyon: Issues of scale, geomorphic setting, and

sampling design. *Journal of Geophysical Research: Earth Surface*, 118(2):361–381, June 2013. ISSN 21699003. doi: 10.1002/jgrf.20050. URL http://doi.wiley.com/10.1002/jgrf.20050.

R B Grayson, C J Gippel, B L Finlayson, and B T Hart. Catchment-wide impacts on water quality: the use of 'snapshot' sampling during stable flow. *Journal of Hydrology*, 199(1-2):121–134, December 1997. ISSN 0022-1694. doi: 10.1016/S0022-1694(96)03275-1.

Nancy B. Grimm, Richard W. Sheibley, Chelsea L. Crenshaw, Clifford N. Dahm, John W. Roach, and Lydia H. Zeglin. N retention and transformation in urban streams. *Journal of the North American Benthological Society*, 24(3):626–642, 2005. URL http://scholar.google.com/scholar?hl=en\&btnG=Search\&q=intitle:N+retention+and+transformation+in+urban+streams\#0.

B. Grizzetti, F. Bouraoui, G. de Marsily, and G. Bidoglio. A statistical method for source apportionment of riverine nitrogen loads. *Journal of Hydrology*, 304(1-4):302–315, March 2005. ISSN 00221694. doi: 10.1016/j.jhydrol.2004.07.036. URL http://linkinghub.elsevier.com/retrieve/pii/S0022169404005013.

François Guillemette and Paul a. del Giorgio. Reconstructing the various facets of dissolved organic carbon bioavailability in freshwater ecosystems. *Limnology and Oceanography*, 56(2):734–748, 2011. ISSN 00243590. doi: 10.4319/lo.2011.56.2.0734. URL http://www.aslo.org/lo/toc/vol_56/issue_2/0734.html.

François Guillemette and Paul a del Giorgio. Simultaneous consumption and production of fluorescent dissolved organic matter by lake bacterioplankton. *Environmental microbiology*, 14(6):1432–43, June 2012. ISSN 1462-2920. doi: 10.1111/j.1462-2920.2012.02728.x. URL http://www.ncbi.nlm.nih.gov/pubmed/22429445.

François Guillemette, S. Leigh McCallister, and Paul A. del Giorgio. Differentiating the degradation dynamics of algal and terrestrial carbon within complex natural dissolved organic carbon in temperate lakes. *Journal of Geophysical Research: Biogeosciences*, pages n/a–n/a, June 2013. ISSN 21698953. doi: 10.1002/jgrg.20077. URL http://doi.wiley.com/10.1002/jgrg.20077.

Wade L Hadwen, Christine S Fellows, Douglas P Westhorpe, Gavin N Rees, Simon M Mitrovic, Brett Taylor, Darren S Baldwin, Ewen Silvester, and Roger Croome. Longitudinal Trends in River Functioning: Patterns of Nutrient and Carbon Processing in Three Australian Rivers. *River Research and Applications*, 26(9):1129–1152, 2010. ISSN 1535-1459. doi: 10.1002/rra.1321.

Anthony F. Harrison, Kenneth Taylor, Andy Scott, Jan Poskitt, David Benham, John Grace, Jacky Chaplow, and Philip Rowland. Potential effects of climate

change on DOC release from three different soil types on the Northern Pennines UK: examination using field manipulation experiments. *Global Change Biology*, 14(3):687–702, March 2008. ISSN 1354-1013. doi: 10.1111/j.1365-2486.2007.01504.x. URL http://doi.wiley.com/10.1111/j.1365-2486.2007.01504.x.

R K Henderson, A Baker, K R Murphy, A Hamblya, R M Stuetz, and S J Khan. Fluorescence as a potential monitoring tool for recycled water systems: A review. *Water research*, 43(4):863–881, 2009. ISSN 0043-1354. doi: 10.1016/j.watres.2008.11.027.

Brian H. Hill, David W. Bolgrien, Alan T. Herlihy, Terri M. Jicha, and Ted R. Angradi. A Synoptic Survey of Nitrogen and Phosphorus in Tributary Streams and Great Rivers of the Upper Mississippi, Missouri, and Ohio River Basins. *Water, Air, & Soil Pollution*, 216(1-4):605–619, August 2010. ISSN 0049-6979. doi: 10.1007/s11270-010-0556-0. URL http://link.springer.com/10.1007/s11270-010-0556-0.

M J Hinton, S L Schiff, and M C English. The significance of storms for the concentration and export of dissolved organic carbon from two Precambrian Shield catchments. *Biogeochemistry*, 36(1):67–88, 1997. ISSN 0168-2563. doi: 10.1023/A:1005779711821.

M J Hinton, S L Schiff, and M C English. Sources and flowpaths of dissolved organic carbon during storms in two forested watersheds of the Precambrian Shield. *Biogeochemistry*, 41(2):175–197, 1998. ISSN 0168-2563. doi: 10.1023/A:1005903428956.

Eran Hood, Michael N Gooseff, and Sherri L Johnson. Changes in the character of stream water dissolved organic carbon during flushing in three small watersheds, Oregon. *Journal of Geophysical Research-Biogeosciences*, 111(G1):G01007–G01007, February 2006. ISSN 0148-0227. doi: 10.1029/2005JG000082.

R P Hooper. Applying the scientific method to small catchment studies: A review of the Panola Mountain experience. *Hydrological Processes*, 15(10):2039–2050, July 2001. ISSN 0885-6087. doi: 10.1002/hyp.255.

R P Hooper, N Christophersen, and N E Peters. Modeling Streamwater Chemistry as a Mixture of Soilwater End-Members - an Application to the Panola Mountain Catchment, Georgia, Usa. *Journal of Hydrology*, 116(1-4):321–343, August 1990. ISSN 0022-1694. doi: 10.1016/0022-1694(90)90131-G.

W A House and M S Warwick. A mass-balance approach to quantifying the importance of in-stream processes during nutrient transport in a large river catchment. *Science of The Total Environment*, 210-211(0):139–152, 1998. ISSN 0048-

9697. doi: 10.1016/S0048-9697(98)00047-3. URL http://www.sciencedirect.com/science/article/pii/S0048969798000473.

Naomi Hudson, Andy Baker, and Darren Reynolds. Fluorescence analysis of dissolved organic matter in natural, waste and polluted waters - A review. *River Research and Applications*, 23(6):631–649, 2007. ISSN 1535-1459. doi: 10.1002/rra.1005.

A Huguet, L Vacher, S Relexans, S Saubusse, J M Froidefond, and E Parlanti. Properties of fluorescent dissolved organic matter in the Gironde Estuary. *Organic Geochemistry*, 40(6):706–719, 2009. ISSN 0146-6380. doi: 10.1016/j.orggeochem.2009.03.002.

James F Hunt and Tsutomu Ohno. Characterization of fresh and decomposed dissolved organic matter using excitation-emission matrix fluorescence spectroscopy and multiway analysis. *Journal of agricultural and food chemistry*, 55(6):2121–8, March 2007. ISSN 0021-8561. doi: 10.1021/jf063336m. URL http://www.ncbi.nlm.nih.gov/pubmed/17305362.

J Hur, M A Williams, and M A Schlautman. Evaluating spectroscopic and chromatographic techniques to resolve dissolved organic matter via end member mixing analysis. *Chemosphere*, 63(3):387–402, April 2006. ISSN 0045-6535. doi: 10.1016/j.chemosphere.2005.08.069.

Shreeram Inamdar, Nina Finger, Shatrughan Singh, Myron Mitchell, Delphis Levia, Harsh Bais, Durelle Scott, and Patrick McHale. Dissolved organic matter (DOM) concentration and quality in a forested mid-Atlantic watershed, USA. *Biogeochemistry*, 108(1-3):55–76, January 2012. ISSN 0168-2563. doi: 10.1007/s10533-011-9572-4. URL http://link.springer.com/10.1007/s10533-011-9572-4.

Insitut Cartogràfic de Catalunya. *Mapa Geològic de Catalunya*, 2002. 1:250.000.

P J Jacobson, K M Jacobson, P L Angermeier, and D S Cherry. Variation in material transport and water chemistry along a large ephemeral river in the Namib Desert. *Freshwater Biology*, 44(3):481–491, July 2000. ISSN 0046-5070. doi: 10.1046/j.1365-2427.2000.00604.x.

R Jaffe, D McKnight, N Maie, R Cory, W H McDowell, and J L Campbell. Spatial and temporal variations in DOM composition in ecosystems: The importance of long-term monitoring of optical properties RID C-2277-2009 RID E-9767-2010. *Journal of Geophysical Research-Biogeosciences*, 113(G4):G04032–G04032, December 2008. ISSN 0148-0227. doi: 10.1029/2008JG000683.

Nianzhi Jiao, Gerhard J Herndl, Dennis a Hansell, Ronald Benner, Gerhard Kattner, Steven W Wilhelm, David L Kirchman, Markus G Weinbauer, Tingwei Luo,

Feng Chen, and Farooq Azam. Microbial production of recalcitrant dissolved organic matter: long-term carbon storage in the global ocean. *Nature reviews. Microbiology*, 8(8):593–9, August 2010. ISSN 1740-1534. doi: 10.1038/nrmicro2386. URL http://www.ncbi.nlm.nih.gov/pubmed/20601964.

Laura T. Johnson, Todd V. Royer, Jael M. Edgerton, and Laura G. Leff. Manipulation of the Dissolved Organic Carbon Pool in an Agricultural Stream: Responses in Microbial Community Structure, Denitrification, and Assimilatory Nitrogen Uptake. *Ecosystems*, 15(6):1027–1038, June 2012. ISSN 1432-9840. doi: 10.1007/s10021-012-9563-x. URL http://link.springer.com/10.1007/s10021-012-9563-x.

Kristin E Judd, Byron C Crump, and George W Kling. Variation in dissolved organic matter controls bacterial production and community composition. *Ecology*, 87(8):2068–79, August 2006. ISSN 0012-9658. URL http://www.ncbi.nlm.nih.gov/pubmed/16937646.

W J Junk, P B Bayley, and R E Sparks. The Flood Pulse Concept in River-Floodplain Systems. *Canadian Special Publication of Fisheries and Aquatic Sciences*, 106:110–127, 1989. ISSN 0706-6481.

R.H. Kadlec and R.L. Knight. *Treatment Wetlands*. CRC Lewis Press, Boca Raton, Florida., 2nd edition, 1996.

O M Karlsson, J S Richardson, and P A Kiffney. Modelling organic matter dynamics in headwater streams of south-western British Columbia, Canada. *Ecological Modelling*, 183(4):463–476, May 2005. ISSN 0304-3800. doi: 10.1016/j.ecolmodel.2004.08.022.

M Kerner, H Hohenberg, S Ertl, M Reckermann, and A Spitzy. Self-organization of dissolved organic matter to micelle-like microparticles in river water. *Nature*, 422(6928):150–154, 2003. ISSN 0028-0836. doi: 10.1038/nature01469.

P M Kiffney, C M Greene, J E Hall, and J R Davies. Tributary streams create spatial discontinuities in habitat , biological productivity , and diversity in mainstem rivers. *Canadian Journal of Fisheries and Aquatic Sciences*, 63(11):2518–2530, 2006. doi: 10.1139/F06-138.

S Kohler, I Buffam, A Jonsson, and K Bishop. Photochemical and microbial processing of stream and soilwater dissolved organic matter in a boreal forested catchment in northern Sweden. *Aquatic Sciences*, 64(3):269–281, 2002. ISSN 1015-1621. doi: 10.1007/s00027-002-8071-z.

T Kohonen. The self-organizing map. *Neurocomputing*, 21(1-3):1–6, October 1998. ISSN 0925-2312. doi: 10.1016/S0925-2312(98)00030-7.

T Kohonen. *Self-Organizing Maps*. Physics and astronomy online library. Springer Berlin Heidelberg, 3rd editio edition, 2001. ISBN 9783540679219.

Julie a Korak, Aaron D Dotson, R Scott Summers, and Fernando L Rosario-Ortiz. Critical analysis of commonly used fluorescence metrics to characterize dissolved organic matter. *Water research*, 49:327–38, February 2014. ISSN 1879-2448. doi: 10.1016/j.watres.2013.11.025. URL http://www.ncbi.nlm.nih.gov/pubmed/24384525.

Piotr Kowalczuk, Gavin H. Tilstone, Monika Zabłocka, Rüdiger Röttgers, and Rob Thomas. Composition of dissolved organic matter along an Atlantic Meridional Transect from fluorescence spectroscopy and Parallel Factor Analysis. *Marine Chemistry*, 157:170–184, December 2013. ISSN 03044203. doi: 10.1016/j.marchem.2013.10.004. URL http://linkinghub.elsevier.com/retrieve/pii/S0304420313001783.

PS Lake. Disturbance, patchiness, and diversity in streams. *Journal of the north american Benthological society*, 19(4):573–592, 2000. URL http://www.jstor.org/stable/1468118.

Joseph R. Lakowicz. *Principles of Fluorescence Spectroscopy*. Springer, 3rd edition, 2006. URL http://www.springer.com/chemistry/analytical+chemistry/book/978-0-387-31278-1.

G N Lance and W T Williams. A General Theory of Classificatory Sorting Strategies .1. Hierarchical Systems. *Computer journal*, 9(4):373–&, 1967. ISSN 0010-4620.

Jean-François Lapierre and Jean-Jacques Frenette. Effects of macrophytes and terrestrial inputs on fluorescent dissolved organic matter in a large river system. *Aquatic Sciences*, 71(1):15–24, February 2009. ISSN 1015-1621. doi: 10.1007/s00027-009-9133-2. URL http://www.springerlink.com/index/10.1007/s00027-009-9133-2.

Scott T. Larned, Thibault Datry, David B. Arscott, and Klement Tockner. Emerging concepts in temporary-river ecology. *Freshwater Biology*, 55(4):717–738, April 2010. ISSN 00465070. doi: 10.1111/j.1365-2427.2009.02322.x. URL http://doi.wiley.com/10.1111/j.1365-2427.2009.02322.x.

Tobias Larsson, Margareta Wedborg, and David Turner. Correction of inner-filter effect in fluorescence excitation-emission matrix spectrometry using Raman scatter RID B-2620-2010 RID A-7870-2010. *Analytica Chimica Acta*, 583(2):357–363, February 2007. ISSN 0003-2670. doi: 10.1016/j.aca.2006.09.067.

A J Lawaetz and C A Stedmon. Fluorescence Intensity Calibration Using the Raman Scatter Peak of Water RID B-5841-2008. *Applied Spectroscopy*, 63(8):936–940, August 2009. ISSN 0003-7028.

Mi-Hee Lee and Jin Hur. Photodegradation-Induced Changes in the Characteristics of Dissolved Organic Matter with Different Sources and Their Effects on Disinfection By-Product Formation Potential. *CLEAN - Soil, Air, Water*, 42 (5):552–560, May 2014. ISSN 18630650. doi: 10.1002/clen.201200685. URL http://doi.wiley.com/10.1002/clen.201200685.

Pierre Legendre and Louis Legendre. *Numerical Ecology*. Elsevier, 2nd englis edition, 1998. ISBN 0444538682.

Gavin R Lloyd, Richard G Brereton, and John C Duncan. Self Organising Maps for distinguishing polymer groups using thermal response curves obtained by dynamic mechanical analysis. *The Analyst*, 133(8):1046–59, August 2008. ISSN 1364-5528. doi: 10.1039/b715390b. URL http://www.ncbi.nlm.nih.gov/pubmed/18645646.

Kathleen a. Lohse, Paul D. Brooks, Jennifer C. McIntosh, Thomas Meixner, and Travis E. Huxman. Interactions Between Biogeochemistry and Hydrologic Systems. *Annual Review of Environment and Resources*, 34(1):65–96, November 2009. ISSN 1543-5938. doi: 10.1146/annurev.environ.33.031207.111141. URL http://www.annualreviews.org/doi/abs/10.1146/annurev.environ.33.031207.111141.

Andrew J. Long and Joshua F. Valder. Multivariate analyses with end-member mixing to characterize groundwater flow: Wind Cave and associated aquifers. *Journal of Hydrology*, 409(1-2):315–327, October 2011. ISSN 00221694. doi: 10.1016/j.jhydrol.2011.08.028. URL http://linkinghub.elsevier.com/retrieve/pii/S0022169411005749.

Miguel Lorite-Herrera, Kevin Hiscock, and Rosario Jimenez-Espinosa. Distribution of Dissolved Inorganic and Organic Nitrogen in River Water and Groundwater in an Agriculturally-Dominated Catchment, South-East Spain. *Water Air and Soil Pollution*, 198(1-4):335–346, March 2009. ISSN 0049-6979. doi: 10.1007/s11270-008-9849-y.

Wolfgang Ludwig, Jean-Luc Probst, and Stefan Kempe. Predicting the oceanic input of organic carbon by continental erosion. *Global Biogeochemical Cycles*, 10 (1):23–41, March 1996. ISSN 08866236. doi: 10.1029/95GB02925. URL http://doi.wiley.com/10.1029/95GB02925.

Brian D Lutz, Emily S Bernhardt, Brian J Roberts, and Patrick J Mulholland. Examining the coupling of carbon and nitrogen cycles in Appalachian streams: the role of dissolved organic nitrogen. *Ecology*, 92(3):720–732, March 2011. ISSN 0012-9658.

Jiahai Ma, Rossana Del Vecchio, Kelli S Golanoski, Erin S Boyle, and Neil V Blough. Optical properties of humic substances and CDOM: effects of borohydride reduction. *Environmental science & technology*, 44(14):5395–402, July 2010. ISSN 0013-936X. doi: 10.1021/es100880q. URL http://www.ncbi.nlm.nih.gov/pubmed/20557095.

Nagamitsu Maie, Kathleen J. Parish, Akira Watanabe, Heike Knicker, Ronald Benner, Tomonori Abe, Karl Kaiser, and Rudolf Jaffé. Chemical characteristics of dissolved organic nitrogen in an oligotrophic subtropical coastal ecosystem. *Geochimica et Cosmochimica Acta*, 70(17):4491–4506, September 2006. ISSN 00167037. doi: 10.1016/j.gca.2006.06.1554. URL http://linkinghub.elsevier.com/retrieve/pii/S0016703706018564.

Nagamitsu Maie, Norman M Scully, Oliva Pisani, and Rudolf Jaffé. Composition of a protein-like fluorophore of dissolved organic matter in coastal wetland and estuarine ecosystems. *Water research*, 41(3):563–70, March 2007. ISSN 0043-1354. doi: 10.1016/j.watres.2006.11.006. URL http://www.ncbi.nlm.nih.gov/pubmed/17187842.

R. Manning. On the flow of water in open channels and pipes. *Transactions of the Institution of Civil Engineers of Ireland*, 20:161–207, 1891.

R J Maranger, M L Pace, P A del Giorgio, N F Caraco, and J J Cole. Longitudinal spatial patterns of bacterial production and respiration in a large River-Estuary: Implications for ecosystem carbon consumption. *Ecosystems*, 8(3):318–330, 2005. ISSN 1432-9840. doi: 10.1007/s10021-003-0071-x.

F C Marhuenda-Egea, E Martínez-Sabater, J Jordá, R Moral, M a Bustamante, C Paredes, and M D Pérez-Murcia. Dissolved organic matter fractions formed during composting of winery and distillery residues: evaluation of the process by fluorescence excitation-emission matrix. *Chemosphere*, 68(2):301–9, June 2007. ISSN 0045-6535. doi: 10.1016/j.chemosphere.2006.12.075. URL http://www.ncbi.nlm.nih.gov/pubmed/17292449.

Eugènia Marti, Jordi Aumatell, Lluís Godé, Manel Poch, and Francesc Sabater. Nutrient retention efficiency in streams receiving inputs from wastewater treatment plants. *Journal of environmental quality*, 33(1):285–93, 2004. ISSN 0047-2425. URL http://www.ncbi.nlm.nih.gov/pubmed/14964383.

Rebecca A Martin and John A Harrison. Effect of High Flow Events on In-Stream Dissolved Organic Nitrogen Concentration. *Ecosystems*, 14(8):1328–1338, December 2011. ISSN 1432-9840. doi: 10.1007/s10021-011-9483-1.

Rebecca a. Martin, Tamara K. Harms, and Nancy B. Grimm. Chronic N loading reduces N retention across varying base flows in a desert river. *Journal of the*

North American Benthological Society, 30(2):559–572, June 2011. ISSN 0887-3593. doi: 10.1899/09-137.1. URL http://www.bioone.org/doi/abs/10.1899/09-137.1.

Josep Mas-Pla and Anna Menció. Estudi hidrològic de la Tordera: Elements per al seguiment de la biodiversitat i la gestió de l'aigua. In Martí Boada, Sílvia Mayo, and Roser Maneja, editors, *Els sistemes socioecològics de la conca de la Tordera*. Institució Catalana d'Història Natural, 1st edition, 2008. ISBN 978-84-7283-983-0.

Josep Mas-Pla, Eva Font, Anna Menció, Mercè Boy, Diego Varga, Anna Freixa, Elisabet Ejarque, Andrea Butturini, and Anna M. Romaní. Evolució hidroquímica i isotòpica de l'aigua superficial a la tordera: implicacions hidrològiques. *VIII Trobada d'Estudiosos del Montseny, Girona*, 2012.

Josep Mas-Pla, Anna Mencio, and Albert Marsinach. Basement Groundwater as a Complementary Resource for Overexploited Stream-Connected Alluvial Aquifers. *Water Resources Management*, 27(1):293–308, January 2013. ISSN 0920-4741. doi: 10.1007/s11269-012-0186-y.

P Massicotte and JJ Frenette. Spatial connectivity in a large river system: resolving the sources and fate of dissolved organic matter. *Ecological Applications*, 21(7): 2600–2617, 2011. URL http://www.esajournals.org/doi/abs/10.1890/10-1475.1.

WNS Mat-Desa, D Ismail, and N NicDaeid. Classification and Source Determination of Medium Petroleum Distillates by Chemometric and Artificial Neural Networks: A Self Organizing Feature Approach. *Analytical chemistry*, 83:7745–7754, 2011. URL http://pubs.acs.org/doi/abs/10.1021/ac202315y.

Sílvia Mayo, Francisco Javier Gómez, and Josep Mas-Pla. L'entorn natural de la conca de la Tordera. In Marti Boada, Sílvia Mayo, and Roser Maneja, editors, *Els sistemes socioecològics de la conca de la Tordera*, page 541. Institució Catalana d'Història Natural, Barcelona, first edit edition, 2008. ISBN 978-84-7283-983-0.

Michael E. McClain, Elizabeth W. Boyer, C. Lisa Dent, Sarah E. Gergel, Nancy B. Grimm, Peter M. Groffman, Stephen C. Hart, Judson W. Harvey, Carol a. Johnston, Emilio Mayorga, William H. McDowell, and Gilles Pinay. Biogeochemical Hot Spots and Hot Moments at the Interface of Terrestrial and Aquatic Ecosystems. *Ecosystems*, 6(4):301–312, June 2003. ISSN 1432-9840. doi: 10.1007/s10021-003-0161-9. URL http://link.springer.com/10.1007/s10021-003-0161-9.

S McDonald, A G Bishop, P D Prenzler, and K Robards. Analytical chemistry of freshwater humic substances. *Analytica Chimica Acta*, 527(2):105–124, December 2004. ISSN 0003-2670. doi: 10.1016/j.aca.2004.10.011.

D M McKnight, E W Boyer, P K Westerhoff, P T Doran, T Kulbe, and D T Andersen. Spectrofluorometric characterization of dissolved organic matter for indication of precursor organic material and aromaticity. *Limnology and Oceanography*, 46(1):38–48, 2001. ISSN 0024-3590.

Diane M. McKnight, George M. Hornberger, Kenneth E. Bencala, and Elizabeth W. Boyer. In-stream sorption of fulvic acid in an acidic stream: A stream-scale transport experiment. *Water Resources Research*, 38(1):6–1–6–12, January 2002. ISSN 00431397. doi: 10.1029/2001WR000269. URL http://doi.wiley.com/10.1029/2001WR000269.

Fangang Meng, Guocheng Huang, Xin Yang, Zengquan Li, J Li, and J Cao. Identifying the sources and fate of anthropogenically impacted dissolved organic matter (DOM) in urbanized rivers. *Water research*, 47(14):5027–5039, 2013. ISSN 0043-1354. doi: 10.1016/j.watres.2013.05.043. URL http://dx.doi.org/10.1016/j.watres.2013.05.043http://www.sciencedirect.com/science/article/pii/S0043135413004715.

Gora Merseburger, Eugenia Marti, Francesc Sabater, and Jesus D Ortiz. Point-source effects on N and P uptake in a forested and an agricultural Mediterranean streams. *Science of the Total Environment*, 409(5):957–967, February 2011. ISSN 0048-9697. doi: 10.1016/j.scitotenv.2010.11.014.

William L. Miller and Richard G. Zepp. Photochemical production of dissolved inorganic carbon from terrestrial organic matter: Significance to the oceanic organic carbon cycle. *Geophysical Research Letters*, 22(4):417–420, February 1995. ISSN 00948276. doi: 10.1029/94GL03344. URL http://doi.wiley.com/10.1029/94GL03344.

B. Montuelle and B. Volat. Use of microbial exoenzymatic activities in aquatic ecosystems studies. *Revue des Sciences de l'Eau*, 6(3):251–268, 1993.

C S Moody, F Worrall, C D Evans, and T G Jones. The rate of loss of dissolved organic carbon (DOC) through a catchment. *Journal of Hydrology*, 492:139–150, June 2013. ISSN 0022-1694. doi: 10.1016/j.jhydrol.2013.03.016.

Kenneth Mopper and Christopher a. Schultz. Fluorescence as a possible tool for studying the nature and water column distribution of DOC components. *Marine Chemistry*, 41(1-3):229–238, January 1993. ISSN 03044203. doi: 10.1016/0304-4203(93)90124-7. URL http://linkinghub.elsevier.com/retrieve/pii/0304420393901247.

M.A. Moran and J.S. Covert. Photochemically mediated linkages between dissolved organic matter and bacterioplankton. In Stuart Findlay and RL Sinsabaugh,

editors, *Aquatic Ecosystems: Interactivity of Dissolved Organic Matter*. Academic Press, Elsevier Science, 2003.

MA Moran and RG Zepp. Role of photoreactions in the formation of biologically labile compounds from dissolved organic matter. *Oceanography*, 42(6), 1997. URL http://www.aslo.info/lo/toc/vol_42/issue_6/1307.pdf.

MA Moran, WM Sheldon, and RG Zepp. Carbon loss and optical property changes during long-term photochemical and biological degradation of estuarine dissolved organic matter. *Limnology and Oceanography*, 45(August 1997):1254–1264, 2000. URL http://www.avto.aslo.info/lo/toc/vol_45/issue_6/1254.pdf.

Khan M G Mostofa, Takahito Yoshioka, Eiichi Konohira, and Eiichiro Tanoue. Photodegradation of fluorescent dissolved organic matter in river waters. *Geochemical Journal*, 41(5):323–331, 2007. ISSN 0016-7002.

P. J. Mulholland, J. L. Tank, J. R. Webster, W. B. Bowden, W. K. Dodds, S. V. Gregory, N. B. Grimm, S. K. Hamilton, S. L. Johnson, E. Martí, W. H. McDowell, J. L. Merriam, J. L. Meyer, B. J. Peterson, H. M. Valett, W. M. Wollheim, and E. Marti. Can Uptake Length in Streams Be Determined by Nutrient Addition Experiments? Results from an Interbiome Comparison Study. *Journal of the North American Benthological Society*, 21(4):544, December 2002. ISSN 08873593. doi: 10.2307/1468429. URL http://apps.webofknowledge.com/full_record.do?product=UA\&search_mode=GeneralSearch\&qid=2\&SID=V1lrl9nTygARXRfYkqc\&page=1\&doc=1.

P.J. Mulholland. Large-scale patterns in dissolved organic carbon concentration, flux and sources. In Stuart E.G. Findlay and Robert L. Sinsabaugh, editors, *Aquatic Ecosystems: Interactivity of Dissolved Organic Matter*. Academic Press, 1st edition, 2003. ISBN 0-12-256371-9.

J. Murphy and J.P. Riley. A modified single solution method for the determination of phosphate in natural waters. *Analytica Chimica Acta*, 27:31–36, 1962. URL http://www.sciencedirect.com/science/article/pii/S0003267000884445.

Kathleen R. Murphy, Colin a. Stedmon, Philip Wenig, and Rasmus Bro. OpenFluor– an online spectral library of auto-fluorescence by organic compounds in the environment. *Analytical Methods*, 6(3):658, 2014. ISSN 1759-9660. doi: 10.1039/c3ay41935e. URL http://xlink.rsc.org/?DOI=c3ay41935e.

Pamela S Naden, Gareth H Old, Caroline Eliot-Laize, Steve J Granger, Jane M B Hawkins, Roland Bol, and Phil Haygarth. Assessment of natural fluorescence as a tracer of diffuse agricultural pollution from slurry spreading on intensely-farmed grasslands. *Water research*, 44(6):1701–1712, March 2010. ISSN 0043-1354. doi: 10.1016/j.watres.2009.11.038.

R J Naiman, J M Melillo, M A Lock, T E Ford, and S R Reice. Longitudinal Patterns of Ecosystem Processes and Community Structure in a Sub-Arctic River Continuum. *Ecology*, 68(5):1139–1156, 1987. ISSN 0012-9658. doi: 10.2307/1939199.

Robert J. Naiman, Henri Déchamps, John Pastor, and Carol A. Johnston. The potential importance of boundaries to fluvial ecosystems. *Journal of the North American Benthological Society*, 7(4):289–306, 1988. URL http://www.jstor.org/discover/10.2307/1467295?uid=3737952\&uid=2\&uid=4\&sid=21104395558717.

Robert J. Naiman, Joshua J. Latterell, Neil E. Pettit, and Julian D. Olden. Flow variability and the biophysical vitality of river systems. *Comptes Rendus Geoscience*, 340(9-10):629–643, September 2008. ISSN 16310713. doi: 10.1016/j.crte.2008.01.002. URL http://linkinghub.elsevier.com/retrieve/pii/S1631071308000266.

Yasunori Nakagawa, Hideaki Shibata, Fuyuki Satoh, and Kaichiro Sasa. Riparian control on NO3-, DOC, and dissolved Fe concentrations in mountainous streams, northern Japan RID A-6909-2008. *Limnology*, 9(3):195–206, December 2008. ISSN 1439-8621. doi: 10.1007/s10201-008-0251-7.

Antonio Nebbioso and Alessandro Piccolo. Molecular characterization of dissolved organic matter (DOM): a critical review. *Analytical and Bioanalytical Chemistry*, 405(1):109–124, January 2013. ISSN 1618-2642. doi: 10.1007/s00216-012-6363-2.

C. Negre. Avaluació de l'estat hidrològic de la tordera. imposicions antròpiques en el balanç hídric., 2004.

Hang Vo-Minh Nguyen, Jin Hur, and Hyun-Sang Shin. Changes in Spectroscopic and Molecular Weight Characteristics of Dissolved Organic Matter in a River During a Storm Event. *Water Air and Soil Pollution*, 212(1-4):395–406, 2010. ISSN 0049-6979. doi: 10.1007/s11270-010-0353-9.

H Ogawa, Y Amagai, I Koike, K Kaiser, and R Benner. Production of refractory dissolved organic matter by bacteria. *Science (New York, N.Y.)*, 292(5518):917–20, May 2001. ISSN 0036-8075. doi: 10.1126/science.1057627. URL http://www.ncbi.nlm.nih.gov/pubmed/11340202.

Merja Oja, Janne Nikkilä, Petri Törönen, Garry Wong, Eero Castrén, and Samuel Kaski. Exploratory Clustering of Gene Expression Profiles of Mutated Yeast Strains. In Wei Zhang and Ilya Shmulevich, editors, *Computational and Statistical Approaches to Genomics*, chapter 5, pages 61–74. Springer US, 2006. ISBN 978-0-387-26287-1. doi: 10.1007/0-387-26288-1_5. URL http://dx.doi.org/10.1007/0-387-26288-1_5.

Jari Oksanen, F. Guillaume Blanchet, Roeland Kindt, Pierre Legendre, Peter R. Minchin, R. B. O'Hara, Gavin L. Simpson, Peter Solymos, M. Henry H. Stevens, and Helene Wagner. *vegan: Community Ecology Package*, 2012. URL `http://CRAN.R-project.org/package=vegan`. R package version 2.0-3.

C L Osburn, D P Morris, K A Thorn, and R E Moeller. Chemical and optical changes in freshwater dissolved organic matter exposed to solar radiation. *Biogeochemistry*, 54(3):251–278, 2001. ISSN 0168-2563. doi: 10.1023/A:1010657428418.

Christopher L Osburn, Leira Retamal, and Warwick F Vincent. Photoreactivity of chromophoric dissolved organic matter transported by the Mackenzie River to the Beaufort Sea. *Marine Chemistry*, 115(1-2):10–20, 2009. ISSN 0304-4203. doi: 10.1016/j.marchem.2009.05.003.

Min-Hye Park, Tae-Hwan Lee, Bo-Mi Lee, Jin Hur, and Dae-Hee Park. Spectroscopic and Chromatographic Characterization of Wastewater Organic Matter from a Biological Treatment Plant. *Sensors*, 10(1):254–265, 2010. ISSN 1424-8220. doi: 10.3390/s100100254.

Young-Seuk Park, Juliette Tison, Sovan Lek, Jean-Luc Giraudel, Michel Coste, and François Delmas. Application of a self-organizing map to select representative species in multivariate analysis: A case study determining diatom distribution patterns across France. *Ecological Informatics*, 1(3):247–257, November 2006. ISSN 15749541. doi: 10.1016/j.ecoinf.2006.03.005. URL `http://linkinghub.elsevier.com/retrieve/pii/S1574954106000525`.

E Parlanti, K Worz, L Geoffroy, and M Lamotte. Dissolved organic matter fluorescence spectroscopy as a tool to estimate biological activity in a coastal zone submitted to anthropogenic inputs. *Organic Geochemistry*, 31(12):1765–1781, 2000. ISSN 0146-6380. doi: 10.1016/S0146-6380(00)00124-8.

RA Payn, JR Webster, PJ Mulholland, HM Valett, and WK Dodds. Estimation of stream nutrient uptake from nutrient addition experiments. *LIMNOLOGY AND OCEANOGRAPHY-METHODS*, 3:174–182, March 2005. URL `http://apps.webofknowledge.com/full\_record.do?product=UA\&search\_mode=GeneralSearch\&qid=4\&SID=V1lrl9nTygARXRfYkqc\&page=1\&doc=1`.

Peter Peduzzi, F Aspetsberger, T Hein, F Huber, S Kargl-Wagner, B Luef, and Y Tachkova. Dissolved organic matter (DOM) and bacterial growth in floodplains of the Danube River under varying hydrological connectivity. *Fundamental and Applied Limnology*, 171(1):49–61, 2008. ISSN 1863-9135. doi: 10.1127/1863-9135/2008/0171-0049.

B J Peterson, W M Wollheim, P J Mulholland, J R Webster, J L Meyer, J L Tank, E Marti, W B Bowden, H M Valett, a E Hershey, W H McDowell, W K

Dodds, S K Hamilton, S Gregory, and D D Morrall. Control of nitrogen export from watersheds by headwater streams. *Science (New York, N.Y.)*, 292(5514): 86–90, April 2001. ISSN 0036-8075. doi: 10.1126/science.1056874. URL `http://www.ncbi.nlm.nih.gov/pubmed/11292868`.

G Pinay, J C Clement, and R J Naiman. Basic principles and ecological consequences of changing water regimes on nitrogen cycling in fluvial systems. *Environmental management*, 30(4):481–491, October 2002. ISSN 0364-152X. doi: 10.1007/s00267-002-2736-1.

N L Poff, J D Allan, M B Bain, J R Karr, K L Prestegaard, B D Richter, R E Sparks, and J C Stromberg. The natural flow regime. *BIOSCIENCE*, 47(11): 769–784, 1997. ISSN 0006-3568. doi: 10.2307/1313099.

G C Poole. Fluvial landscape ecology: addressing uniqueness within the river discontinuum. *Freshwater Biology*, 47(4):641–660, 2002. ISSN 0046-5070. doi: 10.1046/j.1365-2427.2002.00922.x.

Yves T Prairie. Carbocentric limnology: looking back, looking forward. *Canadian Journal of Fisheries and Aquatic Sciences*, 65(3):543–548, 2008. ISSN 0706-652X. doi: 10.1139/F08-011.

Gerry P. Quinn and Michael J. Keough. *Experimental Design and Data Analysis for Biologists*. Cambridge University Press, New York, USA, 10th edition, 2010.

R Development Core Team. *R: A Language and Environment for Statistical Computing*. R Foundation for Statistical Computing, Vienna, Austria, 2012. URL `http://www.R-project.org/`. ISBN 3-900051-07-0.

Pa Raymond and Je Bauer. Bacterial consumption of DOC during transport through a temperate estuary. *Aquatic Microbial Ecology*, 22:1–12, 2000. ISSN 0948-3055. doi: 10.3354/ame022001. URL `http://www.int-res.com/abstracts/ame/v22/n1/p1-12/`.

Peter A Raymond and James E Saiers. Event controlled DOC export from forested watersheds. *Biogeochemistry*, 100(1-3):197–209, 2010. ISSN 0168-2563. doi: 10.1007/s10533-010-9416-7.

John Reardon. Salicylate method for the quantitative determination of ammonia nitrogen, 1969. URL `http://www.freepatentsonline.com/3432395.html`.

J I Rhee, K I Lee, C K Kim, Y S Yim, S W Chung, J Q Wei, and K H Bellgardt. Classification of two-dimensional fluorescence spectra using self-organizing maps. *Biochemical engineering journal*, 22(2):135–144, January 2005. ISSN 1369-703X. doi: 10.1016/j.bej.2004.09.008.

S.P. Rice, M.T. Greenwood, and C.B. Joyce. Tributaries, sediment sources, and the longitudinal organisation of macroinvertebrate fauna along river systems. *Canadian Journal of Fisheries and Aquatic Sciences*, 58(4):824–840, 2001. ISSN 12057533. doi: 10.1139/cjfas-58-4-824. URL http://www.nrc.ca/cgi-bin/cisti/journals/rp/rp2_abst_e?cjfas_f01-022_58_ns_nf_cjfas58-01.

Stephen P Rice, Robert I Ferguson, and Trevor B Hoey. Tributary control of physical heterogeneity and biological diversity at river confluences. *Canadian Journal of Fisheries and Aquatic Sciences*, 63(11):2553–2566, 2006. doi: 10.1139/F06-145.

Ej Rochelle-Newall, Md Pizay, Jj Middelburg, Hts Boschker, and Jp Gattuso. Degradation of riverine dissolved organic matter by seawater bacteria. *Aquatic Microbial Ecology*, 37:9–22, 2004. ISSN 0948-3055. doi: 10.3354/ame037009. URL http://www.int-res.com/abstracts/ame/v37/n1/p9-22/.

Cristina Romera-Castillo, Hugo Sarmento, Xose Anton Alvarez-Salgado, Josep M. Gasol, and Celia Marrase. Erratum: Production of chromophoric dissolved organic matter by marine phytoplankton. *Limnology and Oceanography*, 55 (3):1466–1466, 2010. ISSN 00243590. doi: 10.4319/lo.2010.55.3.1466. URL http://www.aslo.org/lo/toc/vol_55/issue_3/1466.html.

Bernd Rosenstock and Meinhard Simon. Sources and sinks of dissolved free amino acids and protein in a large and deep mesotrophic lake. *Limnology and Oceanography*, 46(3):644–654, 2001. ISSN 00243590. doi: 10.4319/lo.2001.46.3.0644. URL http://www.aslo.org/lo/toc/vol_46/issue_3/0644.html.

Peter J Rousseeuw. Silhouettes: A graphical aid to the interpretation and validation of cluster analysis. *Journal of Computational and Applied Mathematics*, 20(0):53–65, 1987. ISSN 0377-0427. doi: http://dx.doi.org/10.1016/0377-0427(87)90125-7. URL http://www.sciencedirect.com/science/article/pii/0377042787901257.

J G Rowson, H S Gibson, F Worrall, N Ostle, T P Burt, and J K Adamson. The complete carbon budget of a drained peat catchment. *Soil Use and Management*, 26(3):261–273, September 2010. ISSN 0266-0032. doi: 10.1111/j.1475-2743.2010.00274.x.

T V Royer and M B David. Export of dissolved organic carbon from agricultural streams in Illinois, USA. *Aquatic Sciences*, 67(4):465–471, December 2005. ISSN 1015-1621. doi: 10.1007/s00027-005-0781-6.

A Ruggiero, A G Solimini, and G Carchini. Effects of a waste water treatment plant on organic matter dynamics and ecosystem functioning in a Mediterranean stream. *Annales De Limnologie-International Journal of Limnology*, 42(2):97–107, 2006. ISSN 0003-4088. doi: 10.1051/limn/2006014.

B. Sala. Avaluació de l'estat hidromorfològic del riu tordera., 2005.

M Salvia, J F Iffly, P Vander Borght, M Sary, and L Hoffmann. Application of the 'snapshot' methodology to a basin-wide analysis of phosphorus and nitrogen at stable low flow. *Hydrobiologia*, 410:97–102, 1999. ISSN 0018-8158. doi: 10.1023/A:1003892830838.

Jonathan Sanderman, Kathleen A Lohse, Jeffrey A Baldock, and Ronald Amundson. Linking soils and streams: Sources and chemistry of dissolved organic matter in a small coastal watershed. *Water Resources Research*, 45:W03418–W03418, 2009. ISSN 0043-1397. doi: 10.1029/2008WR006977.

Jorge L. Sarmiento and Nicolas Gruber. Sinks for anthropogenic carbon. *Physics Today*, 55(8):30–36, August 2002. ISSN 0031-9228. doi: 10.1063/1.1510279. URL `http://scitation.aip.org/content/aip/magazine/physicstoday/article/55/8/10.1063/1.1510279`.

JR Sedell. The river continuum concept: a basis for the expected ecosystem behavior of very large rivers. In D.P. Dodge, editor, *Proceedings of the International Large River Symposium. Can. Spec. Publ. Aquat. Sci.*, pages 49–55, 1989. URL `http://boto.ocean.washington.edu/lc/RIVERS/25\_sedell\_jr\_49-55.pdf`.

Zheng-Hao Shao, Pin-Jing He, Dong-Qing Zhang, and Li-Ming Shao. Characterization of water-extractable organic matter during the biostabilization of municipal solid waste. *Journal of hazardous materials*, 164(2-3):1191–7, May 2009. ISSN 1873-3336. doi: 10.1016/j.jhazmat.2008.09.035. URL `http://www.ncbi.nlm.nih.gov/pubmed/18963454`.

Shatrughan Singh, Sudarshan Dutta, and Shreeram Inamdar. Land application of poultry manure and its influence on spectrofluorometric characteristics of dissolved organic matter. *Agriculture, Ecosystems & Environment*, 193:25–36, 2014. ISSN 01678809. doi: 10.1016/j.agee.2014.04.019. URL `http://www.sciencedirect.com/science/article/pii/S0167880914002254`.

Robert G M Spencer, Andy Baker, Jason M E Ahad, Gregory L Cowie, Raja Ganeshram, Robert C Upstill-Goddard, and Gunther Uher. Discriminatory classification of natural and anthropogenic waters in two UK estuaries. *Science of the Total Environment*, 373(1):305–323, 2007. ISSN 0048-9697. doi: 10.1016/j.scitotenv.2006.10.052.

B Statzner and B Higler. Questions and Comments on the River Continuum Concept. *Canadian Journal of Fisheries and Aquatic Sciences*, 42(5):1038–1044, 1985. ISSN 0706-652X. doi: 10.1139/f85-129.

C A Stedmon, S Markager, and R Bro. Tracing dissolved organic matter in aquatic environments using a new approach to fluorescence spectroscopy. *Marine Chemistry*, 82(3-4):239–254, 2003. ISSN 0304-4203. doi: 10.1016/S0304-4203(03)00072-0.

Colin A Stedmon and Rasmus Bro. Characterizing dissolved organic matter fluorescence with parallel factor analysis: a tutorial. *Limnology and Oceanography-Methods*, 6:572–579, November 2008. ISSN 1541-5856.

R Stepanauskas, L Leonardson, and L J Tranvik. Bioavailability of wetland-derived DON to freshwater and marine bacterioplankton. *Limnology and Oceanography*, 44(6), 1999. ISSN 0024-3590.

Robert Warner Sterner and James J. Elser. *Ecological Stoichiometry: The Biology of Elements from Molecules to the Biosphere*. Princeton University Press, 2002. ISBN 0691074917. URL `http://books.google.com/books?id=53NTDvppdYUC\&pgis=1`.

Philip G Taylor and Alan R Townsend. Stoichiometric control of organic carbon-nitrate relationships from soils to the sea. *Nature*, 464(7292):1178–1181, 2010. ISSN 0028-0836. doi: 10.1038/nature08985.

J Temnerud, A Duker, S Karlsson, B Allard, S Koehler, and K Bishop. Landscape scale patterns in the character of natural organic matter in a Swedish boreal stream network. *Hydrology and Earth System Sciences*, 13(9):1567–1582, 2009. ISSN 1027-5606.

Johan Temnerud, Jan Seibert, Mats Jansson, and Kevin Bishop. Spatial variation in discharge and concentrations of organic carbon in a catchment network of boreal streams in northern Sweden. *Journal of Hydrology*, 342(1-2):72–87, 2007. ISSN 0022-1694. doi: 10.1016/j.jhydrol.2007.05.015.

J H Thorp and M D Delong. The Riverine Productivity Model - an Heuristic View of Carbon-Sources and Organic-Processing in Large River Ecosystems. *Oikos*, 70 (2):305–308, 1994. ISSN 0030-1299. doi: 10.2307/3545642.

J H Thorp, M C Thoms, and M D Delong. The riverine ecosystem synthesis: Biocomplexity in river networks across space and time. *River Research and Applications*, 22(2):123–147, 2006. ISSN 1535-1459. doi: 10.1002/rra.901.

Joseph A Thouin, Wilfred M Wollheim, Charles J Vorosmarty, Jennifer M Jacobs, and William H McDowell. The biogeochemical influences of NO(3)(-), dissolved O(2), and dissolved organic C on stream NO(3)(-) uptake. *Journal of the North American Benthological Society*, 28(4):894–907, December 2009. ISSN 0887-3593. doi: 10.1899/08-183.1.

Earl Michael Thurman. *Organic geochemistry of natural waters*. Kluwer Academic Press, Amsterdam, 1985. ISBN 9024731437.

Lars Tranvik and Stefan Kokalj. Decreased biodegradability of algal DOC due to interactive effects of UV radiation and humic matter. *Aquatic Microbial Ecology*, 14: 301–307, 1998. URL http://www.int-res.com/abstracts/ame/v14/n3/p301-307/.

Lars J Tranvik, John A Downing, James B Cotner, Steven A Loiselle, Robert G Striegl, Thomas J Ballatore, Peter Dillon, Kerri Finlay, Kenneth Fortino, Lesley B Knoll, Pirkko L Kortelainen, Tiit Kutser, Soren Larsen, Isabelle Laurion, Dina M Leech, S Leigh McCallister, Diane M McKnight, John M Melack, Erin Overholt, Jason A Porter, Yves Prairie, William H Renwick, Fabio Roland, Bradford S Sherman, David W Schindler, Sebastian Sobek, Alain Tremblay, Michael J Vanni, Antonie M Verschoor, Eddie von Wachenfeldt, and Gesa A Weyhenmeyer. Lakes and reservoirs as regulators of carbon cycling and climate. *Limnology and Oceanography*, 54(6):2298–2314, 2009. ISSN 0024-3590. doi: 10.4319/lo.2009.54.6_part_2.2298.

A. Ultsch and H.P. Siemon. Kohonen's Self Organizing Feature Maps for Exploratory Data Analysis. In *Proceedings of International Neural Network Conference (INNC'90)*, pages 305–308, Dordrecht, The Netherlands, 1990. Kluwer.

Joshua F. Valder, Andrew J. Long, Arden D. Davis, and Scott J. Kenner. Multivariate statistical approach to estimate mixing proportions for unknown end members. *Journal of Hydrology*, 460-461:65–76, August 2012. ISSN 00221694. doi: 10.1016/j.jhydrol.2012.06.037. URL http://linkinghub.elsevier.com/retrieve/pii/S0022169412005367.

R L Vannote, G W Minshall, K W Cummins, J R Sedell, and C E Cushing. River Continuum Concept. *Canadian Journal of Fisheries and Aquatic Sciences*, 37(1): 130–137, 1980. ISSN 0706-652X. doi: 10.1139/f80-017.

Eusebi Vázquez, Anna M. Romaní, Francesc Sabater, and Andrea Butturini. Effects of the Dry–Wet Hydrological Shift on Dissolved Organic Carbon Dynamics and Fate Across Stream–Riparian Interface in a Mediterranean Catchment. *Ecosystems*, 10(2):239–251, April 2007. ISSN 1432-9840. doi: 10.1007/s10021-007-9016-0. URL http://link.springer.com/10.1007/s10021-007-9016-0.

Eusebi Vazquez, Stefano Amalfitano, Stefano Fazi, and Andrea Butturini. Dissolved organic matter composition in a fragmented Mediterranean fluvial system under severe drought conditions. *Biogeochemistry*, 102(1-3):59–72, 2011. ISSN 0168-2563. doi: 10.1007/s10533-010-9421-x.

J Vesanto. SOM-based data visualization methods. *Intelligent Data Analysis*, 3(2): 111–126, August 1999. ISSN 1088467X. doi: 10.1016/S1088-467X(99)00013-X. URL http://linkinghub.elsevier.com/retrieve/pii/S1088467X9900013X.

J Vesanto and E Alhoniemi. Clustering of the self-organizing map. *IEEE Transactions on Neural Networks*, 11(3):586–600, May 2000. ISSN 1045-9227. doi: 10.1109/72.846731.

J Vesanto and M Sulkava. Distance matrix based clustering of the Self-Organizing Map. *LECTURE NOTES IN COMPUTER SCIENCE*, 2415:951–956, 2002. ISSN 0302-9743; 3-540-44074-7.

Philippe Vidon, Laura E Wagner, and Emmanuel Soyeux. Changes in the character of DOC in streams during storms in two Midwestern watersheds with contrasting land uses. *Biogeochemistry*, 88(3):257–270, May 2008. ISSN 0168-2563. doi: 10.1007/s10533-008-9207-6.

Peter M. Vitousek, John Aber, Robert W. Howarth, Gene E. Likens, Pamela A. Matson, David W Schindler, William H. Schlesinger, and David G. Tilman. Human alteration of the global nitrogen cycle: Causes and consequences. *Issues in Ecology*, 1:1–16, 1997.

I. Vogeler, R. Cichota, V. O. Snow, T. Dutton, and B. Daly. Pedotransfer Functions for Estimating Ammonium Adsorption in Soils. *Soil Science Society of America Journal*, 75(1):324, 2011. ISSN 1435-0661. doi: 10.2136/sssaj2010.0192. URL https://www.soils.org/publications/sssaj/abstracts/75/1/324.

CJ Volk, CB Volk, and LA Kaplan. Chemical composition of biodegradable dissolved organic matter in streamwater. *Limnology and Oceanography*, 42(1):39–44, 1997. URL http://www.aslo.org/lo/pdf/vol_42/issue_1/0039.pdf.

Zhiwei Wang, Zhichao Wu, and Shujuan Tang. Characterization of dissolved organic matter in a submerged membrane bioreactor by using three-dimensional excitation and emission matrix fluorescence spectroscopy. *Water research*, 43(6): 1533–40, April 2009. ISSN 0043-1354. doi: 10.1016/j.watres.2008.12.033. URL http://www.ncbi.nlm.nih.gov/pubmed/19138782.

JV Ward and JA Stanford. Dynamics of lotic systems. In DD Fontaine and SM Bartell, editors, *Dynamics of lotic ecosystems*, chapter The serial, pages 29–42. Ann Arbor Science Publishers, 1983. URL http://www.nrem.iastate.edu/class/assets/aecl518/DiscussionReadings/Ward_and_Stanford_1983.pdf.

JR Webster and J. L. Meyer. Organic Matter Budgets for Streams: A Synthesis. *Journal of the North American Benthological Society*, 16(1):141–161, 1997.

Ron Wehrens and Lutgarde M C Buydens. Self- and super-organizing maps in R: The kohonen package. *Journal of Statistical Software*, 21(5):1–19, 2007. ISSN 1548-7660.

Bernhard Wehrli. Conduits of the carbon cycle. *Nature*, 503:346–347, 2013.

J L Weishaar, G R Aiken, B A Bergamaschi, M S Fram, R Fujii, and K Mopper. Evaluation of specific ultraviolet absorbance as an indicator of the chemical composition and reactivity of dissolved organic carbon. *Environmental science & technology*, 37(20):4702–4708, 2003. ISSN 0013-936X. doi: 10.1021/es030360x.

Gesa A Weyhenmeyer, Mats Froberg, Erik Karltun, Maria Khalili, Dolly Kothawala, Johan Temnerud, and Lars J Tranvik. Selective decay of terrestrial organic carbon during transport from land to sea. *Global Change Biology*, 18(1):349–355, January 2012. ISSN 1354-1013. doi: 10.1111/j.1365-2486.2011.02544.x.

Tracy N Wiegner, Randee L Tubal, and Richard A MacKenzie. Bioavailability and export of dissolved organic matter from a tropical river during base- and stormflow conditions. *Limnology and Oceanography*, 54(4):1233–1242, July 2009. ISSN 0024-3590. doi: 10.4319/lo.2009.54.4.1233.

Lewis M. William and Michael C. Grant. Relationships between stream discharge and yield of dissolved substances from a Colorado mountain watershed. *Soil Science*, 128(6):353–363, 1979.

Clayton J Williams, Youhei Yamashita, Henry F Wilson, Rudolf Jaffe, and Marguerite A Xenopoulos. Unraveling the role of land use and microbial activity in shaping dissolved organic matter characteristics in stream ecosystems. *Limnology and Oceanography*, 55(3):1159–1171, 2010. ISSN 0024-3590. doi: 10.4319/lo.2010.55.3.1159.

Henry F Wilson and Marguerite A Xenopoulos. Effects of agricultural land use on the composition of fluvial dissolved organic matter. *Nature Geoscience*, 2(1): 37–41, January 2009. ISSN 1752-0894. doi: 10.1038/NGEO391.

Henry F Wilson, James E Saiers, Peter A Raymond, and William V Sobczak. Hydrologic Drivers and Seasonality of Dissolved Organic Carbon Concentration, Nitrogen Content, Bioavailability, and Export in a Forested New England Stream. *Ecosystems*, 16(4):604–616, June 2013. ISSN 1432-9840. doi: 10.1007/s10021-013-9635-6.

MS Wipfli, JS Richardson, and RJ Naiman. Ecological linkages between headwaters and downstream ecosystems: transport of organic matter, invertebrates, and wood down headwater channels1. *Journal of the American Water Resources Association*, 43(1), 2007. URL `http://onlinelibrary.wiley.com/doi/10.1111/j.1752-1688.2007.00007.x/full`.

F. Worrall, T.P. Burt, and J. Adamson. The rate of and controls upon DOC loss in a peat catchment. *Journal of Hydrology*, 321(1-4):311–325, April 2006. ISSN 00221694. doi: 10.1016/j.jhydrol.2005.08.019. URL http://linkinghub.elsevier.com/retrieve/pii/S002216940500394X.

Fred Worrall, Tom Guilbert, and Tim Besien. The flux of carbon from rivers: the case for flux from England and Wales. *Biogeochemistry*, 86(1):63–75, August 2007. ISSN 0168-2563. doi: 10.1007/s10533-007-9145-8. URL http://link.springer.com/10.1007/s10533-007-9145-8.

Jie Xu, Mingming Sun, Zhen Shi, Paul J Harrison, and Hongbin Liu. Response of bacterial metabolic activity to riverine dissolved organic carbon and exogenous viruses in estuarine and coastal waters: implications for CO2 emission. *PloS one*, 9(7):e102490, January 2014. ISSN 1932-6203. doi: 10.1371/journal.pone.0102490. URL http://www.pubmedcentral.nih.gov/articlerender.fcgi?artid=4103809\&tool=pmcentrez\&rendertype=abstract.

Y Yamashita and E Tanoue. Chemical characterization of protein-like fluorophores in DOM in relation to aromatic amino acids. *Marine Chemistry*, 82(3-4):255–271, 2003. ISSN 0304-4203. doi: 10.1016/S0304-4203(03)00073-2.

Liyang Yang and Jin Hur. Critical evaluation of spectroscopic indices for organic matter source tracing via end member mixing analysis based on two contrasting sources. *Water research*, 59:80–9, August 2014. ISSN 1879-2448. doi: 10.1016/j.watres.2014.04.018. URL http://www.ncbi.nlm.nih.gov/pubmed/24784456.

Z Yu, Q Zhang, TEC Kraus, RA Dahlgren, C Anastasio, and RJ Zasoski. Contribution of amino compounds to dissolved organic nitrogen in forest soils. *Biogeochemistry*, 61:173–198, 2002. URL http://link.springer.com/article/10.1023/A:1020221528515.

Jie Zhou, Jun-Jian Wang, Antoine Baudon, and Alex T Chow. Improved Fluorescence Excitation-Emission Matrix Regional Integration to Quantify Spectra for Fluorescent Dissolved Organic Matter. *Journal of environmental quality*, 42(3):925–930, 2013. ISSN 0047-2425. doi: 10.2134/jeq2012.0460.

A Zsolnay, E Baigar, M Jimenez, B Steinweg, and F Saccomandi. Differentiating with fluorescence spectroscopy the sources of dissolved organic matter in soils subjected to drying. *Chemosphere*, 38(1):45–50, 1999. ISSN 0045-6535. doi: 10.1016/S0045-6535(98)00166-0.